1-1-2018

IMPROVEMENT OF POWER QUALITY OF HYBRID GRID BY NON-LINEAR CONTROLLED DEVICE CONSIDERING TIME DELAYS AND CYBER-ATTACKS

Sagnika Ghosh

IMPROVEMENT OF POWER QUALITY OF HYBRID GRID BY NON-LINEAR CONTROLLED DEVICE CONSIDERING TIME DELAYS AND CYBER-ATTACKS

BY

SAGNIKA GHOSH

A Dissertation

Submitted in Partial Fulfillment of the

Requirements for the Degree of

Doctor of Philosophy

Major: Electrical and Computer Engineering

The University of Memphis

August 2018

This dissertation is dedicated to my parents, my sister and my friends for all their love and support that they gave me.

ACKNOWLEDGMENTS

It is my pleasure to acknowledge the roles of several individuals who were instrumental for completion of my Ph.D. study.

First, I would like to express my deepest and sincerest gratitude to Dr. Mohd. Hasan Ali, for his constant support, patience, motivation, enthusiasm, and help during my Ph.D. study here. I cannot but acknowledge the RA support through his CAST project grants from the FedEx Institute of Technology. I am extremely grateful to have him as my advisor, and much more.

I would also like to acknowledge helpful suggestions from my committee members: Dr. Russell Deaton, Dr. Dipankar Dasgupta and Dr. Eddie Jacobs, who devoted their precious time.

I would also like to extend my thanks to the EECE Department for providing me the GA support throughout my years of studies here.

These acknowledgements would not be complete without mentioning my past and present research colleagues of the Electric Power and Energy Systems (EPES) lab. It was a great pleasure working with them and I appreciate their ideas and help.

My deepest appreciation belongs to my family for their patience and understanding. I would also like to thank all my friends for their constant support and encouragement.

With regards to numerous questions about my future academic endeavors from family and friends, I shall answer in the words of Sir Winston Churchill: “Now, this is not the end. It is not even the beginning of the end. But it is, perhaps, the end of the beginning”,

PREFACE

This dissertation is the product of my Ph.D. research papers. Based on chapter III, I have published one journal paper, one conference paper, and one journal paper is under review. Based on chapter IV, I have published one conference paper, and one journal paper is under review. Based on chapter V, I have one accepted conference paper and one journal paper is under review.

Chapter III

- **S. Ghosh** and **M. H. Ali**, "Power Quality Enhancement by Coordinated Operation of Thyristor Switched Capacitor and Optimal Reclosing of Circuit Breakers" *Journal of IET-Generation, Transmission & Distribution*, vol. 9, Issue 12, pp.1301-1307, September 2015.

- **S. Ghosh** and M. H. Ali," Augmentation of Power Quality of Grid-Connected Wind Generator by Fuzzy Logic Controlled TSC," *Proceedings of the IEEE PES Transmission and Distribution (T&D) Conference & Exposition, Denver, USA, April 16-19, 2018.*

- **S. Ghosh** and M. H. Ali," Non-Linear Controlled Thyristor Switched Capacitor for Power Quality Improvement of Hybrid Grid Including Wind Generator," *Submitted at the Journal of Energies.*

Chapter IV

- **S. Ghosh** and Mohd. Hasan Ali," Minimization of Adverse Effects of Time Delay on Power Quality Enhancement in Hybrid Grid," *Submitted at the IEEE Systems Journal.*

- **S. Ghosh** and **M. H. Ali**, "Minimization of Adverse Effects of Time Delay in Smart Power Grid," *Proceedings of the IEEE PES Innovative Smart Grid Technologies (ISGT) Conference*, Paper ID: 219, Washington DC, USA, February 19-22, 2014.

Chapter V

- **S. Ghosh** and Mohd. Hasan Ali," Effects of Cyber-Attacks on the Energy Storage in a Smart Microgrid System," *Proceedings of the IEEE PES GM, 2018 (Accepted and to be presented in August)*

- **S. Ghosh** and Mohd. Hasan Ali.” Mitigating Adverse Effects of Cyber-Attacks on the Power Quality of Microgrid,” *Submitted at the International Journal of Electric Power and Energy Systems.*

ABSTRACT

Ghosh, Sagnika. MS. The University of Memphis. August,2018. Improvement of Power Quality of Hybrid Grid by Non-Linear Controlled Device Considering Time Delays and Cyber-Attacks. Major Professor: Dr. Mohd. Hasan Ali

Power Quality is defined as the ability of electrical grid to supply a clean and stable power supply. Steady-state disturbances such as harmonics, faults, voltage sags and swells, etc., deteriorate the power quality of the grid. To ensure constant voltage and frequency to consumers, power quality should be improved and maintained at a desired level. Although several methods are available to improve the power quality in traditional power grids, significant challenges exist in modern power grids, such as non-linearity, time delay and cyber-attacks issues, which need to be considered and solved. This dissertation proposes novel control methods to address the mentioned challenges and thus to improve the power quality of modern hybrid grids.

In hybrid grids, the first issue is faults occurring at different points in the system. To overcome this issue, this dissertation proposes non-linear controlled methods like the Fuzzy Logic controlled Thyristor Switched Capacitor (TSC), Adaptive Neuro Fuzzy Inference System (ANFIS) controlled TSC, and Static Non-Linear controlled TSC. The next issue is the time delay introduced in the network due to its complexities and various computations required. This dissertation proposes two new methods such as the Fuzzy Logic Controller and Modified Predictor to minimize adverse effects of time delays on the power quality enhancement. The last and major issue is the cyber-security aspect of the hybrid grid. This research analyzes the effects of cyber-attacks on various components such as the Energy Storage System (ESS), the automatic voltage regulator (AVR) of the synchronous generator, the grid side converter (GSC) of the wind generator, and the voltage source converter (VSC) of Photovoltaic (PV) system, located in a hybrid power grid. Also, this dissertation proposes two new techniques such as a Non-Linear (NL) controller and a Proportional-Integral (PI) controller for mitigating the adverse effects of cyber-attacks on the mentioned devices, and a new detection and mitigation technique based on the voltage threshold for the Supercapacitor Energy System (SES).

Simulation results obtained through the MATLAB/Simulink software show the effectiveness of the proposed new control methods for power quality improvement. Also, the proposed methods perform better than conventional methods.

TABLE OF CONTENTS

LIST OF TABLES viii

LIST OF FIGURES x

LIST OF ABBREVIATIONS xii

I. INTRODUCTION 1

A. OVERVIEW OF POWER QUALITY 1
B. MOTIVATION 6
C. OBJECTIVES 7
D. ORIGINALITY OF THE WORK 8
E. ORGANIZATION OF THIS DISSERTATION 10

II. LITERATURE REVIEW 12

A. INTRODUCTION 12
B. TYPES OF POWER QUALITY PROBLEMS 13
C. POWER QUALITY EVALUATION, STANDARDS AND INDICES 19
D. CONVENTIONAL SOLUTIONS FOR POWER QUALITY ISSUES 21
E. SEVERAL CHALLENGES IN POWER QUALITY ISSUES IN MODERN POWER GRID 22
i. Non-Linear Controllers 22
ii. Time Delay 24
iii. Cyber-Attacks 27
F. CONCLUSION 31

III. POWER QUALITY IMPROVEMENT BY NON-LINEAR CONTROLLER BASED THYRISTOR SWITCHED CAPACITOR 33

A. INTRODUCTION 33
B. DESCRIPTION OF POWER SYSTEM 33
i. Synchronous Generator 35
ii. Modelling of Wind Generator 37
iii. Reactive Power Compensating Device: TSC 41
C. CONTROL OF TSC 43
i. Case I: 43
ii. Case II: 53
D. CONCLUSION 81

IV. MINIMIZATION OF ADVERSE EFFECTS OF TIME DELAY ON POWER QUALITY ENHANCEMENT IN HYBRID GRID 82

A. INTRODUCTION 82
B. TIME DELAY ISSUES WITH TSC CONTROLLER 82
i. Time Delay Issue with the TSC Controller 82

C. TIME DELAY MINIMIZATIONS WITH TSC CONTROLLER 84
i. Fuzzy Logic Controller (FLC) Based Method 84
ii. Modified Predictor Method 87
D. SIMULATION RESULTS & DISCUSSION 89
i. Effect of Time Delay Without Minimization Methods 89
ii. Effectiveness of Proposed Minimization Methods in terms of Voltage Index, V_{index} 91
iii. Effectiveness of Proposed Minimization Methods in Terms of Plots 95
iv. Effectiveness of Proposed Minimization Methods in Terms of THD 101
E. CONCLUSION 103

V. CYBERSECURITY ISSUES AND SOLUTIONS FOR THE HYBRID GRID COMPONENTS 105

A. INTRODUCTION 105
B. HYBRID POWER MODEL SYSTEM 105
i. Wind Generator 106
ii. PV 107
iii. Supercapacitor Energy Storage (SES) system 109
C. CYBER SECURITY ISSUES IN HYBRID GRID COMPONENTS 110
i. GSC Controller of Wind Generator 110
ii. VSC Controller of PV 110
iii. AVR Controller of SG 111
iv. SES Controller 112
D. PROPOSED CONTROL ALGORITHMS 113
i. Control Algorithms for GSC, VSC and AVR 113
ii. Check the voltage deviation Control Algorithm for SES 115
E. PROPOSED MITIGATION METHODS 116
i. Non-Linear Controller for GSC, VSC and AVR 116
ii. PI Controller for GSC, VSC and AVR 117
iii. Mitigation Technique for SES 118
F. SIMULATION RESULTS & DISCUSSION FOR THE EFFECTS AND MITIGATION OF CYBER-ATTACKS ON GSC, VSC AND AVR 118
i. Effects and Mitigation of DDoS and FDI Cyber-Attack on GSC Controller of Wind Generator 118
ii. Effects and Mitigation of DDoS and FDI Cyber-Attacks on VSC Controller of PV 127
iii. Effects and Mitigation of DDoS and FDI Cyber-Attacks on AVR Controller of SG 135
iv. Effects and Mitigation of DDoS and FDI Cyber-Attacks on SES 144
v. Index Based Performance Evaluation of the Proposed Mitigation Techniques 153
vi. Analysis of Effects of Different Types Cyber-Attacks on SES 154

G. Conclusion 164

VI. CONCLUSION AND FUTURE WORK 166

A. Conclusion 166
B. Contribution of this Thesis 168
C. Future Work 168

VII. BIBLIOGRAPHY 170

LIST OF TABLES

TABLE I: DELAY VALUES IN VARIOUS COMMUNICATION LINKS 26

TABLE II: GENERATOR PARAMETERS 35

TABLE III: WIND GENERATOR PARAMETERS 39

TABLE IV: PID PARAMETERS 47

TABLE V: VOLTAGE INDICES FOR PCC VOLTAGE FOR PERMANENT FAULTS 51

TABLE VI: VOLTAGE INDICES FOR SYNCHRONOUS GENERATOR (G1 & G2) PERMANENT FAULTS 52

TABLE VII: VOLTAGE INDICES FOR WIND GENERATOR FOR PERMANENT FAULTS 52

TABLE VIII: TOTAL HARMONIC DISTORTION AT PCC FOR PERMANENT FAULTS 53

TABLE X: VOLTAGE INDICES FOR PCC VOLTAGE FOR TEMPORARY FAULTS 76

TABLE XI: VOLTAGE INDICES FOR PCC VOLTAGE FOR PERMANENT FAULTS 77

TABLE XII: VOLTAGE INDICES FOR SYNCHRONOUS GENERATOR (G1 & G2) DURING TEMPORARY FAULTS 77

TABLE XIII: VOLTAGE INDICES FOR SYNCHRONOUS GENERATOR (G1 & G2) PERMANENT FAULTS 78

TABLE XIV: VOLTAGE INDICES FOR WIND GENERATOR FOR TEMPORARY FAULTS 78

TABLE XV: VOLTAGE INDICES FOR WIND GENERATOR FOR PERMANENT FAULTS 79

TABLE XVI: TOTAL HARMONIC DISTORTION AT PCC FOR TEMPORARY FAULTS 80

TABLE XVII: TOTAL HARMONIC DISTORTION AT PCC FOR PERMANENT FAULTS 80

TABLE XVII: MEMBERSHIP FUNCTIONS OF INPUT AND OUTPUT 87

TABLE XVIII: VOLTAGE INDICES 91

TABLE XIX: VOLTAGE INDICES AT PCC FOR 3LG TEMPORARY AND PERMANENT FAULTS 92

TABLE XX: VOLTAGE INDICES AT PCC FOR 1LG TEMPORARY AND PERMANENT FAULTS 93

TABLE XXI: VOLTAGE INDICES OF WIND GENERATOR FOR 3LG TEMPORARY AND PERMANENT FAULTS 94

TABLE XXII: VOLTAGE INDICES OF WIND GENERATOR FOR 1LG TEMPORARY AND PERMANENT FAULTS 95

TABLE XXIII: TOTAL HARMONIC DISTORTION AT PCC FOR 3LG TEMPORARY AND PERMANENT FAULTS 102

TABLE XXIV: TOTAL HARMONIC DISTORTION AT PCC FOR 1LG TEMPORARY AND PERMANENT FAULTS 103

TABLE XXV: PARAMETER VALUES OF THE NON-LINEAR CONTROLLER 117

TABLE XXVI: PARAMETER VALUES OF THE PI CONTROLLER 117

TABLE XXVII: VOLTAGE INDEX VALUES FOR GSC 153

TABLE XXVIII: VOLTAGE INDEX VALUES FOR VSC 153

TABLE XXIX: VOLTAGE INDEX VALUES FOR AVR 154

TABLE XXX: VOLTAGE INDEX FOR SES 154

LIST OF FIGURES

FIGURE 1. POWER QUALITY ISSUES: VOLTAGE SWELL, VOLTAGE SAG, VOLTAGE INTERRUPTION. 13

FIGURE 2. HARMONICS 14

FIGURE 3. IMPULSIVE TRANSIENT 15

FIGURE 4. OSCILLATORY TRANSIENT. 15

FIGURE 5. UNDERVOLTAGE. 16

FIGURE 6. OVERVOLTAGE. 16

FIGURE 7. VOLTAGE FLUCTUATION 17

FIGURE 8: VOLTAGE IMBALANCE. 17

FIGURE 9. VOLTAGE NOTCHING. 17

FIGURE 10. POWER QUALITY PROBLEMS. 18

FIGURE 11. BASIC STEPS INVOLVED IN POWER QUALITY EVALUATION 19

FIGURE 12. HYBRID SYSTEM MODEL. 34

FIGURE 13: THE CONTROL BLOCK OF AUTOMATIC VOLTAGE REGULATOR. 36

FIGURE 14 : THE CONTROL BLOCK OF GOVERNOR MODEL. 37

FIGURE 15. BASIC DIAGRAM OF DFIG WITH CONVERTERS. 38

FIGURE 16. CONTROL BLOCK OF GRID SIDE CONVERTER (GSC). 40

FIGURE 17. CONTROL BLOCK OF ROTOR SIDE CONVERTER (RSC). 40

FIGURE 18. TSC REACTIVE POWER VERSUS FIRING ANGLE. 42

FIGURE 19. SINGLE LINE DIAGRAM OF THYRISTOR SWITCHED CAPACITOR (TSC) MODEL. 43

FIGURE 20. A CONTROL BLOCK FOR SWITCHING OF TSC. 43

FIGURE 21. MEMBERSHIP FUNCTION OF TVD (PU). 44

FIGURE 22. MEMBERSHIP FUNCTION OF FIRING ANGLE, A (DEGREES). 45

FIGURE 23. PID CONTROLLER. 47

FIGURE 24. VOLTAGE RESPONSE AT PCC. 48

FIGURE 25. VOLTAGE RESPONSE OF G1 SYNCHRONOUS GENERATOR. 49

FIGURE 26. VOLTAGE RESPONSE OF G2 SYNCHRONOUS GENERATOR. 49

FIGURE 27. VOLTAGE OF WIND GENERATOR. 50

FIGURE 28. DC LINK VOLTAGE OF WIND GENERATOR. 50

FIGURE 29. ANFIS ARCHITECTURE. 55

FIGURE 30. A CONTROL BLOCK OF CONTROLLER FOR SWITCHING OF TSC. 56

FIGURE 31. VOLTAGE RESPONSES WHEN THE SYSTEM IS SUBJECTED TO 3LG TEMPORARY FAULT AT F3. (A) VOLTAGE AT PCC, (B) TERMINAL VOLTAGE OF WIND GENERATOR, (C) DC LINK VOLTAGE OF THE WIND GENERATOR. 58

FIGURE 32. VOLTAGE RESPONSES WHEN THE SYSTEM IS SUBJECTED TO 3LG TEMPORARY FAULT AT F2. (A) VOLTAGE AT PCC, (B) TERMINAL VOLTAGE OF WIND GENERATOR, (C) DC LINK VOLTAGE OF THE WIND GENERATOR. 60

FIGURE 33. VOLTAGE RESPONSES WHEN THE SYSTEM IS SUBJECTED TO 3LG TEMPORARY FAULT AT F1. (A) VOLTAGE AT PCC, (B) TERMINAL VOLTAGE OF WIND GENERATOR, (C) DC LINK VOLTAGE OF THE WIND GENERATOR. 61

FIGURE 34. VOLTAGE RESPONSES WHEN THE SYSTEM IS SUBJECTED TO 3LG PERMANENT FAULT AT F3. (A) VOLTAGE AT PCC, (B) TERMINAL VOLTAGE OF WIND GENERATOR, (C) DC LINK VOLTAGE OF THE WIND GENERATOR. 63

FIGURE 35. VOLTAGE RESPONSES WHEN THE SYSTEM IS SUBJECTED TO 3LG PERMANENT FAULT AT F2. (A) VOLTAGE AT PCC, (B) TERMINAL VOLTAGE OF WIND GENERATOR, (C) DC LINK VOLTAGE OF THE WIND GENERATOR. 64

FIGURE 36. VOLTAGE RESPONSES WHEN THE SYSTEM IS SUBJECTED TO 3LG PERMANENT FAULT AT F1. (A) VOLTAGE AT PCC, (B) TERMINAL VOLTAGE OF WIND GENERATOR, (C) DC LINK VOLTAGE OF THE WIND GENERATOR. 66

FIGURE 37. VOLTAGE RESPONSES WHEN THE SYSTEM IS SUBJECTED TO 1LG TEMPORARY FAULT AT F3. (A) VOLTAGE AT PCC, (B) TERMINAL VOLTAGE OF WIND GENERATOR, (C) DC LINK VOLTAGE OF THE WIND GENERATOR. 68

FIGURE 38. VOLTAGE RESPONSES WHEN THE SYSTEM IS SUBJECTED TO 1LG TEMPORARY FAULT AT F2. (A) VOLTAGE AT PCC, (B) TERMINAL VOLTAGE OF WIND GENERATOR, (C) DC LINK VOLTAGE OF THE WIND GENERATOR. 69

FIGURE 39. VOLTAGE RESPONSES WHEN THE SYSTEM IS SUBJECTED TO 1LG TEMPORARY FAULT AT F1. (A) VOLTAGE AT PCC, (B) TERMINAL

VOLTAGE OF WIND GENERATOR, (C) DC LINK VOLTAGE OF THE WIND GENERATOR. 71
FIGURE 40. VOLTAGE RESPONSES WHEN THE SYSTEM IS SUBJECTED TO 1LG PERMANENT FAULT AT F3. (A) VOLTAGE AT PCC, (B) TERMINAL VOLTAGE OF WIND GENERATOR, (C) DC LINK VOLTAGE OF THE WIND GENERATOR. 72
FIGURE 41. VOLTAGE RESPONSES WHEN THE SYSTEM IS SUBJECTED TO 1LG PERMANENT FAULT AT F2. (A) VOLTAGE AT PCC, (B) TERMINAL VOLTAGE OF WIND GENERATOR, (C) DC LINK VOLTAGE OF THE WIND GENERATOR. 74
FIGURE 42. VOLTAGE RESPONSES WHEN THE SYSTEM IS SUBJECTED TO 1LG PERMANENT FAULT AT F1. (A) VOLTAGE AT PCC, (B) TERMINAL VOLTAGE OF WIND GENERATOR, (C) DC LINK VOLTAGE OF THE WIND GENERATOR. 75
FIGURE 43. A CONTROL BLOCK FOR SWITCHING OF TSC. 83
FIGURE 44. A CONTROL BLOCK OF CONTROLLER DESIGNED FOR GENERATION REQUIRED FOR SWITCHING OF TSC. 84
FIGURE 45. MEMBERSHIP FUNCTIONS OF FUZZY CONTROLLER INPUTS: (A) ΔV AND (B) DELAY. 86
FIGURE 46. MEMBERSHIP FUNCTIONS OF FUZZY CONTROLLER OUTPUT. 86
FIGURE 47. MODIFIED PREDICTOR MODEL. 88
FIGURE 48. FLOWCHART DIAGRAM OF THE MODIFIED PREDICTOR METHOD. 89

FIGURE 49. VOLTAGE AT PCC FOR 3LG PERMANENT FAULT AT F3. 90

FIGURE 50. VOLTAGE AT PCC FOR 1LG PERMANENT FAULT AT F3. 91

FIGURE 51. VOLTAGE AT PCC FOR 3LG TEMPORARY FAULT AT F3............... 96

FIGURE 52. VOLTAGE OF WIND GENERATOR FOR 3LG TEMPORARY FAULT AT F3... 97

FIGURE 53. VOLTAGE AT PCC FOR 3LG PERMANENT FAULT AT F3 97

FIGURE 54. VOLTAGE OF WIND GENERATOR FOR 3LG PERMANENT FAULT AT F3... 98

FIGURE 55. VOLTAGE AT PCC FOR 1LG TEMPORARY FAULT AT F3............... 99

FIGURE 56. VOLTAGE OF WIND GENERATOR FOR 1LG TEMPORARY FAULT AT F3... 99

FIGURE 57. VOLTAGE AT PCC FOR 1LG PERMANENT FAULT AT F3 100

FIGURE 58. VOLTAGE OF WIND GENERATOR FOR 1LG PERMANENT FAULT AT F3... 100

FIGURE 59. HYBRID GRID SYSTEM. 106

FIGURE 60. EQUIVALENT CIRCUIT OF SOLAR CELL. 108

FIGURE 61. CONTROL BLOCK OF VOLTAGE SOURCE CONVERTER (VSC). . 111

FIGURE 62. CONTROL OF SUPERCAPACITOR ENERGY STORAGE. 113

FIGURE 63. PROPOSED CONTROL ALGORITHM FOR GSC OF WIND GENERATOR, THE VSC OF PV AND THE AVR OF THE SG 115

FIGURE 64. DC REFERENCE VOLTAGE FOR DDOS CYBER-ATTACK FOR GSC 119

FIGURE 65. DC REFERENCE VOLTAGE FOR FDI CYBER-ATTACK FOR GSC 119

FIGURE 66. VOLTAGE AT PCC 120

FIGURE 67. CURRENT AT PCC........ 121

FIGURE 68. POWER AT PCC 121

FIGURE 69. TERMINAL VOLTAGE AT SYNCHRONOUS GENERATOR........ 122

FIGURE 70. TERMINAL VOLTAGE OF WIND GENERATOR 122

FIGURE 71. TERMINAL VOLTAGE OF PV 123

FIGURE 72. VOLTAGE AT PCC 124

FIGURE 73. CURRENT AT PCC........ 124

FIGURE 74. POWER AT PCC 125

FIGURE 75. TERMINAL VOLTAGE OF SYNCHRONOUS GENERATOR. 125

FIGURE 76. TERMINAL VOLTAGE OF WIND GENERATOR. 126

FIGURE 77. TERMINAL VOLTAGE OF PV 126

FIGURE 78. DC REFERENCE VOLTAGE OF VSC OF PV FOR DDOS........ 127

FIGURE 79. DC REFERENCE VOLTAGE OF VSC OF PV FOR FDI 128

FIGURE 80. VOLTAGE AT PCC 129

FIGURE 81. CURRENT AT PCC........ 129

FIGURE 82. POWER AT PCC 130

FIGURE 83. TERMINAL VOLTAGE OF SYNCHRONOUS GENERATOR. 130

FIGURE 84. TERMINAL VOLTAGE OF WIND GENERATOR. 131

FIGURE 85. TERMINAL VOLTAGE OF PV. 131

FIGURE 86. VOLTAGE AT PCC 132

FIGURE 87. CURRENT AT PCC........ 133

FIGURE 88. POWER AT PCC 133

FIGURE 89. TERMINAL VOLTAGE OF SYN. GENERATOR 134

FIGURE 90. TERMINAL VOLTAGE OF WIND GENERATOR 134

FIGURE 91. TERMINAL VOLTAGE OF PV 135

FIGURE 92. E_{FDO} REFERENCE VOLTAGE OF AVR FOR DDOS 136

FIGURE 93. E_{FDO} REFERENCE VOLTAGE OF AVR FOR FDI 136

FIGURE 94. VOLTAGE AT PCC 137

FIGURE 95. CURRENT AT PCC.. 138

FIGURE 96. POWER AT PCC 138

FIGURE 97. TERMINAL VOLTAGE OF SYNCHRONOUS GENERATOR 139

FIGURE 98. TERMINAL VOLTAGE OF WIND GENERATOR 139

FIGURE 99. TERMINAL VOLTAGE OF PV 140

FIGURE 100. VOLTAGE AT PCC 141

FIGURE 101. CURRENT AT PCC.. 141

FIGURE 102. POWER AT PCC 142

FIGURE 103. TERMINAL VOLTAGE OF SYNCHRONOUS GENERATOR 142

FIGURE 104. TERMINAL VOLTAGE OF WIND GENERATOR 143

FIGURE 105. TERMINAL VOLTAGE OF PV 143

FIGURE 106. IGBT GATE PULSE SIGNAL FOR VSC OF SES FOR FDI ATTACK 144

FIGURE 107. VOLTAGE AT PCC 145

FIGURE 108. CURRENT AT PCC.. 146

FIGURE 109. POWER AT PCC 146

FIGURE 110. POWER OF ESS 147

FIGURE 111. TERMINAL VOLTAGE OF SYNCHRONOUS GENERATOR 147
FIGURE 112. TERMINAL VOLTAGE OF WIND GENERATOR 148
FIGURE 113. TERMINAL VOLTAGE OF PV 148
FIGURE 114. VOLTAGE AT PCC 149
FIGURE 115. CURRENT AT PCC.. 150
FIGURE 116. POWER AT PCC 150
FIGURE 117. POWER OF ESS 151
FIGURE 118. TERMINAL VOLTAGE OF SYNCHRONOUS GENERATOR 151
FIGURE 119. TERMINAL VOLTAGE OF WIND GENERATOR 152
FIGURE 120. TERMINAL VOLTAGE OF PV 152
FIGURE 121. VOLTAGE AT PCC 155
FIGURE 122. CURRENT AT PCC.. 155
FIGURE 123. POWER AT PCC 156
FIGURE 124. VOLTAGE AT PCC 157
FIGURE 125. CURRENT AT PCC.. 157
FIGURE 126. POWER AT PCC 158
FIGURE 127. VOLTAGE AT PCC 159
FIGURE 128. CURRENT AT PCC.. 159
FIGURE 129. POWER AT PCC 160
FIGURE 130. TERMINAL VOLTAGE OF SYNCHRONOUS GENERATOR 160
FIGURE 131. TERMINAL VOLTAGE OF WIND GENERATOR 161
FIGURE 132. VOLTAGE AT PCC 162
FIGURE 133. CURRENT AT PCC.. 162

FIGURE 134. POWER AT PCC 163

FIGURE 135. TERMINAL VOLTAGE OF SYNCHRONOUS GENERATOR 163

FIGURE 136. TERMINAL VOLTAGE OF WIND GENERATOR 164

LIST OF ABBREVIATIONS

PQ: Power Quality	1
FACTS: Flexible AC Transmission System	3
SVC: Static VAR Compensator	4
STATCOM: Static Synchronous Compensator	4
TSC: Thyristor Series Capacitor	4
SSSC: Static Synchronous Series Compensator	4
TCSC: Thyristor Controlled Series Capacitor	4
UPFC: Unified Power Flow Controller	4
SMES: Superconducting Magnetic Energy Storage	4
PI: Proportional Integral	4
FLC: Fuzzy Logic Controller	4
PMU: Phasor Measurement Unit	5
SCADA: Supervisory Control and Data Acquisition System	5
ANFIS: Adaptive Neuro Fuzzy Inference System	5
PID: Proportional Integral and Derivative	6
3LG: Three-line-to-ground fault or Three-phase-to-ground fault	7

1LG: One-line-to-ground fault or One-phase-to-ground fault 7

THD: Total Harmonic Distortion 7

ESS: Energy Storage System 7

GSC: Grid Side Converter 7

VSC: Voltage Source Converter 7

AVR: Automatic Voltage Regulator 7

NL: Non- Linear 8

SES: Supercapacitor Energy Storage 8

DDoS: Distributed Denial of Service 8

FDI: False Data Injection 8

EMC: Electromagnetic Compatibility 12

CBEMA: Computer and Business Equipment Manufacturers' Association 13

DFIG: Doubly Fed Induction Generator 22

SG: Synchrounous Generator 23

ANN: Artificial Neural Network 24

GPS: Global Positioning System 24

AMI: Advanced Metering Interface 26

2LG: Two-line-to-ground fault or Two-phase-to-ground fault 29

2LS: Two-line- to-line fault or Two-phase-to-phase fault 29

GOV: Governor 30

PCC: Point of Common Coupling 38

TVD: Total Voltage Deviation 40

FIS: Fuzzy Inference System 44

WACS: Wide Area Control System 78

VSWT: Variable Speed Wind Turbine 102

MPPT: Maximum Power Point Tracking 102

P&O: Perturb & Observe 102

I. INTRODUCTION

A. Overview of Power Quality

Power quality (PQ) definition is contingent on one's frame of reference. From a point of view of a utility, power quality is about reliability. It is important for the utility to show statistics that demonstrate a system to be 99.98 % reliable. But from a manufacturer's point of view, power quality is about successful operation of an equipment [1]. At the end, power quality is all about consumers. The end user's point of view gets preference [2]. Power quality is hence described by the fitness of power from generator to the power supplied to the end user. When the voltage, frequency and phase are synchronized, electrical systems function in their intended manner without significant loss of performance [3]. The quality of power supplied to the consumers is the main factor on which the reliability and cost of any electrical system greatly depend.

PQ is an important issue in power distribution systems, especially where a highly reliable source of power is required. Deterioration of power quality due to steady-state disturbances such as harmonics has been extensively studied [4] [5]. On the other hand, transient disturbances also degrade power quality and, hence are the subject of this dissertation. The source of a power quality problem can be the utility, but it also can be the facility or even the equipment inside the facility. Impact of power quality issues is the most when it begins with the utility. When power quality issues originate from utility's end, it could range from a breaker clearing, which can produce sag [6], under-voltage or outage, to arcing contactors, which may generate impulses. The impact of power quality issues should be mitigated before the power enters the facility. Most of the facility faces problems like loose connections, overloaded circuits and transformers, ground loops and wiring errors.

Most of the new technology or new equipment can produce power quality issues through normal operations like equipment turn-on/off that can include impulse, sag, surge, voltage distortion and repetitive disturbances.

The poor power quality may result in increased power losses, undesirable behavior of equipment, and interference with nearby communication lines. Widespread use of power electronics further burdens the power systems by generating harmonics in the voltages and currents along with increased reactive current [7]. Currently, power quality problems have become more complex at all levels of electrical grid systems. Therefore, power quality issues have received increasing attention by both the end users and utilities [1]. Maintaining the electric power quality within acceptable limits is a significant challenge [8]. In the US, the acceptable voltage and frequency tolerance is +/-5% and +/- 3%, respectively, of the nominal values. The adverse effects of poor power quality are well discussed in [9]. The term power quality is sometimes used with different meaning such as voltage quality, current quality, service quality, supply reliability, quality of supply and quality of consumption [10]. Among all the power quality issues, voltage sag accounts for the highest with 31 % whereas voltage transients are 8% making it the lowest. Because of the increased use of sensitive loads, renewable resources and power electronic equipment produce harmonic and asymmetrical voltages accounting for 20% and 18%, respectively [11].

In 2001, Electric Power Research Institute (EPRI) published a report based on Primen survey in the United States, which showed that the collective loss is $45.7 billion a year due to outages and another $6.7 billion a year due to other PQ phenomena. It was estimated that the U.S. economy loss was between $104 billion to $164 billion due to outages and another $15 billion to $24 billion due to other PQ phenomena [12]. The Leonardo Power Quality

Initiative (LPQI) team published a report about the results of European PQ survey, which comprised of 62 face-to-face interviews across eight European countries in 2008 [13]. The report showed that the PQ loss was about €150 billion, with industrial and services customers wasting around 4% and 0.142% of their annual turnover. In 2001, Taiwan did a survey of interruption cost for 284 high-tech factories. The cost of interruptions was represented as a customer damage function, which gave interruption cost as function of interruption duration. The cost in high-tech was about $37.03/kW for 2 seconds interruption, which was higher than traditional industries [14]. In South Korea, the Korea Electrotechnology Institute in cooperation with Gallup Korea conducted an interview-based survey on 660 industrial customers of various sizes and sectors. The survey presented a method to evaluate productions, sales and extra labor costs respectively, which was incurred from interruption duration and a method to evaluate interruption costs per kw power use according to interruption durations by industrial customer types [15] [16].

To ensure constant voltage and frequency to the consumers, power quality should be improved and maintained at a desired level. The flexible ac transmission system (FACTS) devices are one of the most well-known and reliable solutions to reduce the power quality issues [17]. FACTS devices include the Static VAR Compensator (SVC), Static Synchronous Compensator (STATCOM), Thyristor Switched Capacitor (TSC), Static Synchronous Series Compensator (SSSC), Thyristor Controlled Series Capacitor (TCSC), Unified Power Flow Controller (UPFC), Superconducting Magnetic Energy Storage (SMES), etc. Their benefits include reactive power control, improvement of the stability of the grid, control of active and reactive power flows on the grid, loss minimization, and increased grid efficiency [18].

Just as FACTS devices improve the reliability and quality of power transmission by simultaneously enhancing both power transfer volume and stability, the power electronic controllers are reliable for the distribution systems [19]. Some of these devices are voltage regulator, dynamic voltage restorer, line reactor, surge suppressors, power conditioners, isolation transformers, uninterrupted power supply, proper wiring and grounding, filters, etc. [20]. One important method to improve the power quality is the TSC, which is a device to compensate for the reactive power [21] [22] [23] [24] [25] [26] [27] [28] [29]. The TSC is used because it provides instantaneous response to the changes in the system parameters. The TSC also has another advantage in that it generates no harmonics and requires no filtering. The TSC is also used for power factor improvement, to mitigate harmonics, active and reactive power control, voltage stability [30] [31]. But in all these methods, conventional Proportional-Integral (PI) control techniques were used [32]. However, since the existing power grids are being transitioned into the smart grids, with integration of renewables [33] and sophisticated power electronic controllers power quality enhancement devices should be equipped with intelligent based controllers, such as a fuzzy logic controller (FLC) [34] [35] , neuro fuzzy logic controllers [36]. Moreover, power networks are highly nonlinear. Therefore, it is appropriate to employ nonlinear based intelligent control techniques for smart power grids [37] .

With the integration of renewables sources like wind generator [38] [39], photovoltaic system [40], energy storage system, conventional synchronous generator in the existing grid gives rise to the other two vulnerabilities of the grid [41]. Different types of measurement, monitoring and communicating devices are added to the system like the phasor measurement units (PMUs) and open communication networks which have been extensively used in measurement/monitoring systems [42]. This causes inevitable time delays and reduces the damping performance of the controller, which in turn causes instability in the system [43] [44] [45] [46] [47]. Large time delays not only cause instability of the system, but also affect the power quality of the network [48].

As the renewables relate to the main grid and the total cyber-physical system is monitored and regulated by the Supervisory Control and Data Acquisition System (SCADA) in different layers, cyber-attacks may happen at any points of the supervisory control. This will result in power deficiency in the grid and the controllers will fail to stabilize the system, thus will affect the consumers [49]. The communication between the control center and the controllers can easily be hacked, interrupted or tampered. Consequently, the power quality of the overall grid gets affected.

Based on these backgrounds, this dissertation first deals with the nonlinearity that arises due to the balanced and unbalanced faults occurring at different points in the system. To improve the power quality due to nonlinearity issues, at first the FLC based TSC was proposed and its performance was compared with that of the conventional Proportional-Integral-Derivative (PID) controlled TSC. Later, two new non-linear controllers, namely, the Adaptive Neuro Fuzzy Inference System (ANFIS) controlled TSC and a static Non-Linear controlled TSC were proposed. The effectiveness of these two new controllers was compared with that of the fuzzy controlled TSC. The next issue is the time delay introduced in the network due to its complexities and various computations required. This work deals with minimization of the adverse effects of time delay on the system performance with the help of two methods such as the two inputs based Fuzzy Logic controller and Modified Predictor. The last and major issue is the cyber-security aspect of the hybrid power grid.

This research analyzes the effects of cyber-attacks on different components of the hybrid power system and explores new solutions to mitigate the adverse effects of cyber-attacks.

B. Motivation

Power quality issues occur at various levels of the system that delivers electric power- power plants and the entire area transmission system, transmission lines, major substations, distribution substations, primary and secondary power lines, and distribution transformers and service equipment and building wiring. Power quality issues need to be fixed. There are various devices to mitigate the power quality issues in the network like the FACTS devices, etc. A lot of work has been done with these devices and with the application of non-linear controller, but none of the work focused on the power quality improvement of the grid based on a nonlinear controlled TSC. The characteristics of power grids are inherently non-linear, as power networks are dynamic and their operations are of stochastic nature which leads to power quality disturbances. The integration of renewable sources [50] [51] gives rise to other problems in the network such as time delay and cyber-attacks. Measuring and monitoring [52] of these sources are carried out with the help of new, sophisticated controllers with in return increases the time delay. A lot of work has been done to mitigate the negative effects of time delay, but none of the work considered the time delay aspect for the power quality improvement. The monitoring of the controllers and control parameters are done with the SCADA which is like a control center. The information exchange between the controllers and the control center make the grid vulnerable and makes it prone to cyber-attacks. While much work has been done on the detection and mitigation of cyber-attacks [53], no one has aimed it from the power quality point of view. Thus, this dissertation deals with power quality improvement considering the three significant issues: nonlinearity, time delay and cyber-attack of modern power grids, and proposes new ways to improve the performance of the system.

C. Objectives

The overall objective of this work is to improve the power quality of hybrid power grid system. To realize this objective, this research performed the following tasks:

1) Modelling of non-linear controller based TSC to improve the power quality of the hybrid system:

To improve the power quality of the network consisting of wind and synchronous generators, the ANFIS-control based TSC, fuzzy logic controlled TSC and static non-linear controlled TSC, have been proposed. At first the performance of the FLC based TSC was compared with that of the conventional PID controlled TSC. Later, the effectiveness of the ANFIS controlled TSC and static Non-Linear controlled TSC was compared with that of the fuzzy controlled TSC. The simulations have been performed in the MATLAB/Simulink environment. To demonstrate the effectiveness of the proposed control methods, the balanced (three-phase-to-ground [3LG]) and unbalanced (single-phase-to ground [1LG]), temporary and permanent faults in the power network have been considered. Moreover, to quantify the results, two indices namely the voltage index associated with the wind generator terminal voltage and the voltage index associated with the synchronous generators, have been used. In addition, the power quality in terms of total harmonic distortion (THD) has been evaluated at the point of common coupling for both synchronous generators and the wind generator.

2) Developing controllers to minimize adverse effects of time delay in hybrid power grid:

Two proposed methods, namely the FLC based method and the Modified Predictor method, are used to minimize the adverse effects of time delay on the power quality enhancement of a hybrid power grid. The performance of the FLC based method has been compared with that of the Modified Predictor method in minimizing the adverse effects of time delays. Two indices, namely the voltage index and the THD have been used to evaluate the power quality of the system. Both balanced and unbalanced temporary and permanent faults at different locations in the power network have been considered.

3) Analyzing the effects of cyber-attacks in hybrid grid components and developing method to detect and mitigate the cyber-attack:

The effects of cyber-attacks are analyzed on various components such as the Energy Storage System (ESS), the grid side converter (GSC) of the wind generator, the voltage source converter (VSC) of PV system, and the automatic voltage regulator (AVR) of the SG system located in a hybrid power grid system. The two control techniques such as a Non-Linear (NL) controller and a PI controller for mitigating the adverse effects of cyber-attacks on the GSC, VSC and AVR, and a new detection and mitigation technique based on the voltage threshold for the Supercapacitor Energy Storage (SES) have been proposed. To test the effectiveness of the proposed mitigation methods, two types of cyber-attacks such as the Distributed Denial of Service (DDoS) and False Data Injection (FDI) attacks have been considered. Moreover, a voltage index has been used to numerically evaluate the performance of the proposed control and mitigation methods.

D. Originality of the work

The originality and novelty of the work is stated below:

Although a lot of methods have been explored for power quality enhancement of traditional grids, mostly conventional PI and PID control techniques are used for the TSC. However, the existing power grids are being transitioned into the smart grids, so power quality enhancement devices should be equipped with intelligent based controllers. Based on this background, this dissertation proposes non-linear controllers like the ANFIS control based TSC, fuzzy logic controlled TSC, and static non-linear controlled TSC to improve the power quality of the hybrid power grid system.

Moreover, although much work has been done on the effects of communication delay on the power grid systems, little has been done on how to minimize the adverse impacts of time delays on the performance of the hybrid power grid. Two controllers, namely the FLC based method and the Modified Predictor method, are employed to minimize the adverse effects of time delay on the power quality enhancement of a hybrid power grid consisting of synchronous and variable speed wind generators. The reason to choose the FLC is that, it can handle nonlinearity, uncertainty, imprecision, or fluctuation of the input parameters as well as provides an opportunity to introduce expert knowledge in control rules [54] [37] [55] [56]. This type of controller yields good outcomes under changing operating conditions and time-varying signals. The performance of the FLC based method has been compared with that of the Modified Predictor method in minimizing the adverse effects of time delays.

Furthermore, although much work has been done on cyber security issues recently, but no one has explored the cyber security issues related to the power quality of hybrid grid. Thus, this dissertation analyzes the effects of cyber-attacks on various components such as the ESS [57], GSC of the wind generator [58], the VSC of PV system [59], and the AVR of the SG system located in a hybrid power grid system. To eliminate the adverse effects of cyber-attacks and to detect and mitigate the issues on the GSC, VSC and the AVR, two control techniques such as a NL controller and a PI controller and a new detection and mitigation technique based on the voltage threshold for the SES, have been proposed.

E. Organization of this Dissertation

This dissertation is organized as follows:

Chapter I provides the introduction to this dissertation including the overview, objectives, motivation, originality and the organization of the dissertation.

Chapter II presents the literature review on power quality, power quality evaluation, power quality issues, and power quality improvement methods.

Chapter III discusses the power quality issues due to balanced and unbalanced, temporary and permanent faults in the hybrid power network. This chapter also proposes different non-linear controllers like the ANFIS-control based TSC, the static non-linear controlled TSC, and the Fuzzy Logic control based TSC. At first the performance of the FLC based TSC was compared with that of the conventional PID controlled TSC. Later, the effectiveness of the ANFIS controlled TSC and static Non-Linear controlled TSC was compared with that of the fuzzy controlled TSC.

Chapter IV presents the adverse effects of time delay in a hybrid grid and proposes two methods, namely the FLC based method and the Modified Predictor method, to minimize the adverse effects of time delay on the power quality enhancement of a hybrid power grid.

Chapter V analyses the effects of different cyber-attacks in hybrid grid components and proposes two control techniques such as a NL controller and a PI controller for mitigating the adverse effects of cyber-attacks on the GSC and VSC, and a new detection and mitigation technique based on the voltage threshold for the SES.

Chapter VI provides the conclusion to this dissertation and shows possible future work.

II. LITERATURE REVIEW

A. Introduction

With the introduction and widespread use of sensitive electronic equipment, energy users have become much more aware and sensitive to transients and other power anomalies. Previously, equipment was immune to short-term power fluctuations and did not project problems back into the utility's system. Now, with the introduction of nonlinear devices, harmonics are created which can affect the customer's equipment and the utility's equipment. The utility is no longer just providing power to turn lights on and start motors. As a result, there has been an increase of problems experienced by electrical end-users. The characteristics of electricity like frequency, magnitude, waveform, and symmetry are subject to variations during the normal operation in a supply system due to changes of load, disturbances generated by certain equipment and the occurrence of faults which are mainly caused by external events. Sometimes the equipment installed at the premises of an electricity user can inject disturbances (e.g. harmonic or inter-harmonic distortion, voltage fluctuations etc.) into the distribution networks. Variation in voltage & frequency and waveform distortion (in other words harmonics) are the critical power quality issues.

PQ has become an issue for a long time. All over the world utilities have worked on the improvement of power quality for decades [60] [61] [62]. Every year the network operators in different countries around the world receive many complaints about PQ problems from different groups of customers. It is observed that almost 70% of the PQ disturbances are originated at the customer's premises while 30% are in the network side [63]. Over the last many decades, it has been noticed that equipment always introduces harmonic distortion, but recently the amount of load, fed via power electronic converters has increased enormously, causing more harmonic voltage distortion. Each individual device does not generate much harmonic current, but all of them together cause a serious distortion of the supply voltage [64] [65] [66]. Power quality issues have economic impacts on utilities, equipment, supplier and customers. Power quality issues disrupt manufacturing in large industries and hence there is loss of productivity.

B. Types of Power Quality Problems

There are numerous types of power quality issues and problems, each of which might have varying and diverse causes [67] [68].

Voltage Sags: It is the most common power disturbance. Voltage sag is defined as a short duration reduction in rms (root mean square) voltage between 10 and 90 percent of nominal voltage for one-half cycle to one minute. They occur when very large loads start up, or because of a serious momentary overload or fault in the power system. At a typical industrial site, several severe sags per year are not unusual at the service entrance. Costs associated with sags can range widely, from almost nothing to several million dollars per event. The voltage sag example is shown in Fig. 1 [69].

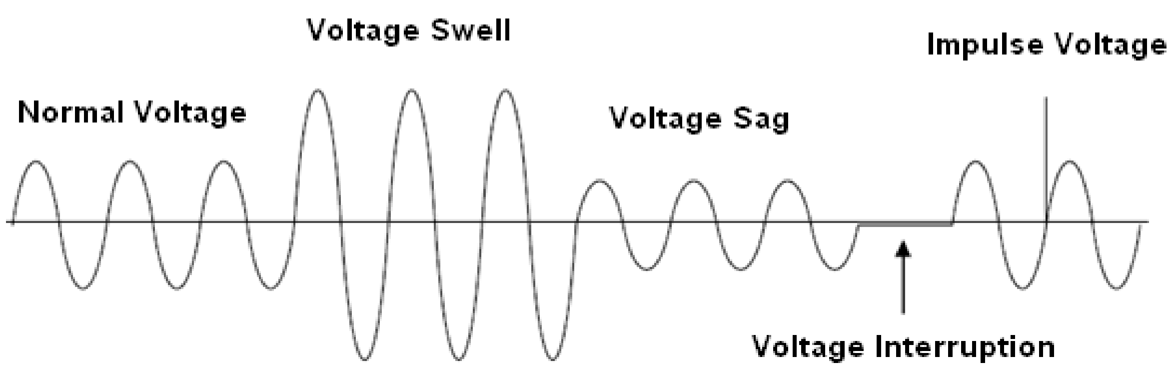

Figure 1. Power Quality Issues: Voltage Swell, Voltage Sag, Voltage Interruption.

Voltage Swell: An increase in voltage between 1.1 and 1.8 pu in rms voltage at the power frequency for durations from 0.5 cycle to 1 min. Swells are characterized by their magnitude and duration. The severity of a voltage swell during a fault condition is a function of the fault location, system impedance, and grounding. Swells can be caused by shutting off loads or switching capacitor banks on. Figure 1 [69] shows an example of voltage swell.

Harmonics: Harmonics are caused by "non-linear" loads, which include motor controls, computers, office equipment, compact fluorescent lamps, light dimmers, televisions and, in general, most electronic loads. High levels of harmonics are not desirable because it increases line losses and decrease equipment lifetime. Harmonics are a recurring distortion of the waveform that can be caused by various devices including variable frequency drives, non-linear power supplies and electronic ballasts [70].An example of a harmonic distortion is shown in Fig. 2 [71].

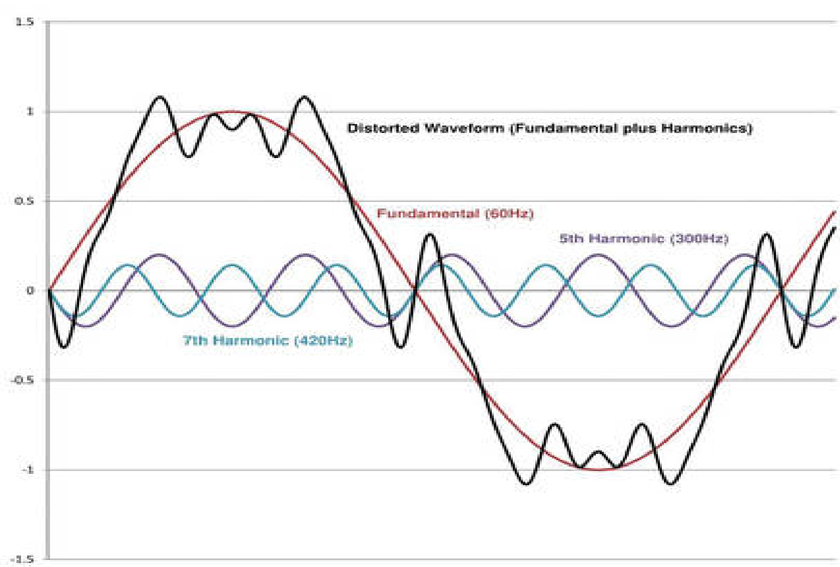

Figure 2. Harmonics

Transient: Transient is that part of the change in a variable that disappears during transition from one steady state operating condition to another. Transients are very short duration events of varying amplitude referred to as surges. Transients can be caused by equipment operation or failure or by weather phenomena like lightning. Electrical components could be damaged by relatively low voltage transients. The effects of transients on a power system depend on the amplitude of the transient and its frequency [1].

Oscillatory transient: It is a sudden, non-power frequency change in the steady-state condition of voltage, current, or both, that includes both positive and negative polarity values. An oscillatory transient consists of a voltage or current whose instantaneous value changes polarity rapidly, as shown in Fig. 3 [1].

Impulsive transient: As shown in Fig. 4 [1], it is a sudden, non–power frequency change in the steady-state condition of voltage, current, or both that is unidirectional in polarity – either primarily positive or negative. It is normally a single, very high impulse like lightning. Impulsive transients are generally described by their rise and decay times.

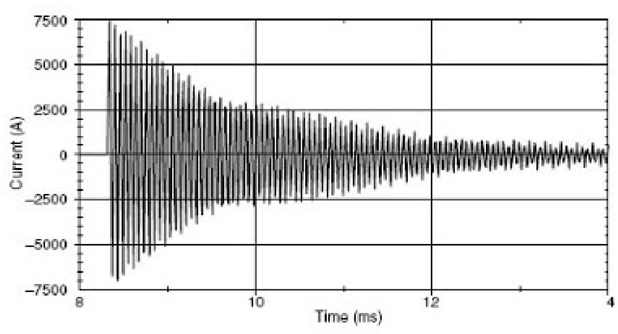

Figure 4. Oscillatory transient.

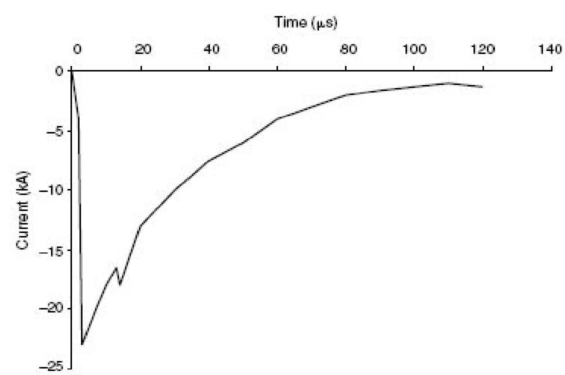

Figure 3. Impulsive transient.

<u>Undervoltage</u>: An undervoltage shown in Fig. 5 [72], is a decrease in the rms ac voltage to less than 90 percent at the power frequency for duration longer than 1 min.

<u>Overvoltage</u>: An overvoltage is an increase in the rms ac voltage greater than 110 percent at the power frequency for duration longer than 1 min. An example of an overvoltage is shown in Fig. 6 [73].

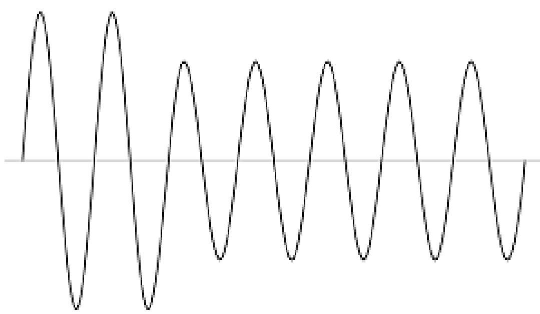

Figure 6. Undervoltage.

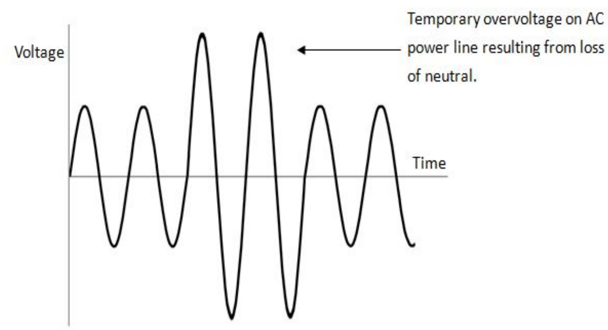

Figure 5. Overvoltage.

<u>Voltage Interruption</u>: When the voltage drops below 10% of its nominal value, it is called an interruption or a blackout. Interruptions have three classifications: momentary (lasting 30 cycles to 3 seconds), temporary (lasting 3 seconds to 1 minute) and sustained (lasting more than 1 minute). Although interruptions are the most severe form of power problem, they are also the least likely to occur. An example of voltage interruption is shown in Fig. 1 [69].

<u>Voltage Imbalance</u>: Voltage imbalance is defined as the maximum deviation from the average of the three-phase voltages, divided by the average of the three-phase voltages, currents, expressed in percent. Figure 7 [74] shows the graph for voltage imbalance.

<u>Voltage Fluctuation</u>: These are systematic variations of the voltage envelope or a series of random voltage changes, the magnitude of which does not normally exceed the voltage ranges of 0.9 to 1.21 pu. It is mainly caused by frequent start/stop of electric motors, arc furnaces, oscillating loads. It leads to under-voltages. Figure 8 [1] shows voltage fluctuation.

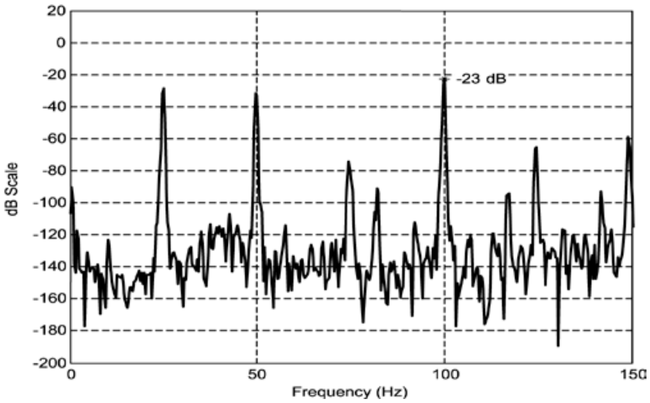

Figure 7. Voltage Fluctuation

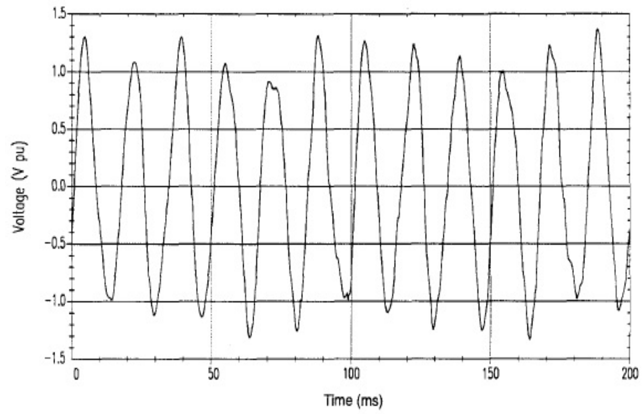

Figure 8: Voltage Imbalance.

Voltage Notching: As shown in Fig. 9 [75], it is a periodic voltage disturbance caused by the normal operation of power electronic devices when current is commutated from one phase to another. During this notching period, there exists a momentary short-circuit between the two commutating phases, reducing the line voltage, the voltage reduction is limited only by the system impedance.

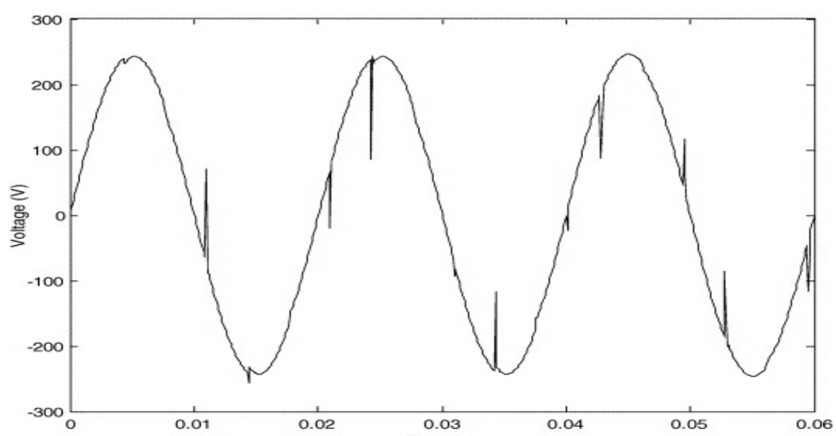

Figure 9. Voltage Notching.

Interharmonics: When the frequency components of voltages and currents are not integer multiples of the frequency at which the supply system operates is defined as interharmonics.

Noise: It is an unwanted electrical signal with broadband spectral content lower than 200 kHz superimposed upon the power system voltage or current in phase conductors, or found on neutral conductors on signal lines. Noise causes data loss and data processing errors. Figure 10 shows the original sinusoidal curve and the curve under influence of noise.

Voltage Spike: The fast variation of the voltage value for durations from a several microseconds to milliseconds. These variations may reach thousands of volts, even in low voltage. It is caused by lightning, switching of lines or power factor correction capacitors, disconnection of heavy loads. Figure 10 shows the curve for voltage spike. Voltage spikes lead to destruction of components and their insulation, data processing errors or data loss, and electromagnetic interference.

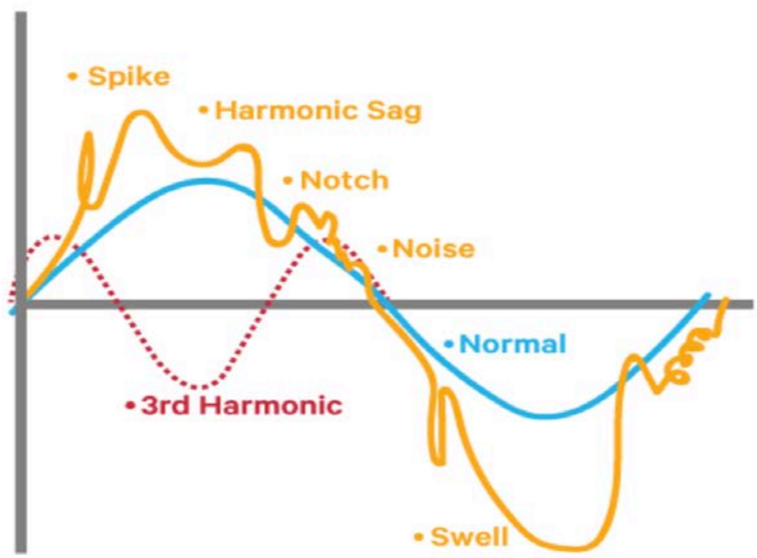

Figure 10. Power Quality Problems.

Due to the above power quality issues, it is necessary to find ways to mitigate those and improve the power quality.

C. Power Quality Evaluation, Standards and Indices

Power quality problems have wide range and different phenomena can occur due to them. Although the occurrence of power quality issues is different and require different mitigation techniques, Fig. 11 provides the basic steps to investigate and finally solve the power quality issue. The steps mentioned in Fig. 10 [76] involves interaction between utility system and end users. Each step mentioned in the figure comes with a major consideration that must be addressed at each step [1].

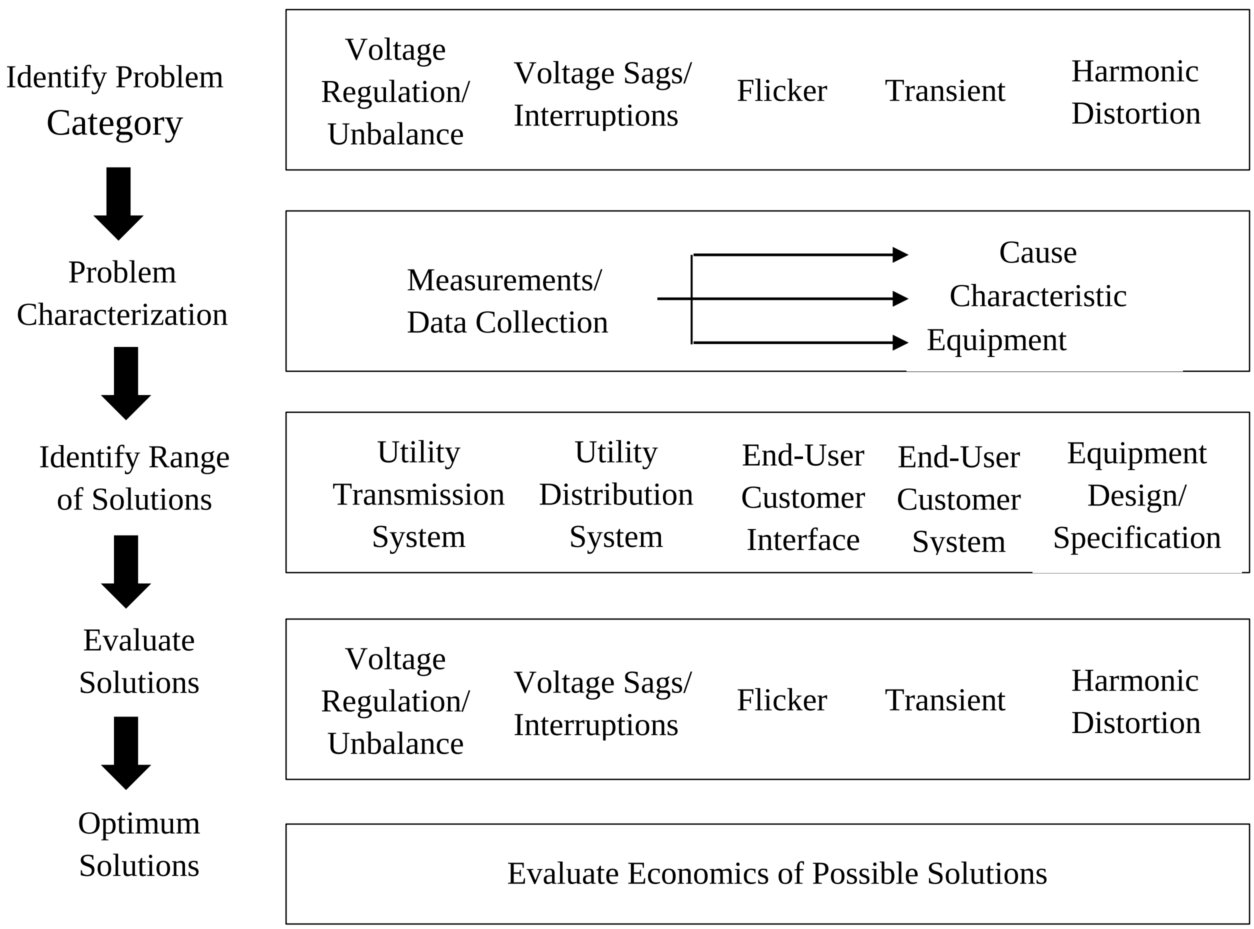

Figure 11. Basic steps involved in Power Quality Evaluation

Some measures have been taken to regulate the minimum PQ level that utilities must provide to consumers and the immunity level that equipment should have to operate properly when the power supplied is within the standards. Standardization organizations like IEC, CENELEC, and IEEE have developed a set of standards with the same purposes. In Europe, the most relevant standards in PQ are the EN 50160 (by CENELEC) and IEC 61000. The IEEE power quality standards do not have such a structured and comprehensive set as compared to IEC [77]. Nonetheless, the IEEE standards give more practical and some theoretical background on the phenomena, which makes it a very useful reference [78].

There are various methods for categorizing the severity of power disturbances. The most used indices for measuring power quality disturbances are listed below.

THD: THD is defined as the measure of the effective value of the harmonic components of a distorted fundamental waveform. In other words, the THD is the summation of all harmonic components of the voltage or current waveform compared against the fundamental component of the voltage or current waveform [79] [80], as shown in (1).

$$THD = \frac{\sqrt{(V_2^2+V_3^2}+V_4^2+\cdots+V_n^2)}{V_1} * 100\% \tag{1}$$

where V_1 is the fundamental voltage, and V_2, V_3… V_n are the higher order harmonic components of the PCC voltage. The higher the THD, the more the distortion on the fundamental signal. The limits of the THD are around 5%.

TDD: Total Demand Distortion (TDD) is the harmonic current distortion against the full load (demand) level of the electrical system.

$$TDD = \sqrt{\frac{(I_2^2 + I_3^2 + I_4^2 + \cdots + I_n^2)}{I_L^2}} * 100\% \tag{2}$$

where I_L is the maximum demand load current, and I_2, I_3… I_n are the higher order harmonic components of the rms value of current.

D. Conventional Solutions for Power Quality Issues

FACTS devices are one of the most well-known and reliable solutions to reduce the power quality issues [81] [82] [83] [84]. Some of the FACTS devices to tackle the power quality issues in transmission and distribution network, reactive power control, improvement of the stability of the grid, control of active and reactive power flows on the grid, loss minimization, and increased grid efficiency, include SVC [85], STATCOM [86], TSC [87], SSSC [88], TCSC [89], UPFC [90], SMES [91]. Other than the above-mentioned FACTS devices, there are several ways to mitigate the power quality issues such as, voltage regulator [92], dynamic voltage restorer [93] [94], line reactor [95], surge suppressors [96], power conditioners [97] [98], isolation transformers [99], uninterrupted power supply [100], proper wiring and grounding, filters [101] [101] [102] [103].

Power quality of the system is also affected by incorporation of renewable energy sources, such as wind and photovoltaic (PV) systems into the existing grid. Lot of works are being done on the construction of energy efficient, reliable, cost effective, sustainable and stable wind energy conversion systems (WECS) [64], [104]. Among renewable energies, wind is one of the most promising one. Due to its rugged structure and low cost of maintenance, induction machines are mostly used as wind generators. But the induction generator has stability problems, especially when integrating with existing power systems, making it a necessity to investigate the power quality of wind power stations with the existing power stations [105] .

Several reports on minimizing the adverse effects of grid disturbances on the doubly fed induction generator (DFIG) based wind farms [106] [39] [107] [108] [109] [110] [111] are available in the literature, and the issues of enhancing the stability of the power networks including both synchronous generators and wind generators by FACTS devices [86] [112]. The integration of renewables into the existing grid require the use of FACTS devices and stabilization power electronic converters, together with fast acting control strategies [113] [114]. New FACTS topologies are emerging to ensure decoupled ac-dc interface, improved voltage security, reactive compensation, voltage and power factor improvement, and loss reduction [113]. They also enhance the security of micro grids, stand-alone ac-dc DG schemes using PV, wind, fuel cell, battery storage, micro gas turbines(MGT), wave/tidal generation CNG/diesel GEN-sets as back-up systems [115] [116] [117] [118].

E. Several Challenges in Power Quality Issues in Modern Power Grid

A modern grid includes a variety of operational and energy measures including smart meters, smart appliances, renewable energy resources, and energy efficient resources. The important features of a modern power grid are reliability, flexibility in network topology, efficiency, load balancing, peak curtailment, sustainability, market-enabling, demand response support, etc. However, with respect to modern power grids, there are 3 major challenges such as nonlinearity, time delay and cyber-attacks, that have serious impact on power quality improvement. These challenges are described in the subsections below.

i. Non-Linear Controllers

When renewable resources, smart meters, etc., are connected or integrated to the existing grid, it is known as the modern grid. The integration of renewables help with the demand response. The ongoing change of energy supply from large, centralized power plants based on nuclear or fossil fuels to smaller, decentralized sources based on renewable energies poses an enormous challenge for design and stable operation of the grid [119]. The structure of the power grid has to be optimized to increase its stability against fluctuations and robustness against failures. However, large-scale failures are consequences of the collective dynamics of the power grid and are often caused by nonlocal mechanisms, one being the non-linearity issue that deteriorates the power quality of the system [120]. As the modern grid consists of various renewables resources, converters, inverters, controllers, switching of the inverters and converters, etc., it adds more nonlinearity to the dynamic nature of the network [121]. However, handling such nonlinearities and stochastic nature of the system is very important [122]. Controller parameters that are optimal for one set of operating conditions might be ineffective for the other sets.

To overcome such challenges, the non-linear dynamics of the power system is considered in the controller design technique [123]. The solution to this non-linear control is the application of different types of non-linear controllers like the exact linearization design method for scalar nonlinear control systems [124], FLCs [125], discrete-time predictive control [126], feedback linearizing control [126], Oscillator-based non-linear controller, bounded integral controller (BIC), ANFIS [127] [128] [129], decentralized nonlinear controller [130] [131], static non-linear control, etc.

FLC tolerates the uncertainty, imprecision, or fluctuation of the input parameters as well as provides an opportunity to introduce expert knowledge in control rules. This type of controller yields good outcomes under changing operating conditions and time-varying input signals. The FLC has been utilized as an efficient tool to stabilize power systems in a wide range of operating conditions and various devices such as power system stabilizer (PSS) and FACTS [34] [132]. One of the powerful tools is the artificial neural network (ANN), which has applications in embedded control systems and information processing

[133]. The ANFIS [134] is an intelligent technique that can be obtained by the combination of Fuzzy Inference System (FIS) and ANN [135] [136]. The imprecision and uncertainty of the system modeling is taken into consideration by the fuzzy logic, while the neural network gives it a sense of adaptability [137] and rapid learning capacity. The ANFIS model has the advantage of having both numerical and linguistic knowledge [138]. The neural network helps in back-propagation to structured network to automate the fuzzy parametric tuning. ANFIS models are also able to explain past data and predict future behaviour.

In this work, to solve the nonlinearity issue, different non-linear controllers are proposed, namely, the ANFIS controlled TSC, static non-linear controlled TSC, and fuzzy controlled TSC. To see the effectiveness of the proposed controllers to improve the power quality of the hybrid grid system, at first the performance of the FLC based TSC was compared with that of the conventional PID controlled TSC. Later, the effectiveness of the ANFIS controlled TSC and static Non-Linear controlled TSC was compared with that of the fuzzy controlled TSC.

ii. Time Delay

In hybrid power grid, the inclusion of the non-linear controllers for wide area power system measurements, power quality enhancement, power system stability, etc., introduces delay in the signals [44]. With the increase in the complexities of the system, new technology PMUs (phasor measurement units) [139] are introduced in the system to measure dynamic data of power system, such as voltage, current, load angle, output power and frequency. All the data measured with the help of PMUs are synchronized by GPS (global positioning system) satellites. The signals, like the voltage response, speed response, rotor angle, etc., are measured and sent to the control center. Since the PMUs are required to send the signals to the control center, they use the existing communication channels [140] thus introducing time delay.

Latency or delay is defined as the time between when the state occurred and when it was acted upon by an application. Each application has its own latency requirements depending upon the kind of system response it is dealing with. Among various delays [141], communication delay also adds to the latency and needs to be minimized. The communication delays on the network are comprised of transmission delays, propagation delays, processing delays, and queuing delays [142]. Each of these delays must be considered to understand the complete behavior of the communication network for a given network [143]. Delay involved between the instant of measurement and that of the signal being available to the controller is typically in the range of microseconds to milliseconds, which depends on the distance, protocol of transmission and several other factors [144]. The system stability and damping performance are affected by the introduction of delay in the system [145] [146] [147] [148]. According to the literature, in wide-area power systems, the time delay can vary from tens to several hundred milliseconds [149]. To maintain the reliability and cost of any electrical system, power quality of the system should be maintained and improved.

In hybrid power grid, communication delays occur at various stages, such as the signal transmission from PMUs to the control centers, from the control centers to the controllers, analog-to-digital (A/D) conversion, online calculation of global input variable, and the time synchronization of signals by GPS. Such delay will affect the controllers and system performance [150]. In wide area control system (WACS) communication networks, data is transmitted in the form of packets. There are several types of time delay [151] like serial delays, which is the amount of delay between two consecutive bits of data sent. Another type of delay is the between packet serial delay which amounts to the time delay between two consecutive packets of data. Routing delay is the time required for data to be sent through a router, and resent to another location. Propagation delays is the time required to transmit data over a communications medium. So, the total time delay can be represented by the following equations:

$$T = T_s + T_b + T_p + T_r \tag{3}$$

$$T_s = \frac{P_s}{D_r} \tag{4}$$

$$T_p = \frac{l}{v} \tag{5}$$

where T_s is the serial delay, T_b is the between packet delay, T_p is the propagation delay, T_r is the routing delay, P_s is the size of the packet (bites/packet), D_r is the data rate of network, l is the length of the communication medium, and v is the velocity at which the data are sent though the communications medium. Table I shows the amount of time delays in communication links [152].

Table I: Delay Values in Various Communication Links

Communication link	Associated delay (ms)
Fiber-optic cables	100-150
Digital microwave links	100-150
Power line (PLC)	150-350
Telephone lines	200-350
Satellite link	500-700

Moreover, methods have been reported to calculate different kinds of time delay [153]. Unlike the small-time delay in local control, in wide-area power systems the time delay can vary from tens to several hundred milliseconds or more [154] [155] [156] [147]. In the Bonneville Power Administration (BPA) system, the latency of fiber optic digital communication has been reported as approximately 38 ms for one way, while latency using modems via microwave is over 80 ms [44]. Communication systems that involve satellites may have even longer delays. The delay of a signal feedback in a wide-area power system is usually considered to be in the order of 100 ms [44]. If routing delay is included, and if many signals are to be routed, there is potential for long delays and variability (uncertainty) in these delays. According to some other reports [157] [158], 150 to 200 milliseconds communication delay values are considered in the design of some actual transient stability control systems. In the past, several studies about the time delay impact on the controlling mechanism and power systems have been performed [159] [160] [161] [162] [153].

Also, some studies have been carried out that minimize the negative effects of time delays on the system performance [151] [163] [164] [165] [166] [167] [168] [169] [170] [171] [172] [173]. All these existing solutions for minimizing time delay effects either consider constant time delays, time varying or random delays. Although much work has been done on the time delay influence and its minimization methods, but the impact of time delay as well as minimization of adverse effects of delay on the improvement of power quality is not well understood.

iii. Cyber-Attacks

The backbone of a modern power system is the cyber or information infrastructure [174], which is primarily used to communicate with different grid components [175]. This network infrastructure uses different communication media, such as serial links, wired cables, wireless or radio/microwave to transmit data and signals to operate, monitor, and control power flow and measurement. In modern power grids [176], for communication between grids and within the grid, different technologies like the substation automation, advance metering infrastructures (AMI), etc., are used. Also, the monitoring and control of the power grid is achieved by SCADA system [177]. All the measurements taken by the PMU are sent to the control center. These communication links are vulnerable and can easily be hacked, making them prone to interruption and susceptible to different types of cyber-attacks [178]. Unauthorized access and the interception of communication channels may inject a false signal to disrupt the SCADA [179]. The cyber-attacks have become sophisticated over the years and successful in targeting the control systems of the power grid [180]. As the controllers of various devices in the hybrid grid are regulated through the SCADA system, there is a high possibility of cyber-attacks on various components of the grid. Consequently, the power quality of the overall grid can be affected.

The following types of cyber-attacks [181] [182] [183] [184] significantly affects the power system.

a) Packet drop attack – Packet drop attack can be triggered at various choke points in the communication path like links, firewalls, proxy servers, encryption device, routers, switches, etc., when a queue within these network points reaches its maximum capacity. These attacks are directed cyber-attacks which can cause packets to drop before reaching the intended destination (e.g. SCADA or field units) and thus help maintain the system stability and security [185].

b) Distributed Denial of Service (DDoS) attacks – These attacks are mainly used for disrupting, blocking or jamming the flow of information through control and communication networks. Recently, there has been an increase in DDoS attacks (with shorter attack duration, but a bigger packet-per-second attack volume) [186] [187] which not only exploit bandwidth but also attack applications that focus on sending bad traffic using those applications' protocols. This type of attack can drastically disrupt the communication in the microgrid cyber infrastructure [188].

c) Bad Data Injection or Tampering Communication data/signal – This type of cyber-attack not only delays signal communication but also pollutes the data in the communication [189]. Such an attack can target a specific type of command and control signal that, for example, activates or deactivates critical field devices for hostile purpose or jams communication. This type of attack can also be considered as false data injection into the system. This data corruption attack can manifest in many ways, one of which is a malware (like Flame), that can make such changes in communication data causing devastating damage to smart grid components including equipment damage, power outage, and misreading of smart meter data [190].

d) Eavesdropping: In Eavesdropping, an attacker may intercept any information communicated by the cyber physical system [191]. In the case of this type of attack, the attacker doesn’t interfere with the working of the cyber physical system, but instead just observes its operation.

(e) Stealthy Deception Attack: In this type of attack, the system components or data is tampered with and the deception could not be detected by the systems detection system [192].

(f) Compromised-Key Attack: A compromised key refers to a secret code obtained by an attacker to interpret secure information [193]. When a compromised key is used, an attacker can secretly gain access to a protected communication, decrypt or alter data, and try to use the compromised key to handle additional compromised keys.

(g) Man-in-the-Middle Attack: In this case, false messages are sent to the operator and can take the form of a false negative or a false positive [194]. This may be the foundation on which the operator takes an action, such as flipping a breaker when it is not required, or it may cause the operator to think everything is fine and not take an action when an action is required.

(h) Jamming Attack: An attacker may jam the wireless channel between sensor nodes and the remote estimator in a cyber-physical system [195].

(i) Replay Attack: Hybrid power systems may be susceptible to replay attacks, especially for smart grid systems whose security protocol that cover the whole system are still not complete [196].

(j) Privacy Leakage on Meters - Utility usage information of the meter broadcast via wireless network can be hacked.

(k)Malware and Software Flaws - Inserting any malware or software, the system can be vulnerable.

(l) *Crash Override Attack*: In this type to attack, the circuit breakers are opened on remote terminal units (RTUs) and create an infinite loop keeping the circuit breakers open even if grid operators attempt to shut down them. This attack results in de-energizing the substations. All the grid operations need to go back on manually.

Although much work has been done on cyber security issues recently, but no one has explored the cyber security issues related to the power quality of hybrid grid. Among the different types of cyber-attacks in power grid, as mentioned in this section, two types, such as the DDoS attack and bad data injection attack, are considered in this work. In a recent study, it is mentioned that the DDoS attacks affect 80% of the electrical enterprises [197] in 14 countries, and thus is one of the most severe attacks [198]. Moreover, the work in [199] states that the Bad data injection is a threatening attack which may cause energy theft of end users, false dispatch on the distribution process, and device breakdown during power generation.

In recent years, many solutions have been proposed to protect and prevent cyber-attacks on smart hybrid grids [200] [201] [57] [202] [203] [204]. Diverse cyber-physical attacks on smart grid and mitigations have been discussed in [205] [206] [207] [208] [209] [210]. A distributed detection method to detect cyber-physical attacks in power networks is reported in [211]. Anomaly Detection and Fault Detection techniques for smart grid are discussed in [212] [213]. In [214], a technique is developed to detect false data injection attacks by observing a subset of measurements and performing calculations based on them to detect malicious data. In this work, to mitigate the adverse effects of cyber-attacks on the hybrid power grid components and to improve the power quality of the system, two controllers such as the Non-Linear controller and PI controller have been proposed.

F. Conclusion

This dissertation focuses on the improvement of the power quality of the hybrid grid system. The literature review focuses on the power quality problems of the conventional grid, power quality evaluation methods and standards, mitigation methods for power quality issues. This chapter also discusses about the challenges in the modern power grid. The literature review shows that power quality study is very important as it has negative impacts on the system performance.

III. POWER QUALITY IMPROVEMENT BY NON-LINEAR CONTROLLER BASED THYRISTOR SWITCHED CAPACITOR

A. Introduction

This chapter involves designing of non-linear controllers such as the Fuzzy logic controlled TSC, ANFIS-control based TSC and static non-linear controlled TSC, to improve the power quality of a hybrid power system, which consists of wind and synchronous generators. Firstly, the performance of the fuzzy control based TSC methods is compared with that of the conventional PID controlled TSC. Next, the other two proposed non-linear controlled TSC are compared with the fuzzy controlled TSC. The simulations have been performed in the MATLAB/Simulink environment. In order to demonstrate the effectiveness of the proposed control methods, the balanced (3LG) and unbalanced (two-line-to ground [2LG], two-line-to-line [2LS], 1LG), temporary and permanent faults in the power network have been considered. Moreover, to quantify the results, three indices namely the voltage index associated with the point of common coupling (PCC), voltage index associated with the wind generator terminal voltage, and the voltage index associated with synchronous generators have been used. In addition, the power quality in terms of THD has been evaluated at the PCC for both synchronous generators and the wind generator.

B. Description of Power System

To analyze the power quality, in this dissertation a hybrid power grid consisting of the IEEE nine bus power system [215] and a doubly fed induction machine based variable speed wind generator has been considered, as shown in Fig. 12. The DFIG-based wind generator is connected at the bus 8 through a 20 KV/575 V step-up transformer. As shown in Fig. 12, the system consists of two synchronous generators with capacities 200 MVA and 130 MVA. The capacity of the wind generator is 9 MVA. The system frequency is 50 Hz and 100

MVA. The system also has an infinite bus connected through transformers and double-circuit transmission lines. The transmission line parameters are represented in the form of resistance, reactance and susceptance per phase per lines. The fault points considered are F1, F2 and F3. The automatic voltage regulator (AVR) and governor (GOV) control models for the synchronous generators have been used in this work. Table II shows the synchronous generator parameters.

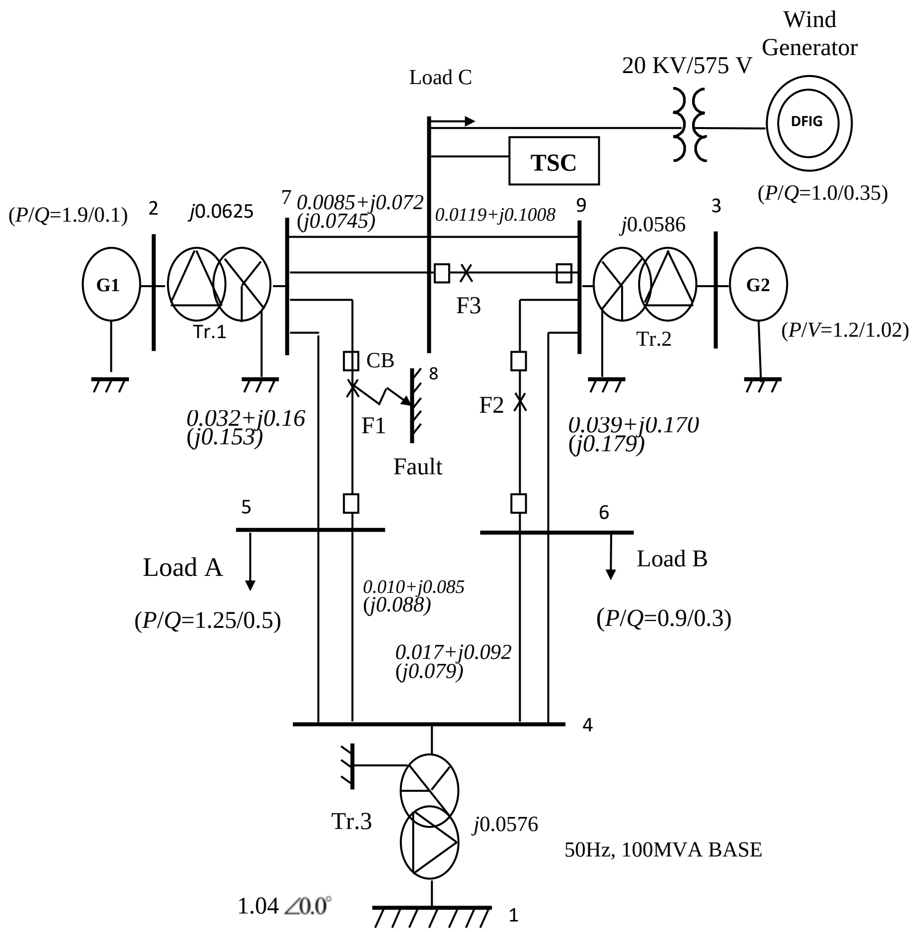

Figure 12. Hybrid System Model.

Table II: Generator Parameters

	G1	G2
MVA	200.000	130.000
r_a (pu)	0.003	0.004
x_a(pu)	0.102	0.078
X_d(pu)	1.651	1.220
X_q(pu)	1.590	1.160
X'_d(pu)	0.232	0.174
X'_q(pu)	0.380	0.250
X''_d(pu)	0.171	0.134
X''_q(pu)	0.171	0.134
T'_{do}(pu)	5.900	8.970
T'_{qo}(pu)	0.535	1.500
T''_{do}(pu)	0.033	0.033
T''_{qo}(pu)	0.078	0.141
H (sec)	9.000	6.000

i. Synchronous Generator

The simplest form of a power system representation is the connection of a synchronous generator to an infinite bus through transmission lines and transformers. Mechanical dynamics of a synchronous generator in a single machine infinite bus system are represented by the following equations:

$$\delta = \omega - \omega_0 \tag{6}$$

$$\omega = -\frac{D}{2H}(\omega - \omega_0) + \frac{\omega_0}{2H}(P_m - P_e) \tag{7}$$

where δ represent the rotor angle of the generator, ω is the running speed of the generator, ω_0 is the synchronous generator which is also the desired speed, H is the inertia constant, P_m is the damping constant of the generator, and P_e is the active electrical power delivered by the generator.

The electrical dynamic of a synchronous generator in a single machine infinite bus system [216] is given by:

$$E_q' = \frac{1}{T_{do}}(E_f - E_q) \tag{8}$$

where E_q' is the quadrature-axis transient voltage, E_q is the quadrature -axis voltage, T_{do} is the direct-axis open-circuit transient time constant, and E_f is the equivalent voltage in the excitation coil of the generator.

Every synchronous generator is equipped with two primary control systems, like the AVR and GOV which are explained below.

1. AVR

The automatic voltage regulator also known as excitation system regulates the field voltage of the synchronous generator. For a large synchronous generator, the exciter may be required to supply field currents [217]. It is also combined with the power system stabilizer to stabilize the voltage of the power grid system. The generator output voltage is compared with a reference voltage and an error is amplified and fed to the field of a special high gain dc generator. The control system block of the AVR is taken from [218] and is shown in Fig. 13, where V_t is the terminal voltage of the synchronous generator, V_{to} is the reference voltage, E_{fdo} is the reference voltage in the excitation coil of the generator, and E_{fd} is the field voltage.

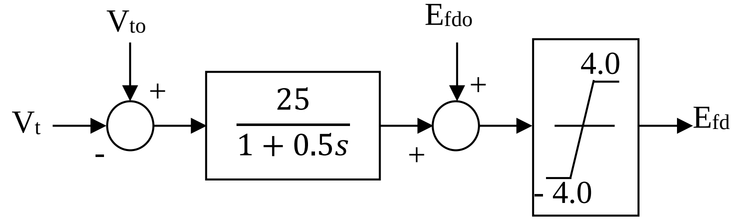

Figure 13: The Control Block of Automatic Voltage Regulator.

2. Governor

The Governor is a device used to control the speed of a prime mover. A governor protects the prime mover from over-speed and keeps the prime mover speed at or near the desired revolutions per minute [219].A governor regulates the speed of a prime mover by properly varying the flow of energy to or from it. It senses speed deviation from its reference value and appropriately changes control valve position in a steam turbine or gate position in a hydraulic turbine. A speed governor allows the operators to change the governor gain (or equivalently the droop) and change the speed and/or load reference [220]. The control structure of GOV is shown in Fig. 14, where ω_m is the measured rotor speed of the synchronous generator, ω_{mo} is the reference rotor speed, P_o is the reference mechanical power and P_m is the mechanical power.

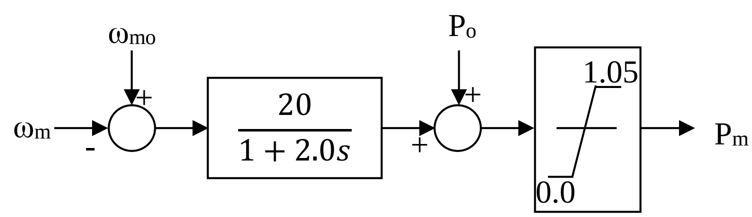

Figure 14 : The Control Block of Governor Model.

ii. Modelling of Wind Generator

For the modelling of wind turbine, a DFIG based wind generator has been used. The controllers used for the wind generator for the grid side converter (GSC) and rotor side converter (RSC) of the DFIG based wind generator are described in [221]. Figure 15 [222] shows the basic diagram of a wind generator. As per the blade element theory [223], the modeling of wind turbine rotor, blade and shaft needs complicated and lengthy computations, and requires detailed and accurate information about rotor geometry. Therefore, a simple approach of modeling the wind turbine blade and shaft is used considering only the electrical characteristics of the power system. Table III shows the wind generator parameters. The power extracted from the wind can be expressed as follows [223]:

$$P_w = \frac{1}{2}\rho * \pi * R^2 * V_w{}^3 * C_p(\lambda, \beta) \quad (9)$$

where P_ω is the extracted power from the wind, ρ is the air density [kg/m^3], R is the blade radius [m], V_w is the wind velocity [m/s], and C_p is the power coefficient which is a function of both tip speed ratio, λ, and blade pitch angle, β [deg].

$$\lambda = \frac{W_r.R}{V_w} \quad (10)$$

where W_r is the rotational speed [rad/s].

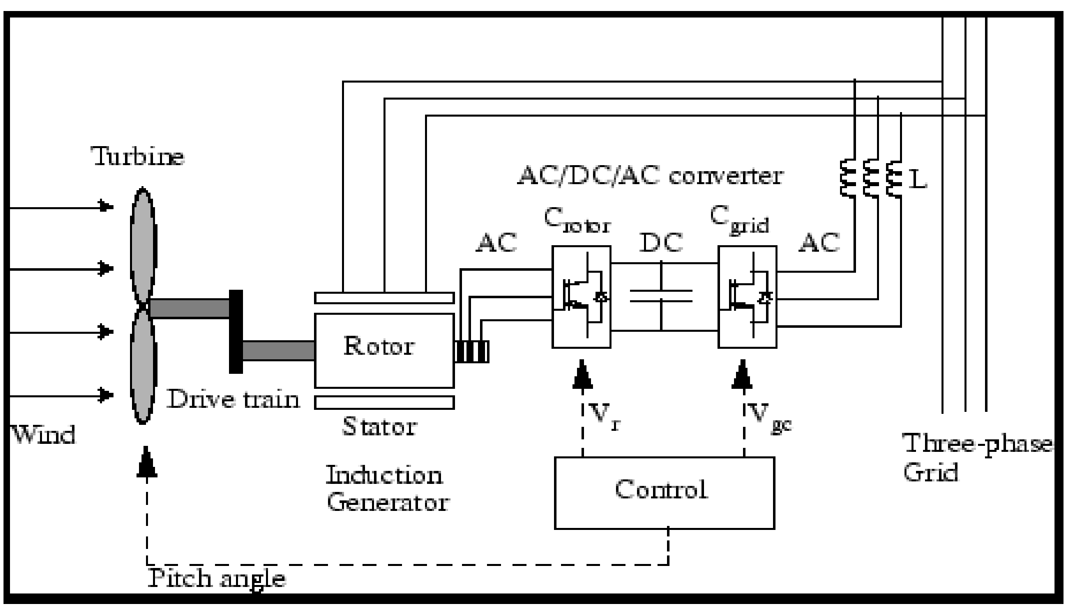

Figure 15. Basic diagram of DFIG with converters.

In this work, the MOD-2 model [223] is considered for the C_p –λ characteristics, which is represented by the following equation (11). Although there are few other equations for the C_p –λ characteristics available in the literature, but this is the most widely accepted one by the wind energy researchers.

$$C_p = \frac{1}{2}(\lambda - 0.022\beta^2 - 5.6)e^{-0.17\lambda} \tag{11}$$

Table III: Wind Generator Parameters

MVA	9
r_1[pu]	0.023
x_1[pu]	0.180
X_{mu}[pu]	30.00
r_2[pu]	0.016
x_2[pu]	0.160
H[sec]	2.000

1. Grid Side Converter (GSC)

The GSC controller of the DFIG based wind generator, shown in Fig. 16, takes the DC link voltage V_{dc} and the rotor line reactive power as inputs to regulate the voltage of the DC link, and generates an independent reactive power that is injected into the grid [224]. The GSC ensures the energy balance on both sides of the dc-link by maintaining the fixed dc-link voltage.

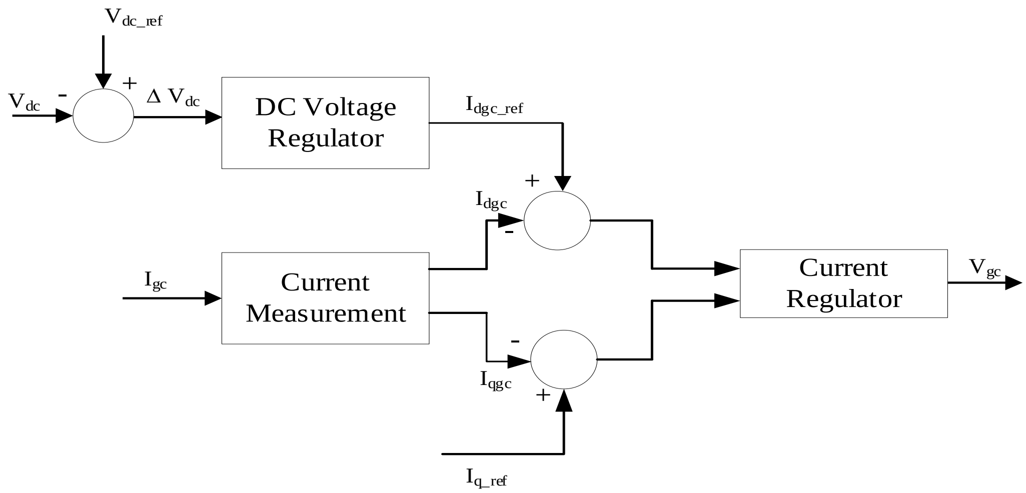

Figure 16. Control block of grid side converter (GSC).

2. Rotor Side Converter (RSC)

Figure 17 represents the structure of rotor side converter. The control of RSC needs the measured rotor current in dq frame to track the reference currents that are generated by the real power and the magnitude of the stator voltage setting, respectively. A current regulator is used to generate the V_r [86].

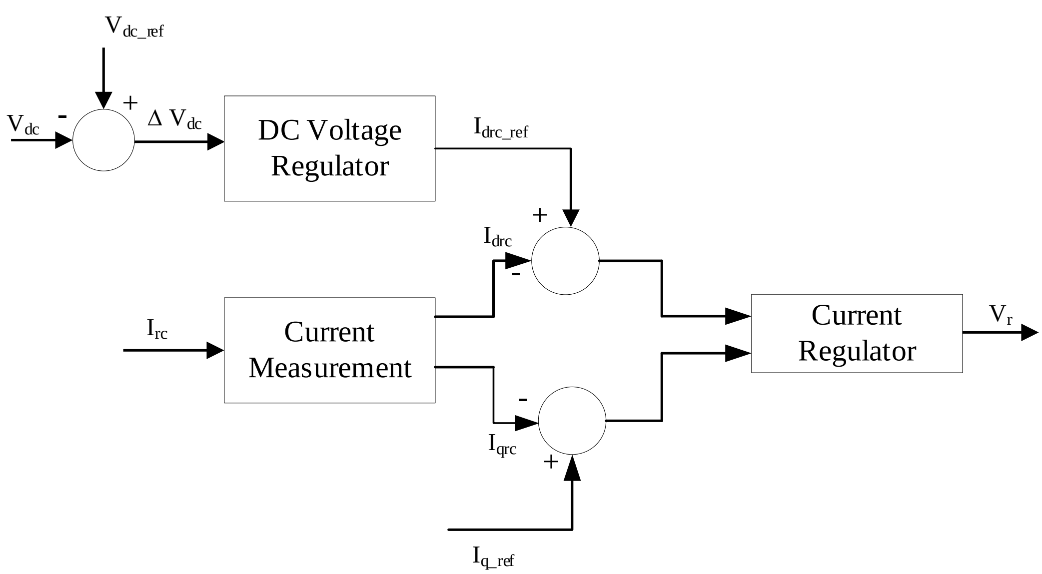

Figure 17. Control block of rotor side converter (RSC).

iii. Reactive Power Compensating Device: TSC

A TSC is a FACTS device used for reactive power compensating in electrical power systems. A TSC normally comprises three main items of equipment: the main capacitor bank, the thyristor valve and a current-limiting reactor, which is usually air-cored. The largest item of equipment in a TSC, the capacitor bank is constructed from rack-mounted outdoor capacitor units, each unit typically having a rating in the range 500 – 1000 kilovars (kVAR). The power capacitor is connected in series with an anti-parallel thyristor [26] [27]. To protect the thyristors, a current limiting inductor (reactor) is used which limits the peak current and the rate of rise of current (di/dt) when the TSC turns on at an incorrect time. In TSC, thyristors are connected in anti-parallel pairs and these pairs are connected in series. The anti-parallel connection of the thyristor makes the flow of current in both directions unlike the commercially available thyristors that can conduct only in one direction.

In this work, the TSC is connected in shunt to the line (shown at bus 8 of Figure 12) as a reactive power compensation device during faults. It consists of capacitors which are usually switched with the help of back to back thyristors as shown in Fig. 19. Thyristors work as a switching device for controlling the switching of the capacitor. Alpha (α) is the switching pulse of the thyristor as shown in Fig. 20. The thyristors are controlled such that the current through the thyristor, I_{TSC} is a function of the firing angle, α. The value of I_{TSC} is obtained using equation (12). The reactive power that would be injected into the system is given by equation (13). Figure 18 shows the graphical representation of the relationship between the TSC reactive power and the firing angle. As the firing angle increases, the delivered reactive power decreases. Therefore, the reactive power diminishes at high firing angles [225]. The thyristors work in full conduction mode when the firing angle, α is 0° and the reactive power is injected into the system and when α is 180◦, the TSC is turned off. The capacity of the capacitor, C, used in this work is 30 MVAR.

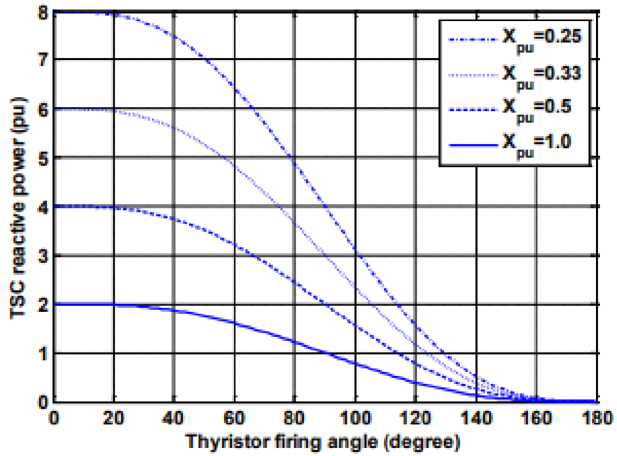

Figure 18. TSC reactive power versus firing angle.

$$I_{TSC} = \frac{2}{\pi}\frac{V_{PCC}}{X_C}[\frac{\sin 2\alpha}{2} + \pi - \alpha] \quad (12)$$

The reactive power is given by,

$$Q = I_{TSC} * V_{PCC} = \frac{2V_{PCC}^2}{\pi X_C}[\frac{\sin 2\alpha}{2} + \pi - \alpha] \quad (13)$$

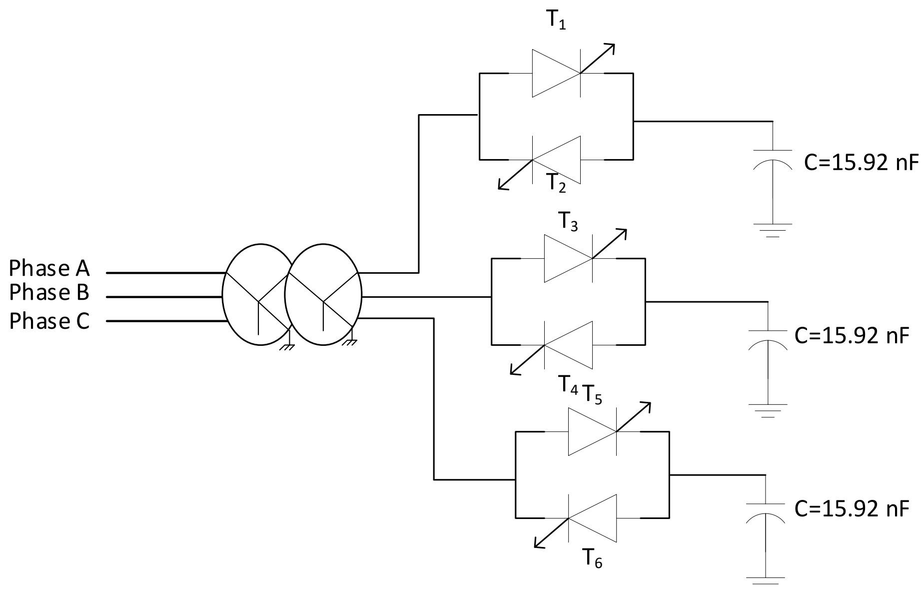

Figure 19. Single line diagram of thyristor switched capacitor (TSC) model.

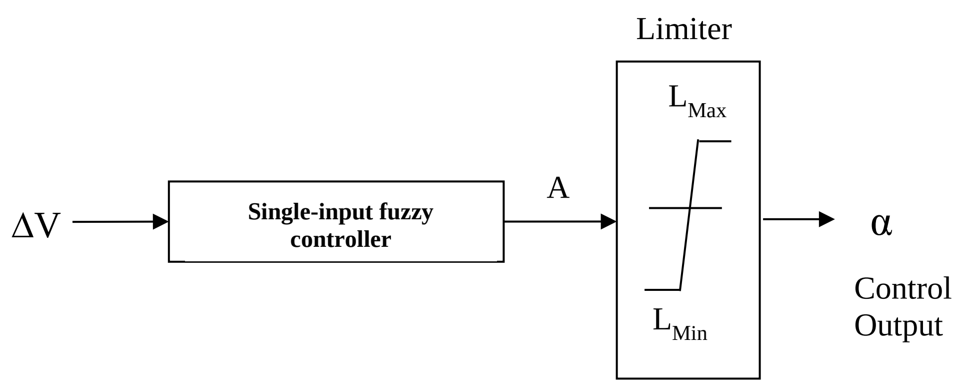

Figure 20. A control block for switching of TSC.

C. Control of TSC

i. Case I:

For case I, the FLC based TSC is proposed for power quality improvement, and the performance of the proposed FLC based TSC is compared with that of the PID controller based TSC.

1. Fuzzy Logic Controller

The proposed fuzzy logic controller design procedure is described below.

a) Fuzzification*:* For the design of the FLC, the total voltage deviation at the PCC and the firing angle of thyristor, are selected as the input and output, respectively. The membership functions for the input and output variables are shown in Fig. 21 and 22, respectively. Through a process of trial and error with various functions, it was found that the triangular membership function leads to better power quality enhancement, thus it is adopted for both input and output variables. In Fig. 21, the symbols are defined as N: negative, Z: zero, and P: positive. In Fig. 22, 1, 2 and 3 are the membership functions of the firing-angle of the thyristors.

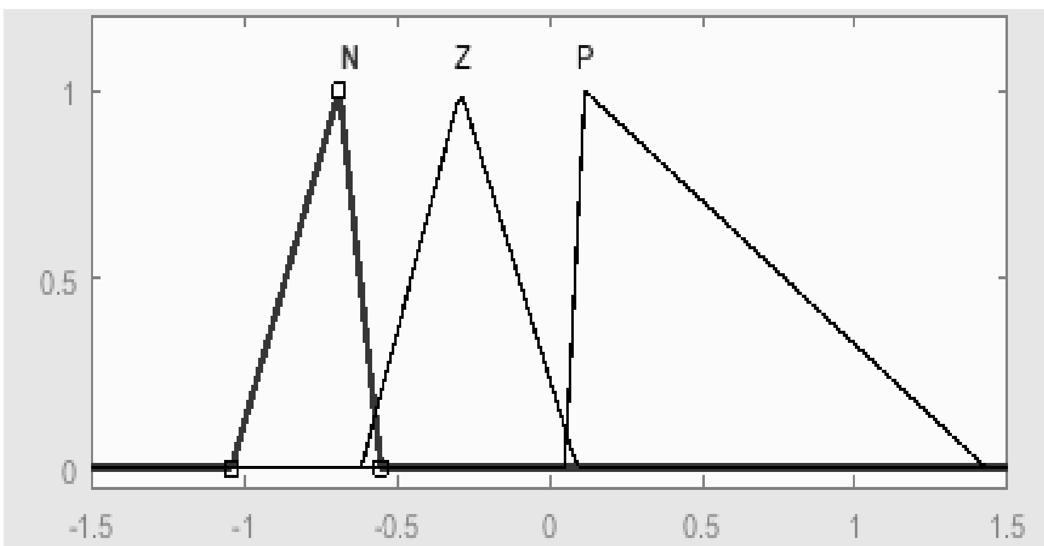

Figure 21. Membership function of TVD (pu).

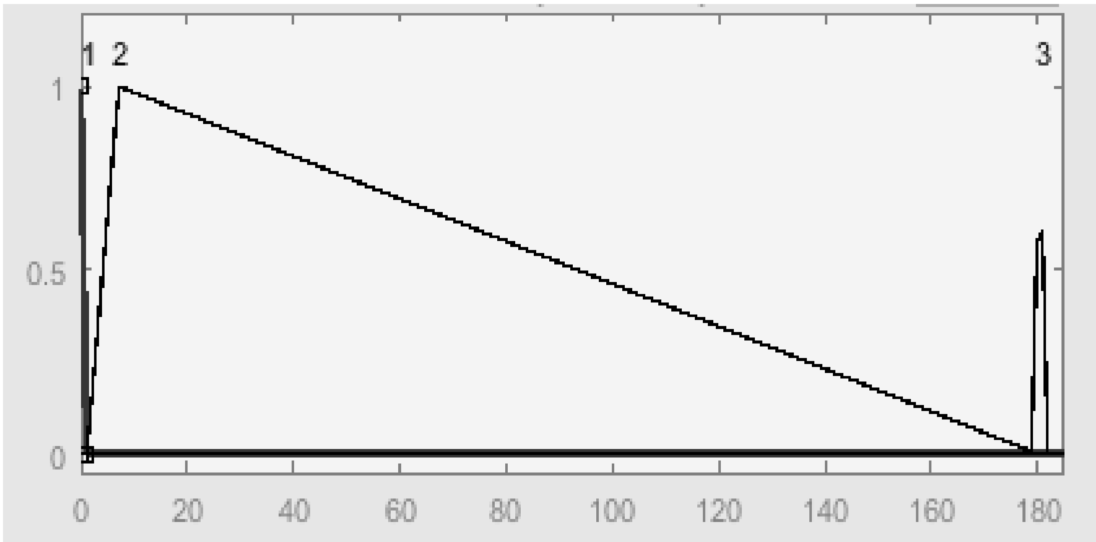

Figure 22. Membership function of firing angle, α (degrees).

The equation of the triangular membership functions used in this work is as follows [226]:

$$\mu_{Ai}(x) = \frac{1}{b}(b - 2\,|\,x - a\,|) \tag{14}$$

where μAi(x) is the value of the grade of membership, “b” is the width, “a” is the coordinate of the point at which the grade of membership is 1, and “x” is the value of the input variable (TVD for this work).

b) Fuzzy Rule Base**:** The proposed fuzzy control strategy is very simple because it has only three control rules. It is important to note that the control rules have been developed from the viewpoint of practical system operation and by trial and error. The rules given in terms of the input variable, TVD, and the output variable, α, are outlined as follows:

- If TVD is P, then the output, α is 0º (1).
- If TVD is N, then the output, α is 100º (2).
- If TVD is Z, then the output, α is 180º (3).

c) Fuzzy Inference: For the inference mechanism of the proposed fuzzy logic controller, Mamdani's method [23] has been utilized. According to Mamdani, the degree of conformity W_i of each fuzzy rule is as follows:

$$W_i = \mu_{Ai}(x) \tag{15}$$

where $\mu_{Ai}(x)$ is the value of grade of membership, and i is the rule number.

d) Defuzzification: The center-of-area method is the most well-known and rather simple defuzzification method [34] [227], which is implemented to determine the output crispy value (i.e., the firing angle of the thyristor, α). Once the input variable is fuzzified and sent to the fuzzy rule base, the output of the rule base is then aggregated and defuzzied. In aggregation, all the output fuzzy sets are added in a logical way, which produces a crisp control signal.

$$\alpha = {\sum W_i C_i} \Big/ {\sum W_i} \tag{16}$$

where Ci is the value of α in the fuzzy rule base.

2. PID Controller

In this work, to see how much effective the proposed fuzzy controlled TSC is, its performance has been compared with that of the PID controlled TSC. The PID control block diagram for the TSC is shown in Fig. 23. The controller takes the TVD at the PCC as an input, and feeds its output to a limiter block. The limiter is used to limit the output of PID controller within the range L_{Min} and L_{Max} as required. The PID controller parameters shown in Table IV are determined by trial and error method for optimizing the best system performance. The control output is the switching pulse of the thyristors shown in Fig. 19.

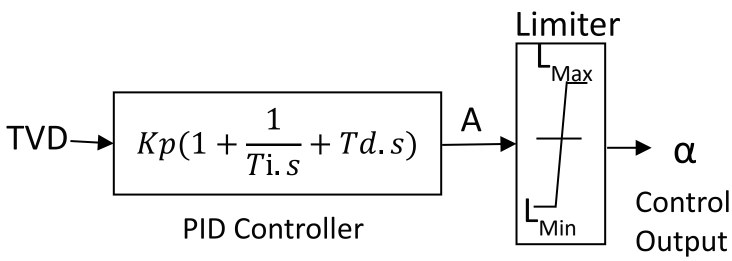

Figure 23. PID Controller.

Table IV: PID Parameters

K_p	T_i	T_d	Limiter	
			L_{max}	L_{min}
100	0.01	10	180	0

3. Simulation Results & Discussion

In this work, both balanced and unbalanced type of permanent faults is considered. It is assumed that the fault occurs at 0.6sec, the circuit breaker opens at 0.7sec, the circuit breaker recloses after 0.7sec and reopens again after 0.1sec of the reclosing instance.

Figures 24-28 show the voltage response at PCC, voltage responses for synchronous generator GI & G2, voltage response of wind generator, and the dc link voltage of the wind generator, due to a 3LG permanent fault at F1 point of Fig. 12. From the responses, it is seen that the fuzzy logic controlled TSC works well to improve the power quality. Also, the performance of the proposed fuzzy controlled TSC is better than that of the PID controlled TSC.

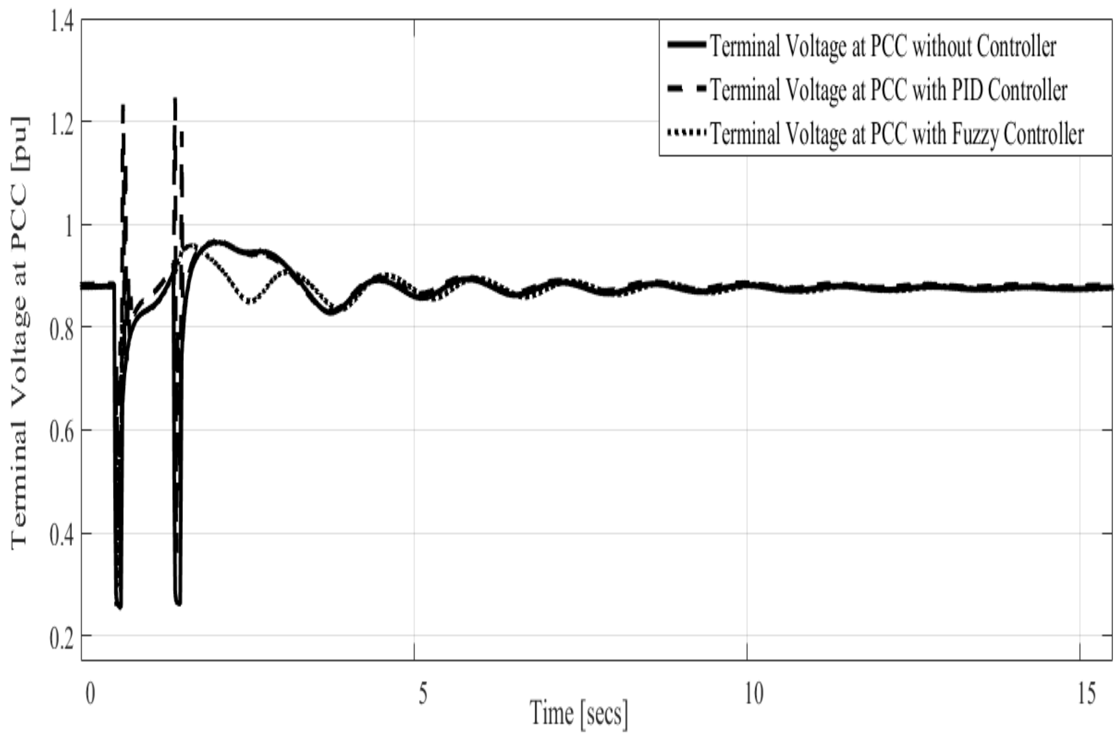

Figure 24. Voltage response at PCC.

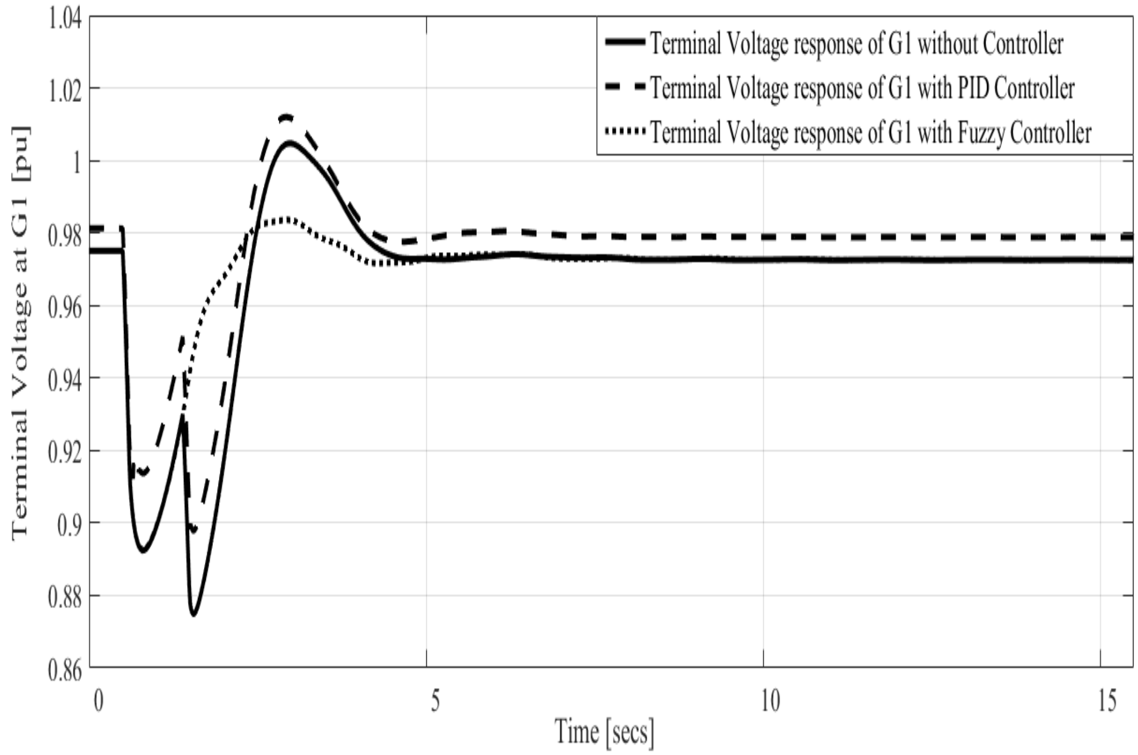

Figure 25. Voltage response of G1 Synchronous Generator.

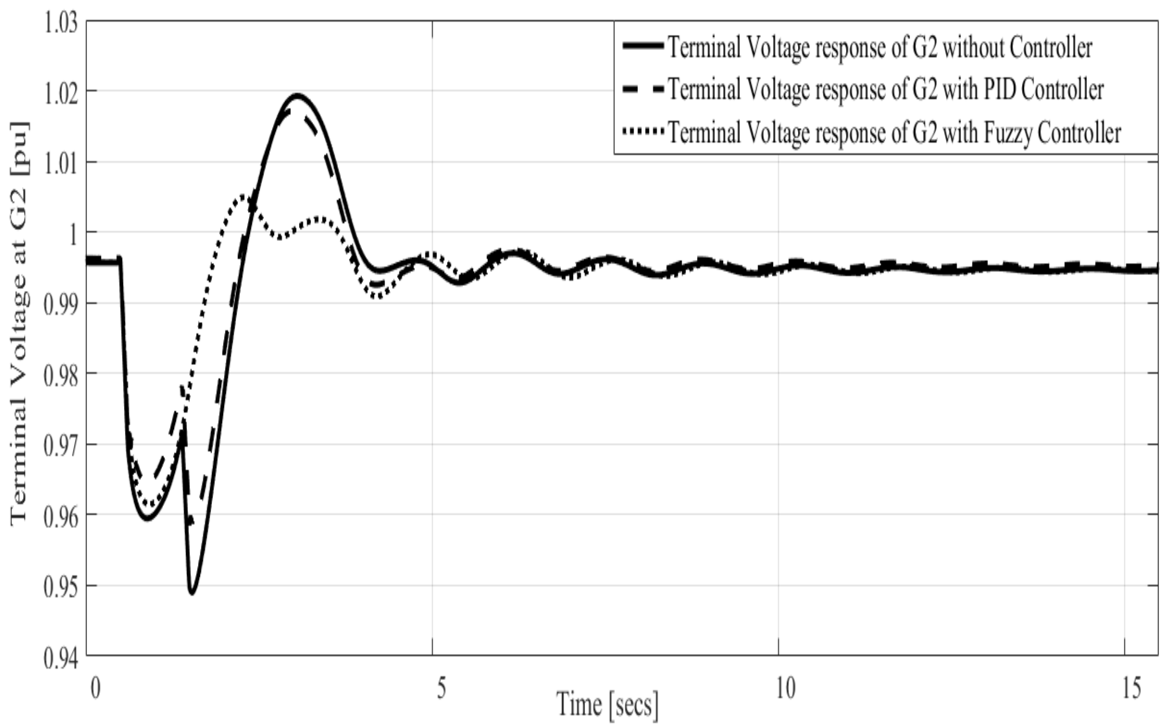

Figure 26. Voltage response of G2 Synchronous Generator.

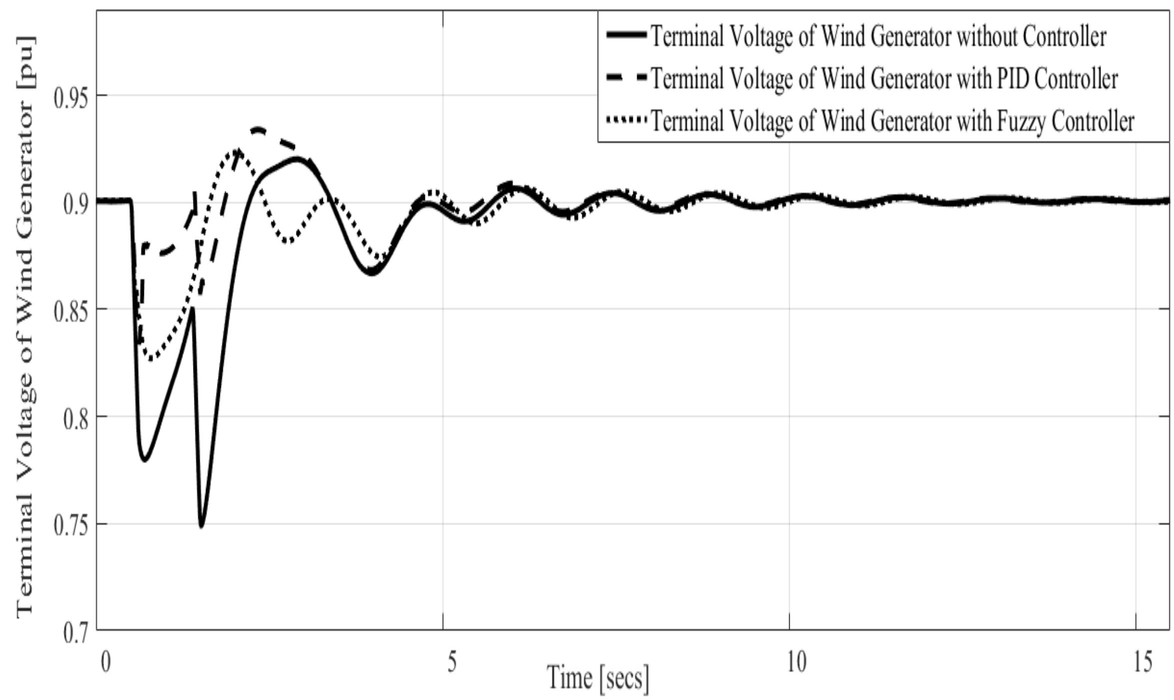

Figure 27. Voltage of Wind Generator.

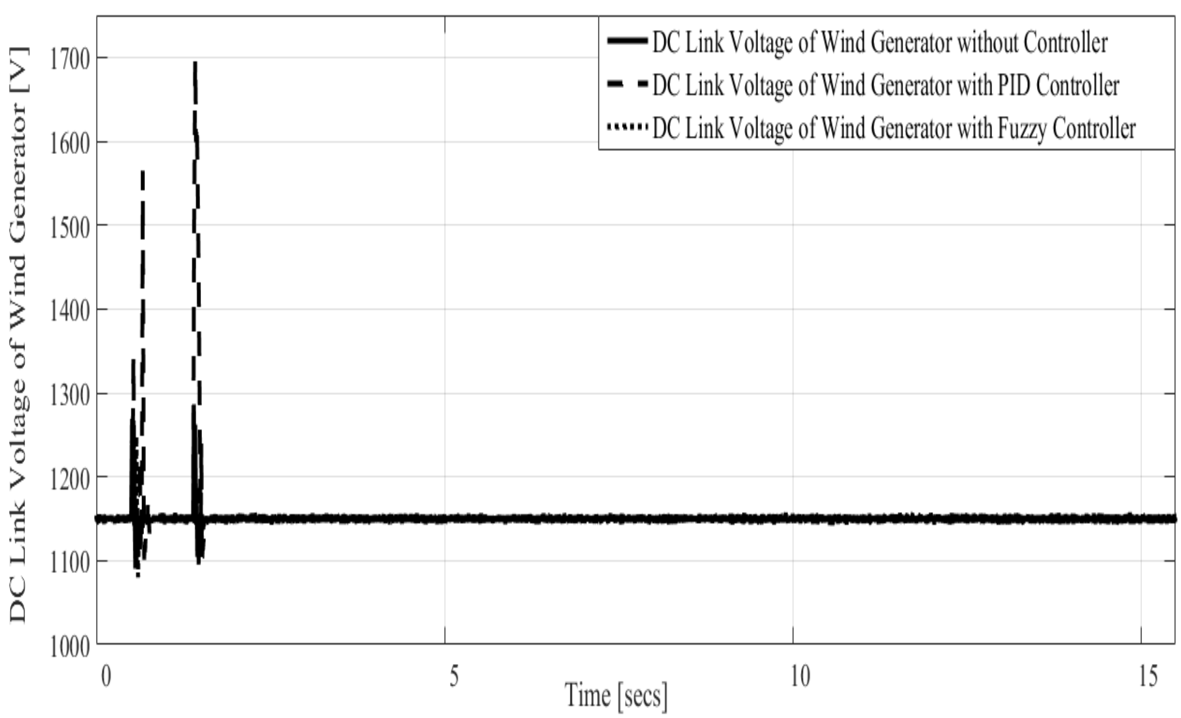

Figure 28. DC link voltage of Wind Generator.

a) Power Quality Analysis in terms of Voltage Index, *Vindex*

To evaluate the effectiveness of the proposed TSC methods in more detail, the voltage index, *Vindex* shown below in (17) is considered.

$$V_{index} = \int_0^T |\Delta V| dt \tag{17}$$

where ΔV indicates the total voltage deviation at the PCC and T is the simulation time of 15 secs. The lower the value of the index, the better the system performance is.

Tables V-VII show the values of voltage indices at PCC, voltage indices of synchronous and wind generators for permanent 3LG faults and 1LG faults at points F1, F2 and F3 of the power system with and without the TSC control method. From the indices it is evident that the fuzzy controlled TSC works better as compared to the PID controlled TSC in improving the power quality.

Table V: Voltage indices for PCC Voltage for permanent faults

Fault Type	Fault Point	Voltage Index PCC		
		Without Control	With PID- TSC	With FLC-TSC
3LG	F1	0.3769	0.2808	0.2469
	F2	0.1774	0.1665	0.1572
	F3	0.6373	0.5016	0.2270
1LG	F1	0.1754	0.1568	0.1502
	F2	0.1036	0.0896	0.0792
	F3	0.6373	0.5016	0.2612

Table VI: Voltage indices for synchronous generator (G1 & G2) permanent faults

Fault Type	Fault Point	Voltage Index G1&G2		
		Without Control	With PID-TSC	With FLC-TSC
3LG	F1	0.2871	0.2682	0.1928
	F2	0.2232	0.1870	0.1560
	F3	0.3290	0.3371	0.3056
1LG	F1	0.1376	0.1440	0.1052
	F2	0.1276	0.0983	0.0122
	F3	0.3290	0.3371	0.0690

Table VII: Voltage indices for wind generator for permanent faults

Fault Type	Fault Point	Voltage Index wind		
		Without Control	With PID-TSC	With FLC-TSC
3LG	F1	0.3269	0.2625	0.2291
	F2	0.1874	0.1706	0.1564
	F3	0.5326	0.4106	0.3124
1LG	F1	0.1602	0.1861	0.1340
	F2	0.0786	0.0704	0.0694
	F3	0.5326	0.4106	0.1883

b) Total Harmonic Distortion (THD) Analysis

THD has been calculated by using the equation (1). Table VIII shows the values of THD for permanent 3LG and 1LG faults at F1, F2 and F3 with fuzzy controlled TSC, PID controlled TSC and without any control method. It is evident from the THD values that the effects of harmonics are reduced when the controllers are used. However, the performance of the proposed fuzzy controlled TSC is better than that of the PID controlled TSC.

Table VIII: Total Harmonic Distortion at PCC for permanent faults

Fault Type	Fault Point	Total Harmonic Distortion at PCC		
		Without Control	With PID-TSC	With FLC-TSC
3LG	F1	4.479	4.059	3.552
	F2	3.295	3.133	1.820
	F3	3.775	3.361	1.058
1LG	F1	5.710	5.547	4.973
	F2	3.295	2.513	1.951
	F3	3.775	3.361	1.707

ii. Case II:

For case II, the proposed two nonlinear controllers such as the ANFIS and static nonlinear controller are explained, and their performance comparison with the fuzzy controller is described.

1. ANFIS Controller

The ANFIS [228] is a simple data learning technique that uses fuzzy logic and ANN to transform given inputs into a desired output through highly interconnected neural network processing elements and information connections, which are weighted to map the numerical inputs into an output. The ANFIS has several features [129] such as: It refines fuzzy IF-THEN rules to describe the behavior of a complex system, it does not require prior human expertise, it is easy to implement and enables fast and accurate learning. It also offers desired data set, greater choice of membership functions to use, strong generalization abilities, and excellent explanation facilities through fuzzy rules.

The algorithms used in this work is the Sugeno-type ANFIS learning and structure. The ANFIS structure is divided into two parts, namely the predecessor and the conclusion part. In fuzzy logic, the two parts are related to each other by rules. For the controller, the Sugeno-type inference system is used, and the rules are given by,

$$\text{If } (x_1 = A_i) \text{ and } (x_2 = B_i) \text{ then } f_i = a_i x_1 + b_i x_2 + c_i \tag{18}$$

where x_1 and x_2 are the inputs to the controller. In this work, x_1 indicates the PCC voltage deviation (ΔV_{PCC}) and x_2 represents the time derivative value of ΔV_{PCC} ($d\Delta V_{PCC}/dt$). Ai and Bi are the fuzzy sets. The output within the fuzzy region is f_i; a_i, b_i and c_i are the controller design parameter rs, i is the number of Membership Functions (MFs) of each input.

Figure 29 shows the five layers architecture of ANFIS in which a circle indicates a fixed node and a square indicates an adaptive node. The structure of ANFIS network is composed of five layers.

Layer 1: This layer consists of inputs variables (ΔV_{PCC} and $d\Delta V_{PCC}/dt$). The membership function used is triangular. The output is developed by sampling the one-dimensional input variable ΔV_{PCC} and $d\Delta V_{PCC}/dt$ uniformly and estimating firing angle (α) for each sampled point.

Layer 2: As shown in Fig. 29, the input layer is multiplied with nodes and the products of the second layer is the input of the third layer, which is the firing strength of a rule [136] [229] [221].

Layer 3: The third layer is known as the rule layer. The nodes in the rule, define the ratio (w_i) of the i^{th} rule's firing strength to the sum of all rules firing strengths. Initial rules are valued after generating the training data. A hybrid leaning algorithm is used to optimize the initial rules by Sugeno-type fuzzy inference system (FIS) [230]. The previous membership functions are found out by the method of back propagation, which is an iterative process. A linear regression analysis is employed for the parameter optimization [231].

Layer 4: This layer (output MF) is called the defuzzication layer. In this layer, the output, i.e., the firing strength and the rule is generated.

Layer 5: The final layer represents the overall structure, which is the summation of all the output from layer 4. The result is then transformed into a crisp output.

In this work, triangular membership functions have been used, where the epochs are 30. The data required for the ANFIS controller is generated from the model with fault in it. After the training is done, the parameters determined are as the following: the nodes in the second layer are 75, linear parameters are 75, nonlinear parameters are 30, training data pairs is 320 and the fuzzy rules are 25.

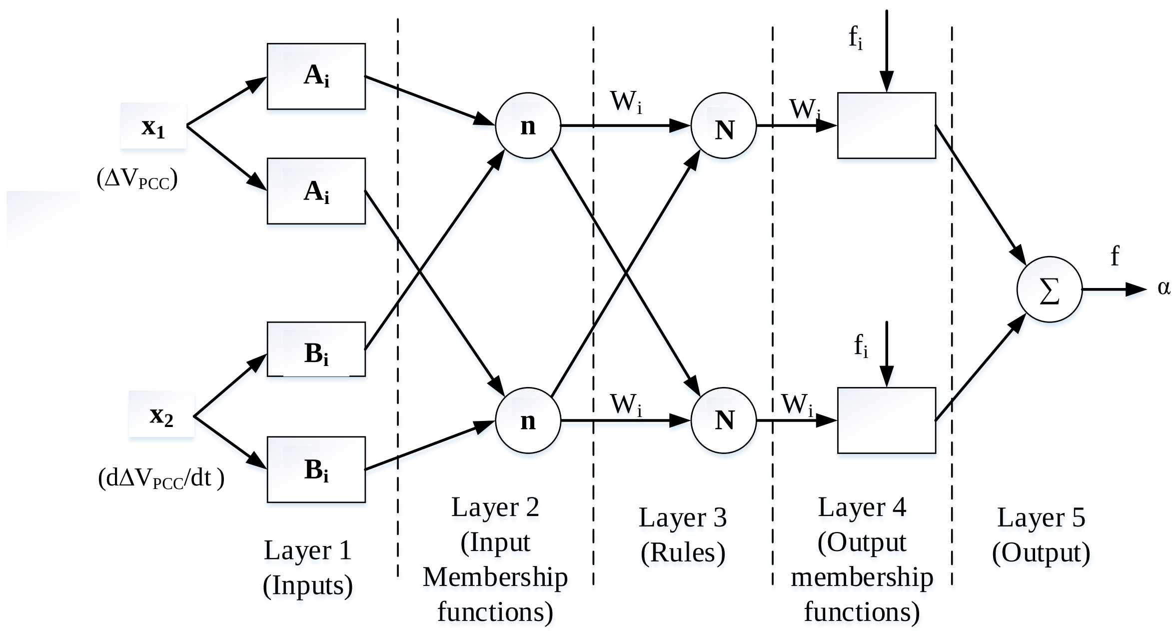

Figure 29. ANFIS Architecture.

2. Static Non-Linear Controller

In this work, a static non-linear controller [232] is implemented for evaluating the performance of the TSC in power quality improvement in more detail. It is noteworthy that, since the integration of the wind generator to a synchronous generator based power network adds nonlinearity, a non-linear controller is incorporated to generate the firing angle of the thyristor. However, for the fault scenarios considered, the performance of the cubic non-linear function is better compared to that of other functions. The equation used for the non-linear controller to generate the firing angle (α) in this work is given by (19),

$$\alpha = K * TVD^3 \tag{19}$$

where TVD indicates the PCC voltage deviation. To make the controller work better and perform well, the parameter K can be tuned. The block diagram of the static non-linear controller is shown in Fig. 30. Through a trial and error approach, K has been set to 0.1 to improve the power quality.

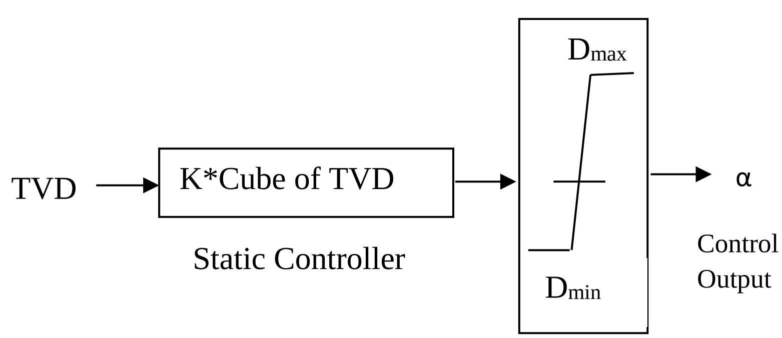

Figure 30. A control block of controller for switching of TSC.

3. Simulation Results & Discussion

In this work, the simulations are executed through the Matlab/Simulink software. Both balanced and unbalanced types of temporary and permanent faults have been considered. It is assumed that the fault occurs at 0.1s, the circuit breaker opens at 0.2s, and the circuit breaker recloses after 0.7sec and reopens again after 0.1sec of the reclosing instance in case of permanent fault.

Figures 31-36 show the voltage responses at PCC, wind generator terminal voltage, and the dc link voltage of the wind generator, due to a 3LG temporary and permanent faults at F3, F2, F1 points in Fig. 12. From the responses, it is seen that the ANFIS controlled TSC and static non-linear controlled TSC work well to improve the power quality. Also, the performance of the proposed controlled TSC is better than that of the fuzzy controlled TSC. The responses also show that the ANFIS controlled TSC performs somewhat better than the static non-linear controlled TSC.

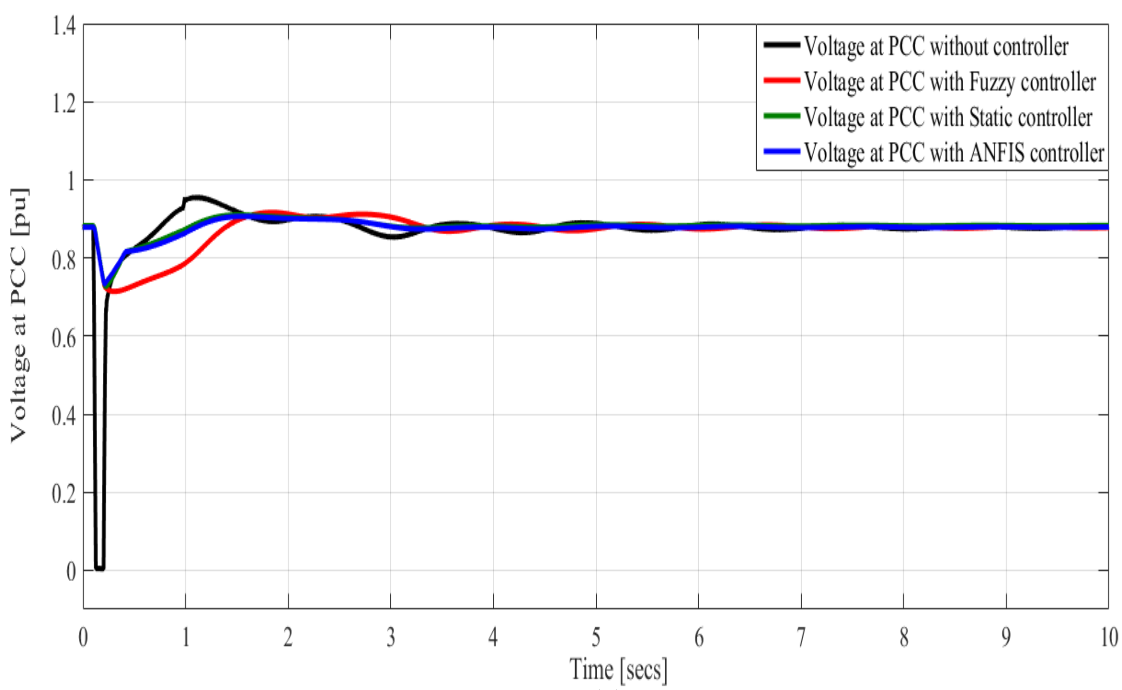

(a)

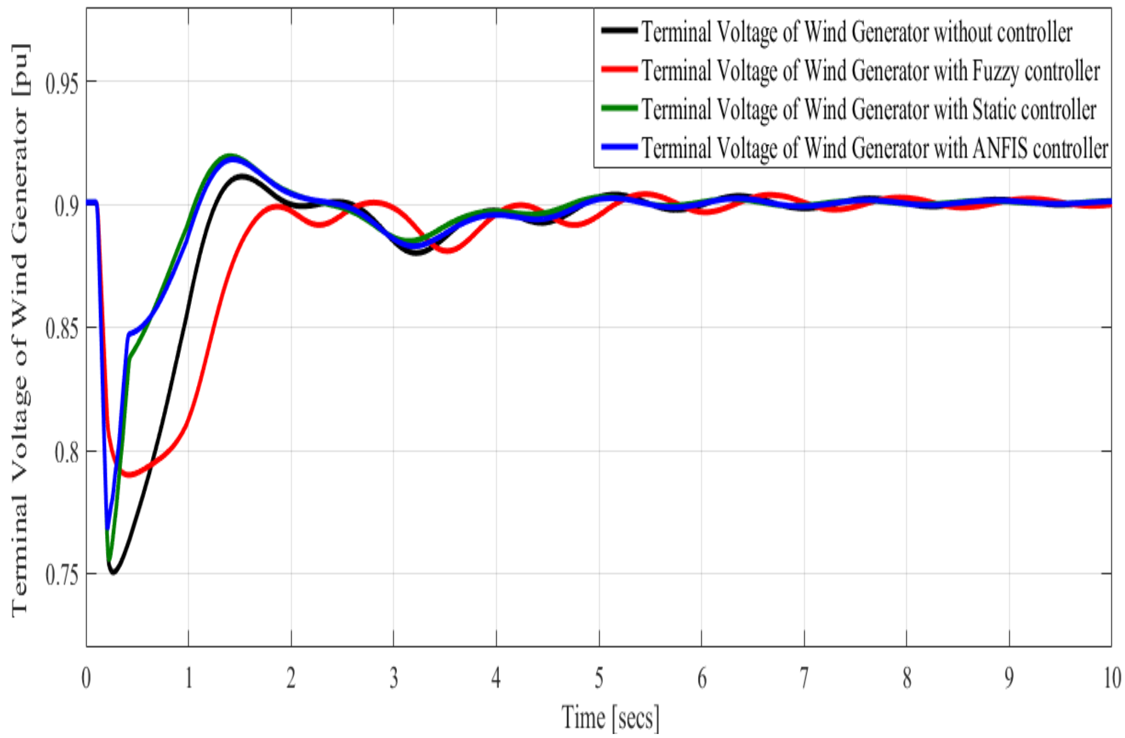

(b)

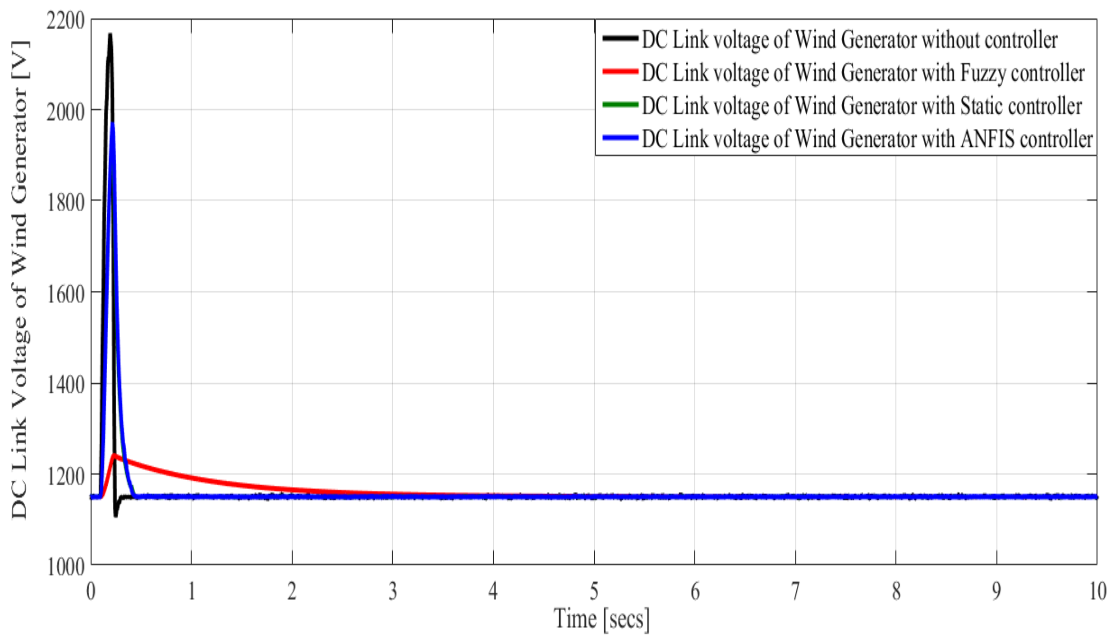

(c)

Figure 31. Voltage responses when the system is subjected to 3LG temporary fault at F3. (a) Voltage at PCC, (b) Terminal voltage of wind generator, (c) DC link voltage of the wind generator.

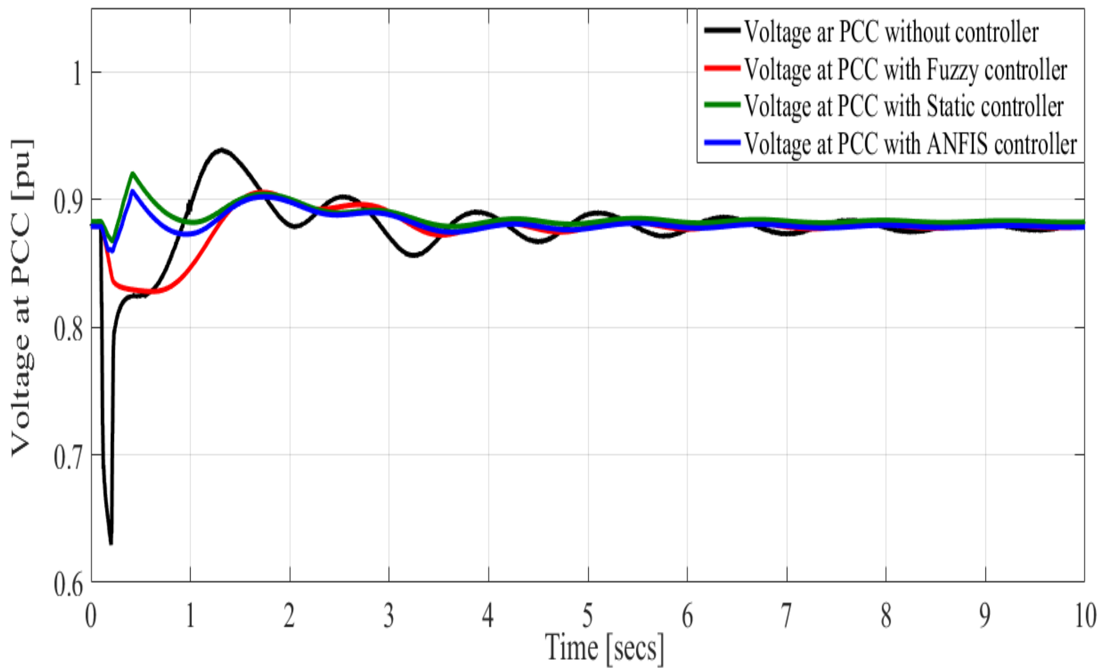
Voltage ar PCC without controller
Voltage at PCC with Fuzzy controller
Voltage at PCC with Static controller
Voltage at PCC with ANFIS controller
Voltage at PCC [pu]
Time [secs]
1
0.9
0.8
0.7
0.6
0
1
2
3
4
5
6
7
8
9
10

(a)

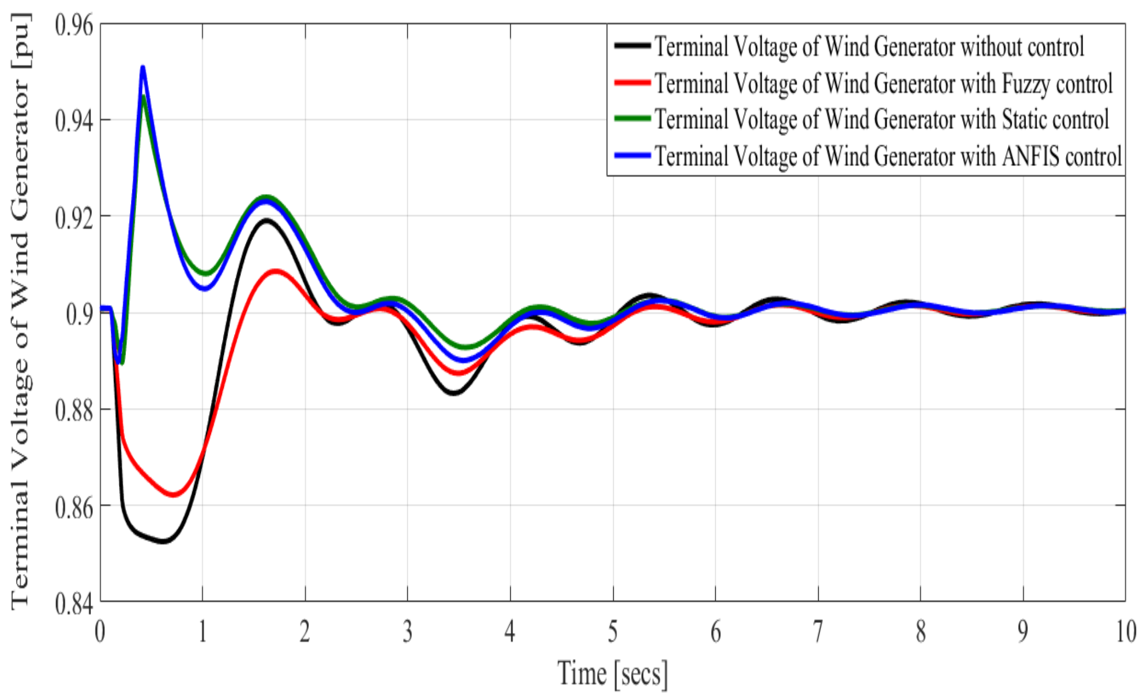
Terminal Voltage of Wind Generator without control
Terminal Voltage of Wind Generator with Fuzzy control
Terminal Voltage of Wind Generator with Static control
Terminal Voltage of Wind Generator with ANFIS control
Terminal Voltage of Wind Generator [pu]
Time [secs]
0.96
0.94
0.92
0.9
0.88
0.86
0.84
0
1
2
3
4
5
6
7
8
9
10

(b)

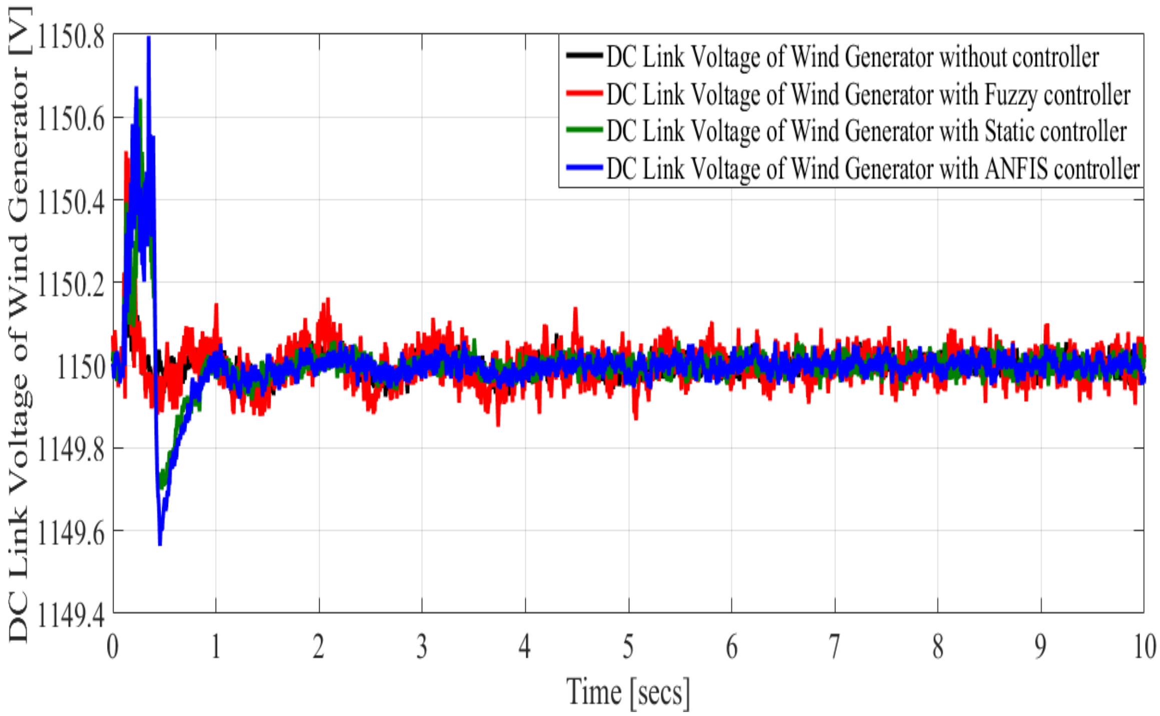

(c)

Figure 32. Voltage responses when the system is subjected to 3LG temporary fault at F2. (a) Voltage at PCC, (b) Terminal voltage of wind generator, (c) DC link voltage of the wind generator.

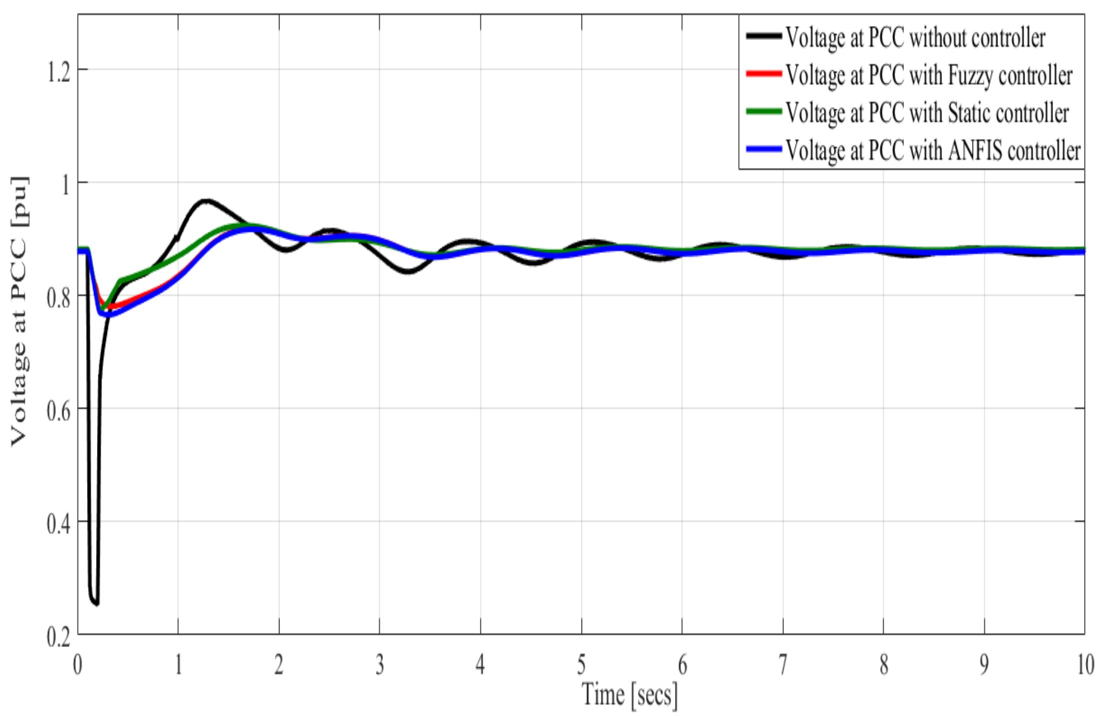

(a)

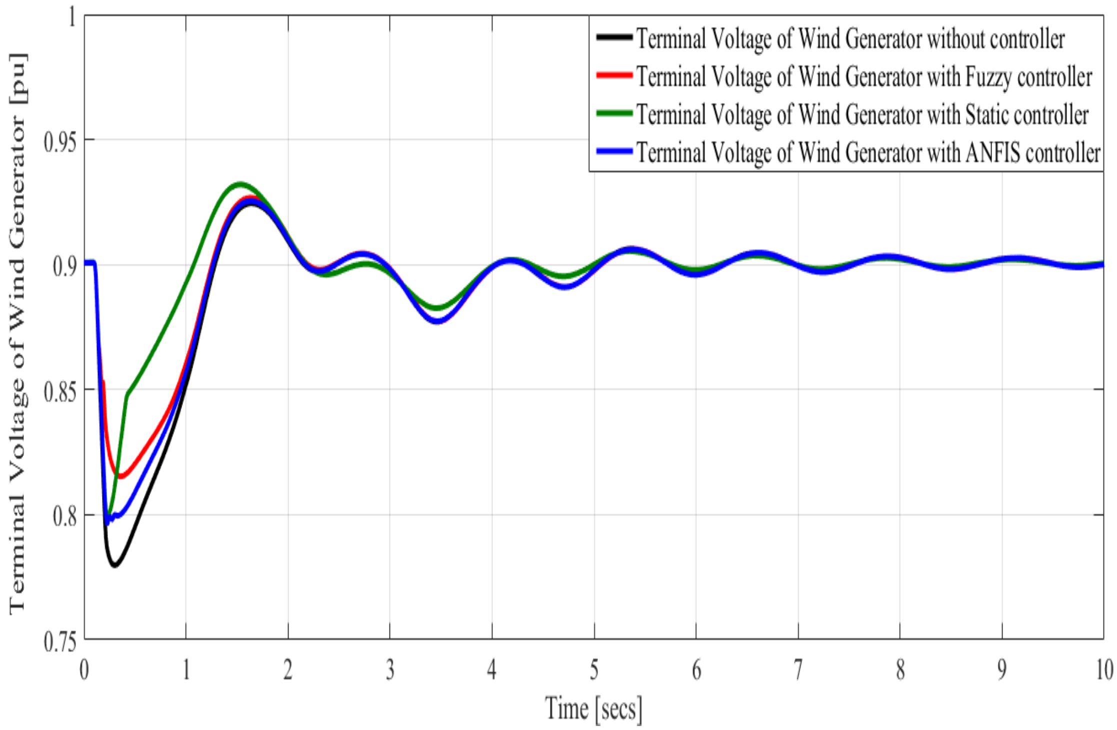

(b)

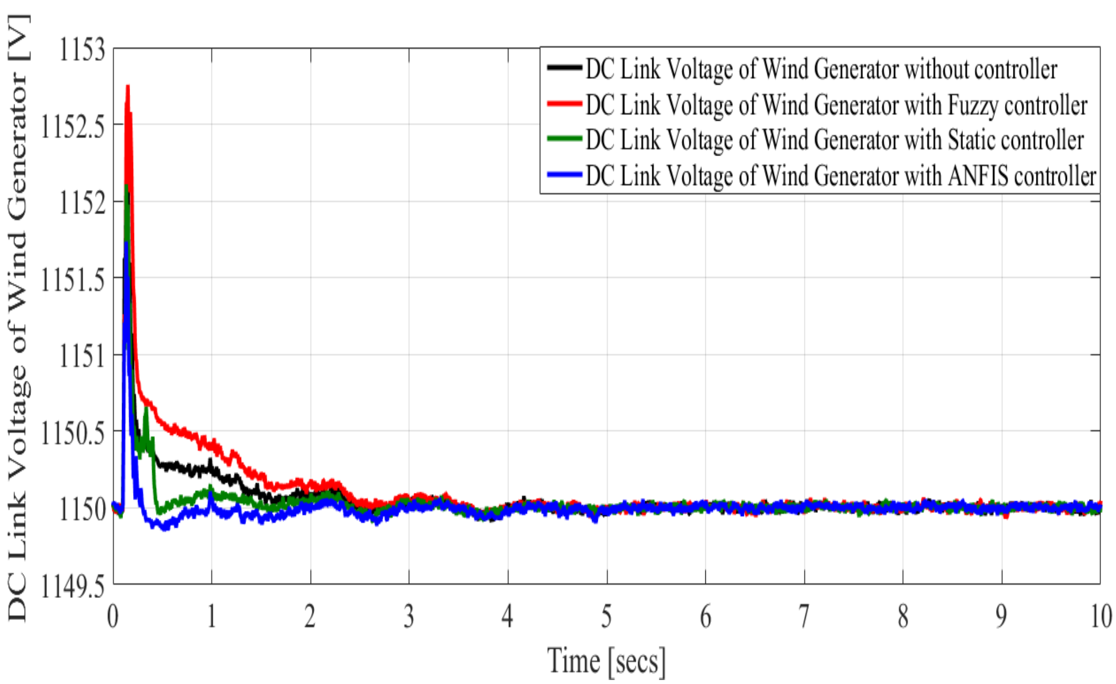

(c)

Figure 33. Voltage responses when the system is subjected to 3LG temporary fault at F1. (a) Voltage at PCC, (b) Terminal voltage of wind generator, (c) DC link voltage of the wind generator.

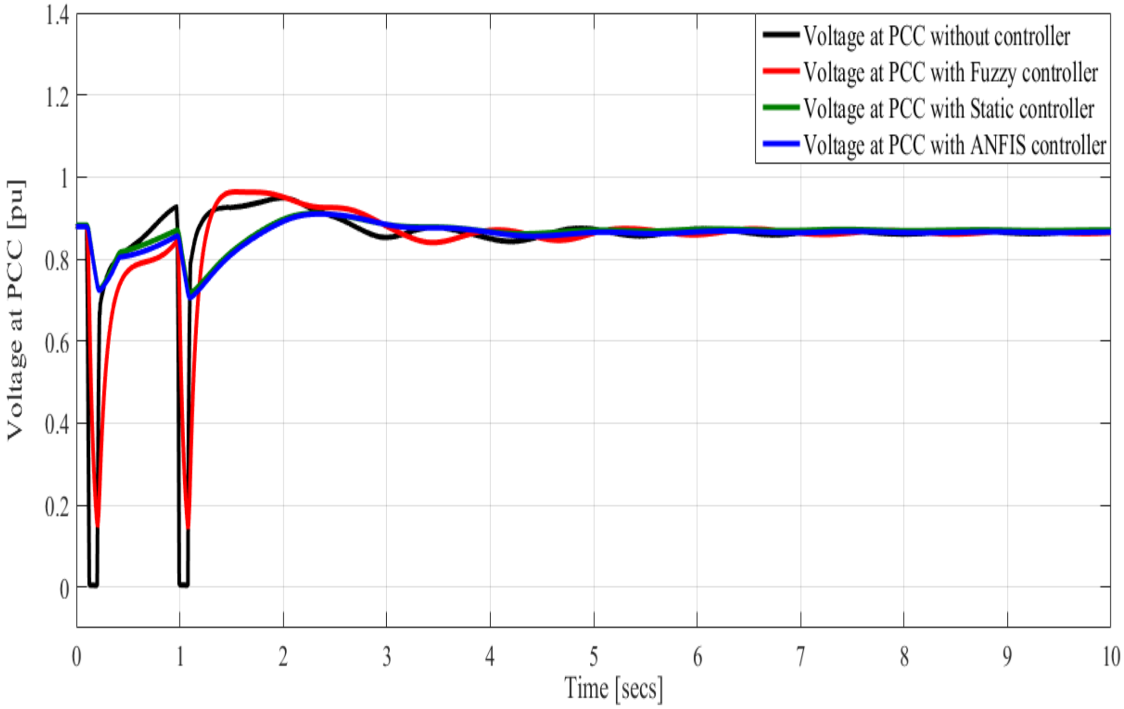

Voltage at PCC without controller
Voltage at PCC with Fuzzy controller
Voltage at PCC with Static controller
Voltage at PCC with ANFIS controller
Voltage at PCC [pu]
Time [secs]

(a)

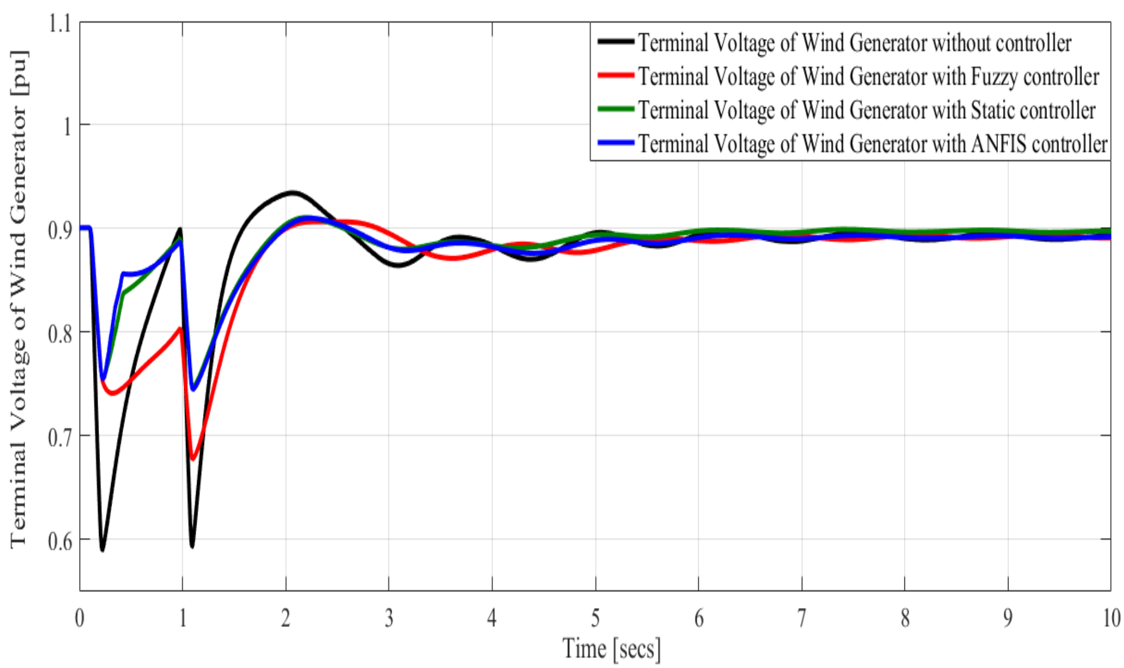

Terminal Voltage of Wind Generator without controller
Terminal Voltage of Wind Generator with Fuzzy controller
Terminal Voltage of Wind Generator with Static controller
Terminal Voltage of Wind Generator with ANFIS controller
Terminal Voltage of Wind Generator [pu]
Time [secs]

(b)

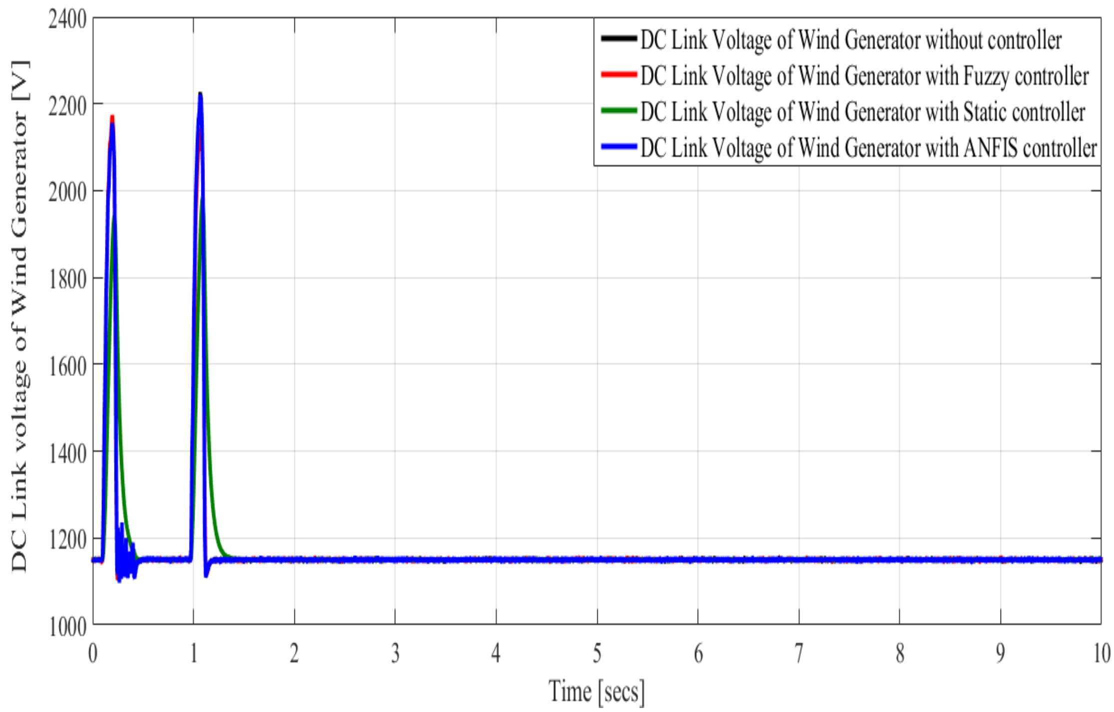

(c)

Figure 34. Voltage responses when the system is subjected to 3LG permanent fault at F3. (a) Voltage at PCC, (b) Terminal voltage of wind generator, (c) DC link voltage of the wind generator.

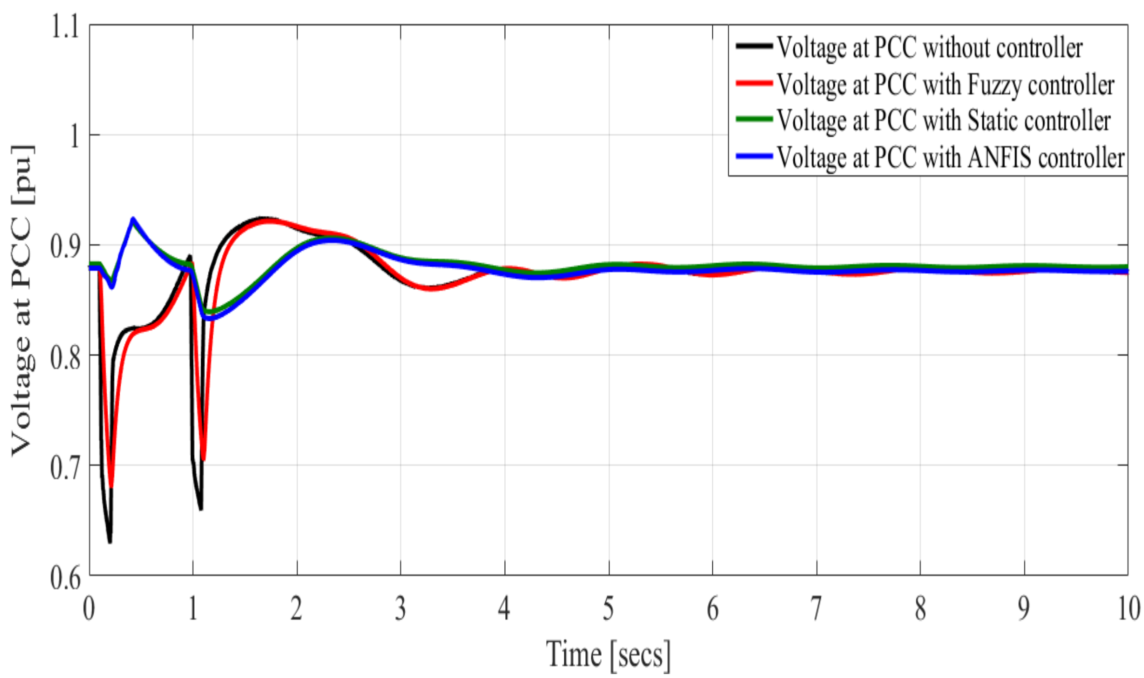

(a)

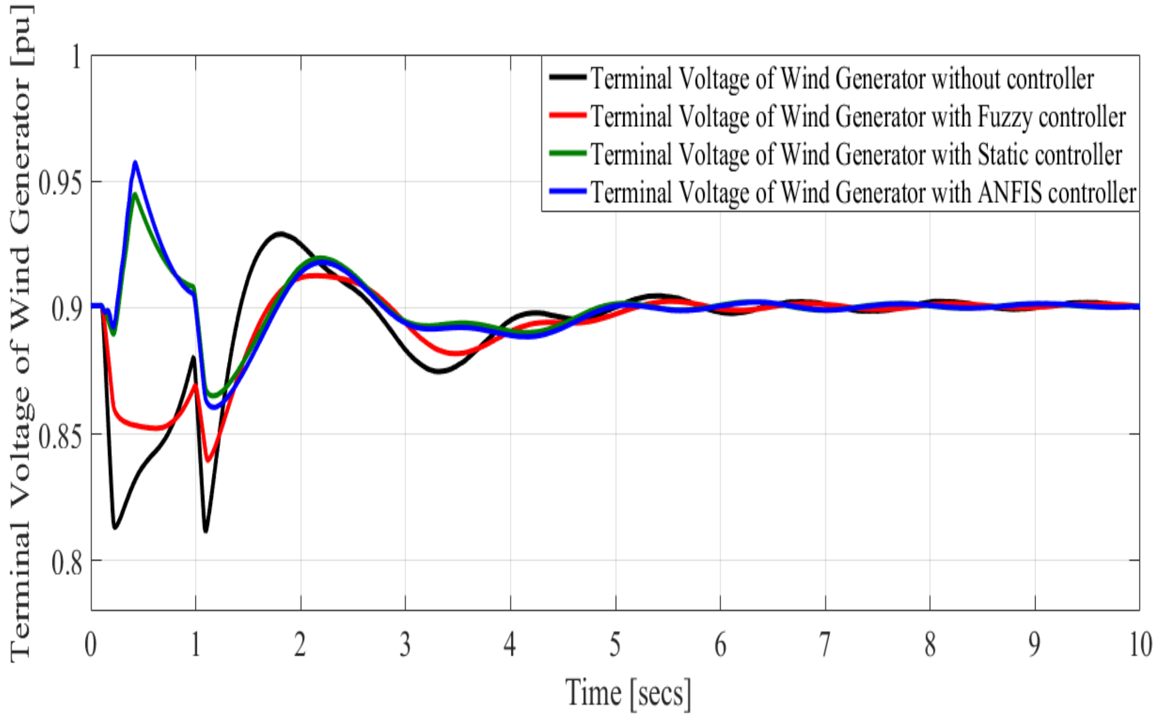

(b)

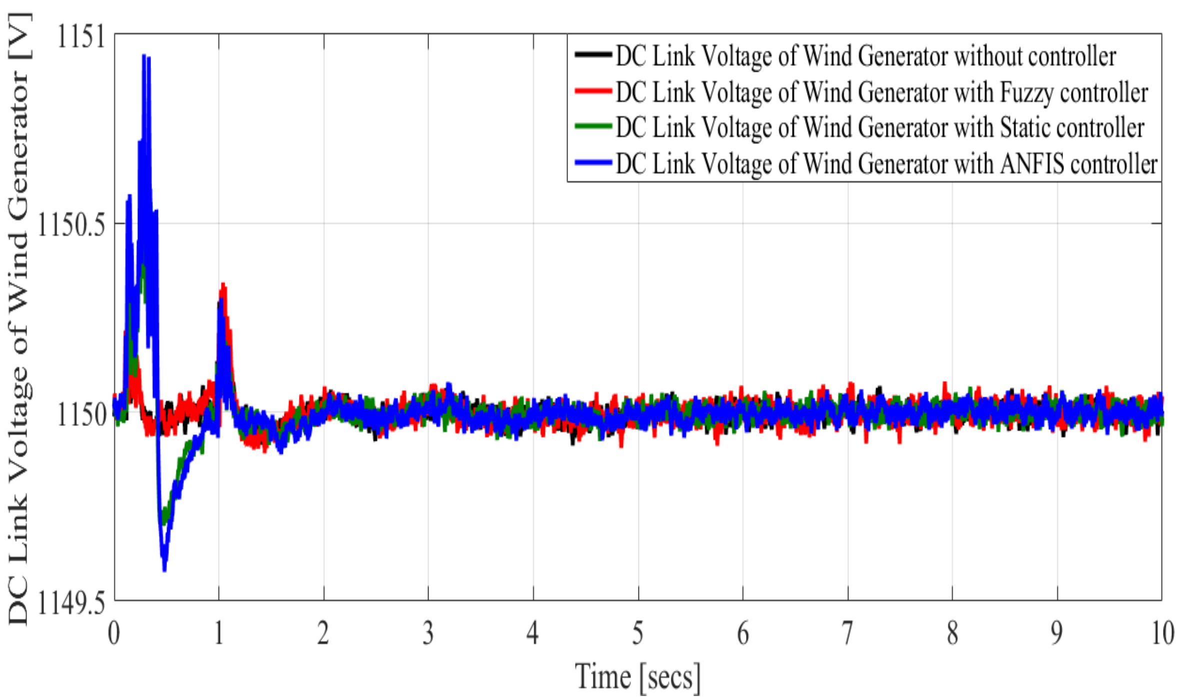

(c)

Figure 35. Voltage responses when the system is subjected to 3LG permanent fault at F2. (a) Voltage at PCC, (b) Terminal voltage of wind generator, (c) DC link voltage of the wind generator.

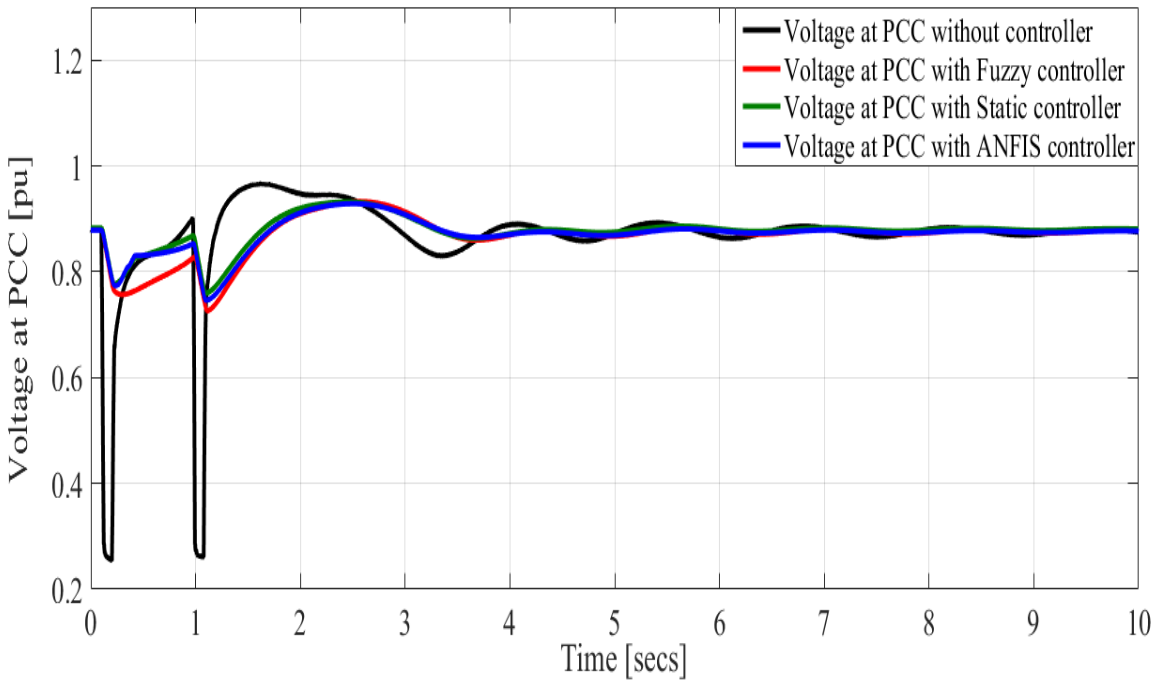

Voltage at PCC without controller
Voltage at PCC with Fuzzy controller
Voltage at PCC with Static controller
Voltage at PCC with ANFIS controller
Voltage at PCC [pu]
Time [secs]
0.2
0.4
0.6
0.8
1
1.2
0
1
2
3
4
5
6
7
8
9
10

(a)

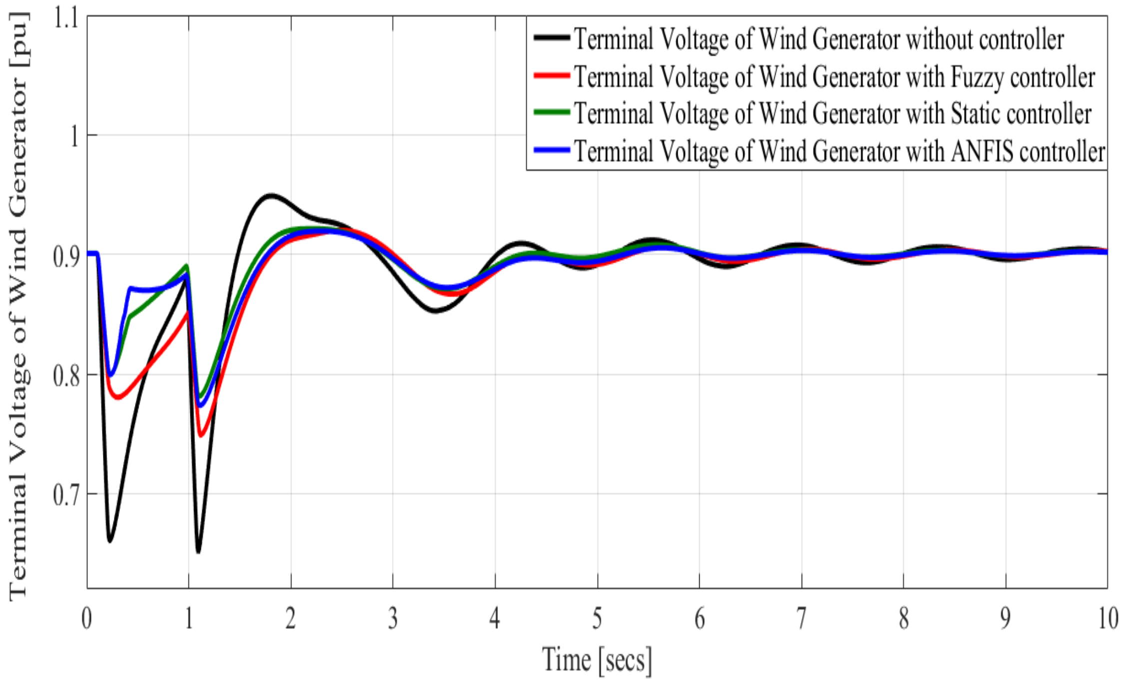

Terminal Voltage of Wind Generator without controller
Terminal Voltage of Wind Generator with Fuzzy controller
Terminal Voltage of Wind Generator with Static controller
Terminal Voltage of Wind Generator with ANFIS controller
Terminal Voltage of Wind Generator [pu]
Time [secs]
0.7
0.8
0.9
1
1.1
0
1
2
3
4
5
6
7
8
9
10

(b)

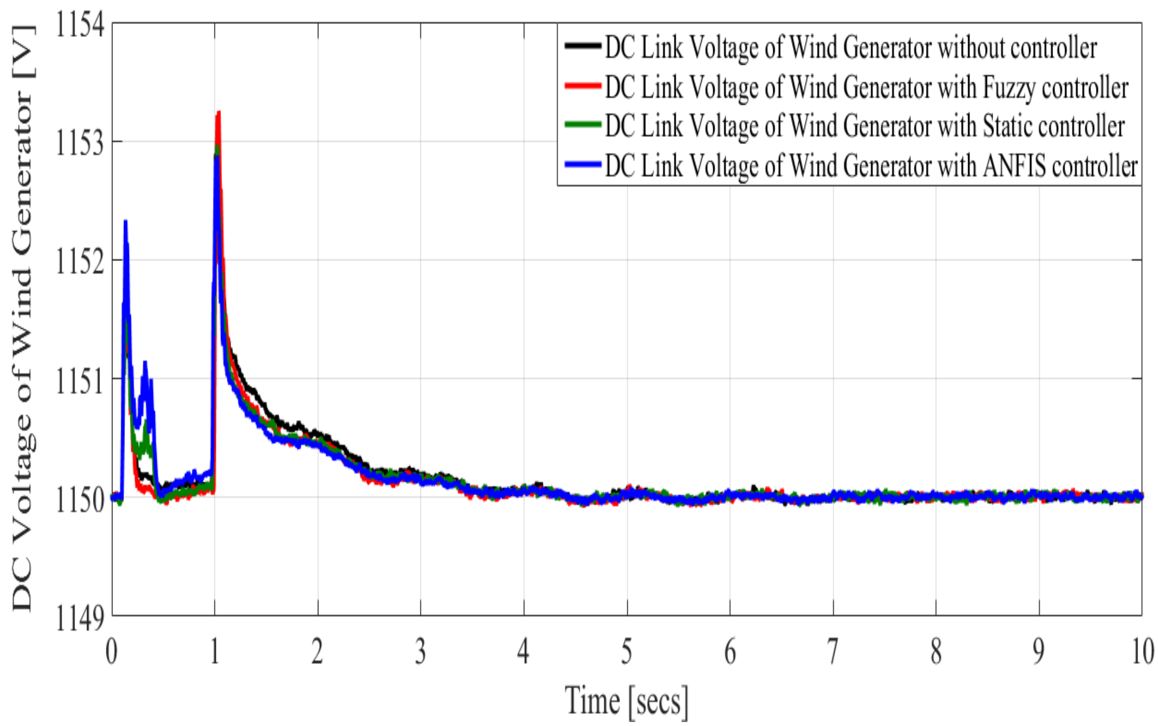

(c)

Figure 36. Voltage responses when the system is subjected to 3LG permanent fault at F1. (a) Voltage at PCC, (b) Terminal voltage of wind generator, (c) DC link voltage of the wind generator.

Figures 37- 42 show the voltage responses at the PCC, wind generator terminal voltage, and the dc link voltage of the wind generator, due to a 1LG temporary and permanent faults at F3, F2, F1 points in Fig. 12. From the responses, it is seen that the ANFIS controlled TSC and static non-linear controlled TSC work well to improve the power quality. Also, the performance of the proposed controlled TSC is better than that of the fuzzy controlled TSC. The responses also show that the ANFIS controlled TSC performs somewhat better than the static non-linear controlled TSC.

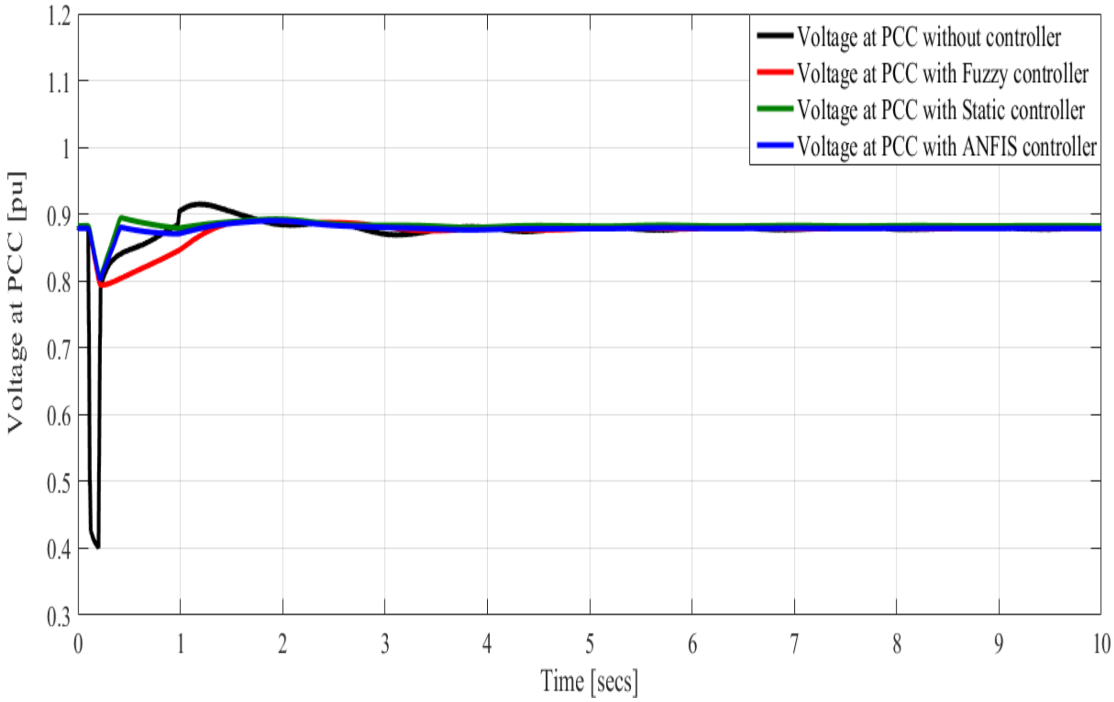
Voltage at PCC without controller
Voltage at PCC with Fuzzy controller
Voltage at PCC with Static controller
Voltage at PCC with ANFIS controller
Voltage at PCC [pu]
Time [secs]
1.2
1.1
1
0.9
0.8
0.7
0.6
0.5
0.4
0.3
0
1
2
3
4
5
6
7
8
9
10

(a)

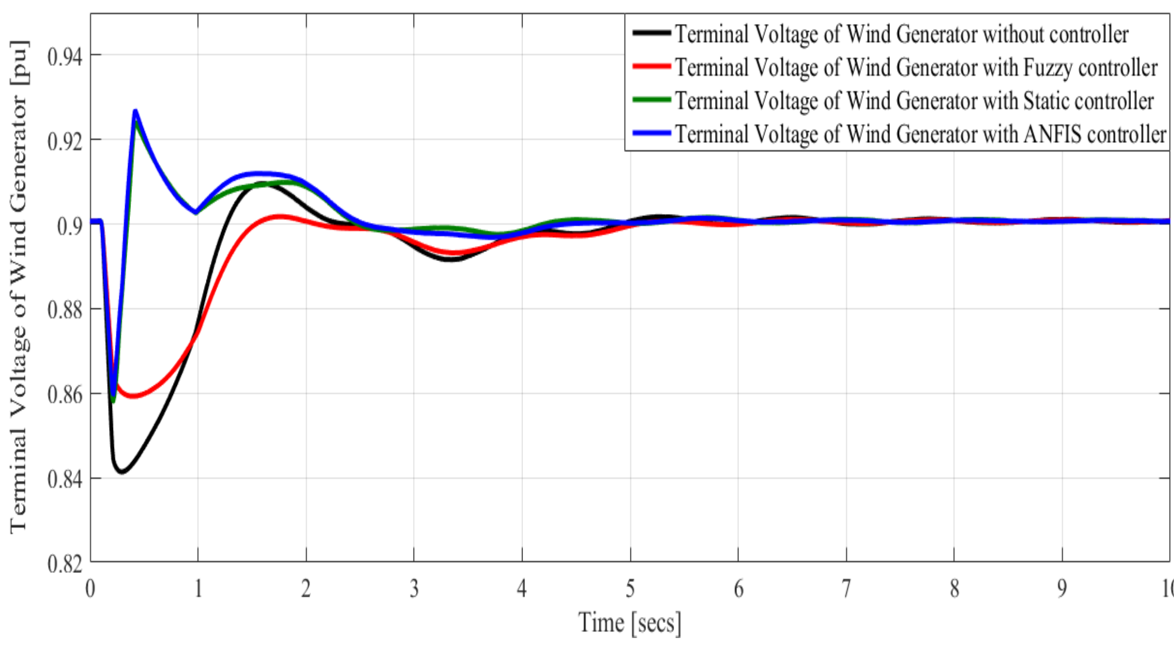
Terminal Voltage of Wind Generator without controller
Terminal Voltage of Wind Generator with Fuzzy controller
Terminal Voltage of Wind Generator with Static controller
Terminal Voltage of Wind Generator with ANFIS controller
Terminal Voltage of Wind Generator [pu]
Time [secs]
0.94
0.92
0.9
0.88
0.86
0.84
0.82
0
1
2
3
4
5
6
7
8
9
10

(b)

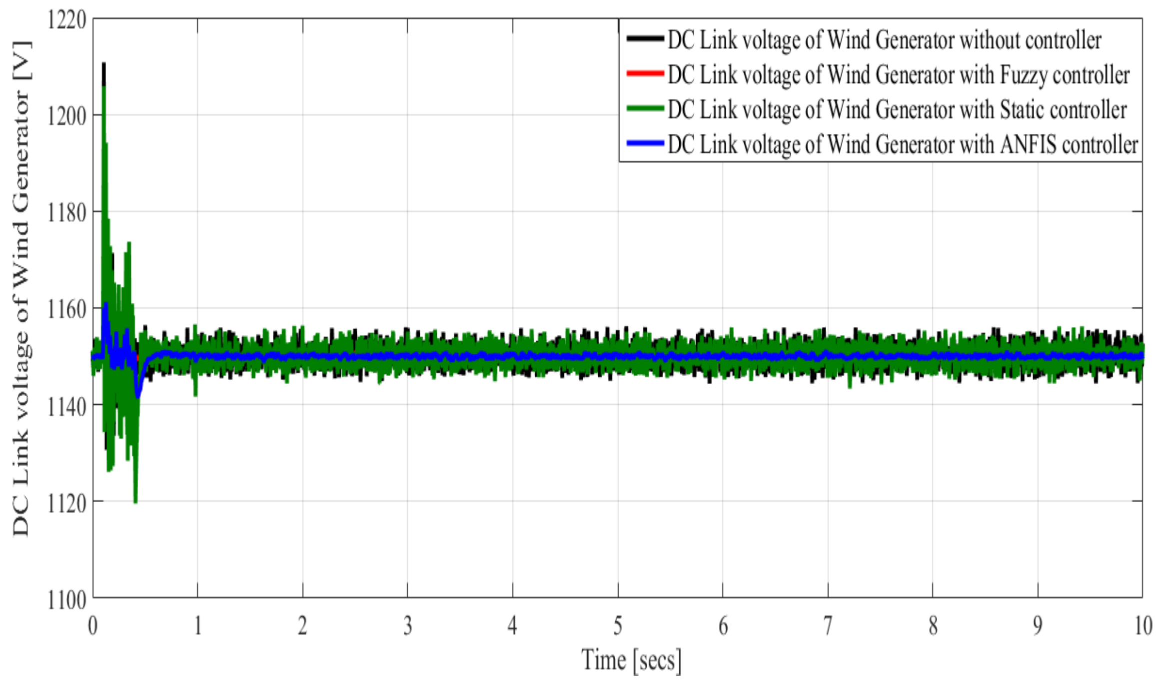

(c)

Figure 37. Voltage responses when the system is subjected to 1LG temporary fault at F3. (a) Voltage at PCC, (b) Terminal voltage of wind generator, (c) DC link voltage of the wind generator.

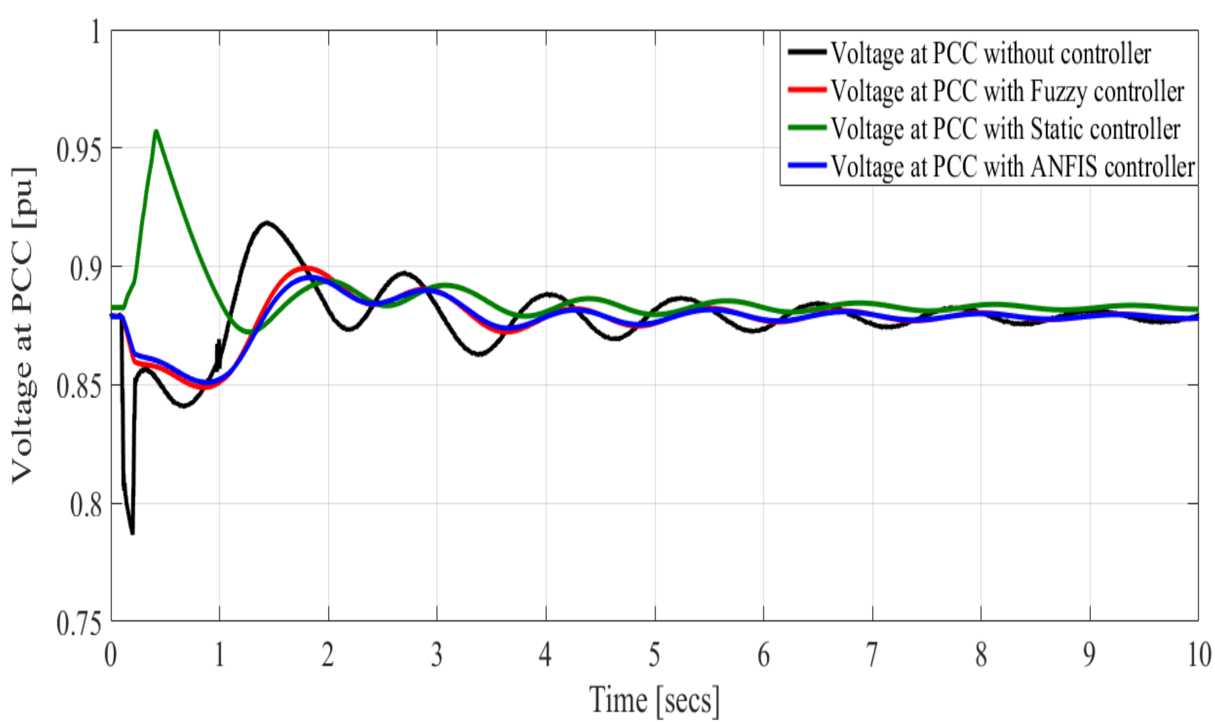

(a)

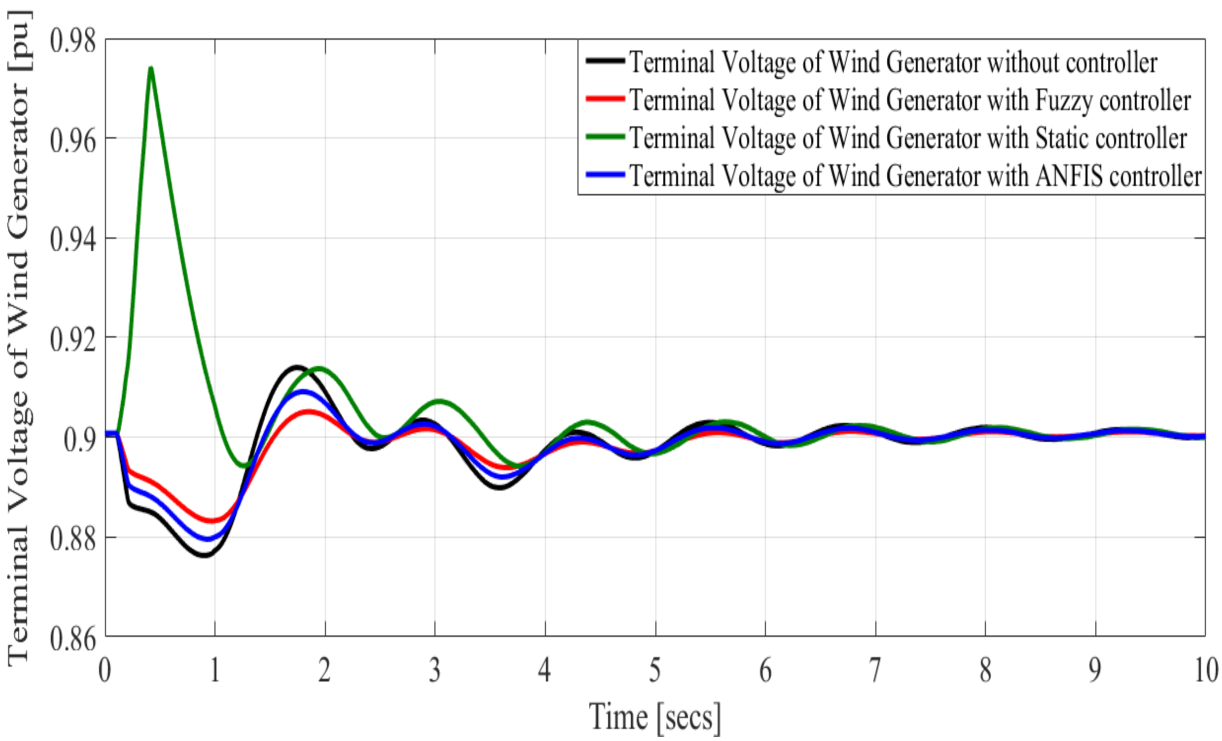

(b)

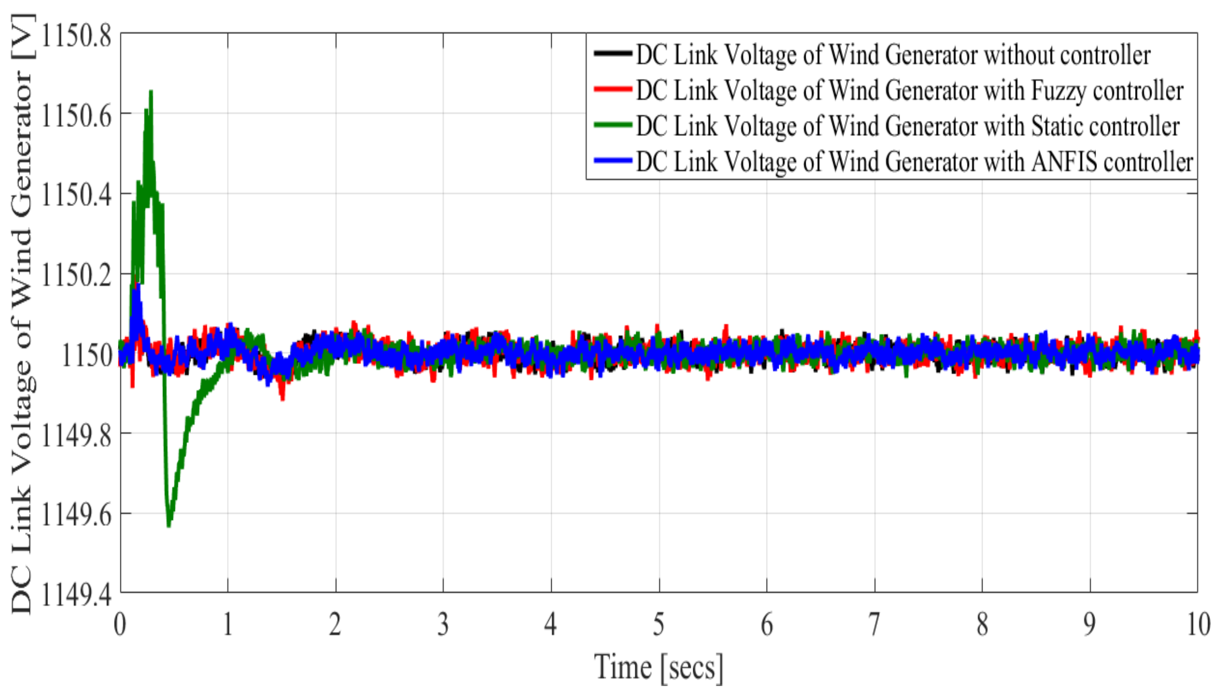

(c)

Figure 38. Voltage responses when the system is subjected to 1LG temporary fault at F2. (a) Voltage at PCC, (b) Terminal voltage of wind generator, (c) DC link voltage of the wind generator.

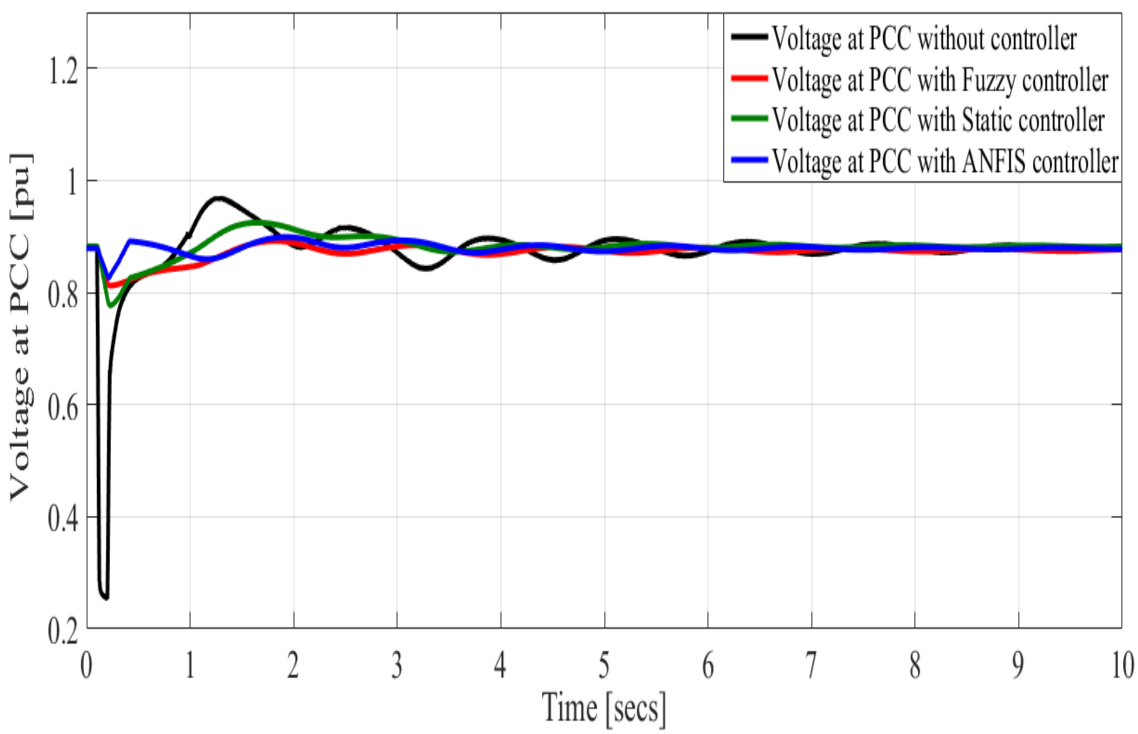
Voltage at PCC without controller
Voltage at PCC with Fuzzy controller
Voltage at PCC with Static controller
Voltage at PCC with ANFIS controller
Voltage at PCC [pu]
Time [secs]

(a)

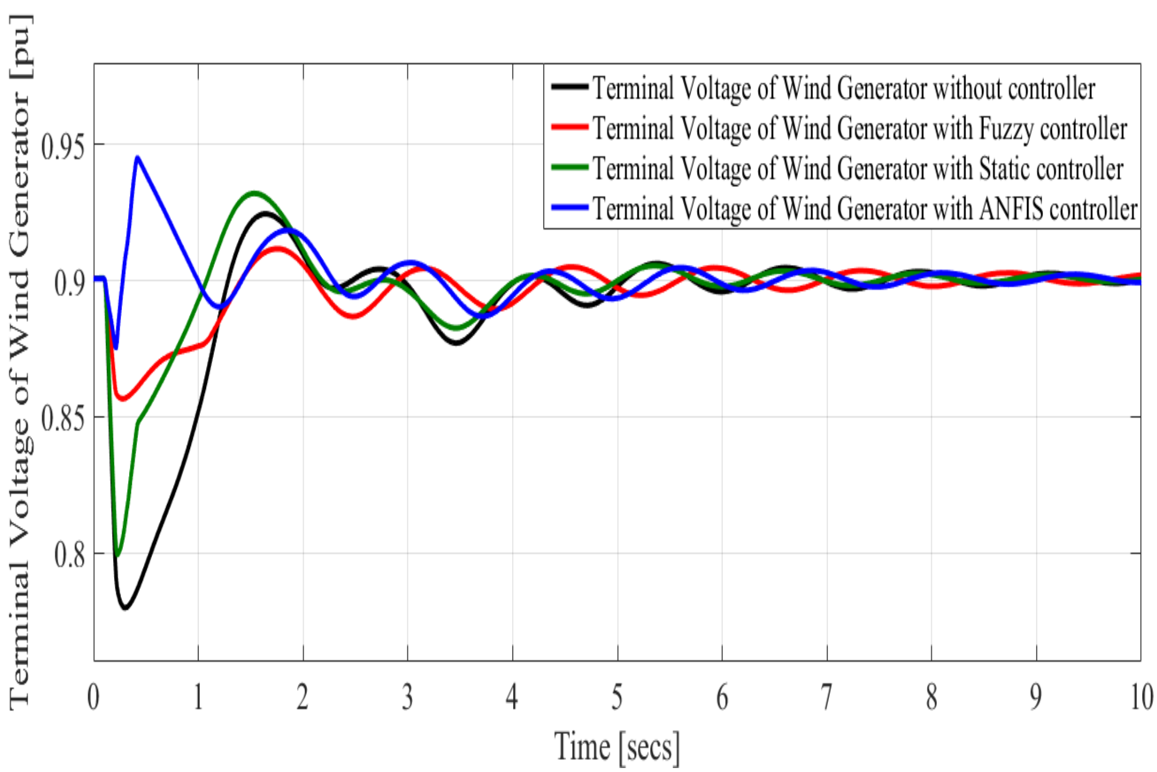
Terminal Voltage of Wind Generator without controller
Terminal Voltage of Wind Generator with Fuzzy controller
Terminal Voltage of Wind Generator with Static controller
Terminal Voltage of Wind Generator with ANFIS controller
Terminal Voltage of Wind Generator [pu]
Time [secs]

(b)

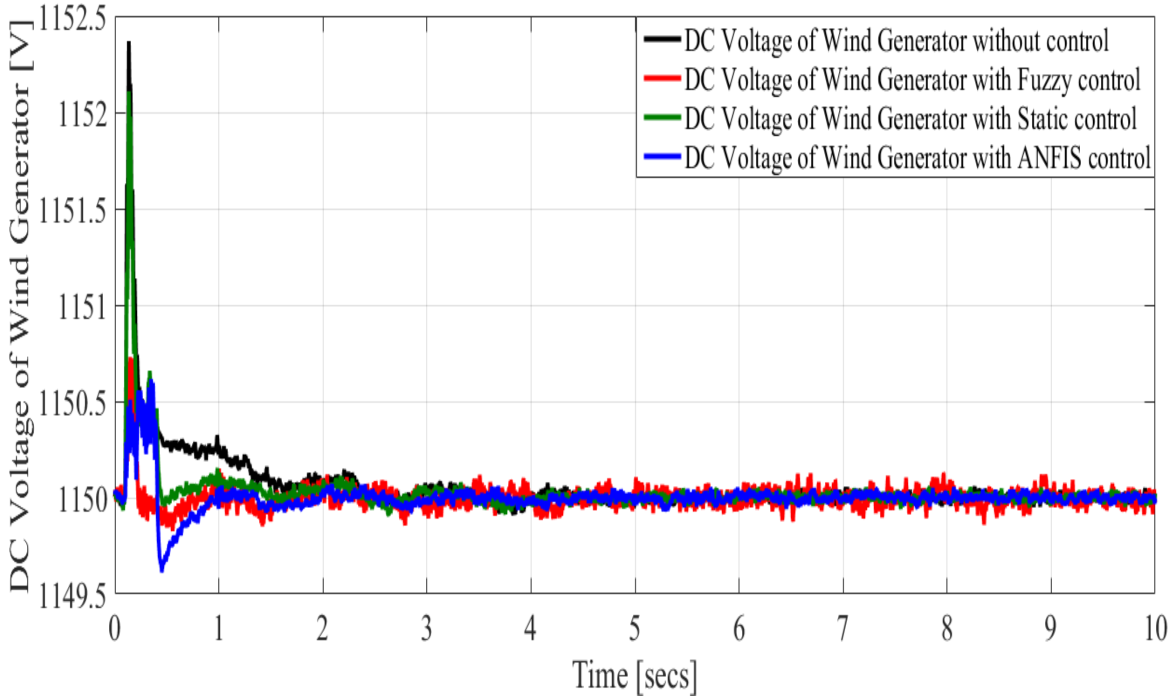

(c)

Figure 39. Voltage responses when the system is subjected to 1LG temporary fault at F1. (a) Voltage at PCC, (b) Terminal voltage of wind generator, (c) DC link voltage of the wind generator.

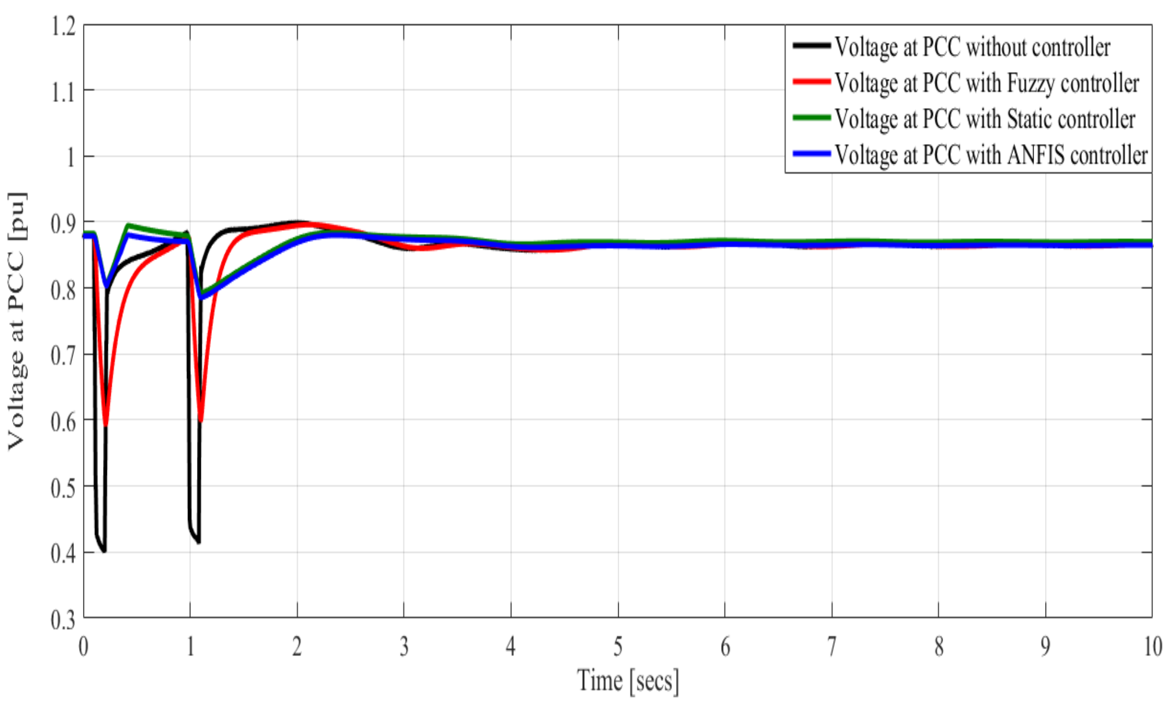

(a)

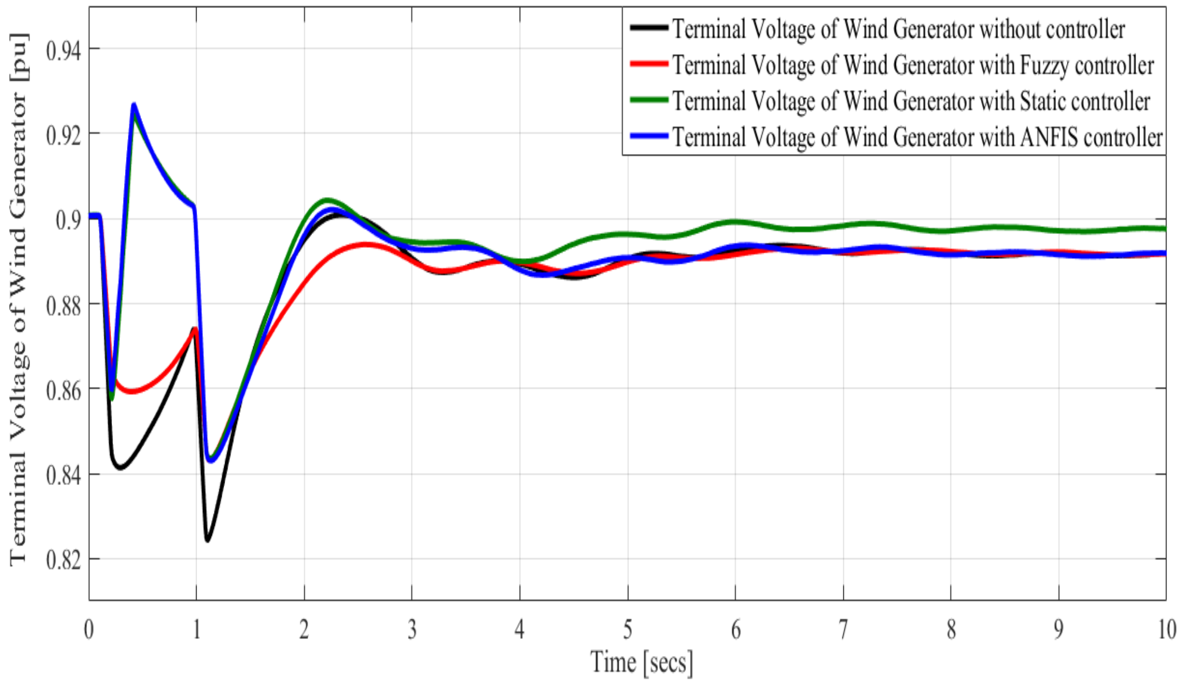

(b)

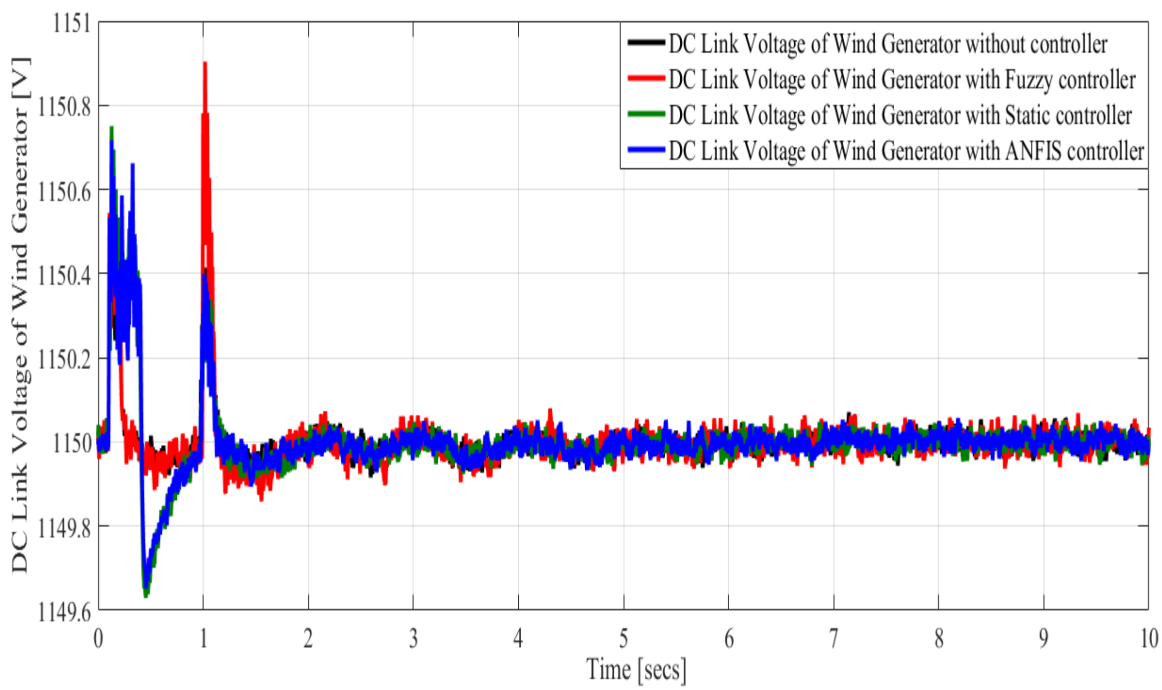

(c)

Figure 40. Voltage responses when the system is subjected to 1LG permanent fault at F3. (a) Voltage at PCC, (b) Terminal voltage of wind generator, (c) DC link voltage of the wind generator.

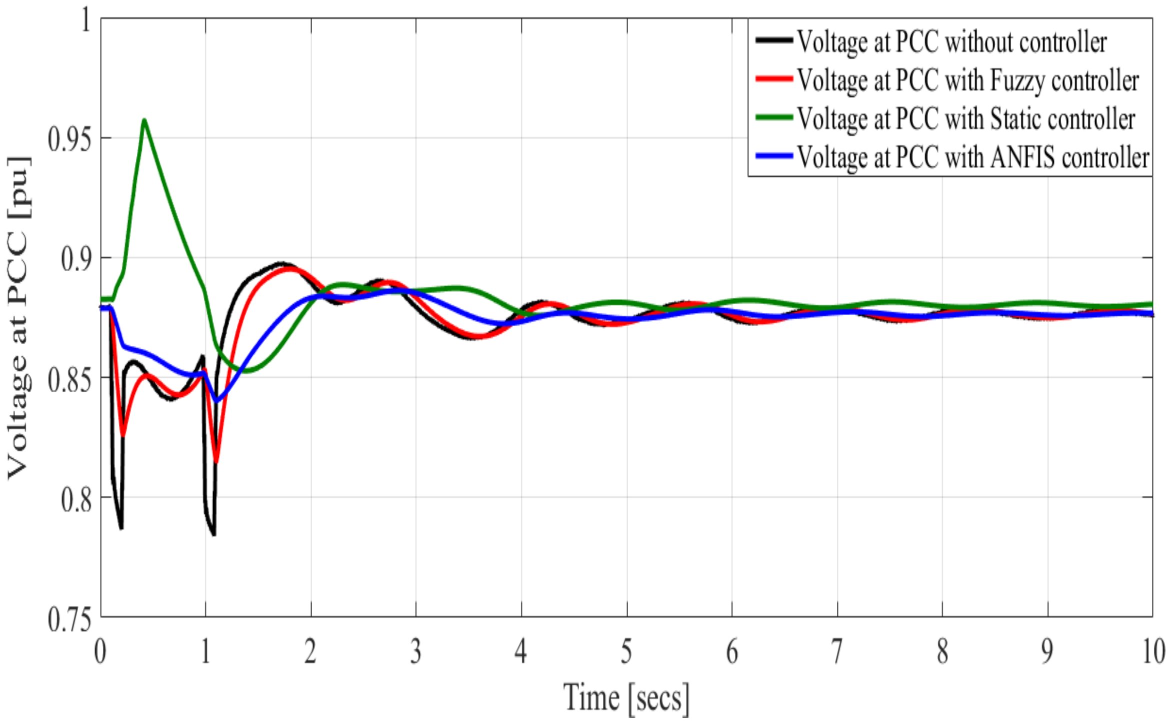

Voltage at PCC without controller
Voltage at PCC with Fuzzy controller
Voltage at PCC with Static controller
Voltage at PCC with ANFIS controller
Voltage at PCC [pu]
Time [secs]

(a)

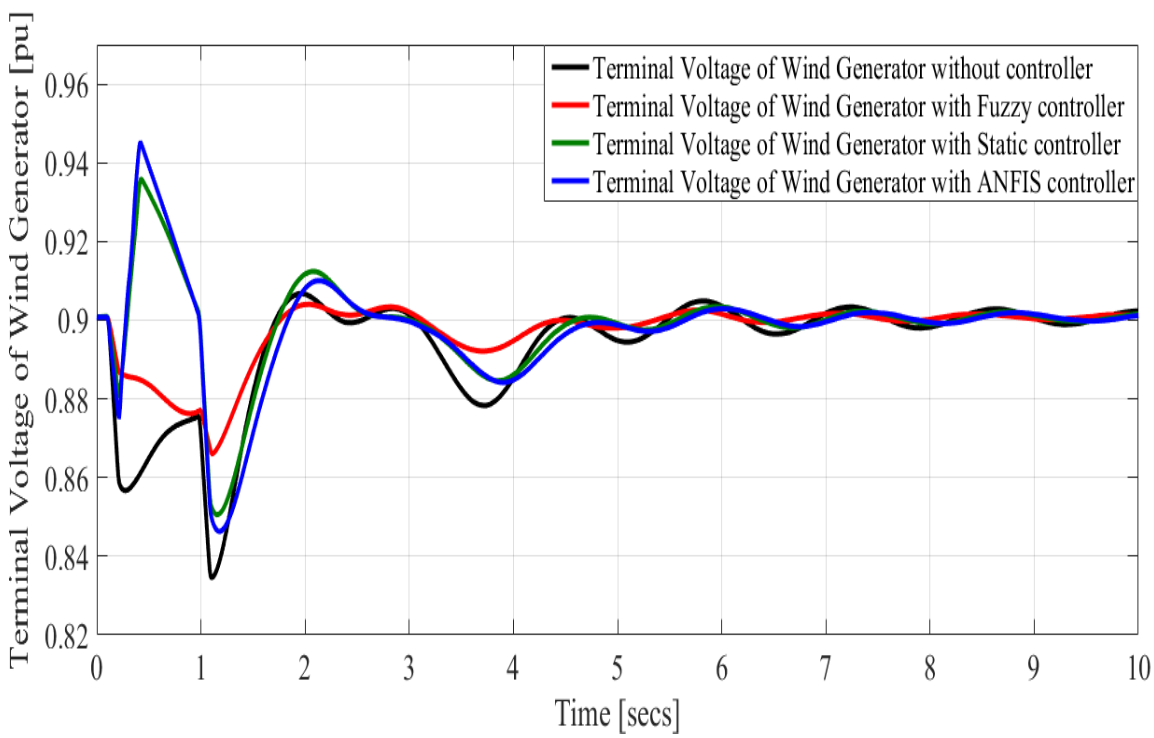

Terminal Voltage of Wind Generator without controller
Terminal Voltage of Wind Generator with Fuzzy controller
Terminal Voltage of Wind Generator with Static controller
Terminal Voltage of Wind Generator with ANFIS controller
Terminal Voltage of Wind Generator [pu]
Time [secs]

(b)

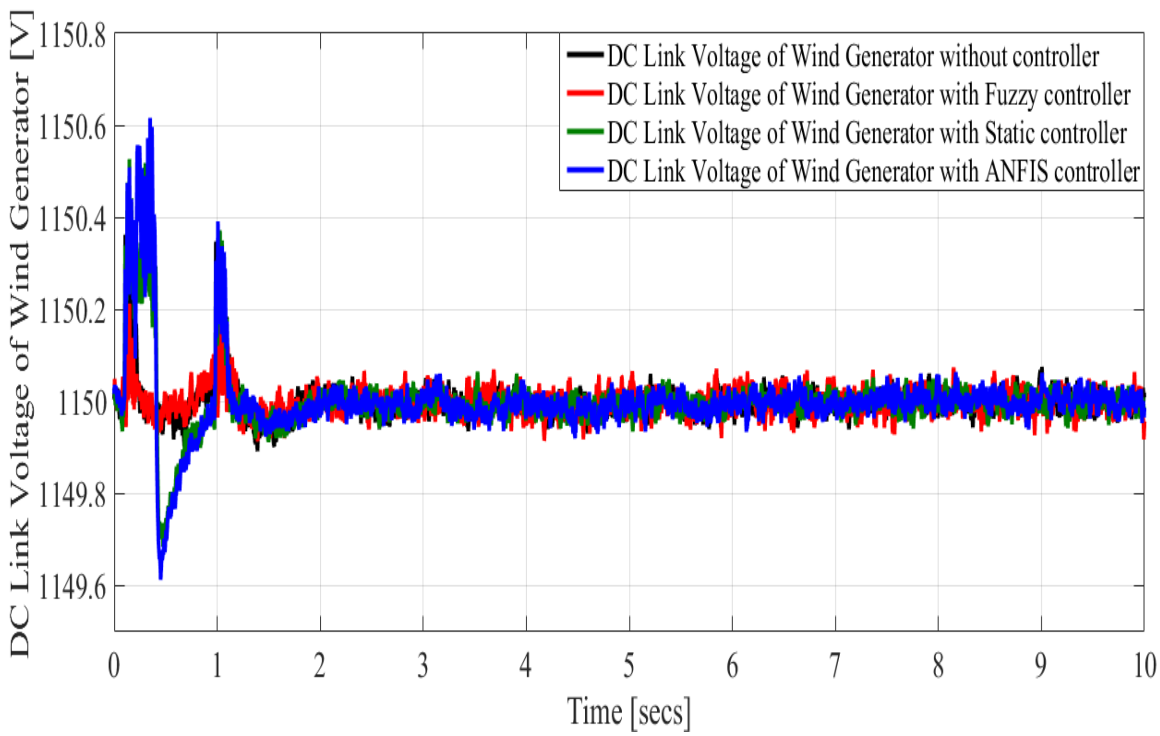

(c)

Figure 41. Voltage responses when the system is subjected to 1LG permanent fault at F2. (a) Voltage at PCC, (b) Terminal voltage of wind generator, (c) DC link voltage of the wind generator.

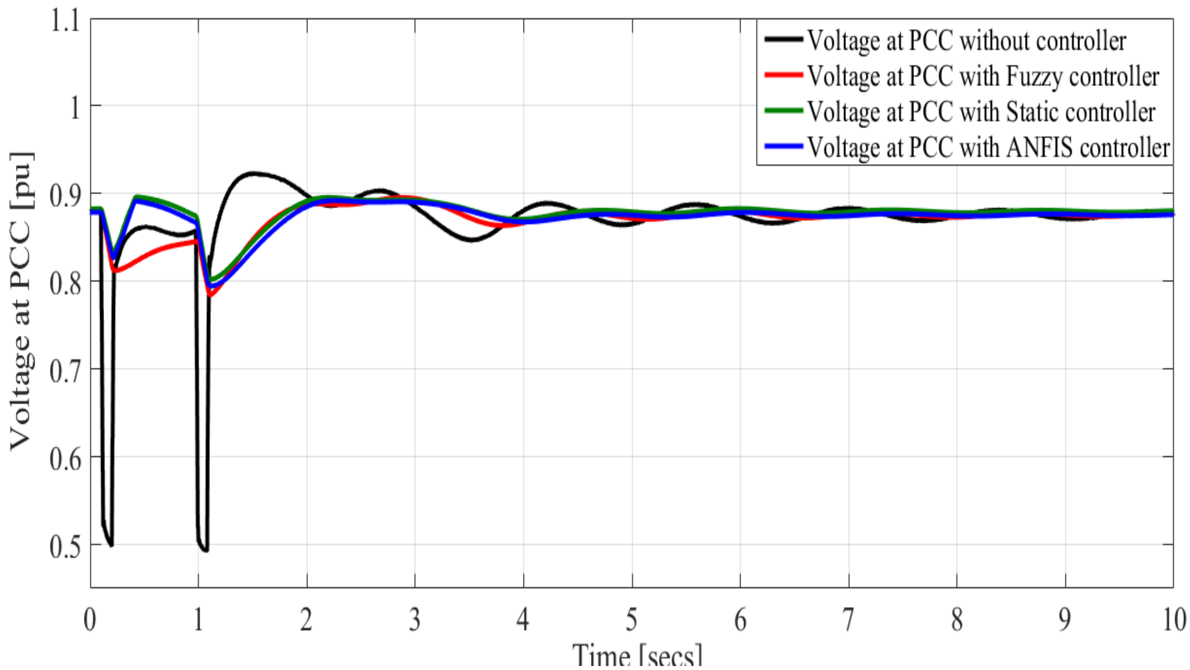

(a)

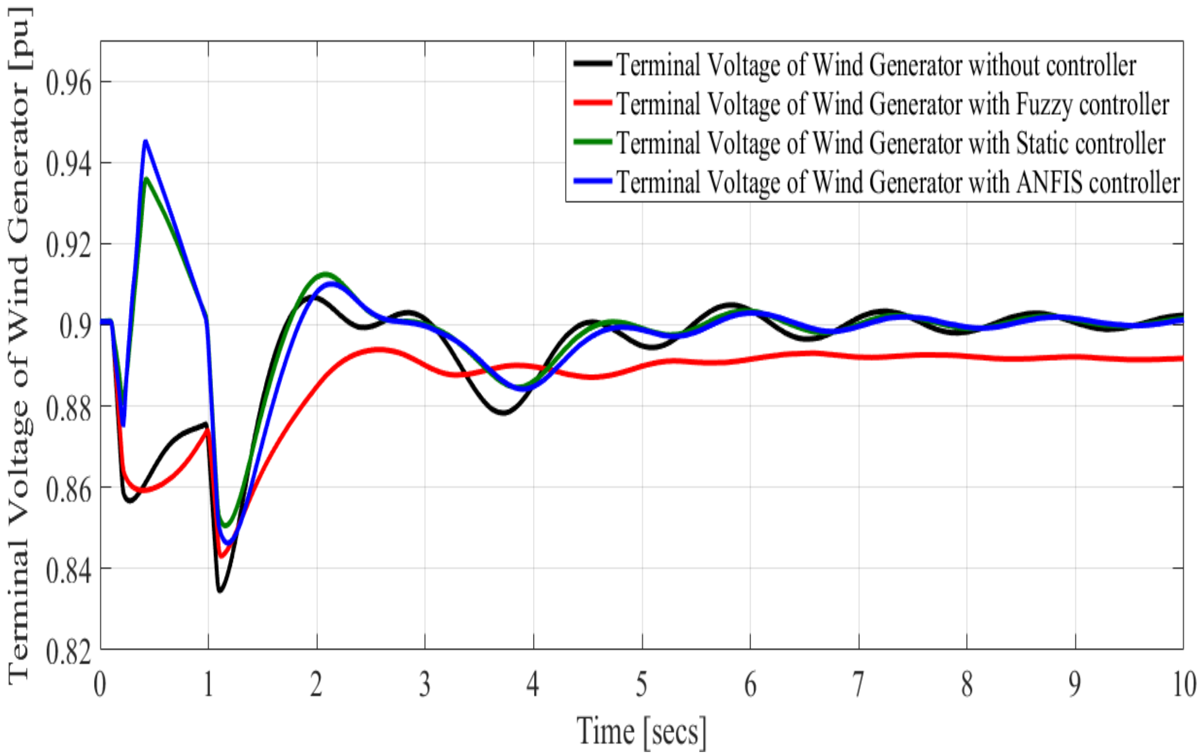

(b)

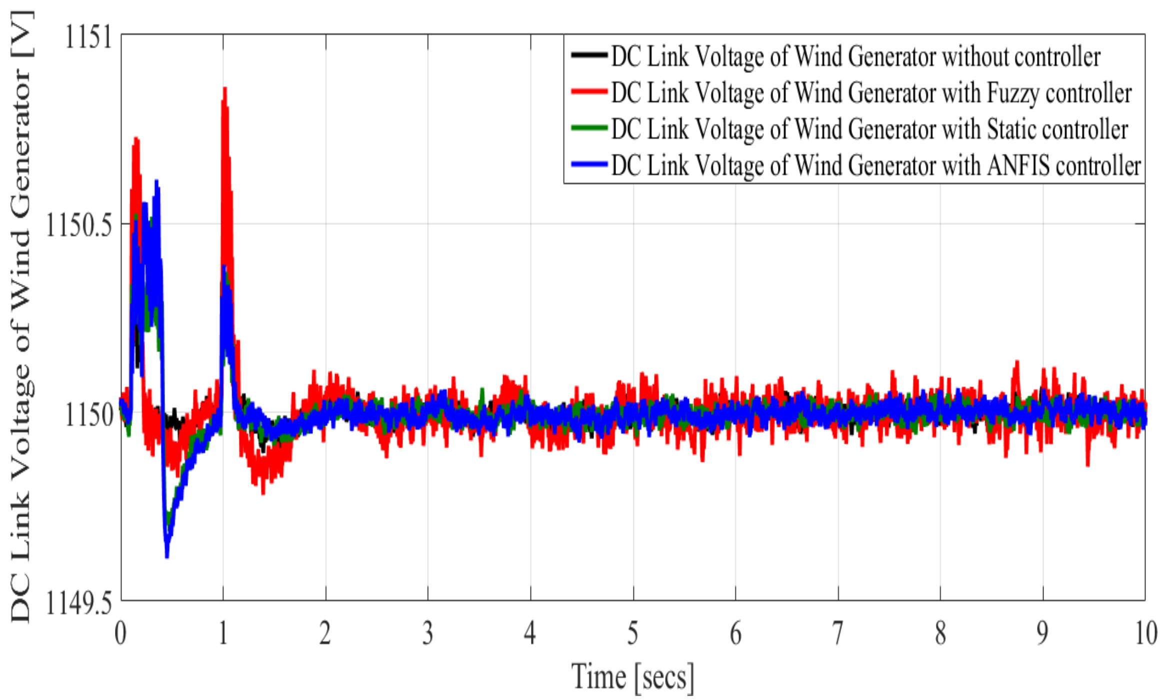

(c)

Figure 42. Voltage responses when the system is subjected to 1LG permanent fault at F1. (a) Voltage at PCC, (b) Terminal voltage of wind generator, (c) DC link voltage of the wind generator.

a) Power Quality Analysis in terms of Voltage Index, V_{index}

Tables X-XV show the values of voltage indices at PCC, voltage indices of synchronous and wind generators for temporary and permanent 3LG, 1LG, 2LG and 2LS faults at points F1, F2 and F3 of the power system with and without the TSC control methods. The voltage index is calculated using the equation (15). From the indices it is shown that the proposed ANFIS controlled TSC and static non-linear controlled TSC perform better as compared to the fuzzy controlled TSC in improving the power quality. It is also observed from the responses that the performance of ANFIS controlled TSC is somewhat better than that of the static non-linear controlled TSC.

Table IX: Voltage indices for PCC Voltage for temporary faults

Fault Type	Fault Point	Voltage Index PCC (Temp)			
		Without Control	With Fuzzy- TSC	With SNC-TSC	With ANFIS-TSC
3LG	F1	0.3474	0.3417	0.3242	0.3120
	F2	0.1506	0.1489	0.1346	0.1387
	F3	0.3777	0.3659	0.3534	0.3492
1LG	F1	0.1942	0.1676	0.1808	0.1620
	F2	0.0901	0.0719	0.1225	0.0898
	F3	0.2895	0.2715	0.2292	0.2675
2LG	F1	0.1943	0.1670	0.1661	0.1713
	F2	0.1193	0.1011	0.1055	0.1062
	F3	0.1885	0.1754	0.1729	0.1681
2LS	F1	0.2418	0.1326	0.1661	0.1642
	F2	0.1193	0.1011	0.1055	0.1069
	F3	0.1885	0.1754	0.1729	0.1681

Table X: Voltage indices for PCC Voltage for permanent faults

Fault Type	Fault Point	Voltage Index PCC			
		Without Control	With Fuzzy- TSC	With SNC-TSC	With ANFIS-TSC
3LG	F1	0.3474	0.3417	0.3242	0.3120
	F2	0.1506	0.1489	0.1346	0.1387
	F3	0.3777	0.3659	0.3534	0.3492
1LG	F1	0.1942	0.1676	0.1808	0.1620
	F2	0.0901	0.0719	0.1225	0.0898
	F3	0.2895	0.2715	0.2292	0.2675
2LG	F1	0.2935	0.2644	0.2458	0.26
	F2	0.1358	0.09916	0.1158	0.1411
	F3	0.3667	0.3199	0.3262	0.1573
2LS	F1	0.3491	0.1676	0.302	0.192
	F2	0.09008	0.1240	0.1225	0.0898
	F3	0.4031	0.1465	0.2292	0.2678

Table XI: Voltage indices for synchronous generator (G1 & G2) during temporary faults

Fault Type	Fault Point	Voltage of G1 & G2 Voltage Index			
		Without Control	With Fuzzy- TSC	With SNC-TSC	With ANFIS-TSC
3LG	F1	0.2939	0.2154	0.2210	0.2164
	F2	0.2541	0.1851	0.2006	0.1763
	F3	0.2601	0.1986	0.2061	0.1980
1LG	F1	0.1940	0.1375	0.1213	0.1647
	F2	0.1860	0.1221	0.1686	0.1037
	F3	0.1729	0.1121	0.1395	0.1059
2LG	F1	0.1442	0.1699	0.1878	0.1918
	F2	0.1229	0.1586	0.1766	0.1496
	F3	0.1206	0.1601	0.1720	0.1505
2LS	F1	0.1940	0.1375	0.1878	0.1647
	F2	0.1229	0.1586	0.1766	0.1509
	F3	0.1206	0.1601	0.1720	0.1505

Table XII: Voltage indices for synchronous generator (G1 & G2) permanent faults

Fault Type	Fault Point	Voltage of G1 & G2 Voltage Index (Perm)			
		Without Control	With Fuzzy- TSC	With SNC-TSC	With ANFIS-TSC
3LG	F1	0.2769	0.2593	0.2691	0.2588
	F2	0.2615	0.2142	0.2165	0.2125
	F3	0.2569	0.2426	0.2040	0.2140
1LG	F1	0.1309	0.1211	0.1051	0.1020
	F2	0.1164	0.0913	0.1088	0.1017
	F3	0.1673	0.1590	0.1542	0.1584
2LG	F1	0.1970	0.1875	0.1081	0.1754
	F2	0.1640	0.1428	0.1488	0.1216
	F3	0.1877	0.1576	0.1441	0.1327
2LS	F1	0.277	0.1311	0.1672	0.1200
	F2	0.2164	0.1863	0.1588	0.1317
	F3	0.2569	0.1124	0.1842	0.1548

Table XIII: Voltage indices for wind generator for temporary faults

Fault Type	Fault Point	Wind Generator Voltage Index (Temp)			
		Without Control	With Fuzzy- TSC	With SNC-TSC	With ANFIS-TSC
3LG	F1	0.2230	0.1117	0.0842	0.0983
	F2	0.1315	0.0538	0.0487	0.0484
	F3	0.2026	0.1078	0.0862	0.0836
1LG	F1	0.2226	0.0518	0.0835	0.0533
	F2	0.0865	0.0549	0.0551	0.0429
	F3	0.0907	0.0475	0.0299	0.0322
2LG	F1	0.1671	0.07504	0.05321	0.05741
	F2	0.1065	0.03922	0.0506	0.04522
	F3	0.1519	0.08064	0.0533	0.05577
2LS	F1	0.2226	0.05179	0.05321	0.05327
	F2	0.1065	0.03922	0.0506	0.0456
	F3	0.1519	0.08064	0.0533	0.05059

Table XIV: Voltage indices for wind generator for permanent faults

Fault Type	Fault Point	Wind generator Voltage Index			
		Without Control	With Fuzzy- TSC	With SNC-TSC	With ANFIS-TSC
3LG	F1	0.2457	0.1893	0.1368	0.1375
	F2	0.1389	0.0841	0.0634	0.0703
	F3	0.2371	0.2102	0.1742	0.2030
1LG	F1	0.1498	0.0627	0.0625	0.0615
	F2	0.0732	0.0472	0.0622	0.0444
	F3	0.1673	0.0886	0.0718	0.0593
2LG	F1	0.2253	0.1062	0.0777	0.08651
	F2	0.102	0.04754	0.0687	0.06258
	F3	0.2651	0.1503	0.1200	0.01475
2LS	F1	0.3099	0.06267	0.1339	0.06795
	F2	0.07321	0.07256	0.06223	0.04442
	F3	0.3371	0.05451	0.07181	0.1107

b) THD Analysis

Tables XVI-XVII show the THD values for temporary and permanent 3LG, 1LG, 2LG and 2LS faults at points F1, F2 and F3 with the ANFIS controlled TSC, static non-linear controlled TSC, fuzzy controlled TSC and without any control method. The THD index is calculated using equation (16). From the THD values, it is observed that the proposed controllers reduced the effects of harmonics. However, the performance of the ANFIS controlled TSC and static non-linear controlled TSC is better than that of the fuzzy controlled TSC. It is also clear from the indices that the ANFIS controlled TSC is somewhat better than the static non-linear controlled TSC.

Table XV: Total Harmonic Distortion at PCC for temporary faults

Fault Type	Fault Point	THD (Temp)			
		Without Control	With Fuzzy- TSC	With SNC-TSC	With ANFIS-TSC
3LG	F1	2.025	0.7933	0.8062	0.7913
	F2	2.686	0.7948	0.8168	0.7793
	F3	1.047	0.9177	0.8900	0.7465
1LG	F1	2.677	0.8258	0.7915	0.6922
	F2	2.053	0.8020	0.4290	0.7846
	F3	2.963	1.6503	1.352	1.112
2LG	F1	1.004	0.8102	0.7939	0.8353
	F2	5.618	0.8304	0.8757	0.8547
	F3	2.41	0.7664	0.9458	0.6943
2LS	F1	2.677	0.8258	0.7939	0.9922
	F2	5.618	0.8304	0.8757	0.6910
	F3	2.41	0.7664	0.9458	0.6943

Table XVI: Total Harmonic Distortion at PCC for permanent faults

Fault Type	Fault Point	THD (Perm)			
		Without Control	With Fuzzy- TSC	With SNC-TSC	With ANFIS-TSC
3LG	F1	2.400	0.8132	0.8042	0.8068
	F2	1.382	0.8267	0.8180	0.8139
	F3	2.482	0.8457	1.2130	0.6469
1LG	F1	1.289	0.9869	0.7905	0.8169
	F2	1.215	0.8651	0.8317	0.7875
	F3	2.915	0.1049	0.8773	0.7340
2LG	F1	2.188	0.8156	0.7741	0.0002
	F2	3.005	0.7372	0.7	0.8229
	F3	4.762	1.019	0.7379	0.3174
2LS	F1	1.171	0.1869	0.8209	0.8169
	F2	4.215	0.7694	0.8317	0.7875
	F3	4.303	0.6745	0.8773	0.7427

D. Conclusion

This chapter deals with the nonlinearity issue in a hybrid power grid. Different non-linear controllers based TSC are proposed and designed to improve the power quality of the system. Both balanced and unbalanced faults at different points are considered. Based on the results, the following conclusions are made:

1. The proposed fuzzy logic controlled TSC is effective to enhance the power quality of the hybrid system. Also, the performance of the fuzzy logic controlled TSC is better than that of the PID controlled TSC.
2. The proposed ANFIS and static nonlinear control based TSC methods are effective to enhance the power quality of the hybrid grid system.
3. Except few cases, the performance of the ANFIS and static nonlinear control based TSC methods are better than that of the fuzzy controlled TSC.
4. The ANFIS controlled TSC is somewhat better than the static non-linear controlled TSC.

IV. MINIMIZATION OF ADVERSE EFFECTS OF TIME DELAY ON POWER QUALITY ENHANCEMENT IN HYBRID GRID

A. Introduction

This chapter deals with one of the most challenging issues of the modern power grid, i.e., the communication delay, which has adverse effects on the power quality of a system. At first, the effects of time delay on the system performance is analyzed. Later, two methods, namely the FLC based method and the Modified Predictor method, are proposed to minimize the adverse effects of time delay on the power quality enhancement of a hybrid power grid consisting of synchronous and variable speed wind generators. The device used for power quality enhancement is the TSC. Time delays ranging from 0-700 ms have been considered for the analysis. Both balanced and unbalanced temporary and permanent faults at different locations in the power network have been considered. Two indices, namely the voltage index and the THD have been used to evaluate the power quality of the system. The performance of the FLC based method has been compared with that of the Modified Predictor method. Simulations have been performed by using the Matlab/Simulink software. The hybrid power system considered for the analysis of the power quality due to communication delay in this chapter has already been introduced in chapter III (Figure 10).

B. Time Delay Issues with TSC Controller

i. Time Delay Issue with the TSC Controller

As shown in Figure 11, the TSC is connected to the line via a step-down transformer. There are six back-to-back thyristors connected with the capacitors [87]. These capacitors are switched with the help of the thyristors. The reactive power capacity of the capacitor, C, used is 28 MVAR. Here it is operating only when the error percentage is more than 2% between the reference and terminal voltages. The output of the controller is alpha (α) which is the switching pulse of the thyristors. The effects of time delay have been analyzed first by considering a single-input based FLC for the TSC. Figure 43 shows the control block for switching of the single-input fuzzy controlled TSC for the transient stability control. It is to note here that, this single-input fuzzy controller has not been used for minimizing the negative effects of time delay.

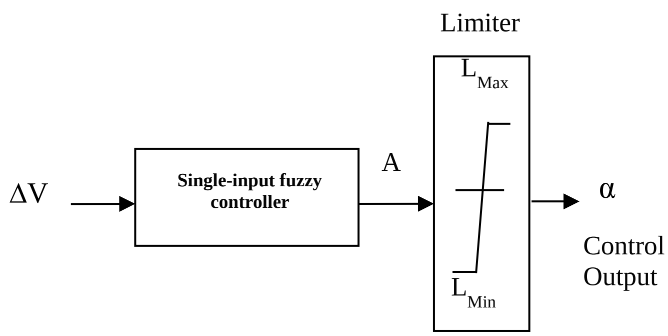

Figure 43. A control block for switching of TSC.

Figure 44 shows a closed-loop control system for the TSC utilizing the GPS. As shown in Fig. 43, the controller input (ΔV) has been obtained from the control center, and delays are induced during the communication of the signals, which ultimately gets the generation of the controller output (alpha) delayed, and deteriorates the power quality of the system.

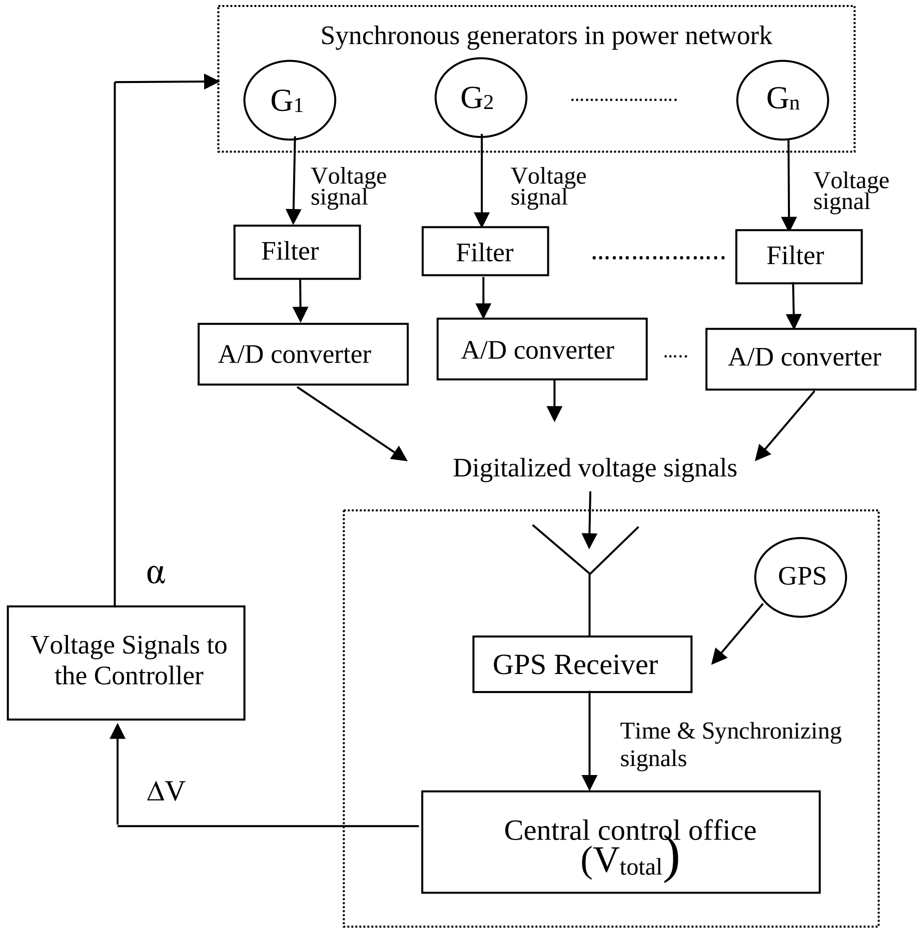

Figure 44. A control block of controller designed for generation required for switching of TSC.

C. Time Delay Minimizations with TSC Controller

i. Fuzzy Logic Controller (FLC) Based Method

This work uses the 2-Input based FLC for the minimization of the adverse effects of time delays on the performance of the TSC. The inputs to the FLC are the total voltage deviation at the PCC, ΔV, and the delay of the feedback signal (D). The output of the controller is alpha (α), the firing angle of the thyristor. During the process of designing the controller, the signal latency lies between 0 to 700 ms that cover all practical cases [43]. The proposed FLC is described below.

a) Fuzzification: In the fuzzification step, the grade of membership is determined. Figures 45 and 46 show the input and output triangular type membership functions, respectively, which have been calculated through a series of trial and error. In Fig. 45 (a & b), the symbols are defined as NB: negative big, NM: negative medium, Z: zero, PM: positive medium, PB: positive big, N: negative, P: positive. In Figure 46, NB, NM, Z, PM, and PB are the membership functions of the firing-angle of the thyristors, alpha (α). In this work, the equation in (14) has been used to calculate the grade of membership values.

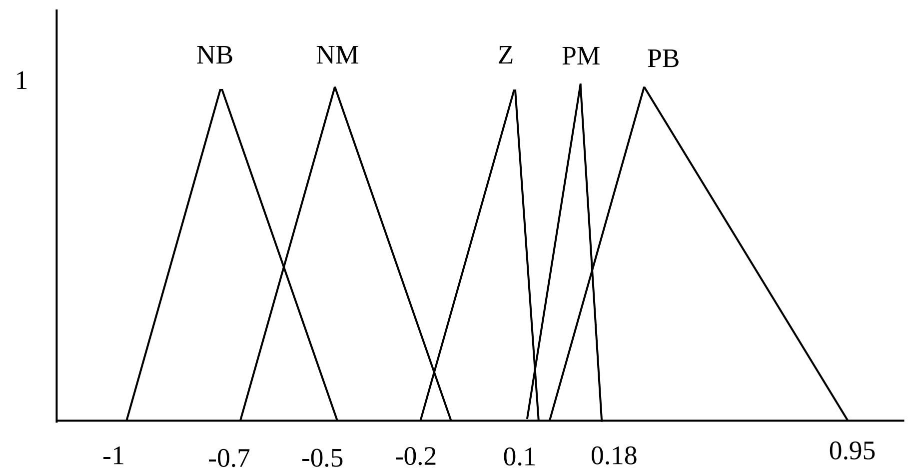

(a)

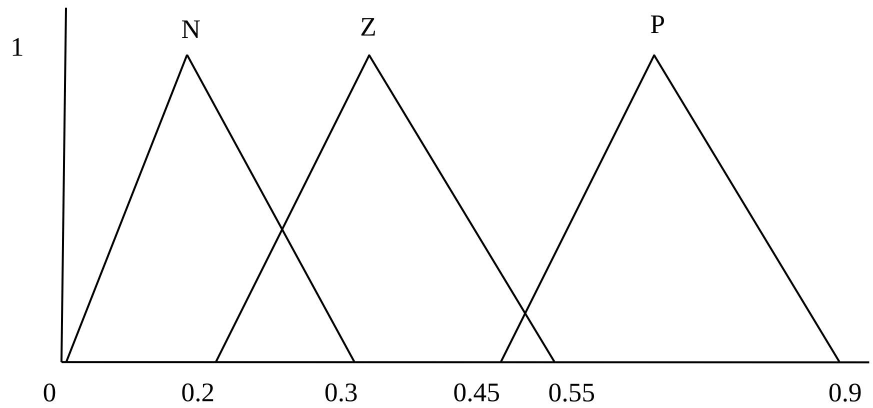

(b)

Figure 45. Membership functions of fuzzy controller inputs: (a) ΔV and (b) Delay.

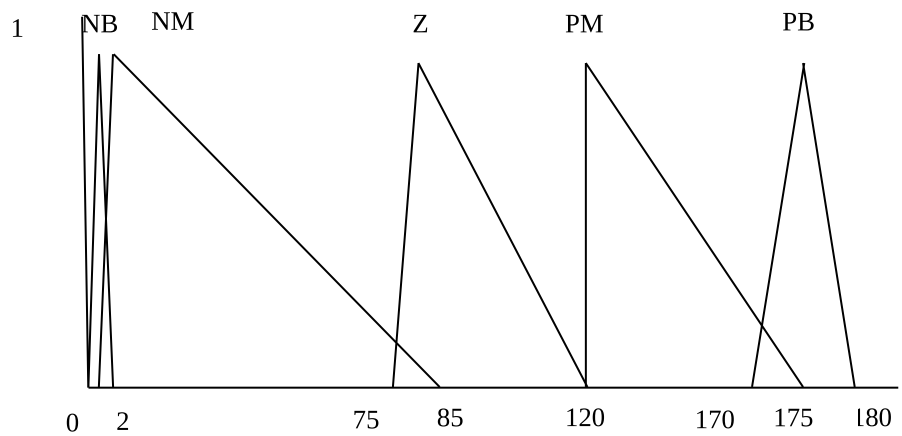

Figure 46. Membership functions of fuzzy controller output.

b) Rule Base: The rules for this membership functions are developed with the viewpoint of practical system and by trial and error. The control rules mentioned in terms of the linguistic input and output variables are given in Table XVII.

Table XVII: Membership functions of input and output

D \ ΔV	NB	NM	Z	PM	PB
N	PB	PM	Z	NM	NB
Z	PB	PM	Z	NM	NB
P	PB	PM	Z	NM	NB

c) Fuzzy Inference: Equation (20) shows the degree of conformity Wi of each fuzzy rule based on Mamdani's method.

$$W_i = \mu_{Ai}(\Delta V) \times \mu_{Bi}(D) \quad (20)$$

where μAi(x)(ΔV) and μBi (D) are the values of grade of membership, and i is the rule number.

d) Defuzzification: To determine the crispy output (i.e., the firing angle of the thyristor, α) for the controller, the center-of-area method given by the equation (16) is used.

ii. Modified Predictor Method

The model-free predictor framework performs a frequency-domain study as a first step to understand the performance characteristics of the predictor. Specifically, this analysis reveals the relationship between the design parameter of the predictor, time delay, and steady-state performance. This helps establish the fundamental performance limitations of the predictor beyond a certain frequency determined by the time delay. Figure 47 illustrates the signal which has transmission delay corrected by the proposed modified predictor method, and then go to the controller.

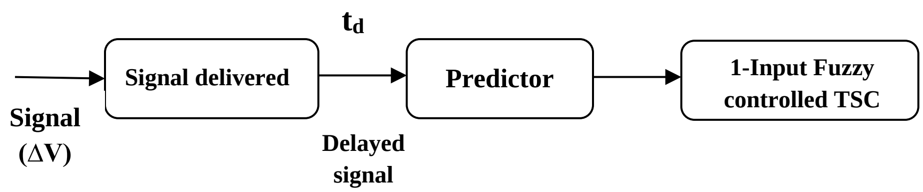

Figure 47. Modified Predictor Model.

The flow diagram for the modified predictor method is shown in Figure 48. The algorithm of the predictor method can modify the delayed signal to the original curve before inputting it into controller. The versatility of the predictor method is that, it can adapt to any controllers. If the time delay is td, the predicted ΔV can be obtained from the measured point, previous measured point and changing rate [9]:

$$\Delta \mathrm{V}_{p} = \Delta \mathrm{V}_{previous} + t_d . \Delta V . c \tag{21}$$

$$\Delta V = \frac{\Delta V_k - \Delta V_{(k-1)}}{\Delta t} \tag{22}$$

where p is the predicted point, k is measured point, c is a constant and ΔV is changing rate of the input to the controller. Here c is 0.25 that has been determined by trial and error.

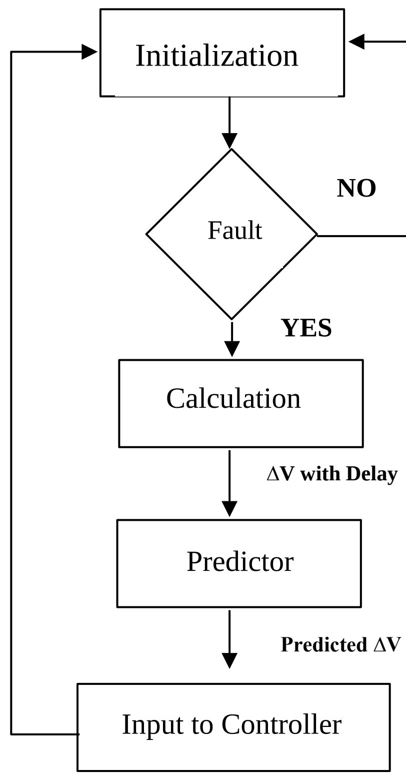

Figure 48. Flowchart diagram of the Modified Predictor Method.

D. Simulation Results & Discussion

In this work, both effects of communication delays and minimization of negative effects of the delays on the performance of the TSC controller for the power quality improvement of the hybrid grid are investigated. Simulations have been performed by using the Matlab/Simulink software.

i. Effect of Time Delay Without Minimization Methods

In this work, at first the impact of time delays on the performance of single-input fuzzy controlled TSC was explored. Based on the Table XVII, five different amounts of latency are considered, such as 100 ms, 200 ms, 350 ms, 500 ms and 700 ms. It was found that, increase in the time delay of the controller signal diminishes the performance of the controller. Figures 49-50 show the response of voltage at the PCC for a permanent 3LG and 1LG fault at F3 point with no controller, controller without delay and controller with 700 ms delay. Table XVIII shows the voltage indices for the 3LG permanent fault at points F1, F2, and F3. The indices in Table XVIII show that the time delay diminishes the performance of the TSC controller.

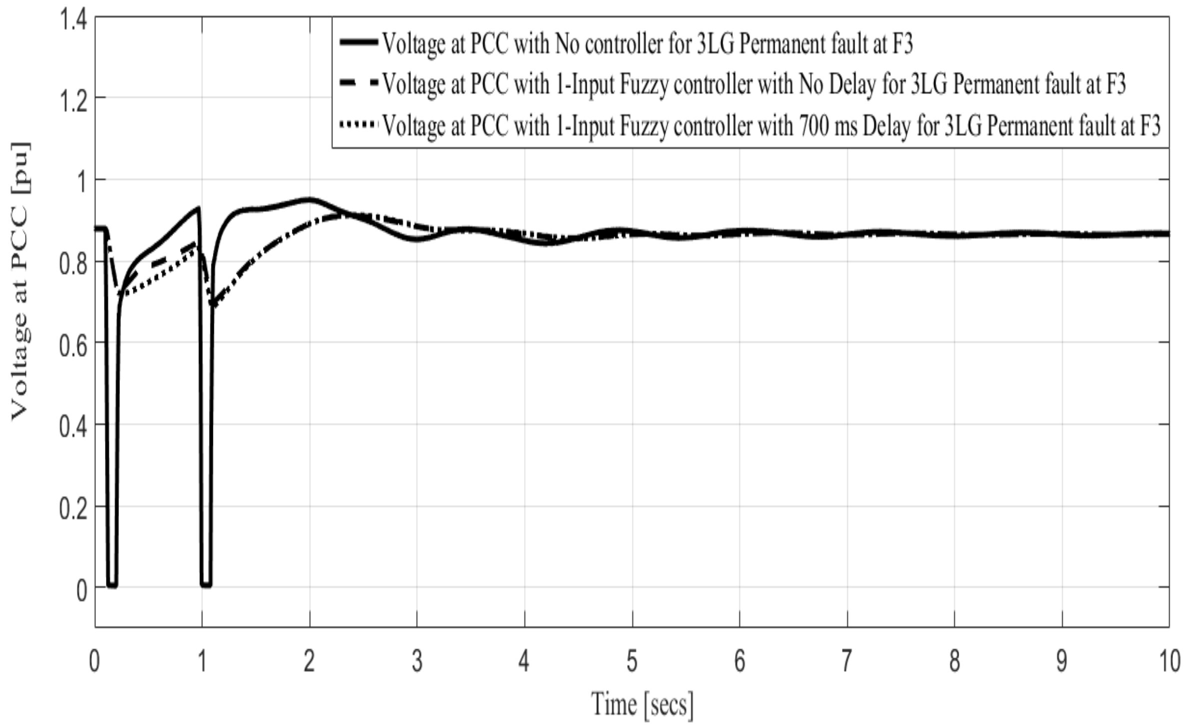

Figure 49. Voltage at PCC for 3LG Permanent fault at F3.

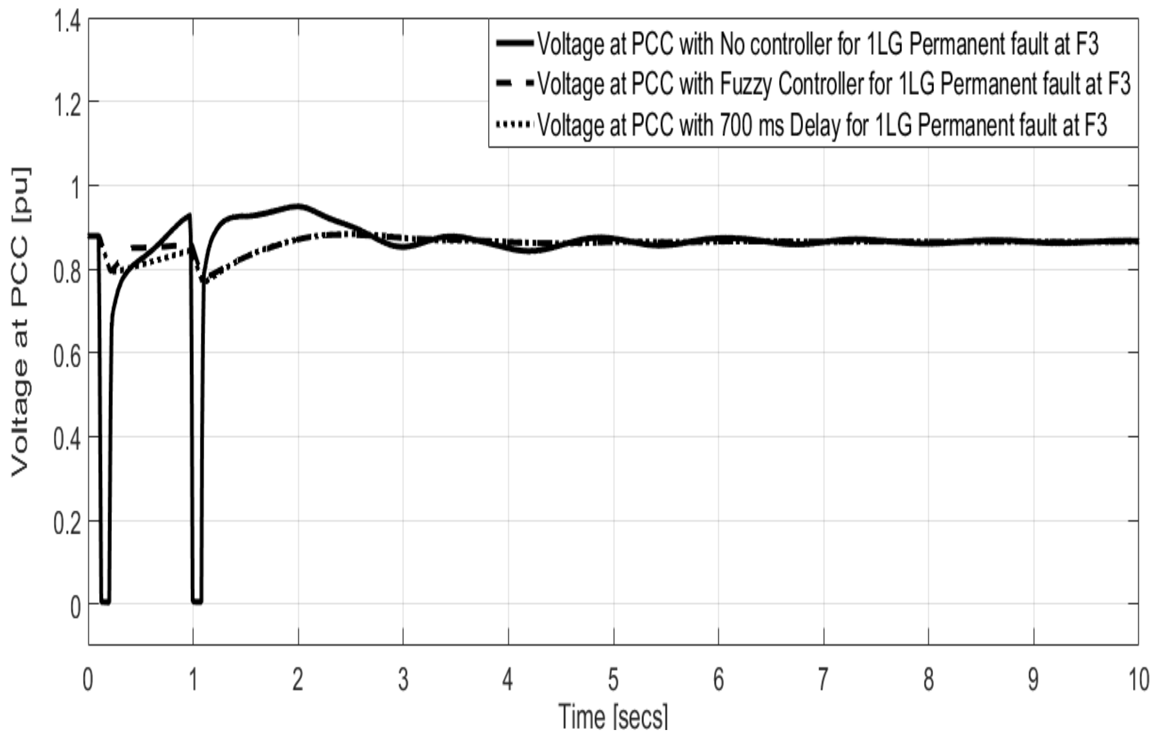

Figure 50. Voltage at PCC for 1LG Permanent fault at F3.

Table XVIII: Voltage indices

Fault Type	Fault point	No Controller	1-Input Fuzzy	1-Input Fuzzy +700ms delay
3LG Perm	F1	0.3479	0.2123	0.3112
	F2	0.2475	0.1001	0.1535
	F3	0.3905	0.3663	0.3815

ii. Effectiveness of Proposed Minimization Methods in terms of Voltage Index, V_{index}

To evaluate the effectiveness of the proposed delay minimization methods, the voltage index, V_{index} mentioned in (17) has been considered. The lower value of the index indicates the better system performance.

Tables XIX-XX show the values of voltage indices at the PCC in case of the modified predictor and fuzzy controlled delay minimization methods for temporary and permanent

3LG and 1LG faults, respectively, at points F1, F2 and F3 of the power system with 700 ms, 500 ms, 350 ms, 200 ms and 100 ms delays. From the indices it is shown that the fuzzy controlled method and predictor method minimize the delay effects and improve the power quality of the system. It is also seen that, in most cases the fuzzy controlled method works better than the modified predictor method.

Table XIX: Voltage Indices at PCC for 3LG Temporary and Permanent Faults

Delay Value	Fault Type	Fault Point	Voltage Indices at PCC		
			No compensation	Predictor Method	2 Input Fuzzy
700 ms	3LG Temp	F1	0.2437	0.2101	0.2103
		F2	0.1420	0.1146	0.1170
		F3	0.2297	0.1965	0.1964
	3LG Perm	F1	0.3112	0.3110	0.3001
		F2	0.1535	0.1405	0.1389
		F3	0.3815	0.3685	0.3681
500 ms	3LG Temp	F1	0.2436	0.2095	0.2107
		F2	0.1320	0.1245	0.1212
		F3	0.2297	0.1986	0.1972
	3LG Perm	F1	0.3478	0.3108	0.3011
		F2	0.1535	0.1498	0.1381
		F3	0.3905	0.3715	0.3689
350 ms	3LG Temp	F1	0.2437	0.2099	0.2103
		F2	0.1452	0.1356	0.1317
		F3	0.2297	0.1978	0.1964
	3LG Perm	F1	0.3479	0.3105	0.3100
		F2	0.1534	0.1479	0.1389
		F3	0.3905	0.3704	0.3681
200 ms	3LG Temp	F1	0.2437	0.2096	0.2108
		F2	0.1421	0.1147	0.1163
		F3	0.2296	0.1968	0.1957
	3LG Perm	F1	0.3478	0.3104	0.3117
		F2	0.2345	0.2278	0.2143
		F3	0.3905	0.3799	0.3706
100 ms	3LG Temp	F1	0.2263	0.2096	0.2078
		F2	0.1273	0.1146	0.1118
		F3	0.2165	0.1976	0.1961
	3LG Perm	F1	0.3301	0.3104	0.3084
		F2	0.1470	0.1298	0.1229
		F3	0.3843	0.3702	0.3694

Table XX: Voltage Indices at PCC for 1LG Temporary and Permanent Faults

Delay Value	Fault Type	Fault Point	Voltage Indices at PCC		
			No compensation	Predictor Method	2 Input Fuzzy
700 ms	1LG Temp	F1	0.1518	0.1461	0.1465
		F2	0.1092	0.0949	0.0910
		F3	0.1115	0.1091	0.1070
	1LG Perm	F1	0.1903	0.1864	0.1879
		F2	0.0888	0.0850	0.0810
		F3	0.2355	0.2286	0.2249
500 ms	1LG Temp	F1	0.1520	0.1460	0.1426
		F2	0.1092	0.1085	1.075
		F3	0.1115	0.1087	0.1024
	1LG Perm	F1	0.1903	0.1805	0.1812
		F2	0.0803	0.0775	0.0771
		F3	0.2355	0.2251	0.2145
350 ms	1LG Temp	F1	0.1520	0.1414	0.1450
		F2	0.0918	0.0874	0.8541
		F3	0.1036	0.1009	0.0987
	1LG Perm	F1	0.1903	0.1852	0.1879
		F2	0.0803	0.0789	0.0734
		F3	0.2355	0.2295	0.2289
200 ms	1LG Temp	F1	0.1546	0.1513	0.1501
		F2	0.1099	0.0949	0.0954
		F3	0.1114	0.1067	0.1090
	1LG Perm	F1	0.1903	0.1817	0.1860
		F2	0.1083	0.0984	0.0896
		F3	0.2354	0.2296	0.2224
100 ms	1LG Temp	F1	0.1521	0.1423	0.1389
		F2	0.1098	0.0968	0.0915
		F3	0.1081	0.1054	0.1023
	1LG Perm	F1	0.1903	0.1852	0.1879
		F2	0.1089	0.0918	0.0896
		F3	0.2424	0.2311	0.2264

Tables XXI-XXII show the voltage indices of wind generators in case of the modified predictor and fuzzy controlled delay minimization methods for temporary and permanent 3LG and 1LG faults, respectively, at points F1, F2 and F3 of the power system with 700 ms, 500 ms, 350 ms, 200 ms and 100 ms delays. From the indices it is shown that the fuzzy controlled method and predictor method minimize the delay effects and improve the power quality of the system. It is also seen that, in most cases the fuzzy controlled method works better than the modified predictor method.

Table XXI: Voltage Indices of Wind Generator for 3LG Temporary and Permanent Faults

Delay value	Fault Type	Fault Point	Voltage Indices of Wind Generator		
			No compensation	Predictor method	Fuzzy method
700 ms	3LG Temp	F1	0.2227	0.1929	0.1923
		F2	0.1313	0.1112	0.1110
		F3	0.2028	0.1723	0.1727
	3LG Perm	F1	0.2758	0.2751	0.2735
		F2	0.1395	0.1341	0.1332
		F3	0.3370	0.3200	0.3199
500 ms	3LG Temp	F1	0.2228	0.1917	0.1921
		F2	0.1318	0.1110	0.1105
		F3	0.2027	0.1742	0.1721
	3LG Perm	F1	0.3108	0.2749	0.2756
		F2	0.1393	0.1245	0.1214
		F3	0.3372	0.3228	0.3195
350 ms	3LG Temp	F1	0.2225	0.1920	0.1922
		F2	0.1313	0.1111	0.1110
		F3	0.2031	0.1947	0.1727
	3LG Perm	F1	0.3105	0.2753	0.2742
		F2	0.1395	0.1295	0.1230
		F3	0.3370	0.3232	0.3197
200 ms	3LG Temp	F1	0.2230	0.1914	0.1913
		F2	0.1314	0.1112	0.1102
		F3	0.2029	0.1723	0.1732
	3LG Perm	F1	0.3106	0.2749	0.2750
		F2	0.3415	0.3321	0.3189
		F3	0.3373	0.3194	0.3209
100 ms	3LG Temp	F1	0.2060	0.1914	0.1910
		F2	0.1201	0.1111	0.1122
		F3	0.1877	0.1742	0.1703
	3LG Perm	F1	0.2933	0.2746	0.2741
		F2	0.1569	0.1395	0.1378
		F3	0.3326	0.3221	0.3192

Table XXII: Voltage Indices of Wind Generator for 1LG Temporary and Permanent Faults

Delay Value	Fault Type	Fault Point	Voltage Indices of Wind Generator		
			No compensation	Predictor Method	2 Input Fuzzy
700 ms	1LG Temp	F1	0.1321	0.1222	0.1216
		F2	0.1085	0.0993	0.0962
		F3	0.0910	0.0896	0.0886
	1LG Perm	F1	0.1495	0.1433	0.1428
		F2	0.1074	0.1015	0.0986
		F3	0.1858	0.1703	0.1674
500 ms	1LG Temp	F1	0.1321	0.1223	0.1137
		F2	0.0855	0.0841	0.0840
		F3	0.1098	0.0963	0.0945
	1LG Perm	F1	0.1497	0.1434	0.1417
		F2	0.1073	0.0894	0.0853
		F3	0.1015	0.1571	0.1526
350 ms	1LG Temp	F1	0.1317	0.1275	0.1216
		F2	0.1054	0.0993	0.0845
		F3	0.1075	0.0943	0.0812
	1LG Perm	F1	0.1495	0.1396	0.1329
		F2	0.1096	0.0894	0.0785
		F3	0.1674	0.1523	0.1513
200 ms	1LG Temp	F1	0.1365	0.1345	0.1311
		F2	0.1017	0.0991	0.0856
		F3	0.1046	0.0965	0.0845
	1LG Perm	F1	0.1497	0.1457	0.1482
		F2	0.0952	0.0894	0.0724
		F3	0.1965	0.1850	0.1674
100 ms	1LG Temp	F1	0.1339	0.1278	0.1245
		F2	0.1018	0.1007	0.0875
		F3	0.0958	0.0895	0.0849
	1LG Perm	F1	0.1495	0.1396	0.1329
		F2	0.0937	0.0916	0.0755
		F3	0.753	0.1672	0.1655

iii. Effectiveness of Proposed Minimization Methods in Terms of Plots

Figures 51-54 show the voltage responses at the PCC and voltage response of wind generator due to a 3LG temporary and permanent fault at point F3 for 700 ms latency. From the responses it is seen that the delay minimization methods work well and improve the power quality of the system. However, in most cases the fuzzy logic controlled based method performs better than the modified predictor method in improving the power quality of the hybrid grid.

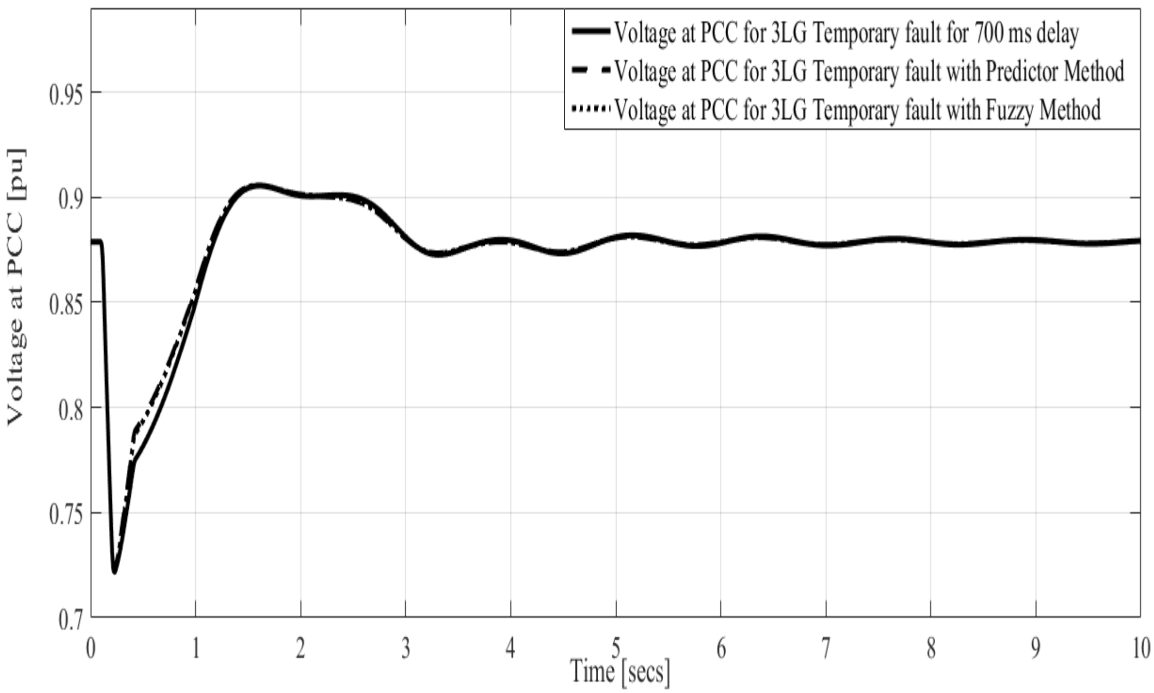

Figure 51. Voltage at PCC for 3LG Temporary fault at F3

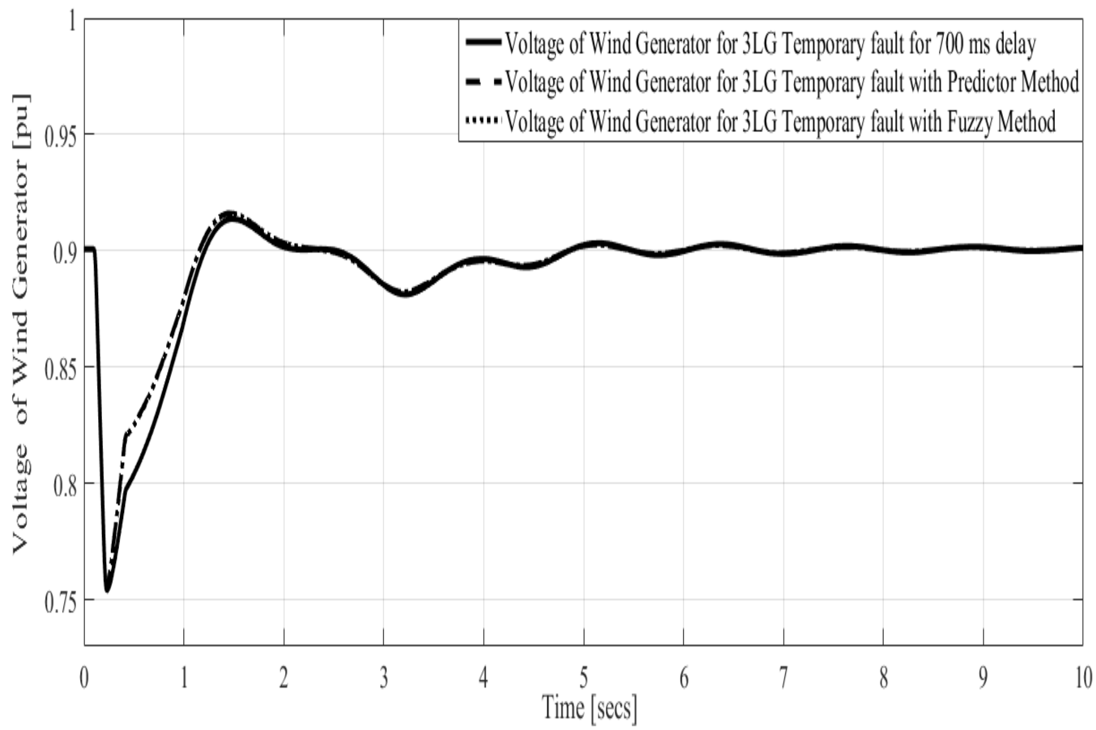

Figure 52. Voltage of Wind Generator for 3LG Temporary fault at F3

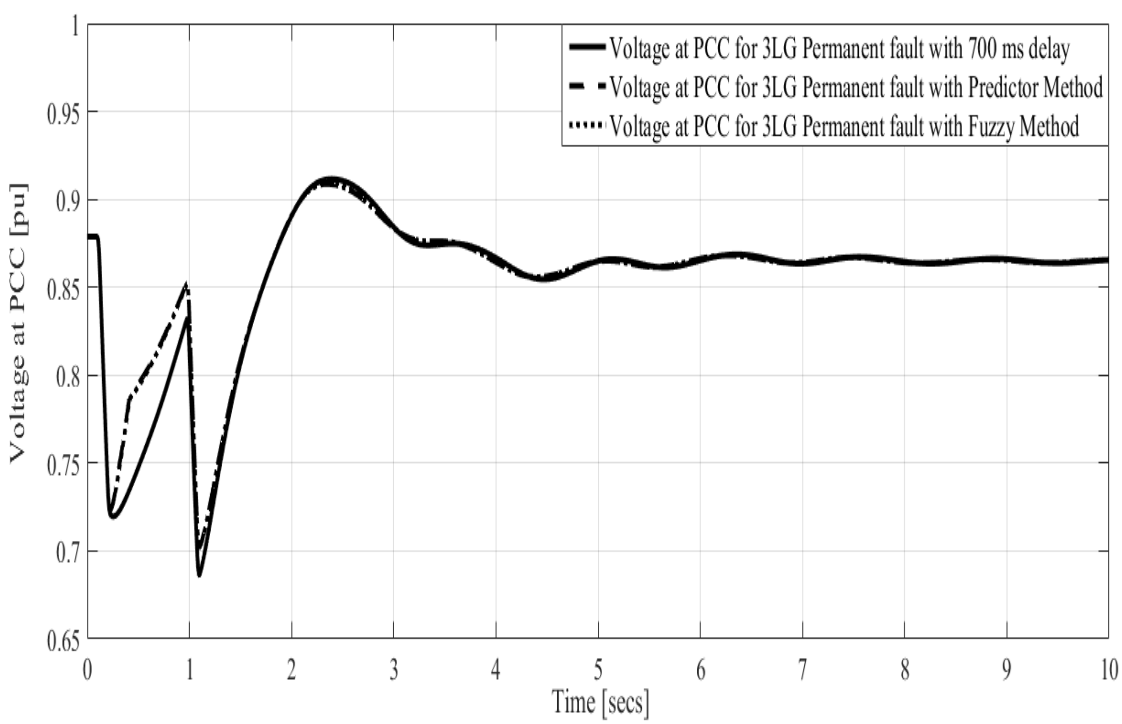

Figure 53. Voltage at PCC for 3LG Permanent fault at F3

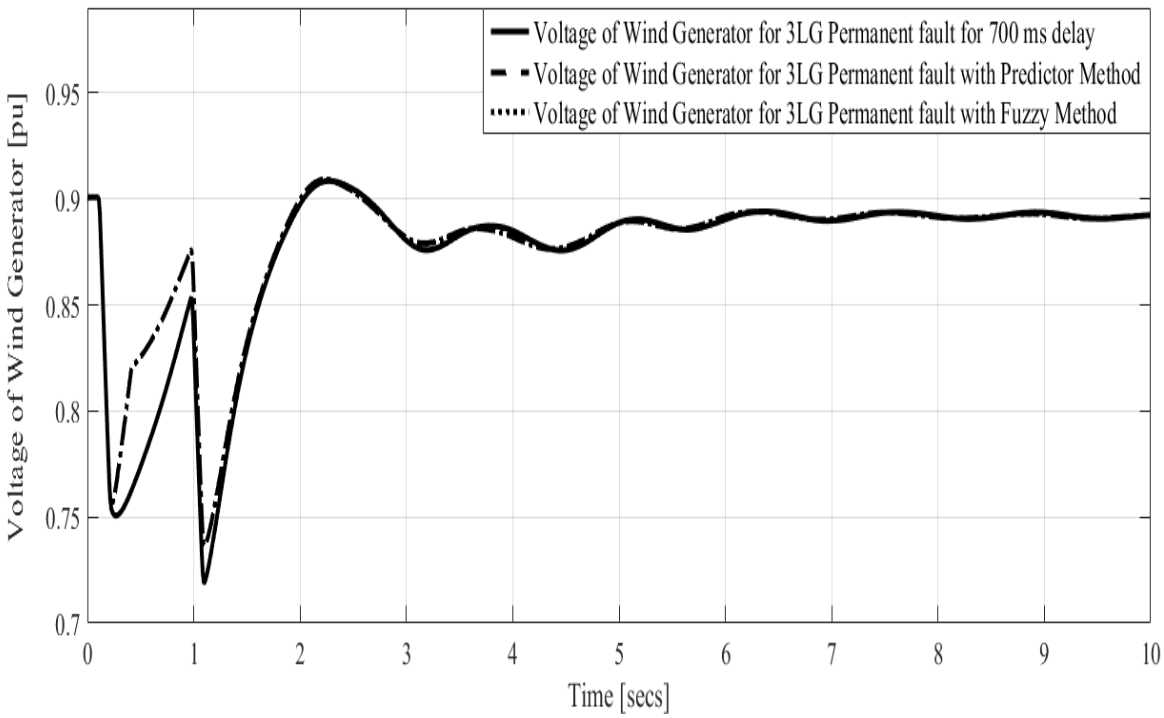

Figure 54. Voltage of Wind Generator for 3LG Permanent fault at F3

Figures 55-58 show the voltage responses at the PCC, voltage response of wind generator due to a 1LG temporary and permanent fault at point F3 for 700 ms latency. From the responses it is seen that the delay minimization methods work well and improve the power quality of the system. The results also show that in most cases the fuzzy logic controlled based method performs better than the modified predictor method.

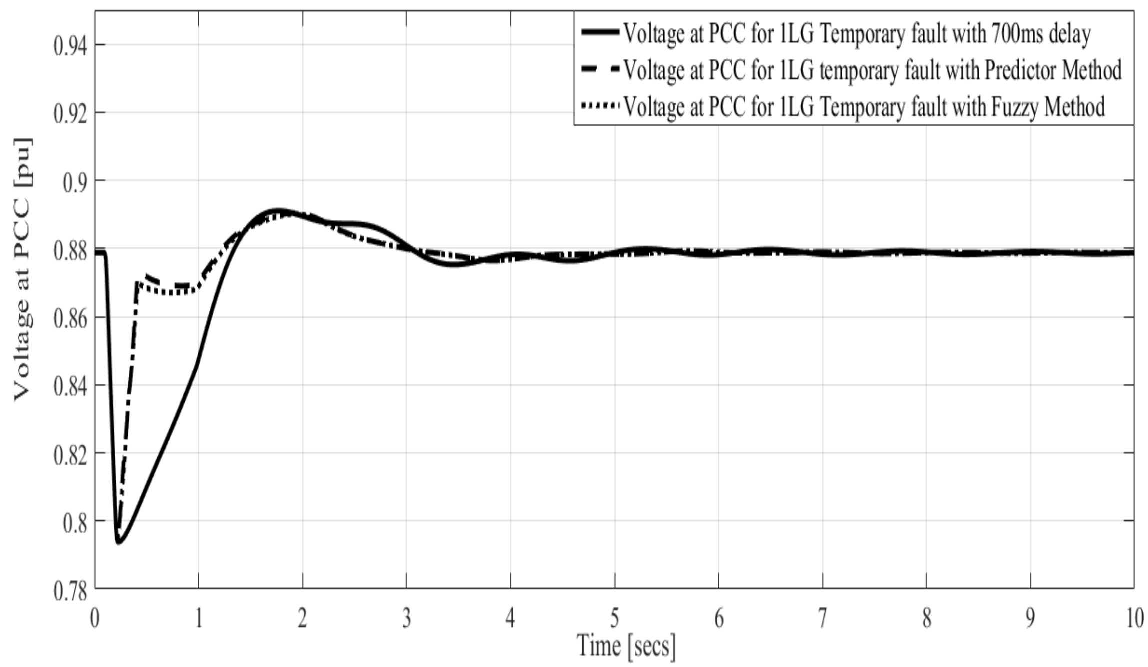

Figure 55. Voltage at PCC for 1LG Temporary fault at F3

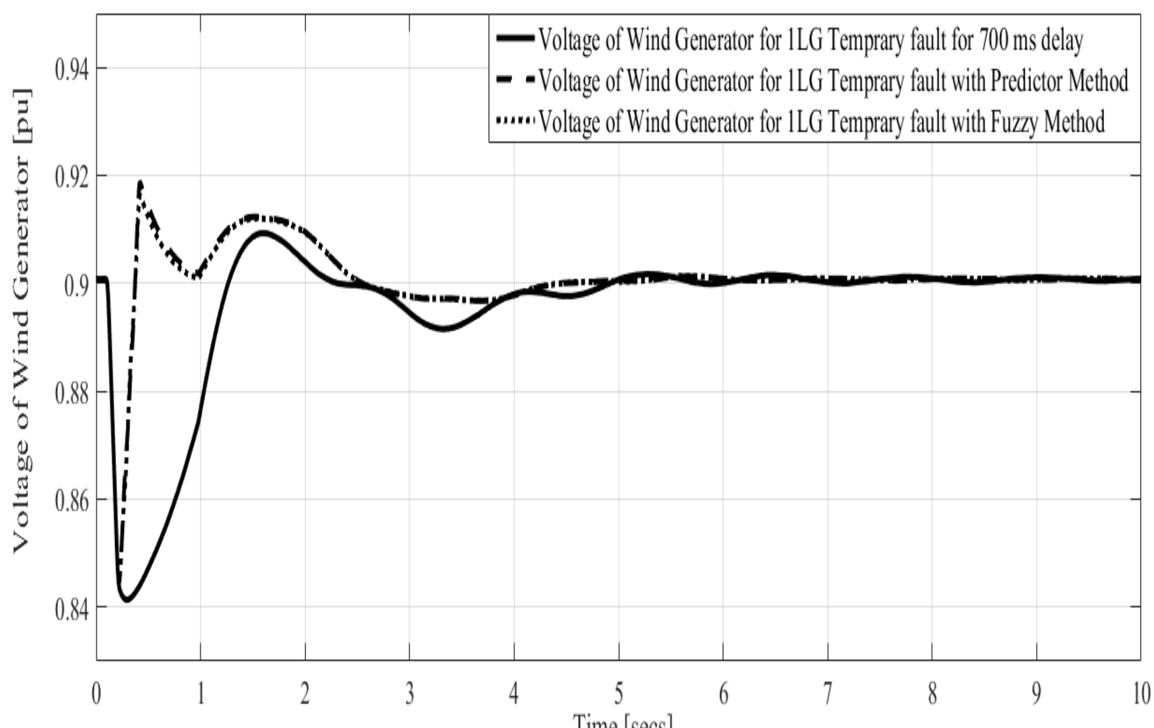

Figure 56. Voltage of Wind Generator for 1LG Temporary fault at F3

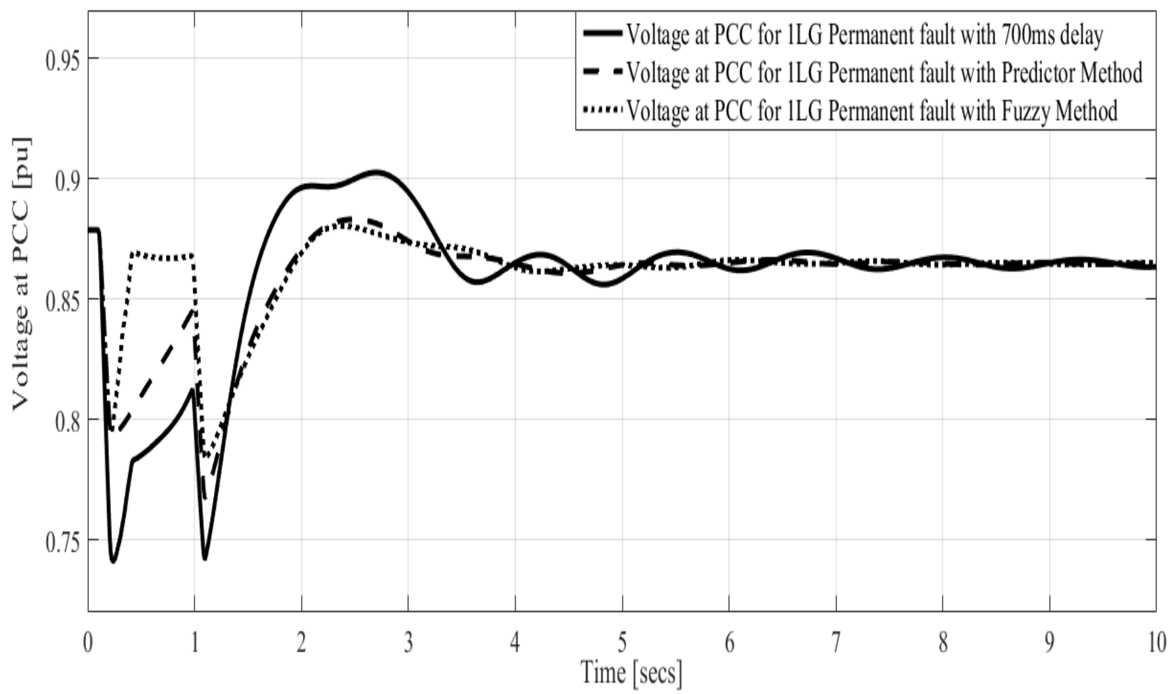

Figure 57. Voltage at PCC for 1LG Permanent fault at F3

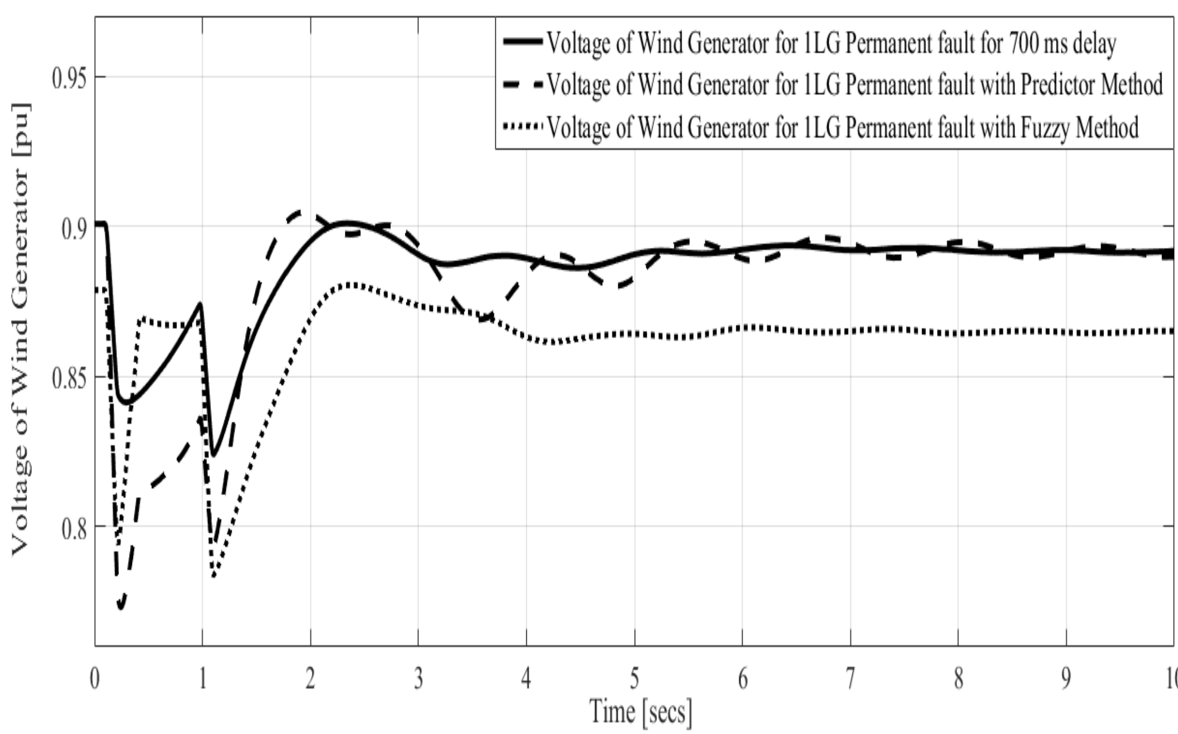

Figure 58. Voltage of Wind Generator for 1LG Permanent fault at F3

iv. Effectiveness of Proposed Minimization Methods in Terms of THD

The THD of the PCC voltage is calculated by using the equation (1). Tables XXIII-XXIV show the values of THD in case of predictor method and 2-input fuzzy delay minimization methods for temporary and permanent 3LG and 1LG faults at points F1, F2 and F3 of the power system with 700ms, 500ms, 350ms, 200ms and 100ms delays. From the indices it is shown that the fuzzy controlled method and the predictor method minimize the delay effects and improve the power quality of the system. However, in most cases the fuzzy logic controlled based method performs better than the modified predictor method.

Table XXIII: Total Harmonic Distortion at PCC for 3LG Temporary and Permanent faults

Fault Type		Fault Point	Total Harmonic Distortion at PCC		
			No Compensation	Predictor Method	2 Input Fuzzy
700 ms	3LG Temp	F1	3.129	2.213	1.840
		F2	3.172	2.712	1.635
		F3	1.087	0.9870	1.010
	3LG Perm	F1	2.270	2.026	1.687
		F2	1.402	1.213	1.145
		F3	2.388	2.241	1.683
500 ms	3LG Temp	F1	2.342	1.809	2.258
		F2	2.972	2.566	2.574
		F3	3.122	2.985	2.456
	3LG Perm	F1	1.166	1.147	1.1345
		F2	2.244	2.217	1.969
		F3	1.974	1.321	1.419
350 ms	3LG Temp	F1	5.710	2.694	2.087
		F2	3.419	2.987	1.778
		F3	3.529	3.202	3.072
	3LG Perm	F1	1.478	1.131	1.102
		F2	1.845	1.456	1.258
		F3	3.451	1.098	1.962
200 ms	3LG Temp	F1	2.016	1.294	1.944
		F2	1.112	1.108	1.105
		F3	1.987	1.868	1.641
	3LG Perm	F1	1.715	1.148	1.126
		F2	3.589	3.368	1.541
		F3	2.737	1.113	1.168
100 ms	3LG Temp	F1	4.618	3.918	3.266
		F2	2.608	2.232	1.918
		F3	1.676	1.547	1.456
	3LG Perm	F1	2.270	1.616	1.471
		F2	3.827	2.456	2.136
		F3	1.767	1.017	1.034

Table XXIV: Total Harmonic Distortion at PCC for 1LG Temporary and Permanent faults

Delay Value	Fault Type	Fault Point	Total Harmonic Distortion at PCC		
			No compensation	Predictor Method	2 Input Fuzzy
700 ms	1LG Temp	F1	2.912	1.343	1.072
		F2	2.140	2.083	1.163
		F3	1.896	1.264	1.185
	1LG Perm	F1	2.444	2.117	2.015
		F2	4.546	4.256	4.025
		F3	1.139	1.064	1.046
500 ms	1LG Temp	F1	2.334	2.034	1.674
		F2	3.922	3.073	2.569
		F3	2.604	2.224	2.156
	1LG Perm	F1	1.030	0.7230	0.8413
		F2	2.880	2.456	2.123
		F3	3.208	3.156	3.063
350 ms	1LG Temp	F1	1.879	1.136	1.125
		F2	1.485	1.236	1.115
		F3	2.891	2.693	2.505
	1LG Perm	F1	2.866	2.162	2.009
		F2	3.236	2.671	2.251
		F3	3.945	2.485	2.098
200 ms	1LG Temp	F1	2.623	1.742	1.788
		F2	4.589	2.949	2.063
		F3	4.280	3.001	1.789
	1LG Perm	F1	2.583	2.411	2.392
		F2	3.423	2.786	1.587
		F3	2.769	2.660	2.333
100 ms	1LG Temp	F1	2.258	2.145	2.085
		F2	1.756	1.643	1.588
		F3	1.266	1.1152	1.1045
	1LG Perm	F1	2.866	2.162	2.009
		F2	1.958	1.827	1.609
		F3	1.856	1.389	1.245

E. Conclusion

This chapter analyzes the effects of time delay on a hybrid power grid and proposes two methods to minimize the adverse effects of time delays on the power quality enhancement. Both balanced and unbalanced temporary and permanent faults at different locations in the power network have been considered. The following conclusions can be made based on the simulation results.

1. The proposed methods such as the two inputs based fuzzy controller and Modified Predictor Method are effective in reducing the negative effects of time delay on the power quality improvement of the hybrid power system.
2. The fuzzy controlled method performs better than the modified predictor method in most of the cases.
3. In some cases, like the 2LG temporary fault at points F2 and F1, the performance of the Modified Predictor method is better than that of the 2-Input Fuzzy controller method.

V. CYBERSECURITY ISSUES AND SOLUTIONS FOR THE HYBRID GRID COMPONENTS

A. Introduction

Cybersecurity has been a crucial issue for the modern power grid that needs to be solved. This chapter investigates the effects of cyber-attacks on the ESS, GSC of the wind generator, VSC of the PV system, and the AVR of the synchronous generator located in a hybrid power grid. Also, this chapter proposes two new methods based on NL controller and PI controller to mitigate the adverse effects of cyber-attacks on the mentioned GSC and VSC components, and a new detection and mitigation technique based on the voltage threshold for the ESS. To test the effectiveness of the proposed methods, two types of cyber-attacks, namely the DDoS and FDI, targeting the controllers of the ESS, GSC and VSC have been considered. Moreover, a voltage index has been used to numerically evaluate the performance of the proposed controllers. Simulations have been performed by using the Matlab/Simulink software.

B. Hybrid Power Model System

This work uses the hybrid power system model depicted in Fig. 59 for cyber security analysis. It consists of one SG [4MW]-based single machine infinite-bus system, to which one PV farm of 2 MW, one DFIG-based wind farm of 2 MW and one SES of 2 MW capacity are integrated through a short distribution line. These energy sources are delivering power to the power grid through double circuit distribution lines. The SG is equipped with AVR and GOV control systems [208]. The SG parameters used for the design consideration are available in [208].

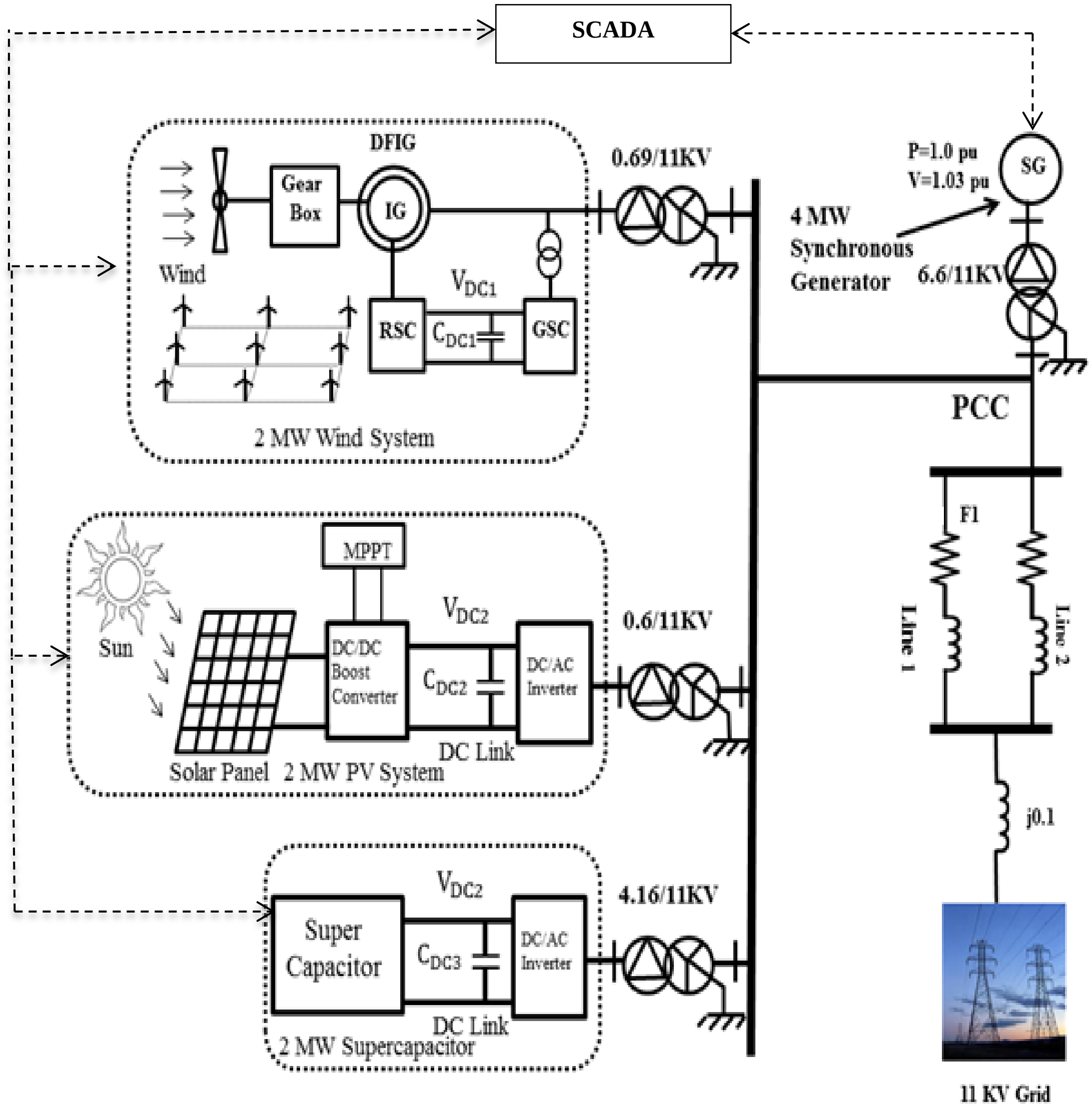

Energy Storage System

Figure 59. Hybrid grid system.

i. Wind Generator

Although a practical wind power station consists of many generators, it is considered to contain a large equivalent aggregated single generator. An equivalent aggregated variable-speed wind turbine (VSWT) through an equivalent gearbox [14] drives the wind generator. The DFIG stator winding is connected to the grid by 0.69/11kV step-up transformer, whereas the rotor winding is connected to the low voltage side of the step-up transformer through the power electronic converters, namely RSC and GSC and a transformer. A dc link is connected between the RSC (Fig. 17) and GSC (Fig. 16). The GSC is used to maintain a constant dc-link voltage and regulate the stator voltage. The modelling of the DFIG is already explained in chapter III.

ii. PV

The PV plant consists of many PV modules connected in series-parallel combination to attain the desired power level, and it is connected to the PCC by a boost converter [233] [234] and an equivalent aggregated dc to ac inverter [235]. A PV system connected to the grid consists of a PV array, a maximum power point tracking technique (MPPT), which is used to extract maximum power from the PV arrays. The perturb and observe (P&O) based MPPT [236] for the PV is implemented on the boost converter for extracting the maximum PV power at all environment conditions. Large PV plants are composed of several PV panels or modules. In this work, 50 KC200GT PV modules are connected in series per string, and 200 parallel strings [237].

Figure 60 shows the equivalent circuit of individual PV cell that includes one diode, one shunt resistance, R_{sh} (with high value in KΩ range) representing the leakage current loss, and the series resistance, R_s (very small value) that represents the losses due to metallic contacts (grid contacts, current collecting bus, etc.).

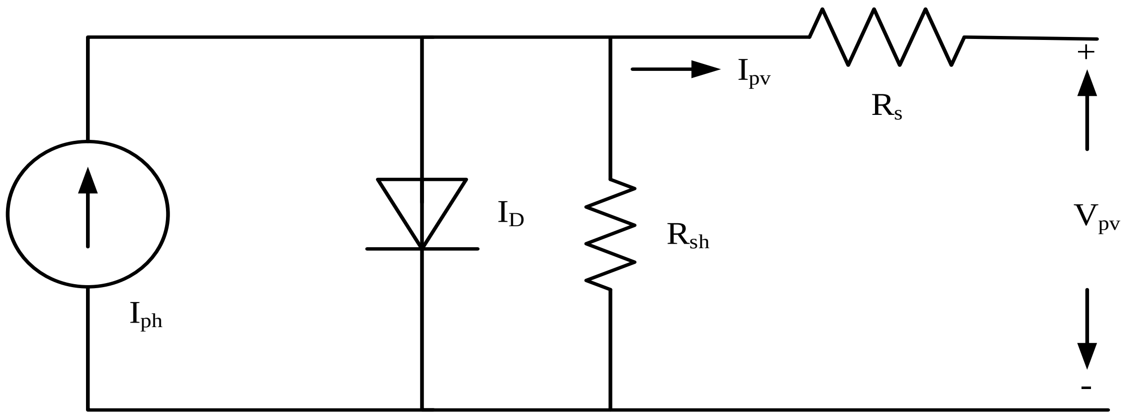

Figure 60. Equivalent circuit of solar cell.

The current produced by the PV can be represented by the following equations [238] [239]:

$$I = I_L - I_D - I_{sh} \tag{23}$$

$$I_D = I_0 \left\{ exp\left[\frac{qV_D}{nkT}\right] - 1 \right\} \tag{24}$$

$$I = I_L - I_0 \left\{ exp\left[\frac{qV_D}{nkT}\right] - 1 \right\} - \frac{V_D}{R_{sh}} \tag{25}$$

where I_L is the photo generated current, I_D is the current across the diode, I_{sh} is the shunt current, I_0 is the reverse saturation current, n is the diode ideality factor (1 for an ideal diode), q is elementary charge, k is Boltzmann's constant ($1.38*10^{-23}$ J/K), T is absolute temperature, and V_D is the diode voltage.

The voltage produced at the terminal of the PV cell can be represented by:

$$V = V_D - IR_S \tag{26}$$

$$V = n\frac{kT}{q}ln\left(\frac{I_L - I}{I_0} + 1\right) - IR_S \tag{27}$$

The DC link voltage V_{DC}, i.e., the voltage output of the boost converter is obtained depending upon the duty cycle, *D*, and the PV terminal voltage, V_{PV}, as represented by the following equation [238]:

$$V_{DC} = \frac{V_{PV}}{1 - D} \tag{28}$$

iii. Supercapacitor Energy Storage (SES) system

To maintain the efficient flow of power, utility operators must attempt to steady the supply and demand consistently to meet peak demand. The integration of renewable resources has helped serve the problem of demand [240]. But the intermittent nature of these resources adds to the grid's need for frequency, power and voltage regulations. Energy storage can compensate those fluctuations in power, frequency and voltage, and thus deliver smoothed power to the customer. There are several types of energy storage available, battery energy storage being the most commonly used because of its high energy density [241]. But batteries take a long time to discharge and recharge, which limits their ability to deliver power. In applications demanding high power, over-engineering the battery will rarely be the right solution, and will typically result in increased size, weight, and cost, and/or reduced cycle life and energy.

Supercapacitors combine the energy storage properties of batteries with the power discharge characteristics of capacitors. Supercapacitors are devices that can be used as energy storage systems, and have power densities and high energy, a large life expectancy and high efficiency, nearly 95% [242] [243] [244]. The possibility of fast charge and discharge without loss of efficiency, for thousands of cycles, makes the supercapacitor a suitable choice as the ESS [245] [246] [247]. Also, supercapacitors have the capacity to recharge in a very short time having a great facility to supply high and frequent power demand peaks.

To maintain constant power at the PCC, the SES of 2MW capacity is connected to the system using bi-directional buck- boost converter. While the SES can be used for power fluctuations minimization of the hybrid power system, in this work it has been used as the backup power only. In addition to renewables sources, the other important component of the hybrid grid system is the central control center, (i.e., the SCADA). It controls all the components in the system. It also facilitates bi-directional flow of information between the different controllers and itself.

C. Cyber Security Issues in Hybrid Grid Components

i. GSC Controller of Wind Generator

As the SCADA sends signals to the GSC controller for its functioning, any cyber-attacks can interfere with the signals and affect the working of the GSC. For example, the intruder can change the set point of V_{dc_ref} as shown in Fig. 16.

ii. VSC Controller of PV

The VSC controller of the PV as shown in Fig. 61, takes the DC link voltage V_{dc} and converts it into AC. The VSC control system [248] uses two control loops: an external control loop which regulates the DC link voltage and an internal control loop which regulates I_d and I_q grid currents (active and reactive current components). I_d current reference is the output of the DC voltage external controller. I_q current reference is set to zero to maintain unity power factor. V_d and V_q voltage outputs of the current controller are converted to three modulating signals U_{abc_ref} used by the Pulse Width Modulator (PWM) Generator.

However, since the SCADA sends signals to the VSC controller for its functioning, any cyber-attacks can interfere with the signals and affect the working of the VSC. For example, the intruder can change the set point of V_{del_ref} as shown in Fig. 61.

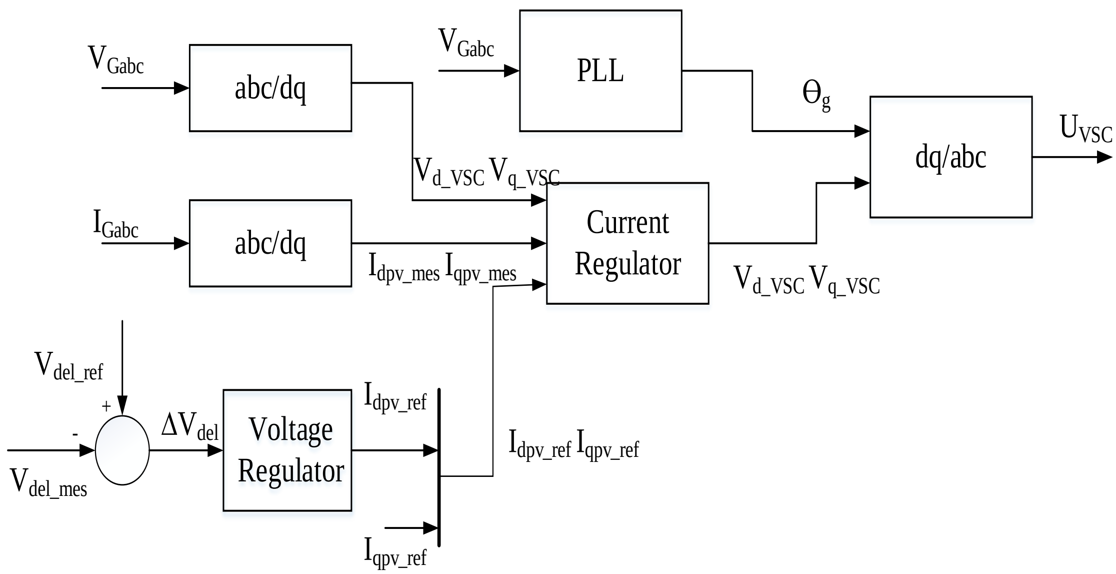

Figure 61. Control block of voltage source converter (VSC).

iii. AVR Controller of SG

The control system block of the automatic voltage regulator is shown in fig. 12. The SCADA communicates with the AVR and send necessary signals. Therefore, the controller of AVR can be under cyber-attacks. For example, the attacker can manipulate the E_{fdo} signal that can affect the generator terminal voltage as shown in Fig. 13.

iv. SES Controller

Figure 62 shows the control of SES system. Super-Capacitor exchanges power using a buck-boost type of power converter. The converter works in buck mode when the super-capacitor gets charged, and in boost mode the super-capacitor discharges. These varying functions occur because super-capacitor terminal potential is always expected to be less than the node side voltage. The DC link capacitor (dcCap) is used to limit voltage ripple during boost mode. In boost mode when the 'Discharge' IGBT is ON, it is the DC link capacitor that supplies energy to the grid while the super-capacitor is transferring energy to the inductor. When the 'Discharge' IGBT is OFF, the DC link capacitor is charged from the SES (the stored energy in L), and the DC link voltage increases. The design of the inductor and DC link capacitor is described elaborately in [249].

As shown in Fig. 62, the SES is connected to the SCADA through wires or wireless network. Therefore, it can be affected by cyber-attacks. For example, at any point in time, any set point of the SES system can be altered by the intruder which can make the SES fully disabled or function partially.

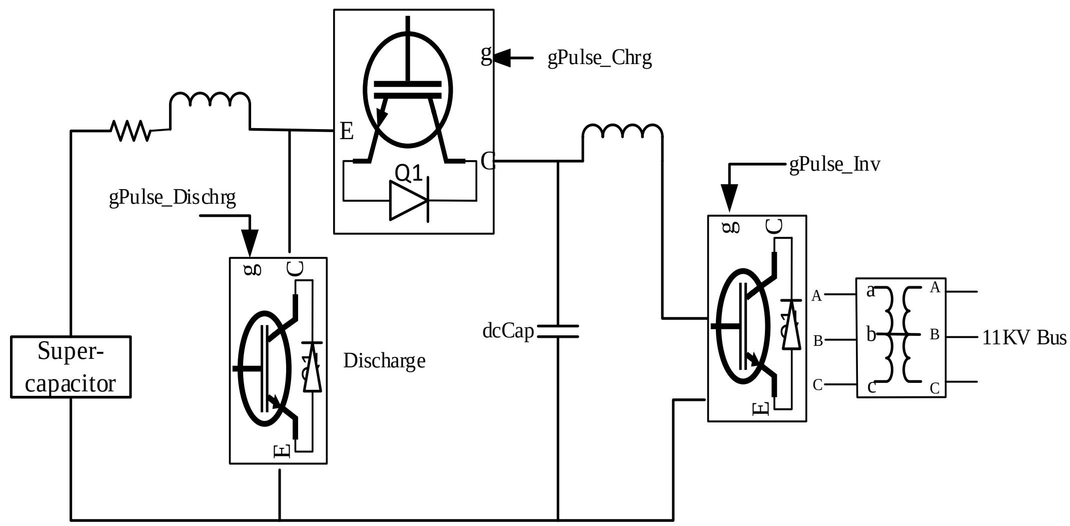

Figure 62. Control of supercapacitor energy storage.

D. Proposed Control Algorithms

All kinds of vulnerabilities in a power system have direct impact on the PCC voltage. So, our main objective is to regain the PCC voltage at its required level within the shortest possible time following cyber-attacks.

i. Control Algorithms for GSC, VSC and AVR

In this work, two types of controllers, such as a simple non-linear controller and a PI controller have been proposed to mitigate the adverse effects of cyber-attacks on the GSC of the DFIG, the VSC of the PV system and the AVR of the SG. Figure 63 shows the basic algorithm of the proposed detection and mitigation techniques. The input to the proposed controller is the PCC voltage. In the proposed detection and mitigation technique, the first step is to check the voltage deviation (ΔV_{pcc}) at the PCC. If there is any deviation, then it indicates either a network fault or a cyber-attack. The next step is to check the reference values of the different controller parameters like any change in reference DC voltage of the

GSC (V_{dc_ref}) of the wind generator, the change in reference DC voltage of the VSC (V_{del_ref}) of the PV system and the change in the reference voltage (E_{fdo}) of the AVR of the SG system. The changes in the reference values indicate cyber-attacks, and this constitutes the detection technique. The next section of the control algorithm is for mitigation of the adverse effects of cyber-attacks. When cyber-attack is detected, the controller for the mitigation of cyber-attacks is activated. The performance of the controller is constantly monitored and if the reference value returns at its original value, the controller is deactivated.

It is to note here that, after operation the controllers will be disconnected from the data cloud of SCADA system so that no intruder effect can hamper this controller. The controller will come into action for a very brief period and once the system regains its stability and quality, the controller will get disconnected from the network. The very limited time of operability will enable the controller to function securely.

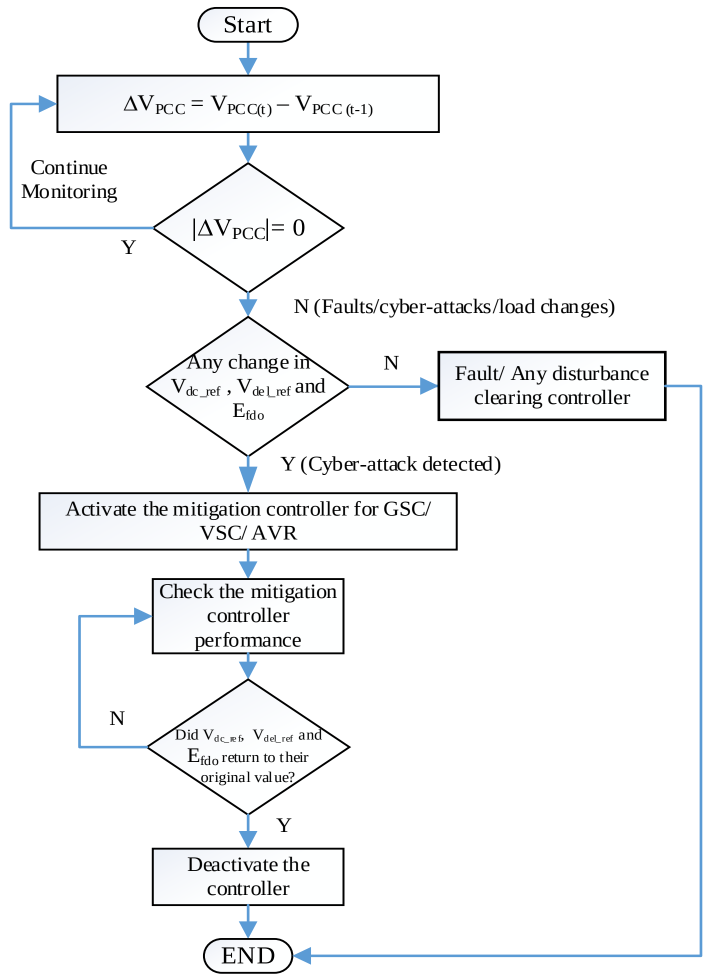

Figure 63. Proposed control algorithm for GSC of wind generator, the VSC of PV and the AVR of the SG

ii. Check the voltage deviation Control Algorithm for SES

For the proposed detection and mitigation technique for the SES, the first step is to check the voltage deviation (ΔV_{pcc}) at the PCC. If there is any deviation, then it indicates either a fault or a cyber-attack. The next step is to check the amount of P_{SES}. As the PV system switches off at night, the SES is on. The availability of 2 MW power is required. If the P_{SES} is 2MW with the required constant pulses for the insulated gate bipolar transistor (IGBT) of the VSC, but the ΔV_{pcc} is not zero, then it indicates a fault or other disturbance and the fault clearing controller is triggered. The cyber-attack could happen due to any change in the gate signal of IGBT of the VSC. When the IGBT gate signal is altered, the power output of the SES changes. Therefore, if the $P_{SES} < 2MW$ and the IGBT gate pulses are changed from their constant values, then it indicates a cyber-attack and accordingly the proposed mitigation technique is activated.

E. Proposed Mitigation Methods

i. Non-Linear Controller for GSC, VSC and AVR

As the power grid is highly non-linear, application of non-linear controllers in grid is highly preferred. This control action can be governed by any nonlinear differential equations or any other mathematical model. In this work, a simple nonlinear function has been used as shown in the following:

$$V_{dc\_ref(GSC)} = \left(k_1 \times |\Delta V_{pcc}|^2\right) \tag{29}$$

$$V_{del\_ref\,(VSC)} = \left(k_2 \times |\Delta V_{pcc}|^2\right) \tag{30}$$

$$E_{fdo(AVR)} = \left(k_3 \times |\Delta V_{pcc}|^2\right) \tag{31}$$

where k_1 , k_2 and k_3 are constant values and ΔV_{pcc} is the input to the controller. By tuning the values of k_1, k_2, and k_3 the required values of the $V_{dc\_ref(GSC)}$, $V_{del\_ref(VSC)}$ and $E_{dfo(AVR)}$ are obtained. The parameters have been set in such a way as the controller can handle any kind of voltage deviation from very high to very low. The parameters of the controller have been shown in Table XXV.

Table XXV: Parameter Values of the Non-Linear controller

Non-linear Controller			
Type of Attack	K_1 (GSC)	K_2 (VSC)	K_3 (AVR)
DDoS	0.000008	0.058	3500
FDI	1290	0.06009	2560

ii. PI Controller for GSC, VSC and AVR

The PI controller is one of the popular controllers that is being used extensively in industrial control. The transfer function that has been used for the PI controller in Laplace domain (s) is as follows:

$$V_{dc\_ref(GSC)} = |\Delta V_{pcc}| \left[K_{p1} + \frac{1}{s} K_{i1}\right] \quad (32)$$

$$V_{del\_ref(VSC)} = |\Delta V_{pcc}| \left[K_{p2} + \frac{1}{s} K_{i2}\right] \quad (33)$$

$$E_{fdo(AVR)} = |\Delta V_{pcc}| \left[K_{p3} + \frac{1}{s} K_{i3}\right] \quad (34)$$

where K_{p1}, K_{p2}, K_{p3}, K_{i1}, K_{i2} and K_{i3} are the proportional and integral gain of the PI controller, respectively. ΔV_{pcc} is the input to the controller and $V_{dc\_ref\ (GSC)}$, $V_{del\_ref\ (VSC)}$ and $E_{dfo(AVR)}$ are the output variable of the controller, respectively. The values of the parameters K_{p1}, K_{p2}, K_{p3}, K_{i1}, K_{i2} and K_{i3} are shown in Table XXVI. These values have been obtained by trial and error and they can handle any abrupt change in the input.

Table XXVI: Parameter Values of the PI controller

PI Controller						
Type of Attack	K_{p1} (GSC)	K_{p2} (VSC)	K_{p3} (AVR)	K_{i1} (GSC)	K_{i2} (VSC)	K_{i3} (AVR)
DDoS	0.09	0.008	100	0.06	0.028	0.95
FDI	10000	0.09	100	0.92	0.55	0.75

iii. Mitigation Technique for SES

The proposed mitigation technique for the SES monitors the power level of the energy storage and the IGBT gate signals. Any change in the gate signal value triggers the controller and overrides the signal sent from the SCADA. The gate signal is changed back to the required constant values and makes the value of the P_{ESS} equal to 2 MW.

F. Simulation Results & Discussion for the Effects and Mitigation of Cyber-Attacks on GSC, VSC and AVR

i. Effects and Mitigation of DDoS and FDI Cyber-Attack on GSC Controller of Wind Generator

For this scenario, it is assumed that the DDoS and FDI attack on the GSC of the wind generator occurs (i.e., V_{dc} reference value is changed) at 0.5 secs. The controller starts operation at 0.6 secs. Figures 64-65 show the DC link reference voltage (V_{dc_ref}) of the GSC with and without DDoS and FDI cyber-attack respectively. From the response, it is evident that the DDoS and FDI cyber-attack changes the dc reference voltage and deteriorates the performance of the system. Moreover, the proposed controllers could make the dc reference voltage back to its original value. For the DDoS and FDI attack on the GSC of the wind generator, the PI controller perform better than the Non-Linear controller.

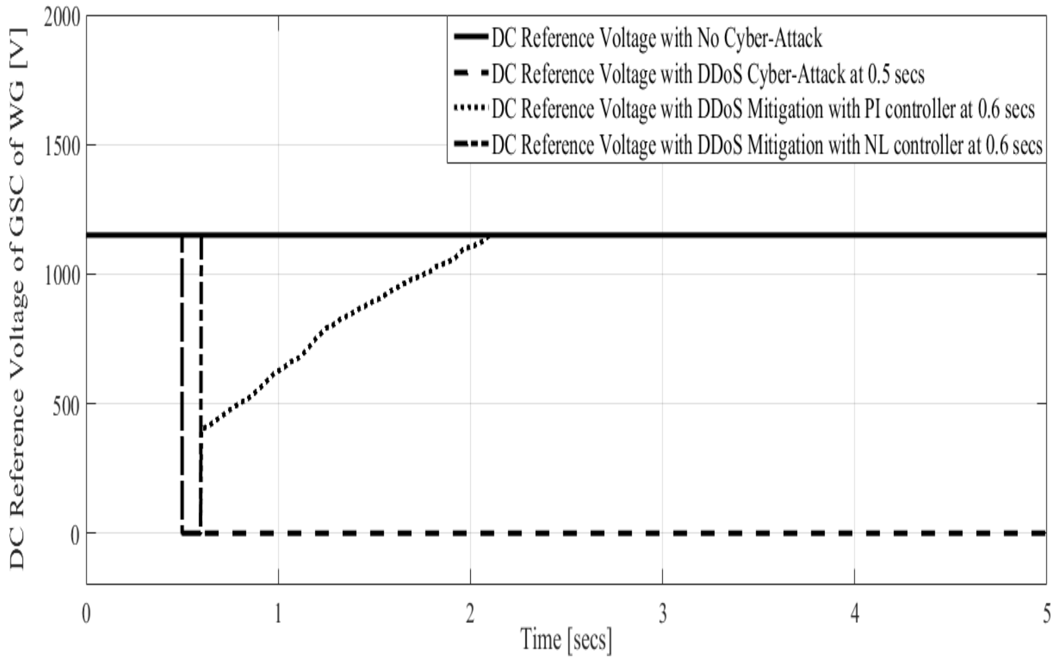

Figure 64. DC reference voltage for DDoS cyber-attack for GSC

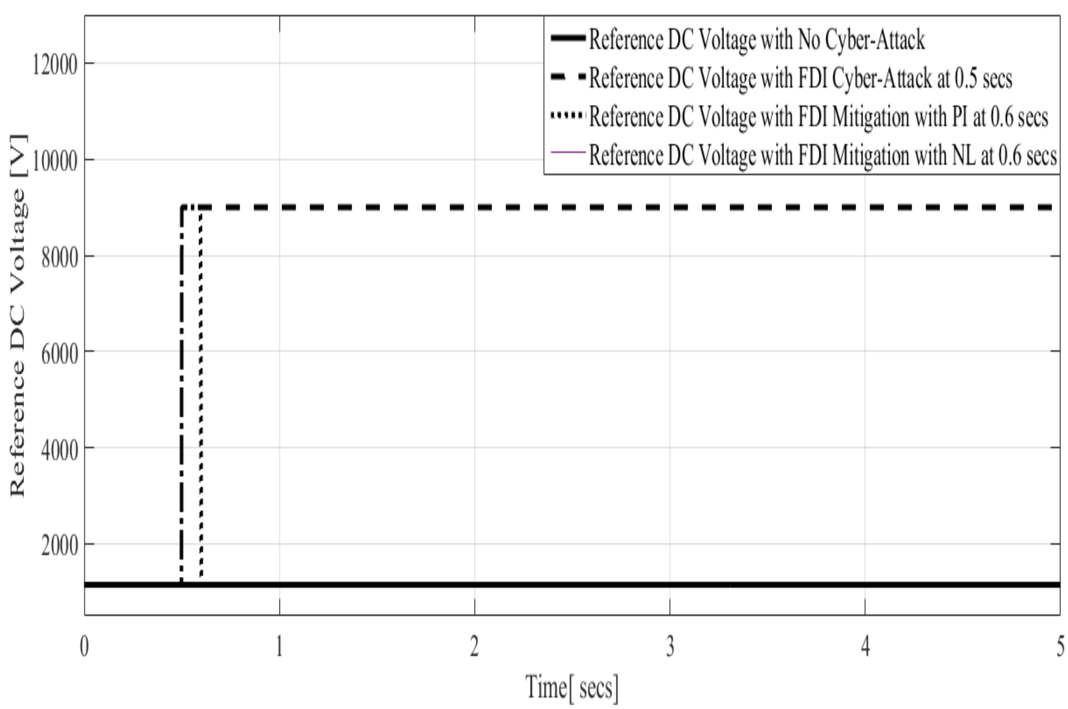

Figure 65. DC reference voltage for FDI cyber-attack for GSC

1. DDoS Attack Case

Figures 66-71 show the voltage responses at PCC, current at PCC, power at PCC, terminal voltage of synchronous generator, terminal voltage of wind generator and terminal voltage of PV. From the responses, it is shown that the DDoS cyber-attack affects the power quality of the hybrid grid. Moreover, the two proposed controllers mitigate the adverse effects of cyber-attack well and improve the power quality. However, the PI controller performs better than the Non-Linear controller.

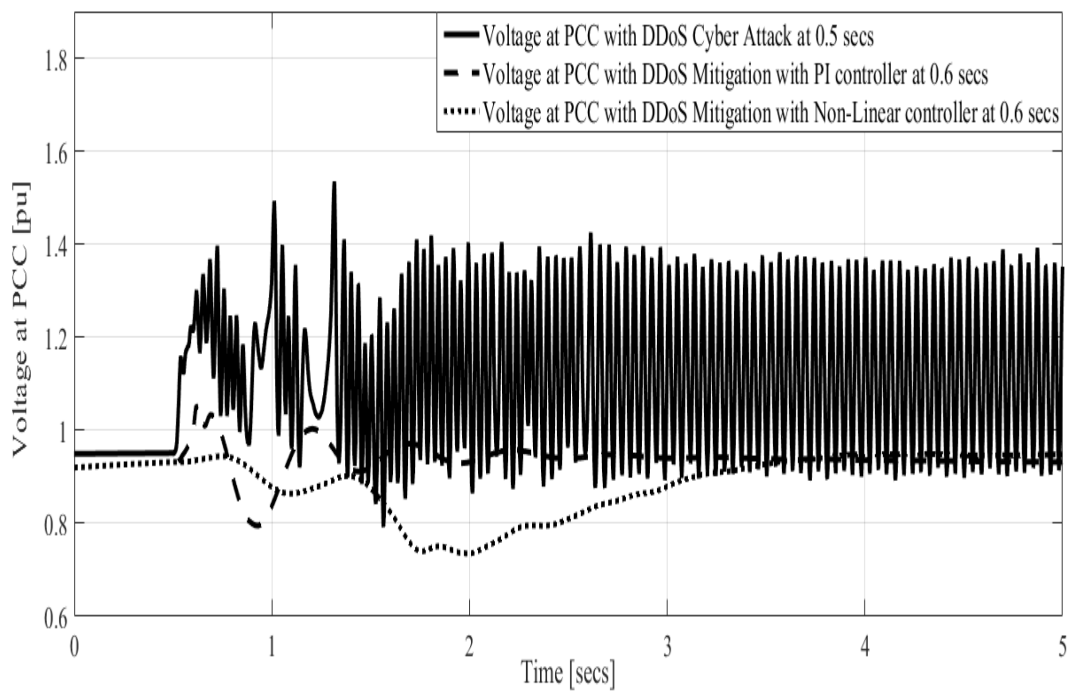

Figure 66. Voltage at PCC

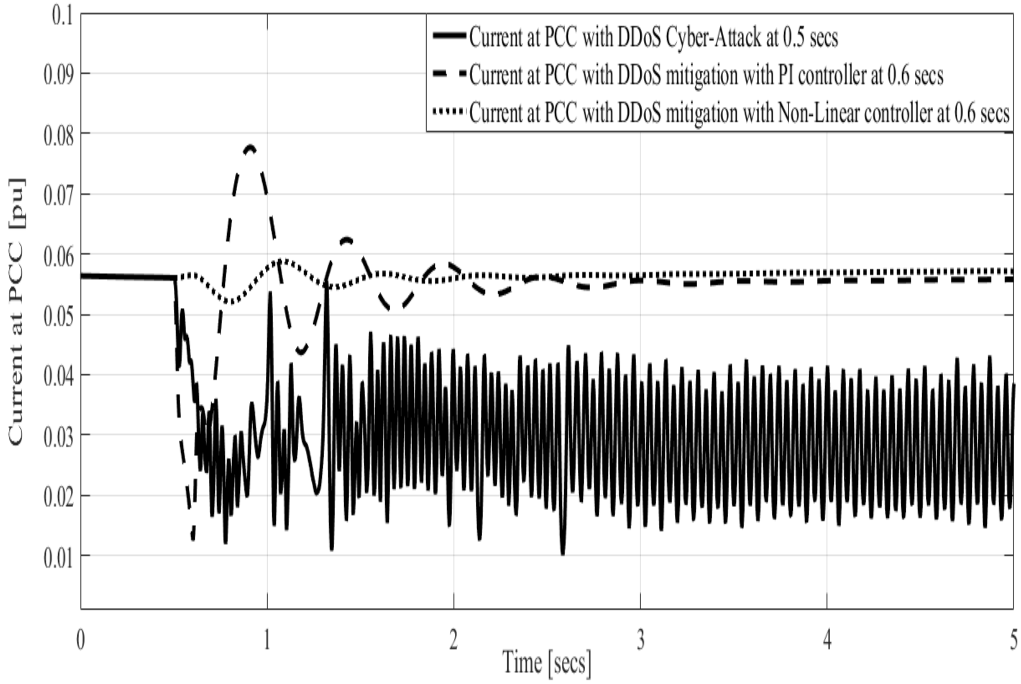

Figure 67. Current at PCC

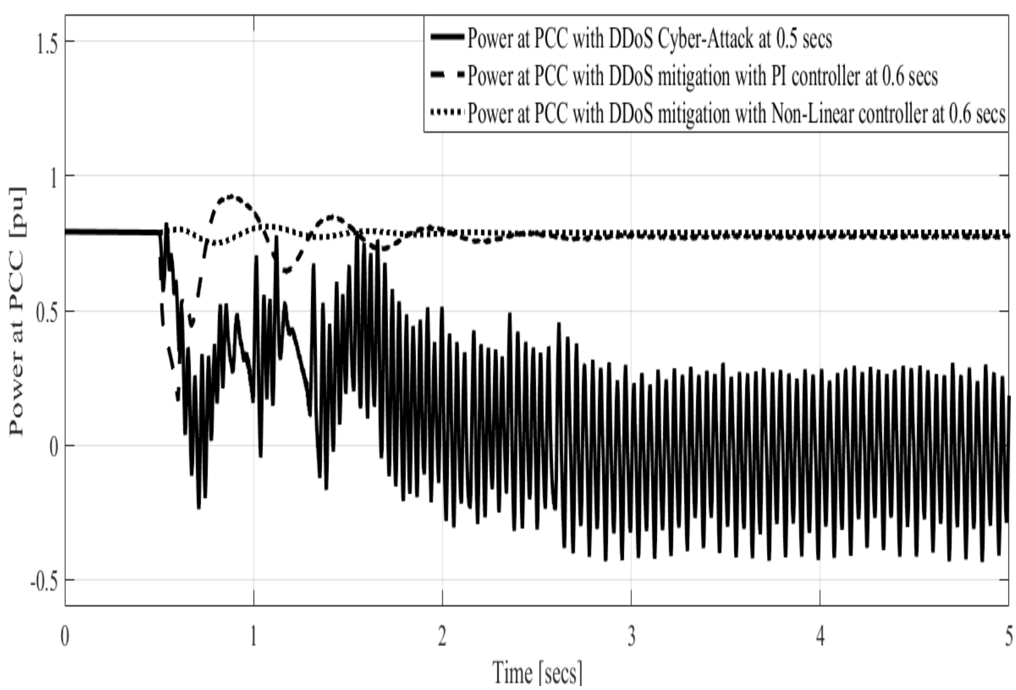

Figure 68. Power at PCC

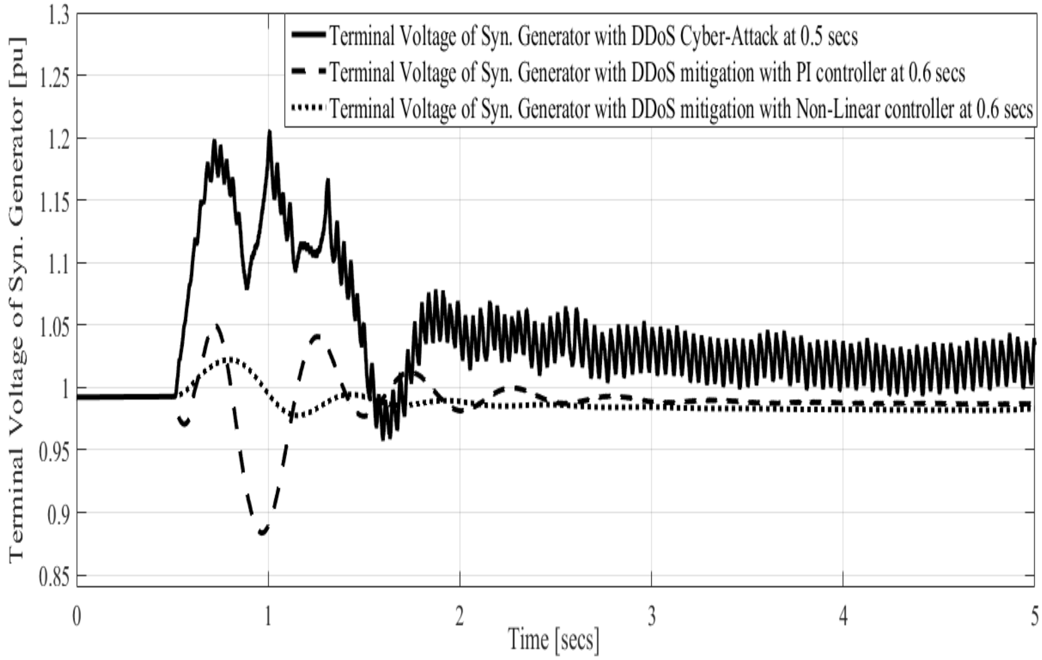

Figure 69. Terminal Voltage at Synchronous Generator

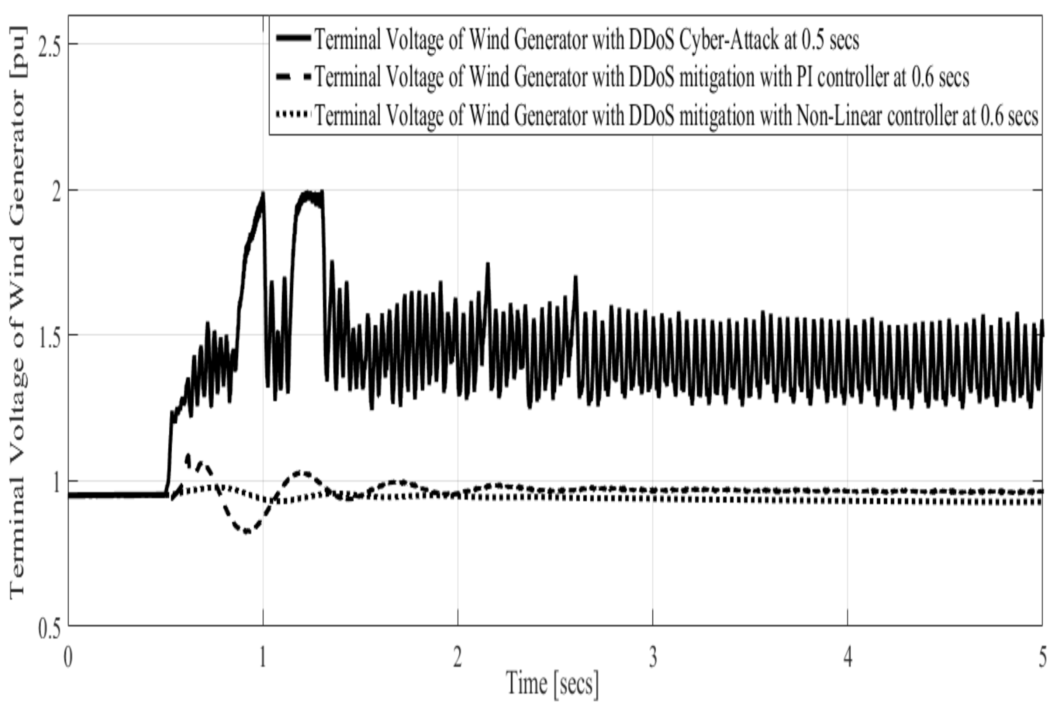

Figure 70. Terminal Voltage of Wind Generator

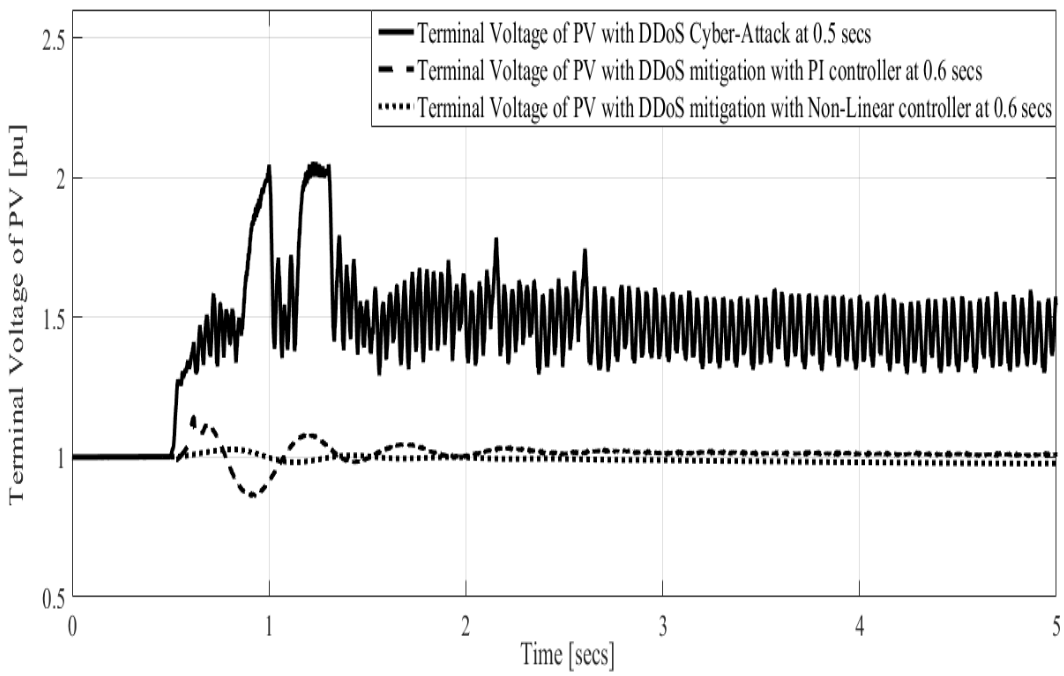

Figure 71. Terminal Voltage of PV

2. FDI Attack Case

Figures 72-77 show voltage responses at PCC, current at PCC, power at PCC, terminal voltage of synchronous generator, terminal voltage of wind generator and terminal voltage of PV. From the responses, it is shown that the FDI cyber-attack affects the power quality of the hybrid grid. Also, the two proposed controllers mitigate the adverse effects of cyber-attack well and improve the power quality. However, the PI controller performs better than the Non-Linear controller.

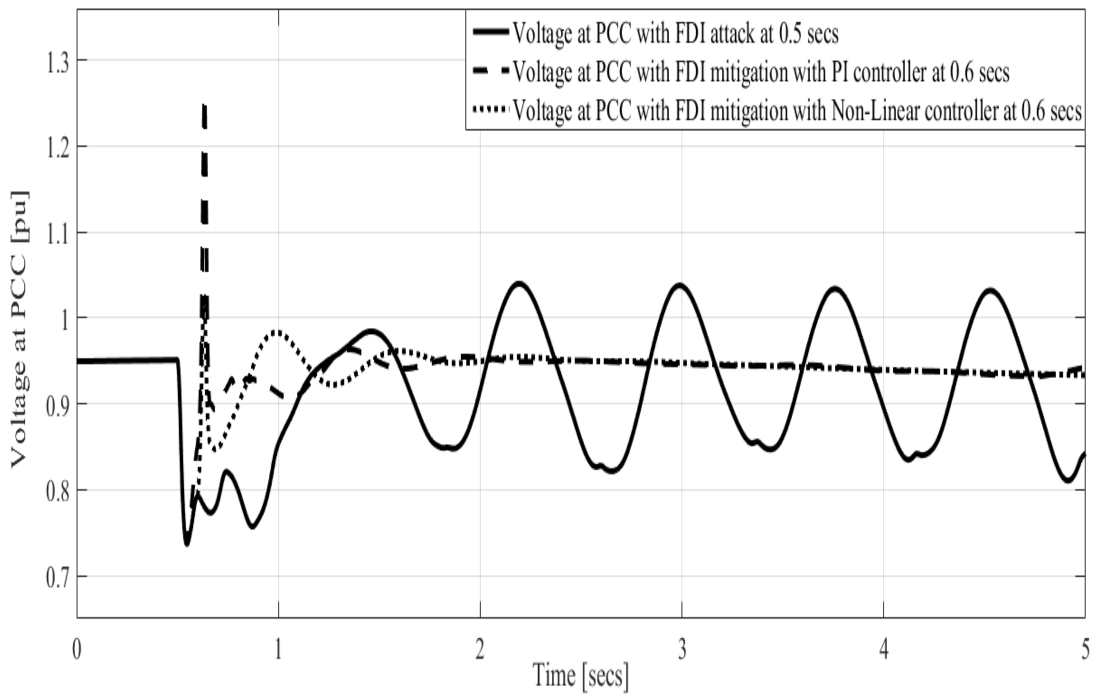

Figure 72. Voltage at PCC

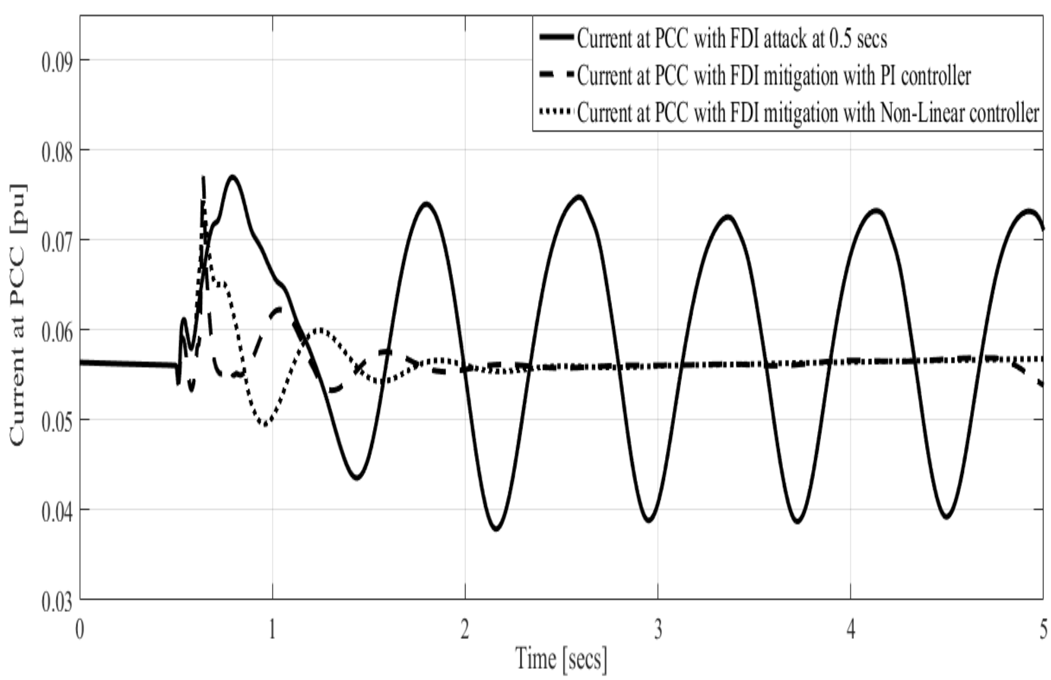

Figure 73. Current at PCC

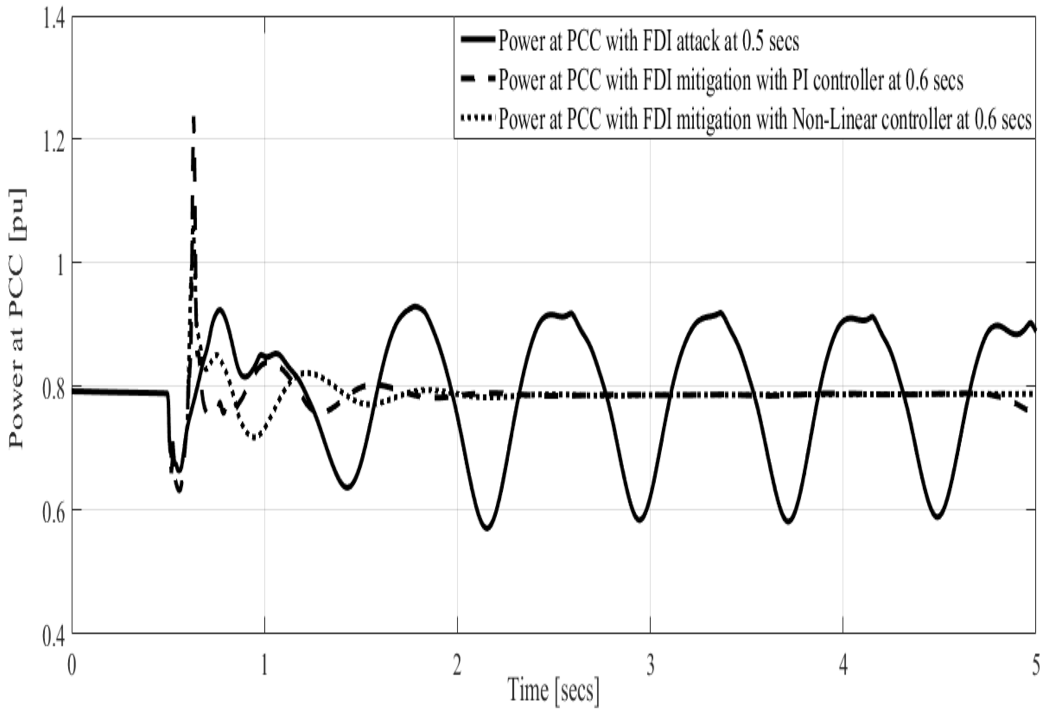

Figure 74. Power at PCC

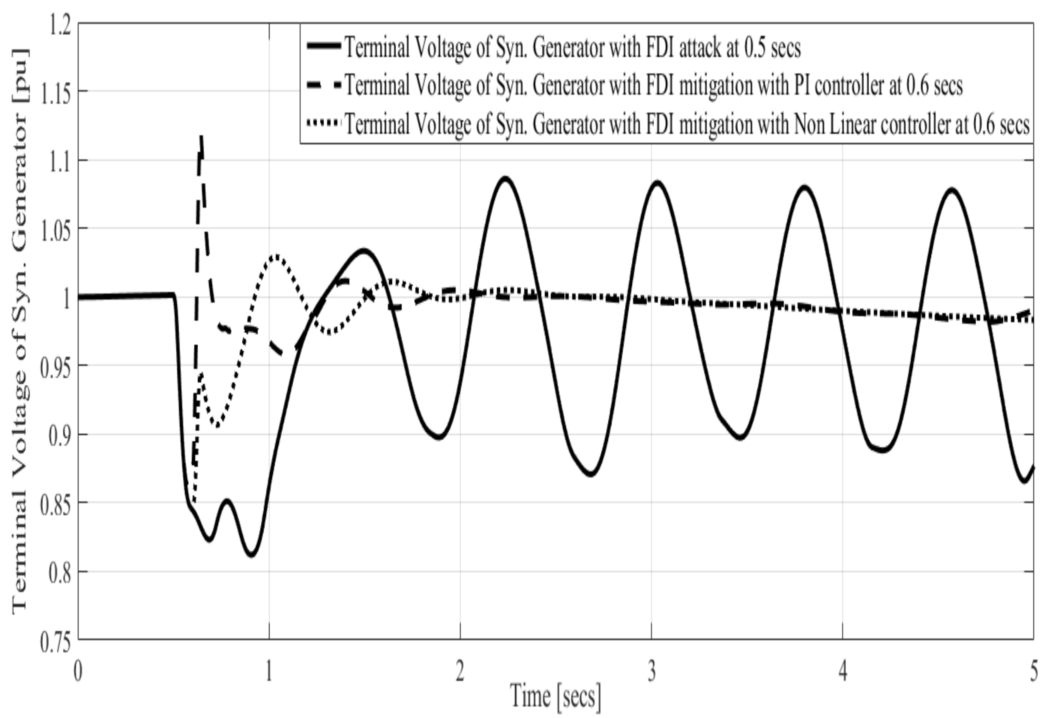

Figure 75. Terminal Voltage of Synchronous Generator.

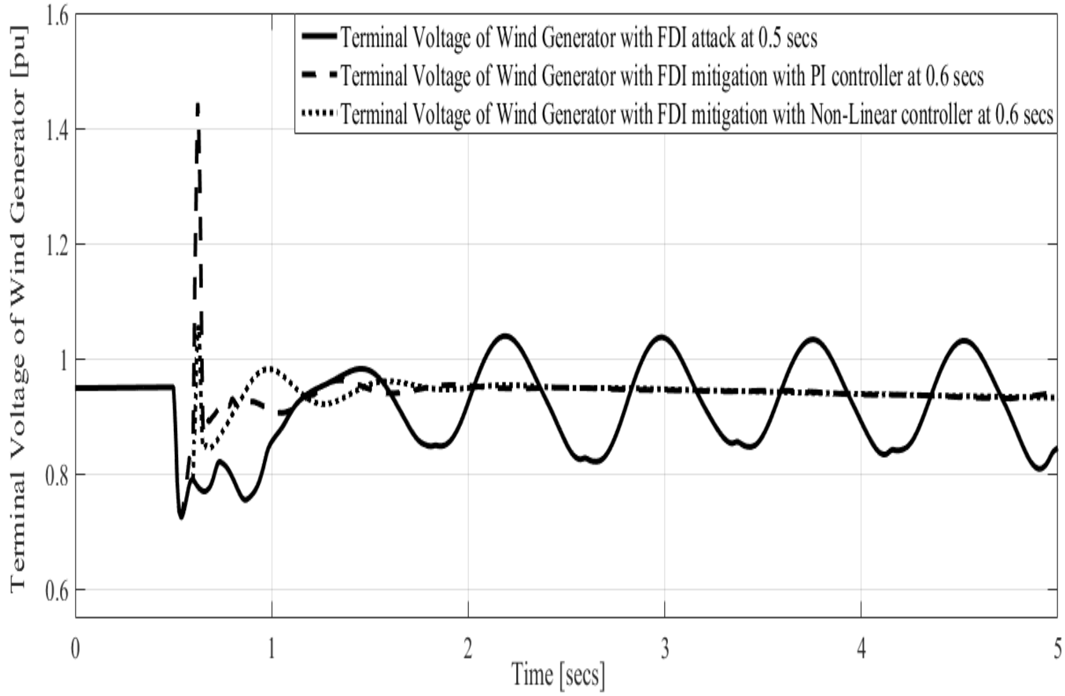

Figure 76. Terminal Voltage of Wind Generator.

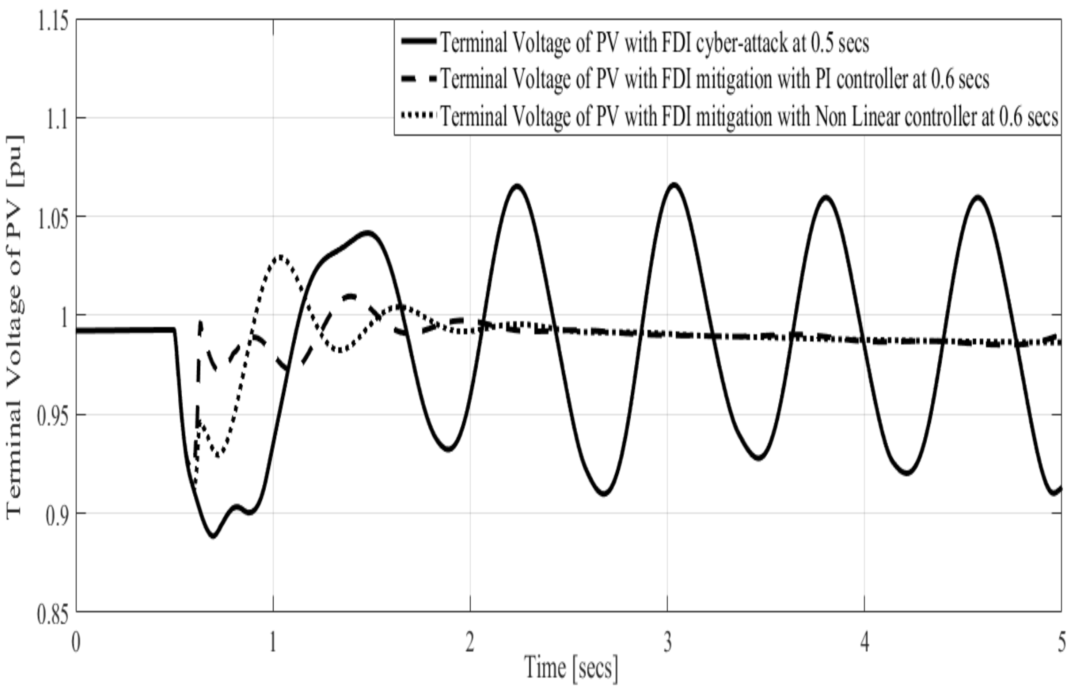

Figure 77. Terminal Voltage of PV

ii. Effects and Mitigation of DDoS and FDI Cyber-Attacks on VSC Controller of PV

For this scenario, it is assumed that the DDoS and FDI attacks affect the VSC controller of the PV at 0.5 secs and continues until 5 sec. To mitigate the cyber-attack, the controllers start operating at 0.6 secs and improve the performance of the system. Figures 78-79 show the DC reference voltage (V_{del_ref}) of the VSC of the PV system with and without the DDoS and FDI cyber-attacks and with the proposed controllers. From the response, it is evident that the DDoS and FDI cyber-attacks change the dc reference voltage and deteriorate the performance of the system. Also, the proposed controllers can detect the cyber-attack and mitigate the adverse effects. However, for the DDoS attack on the VSC of the PV, the PI controller performs better than the Non-Linear controller, and for the FDI attack, the Non-Linear controllers performs better.

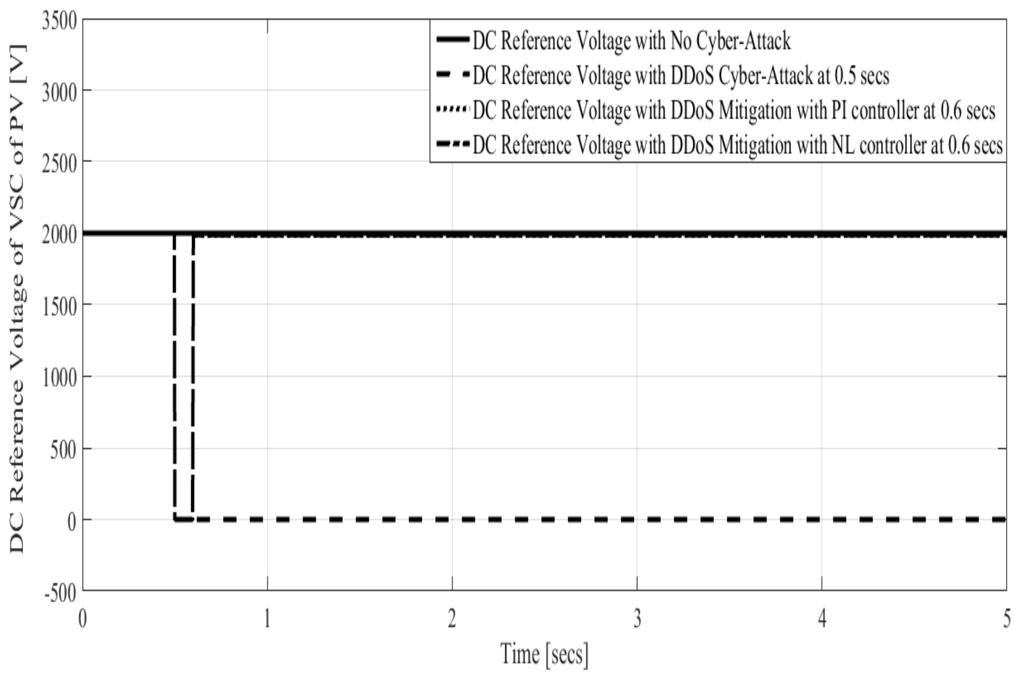

Figure 78. DC Reference Voltage of VSC of PV for DDoS

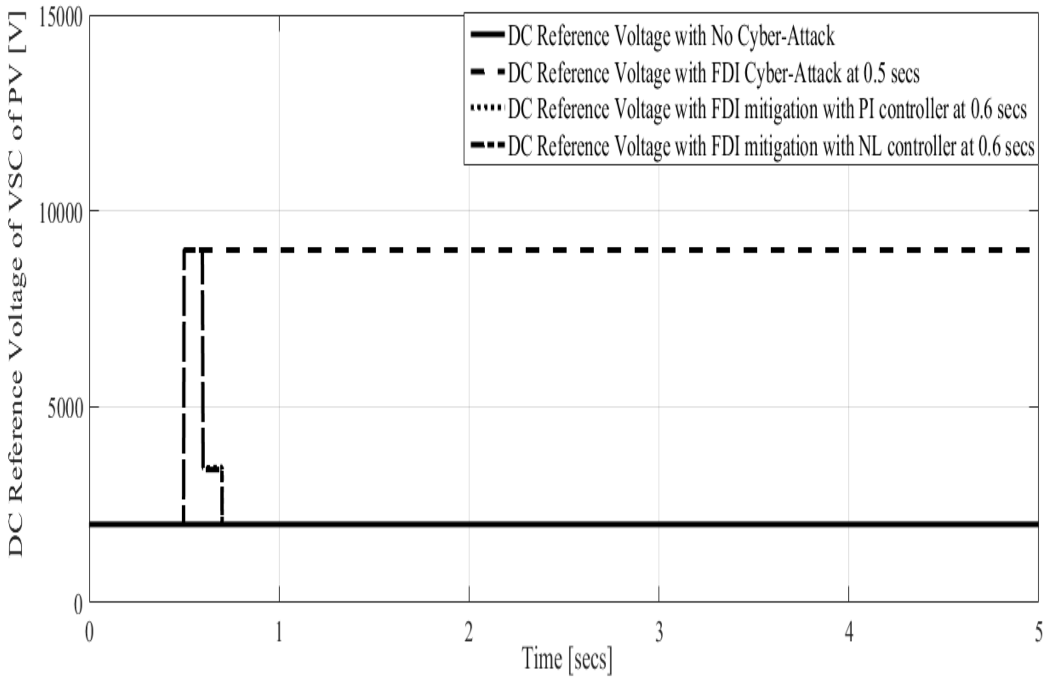

Figure 79. DC Reference Voltage of VSC of PV for FDI

1. DDoS Attack Case

Figures 80-85 show the voltage responses at the PCC, current at PCC, power at PCC, terminal voltage of synchronous generator, terminal voltage of wind generator and terminal voltage of PV. From the responses, it is observed that the DDoS cyber-attack affects the performance of the hybrid grid, but the proposed controllers mitigate the adverse effects of the cyber-attack. However, the PI controller performs better than the Non-Linear controller.

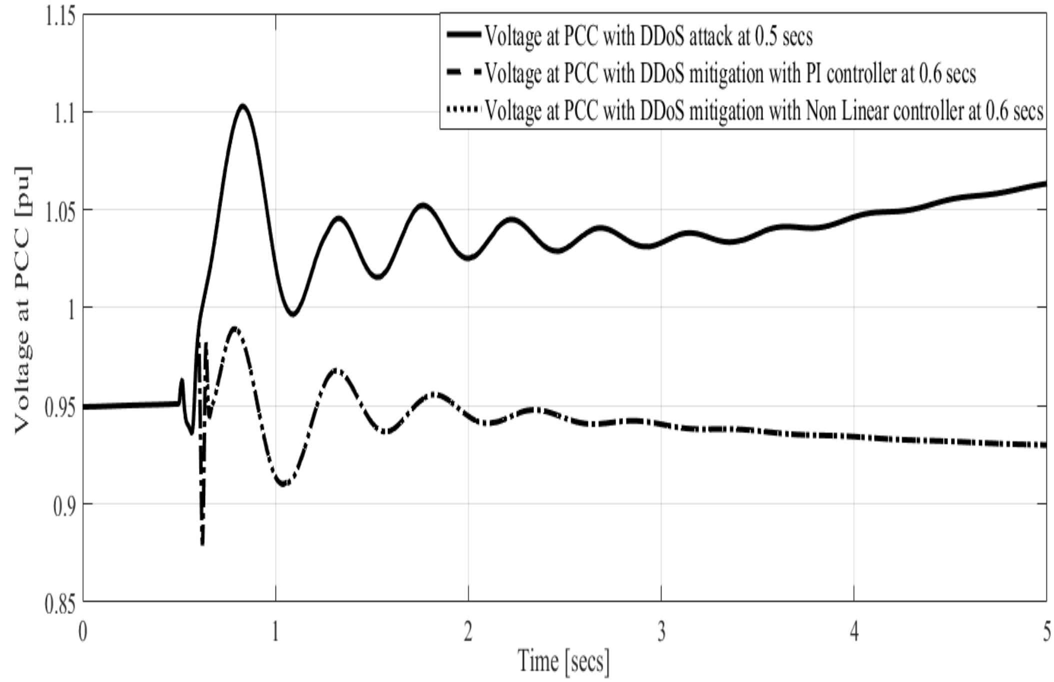

Figure 80. Voltage at PCC

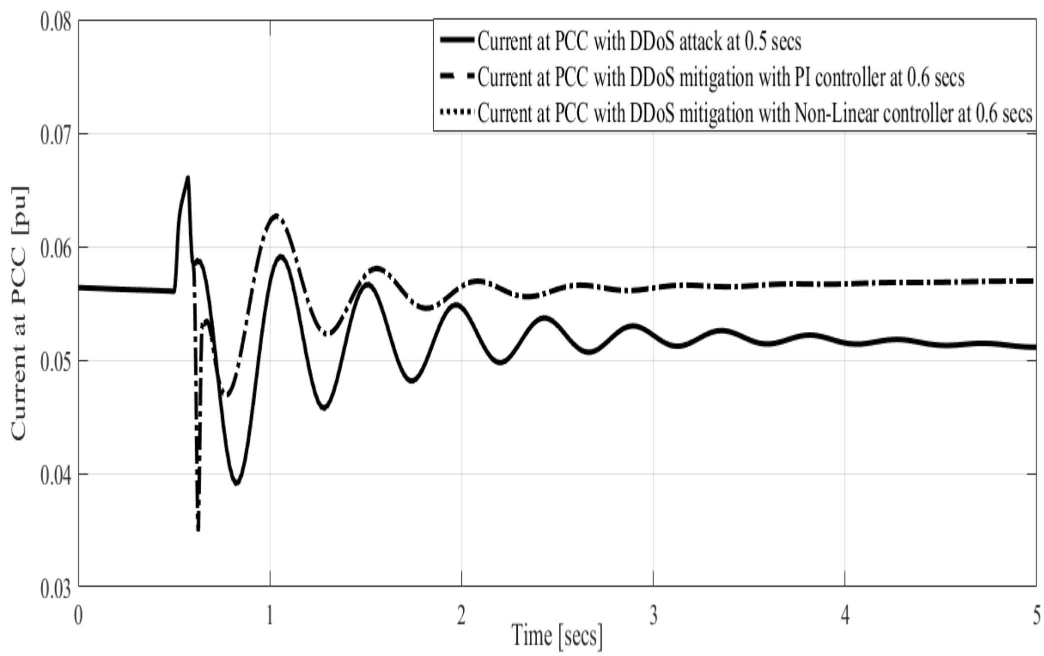

Figure 81. Current at PCC

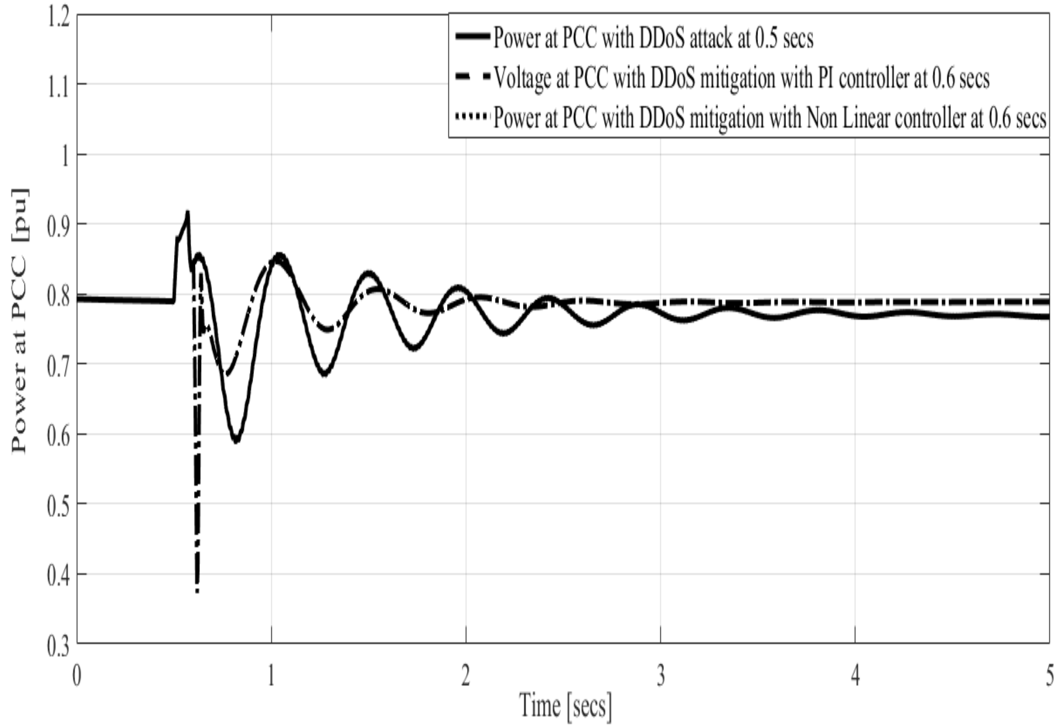

Figure 82. Power at PCC

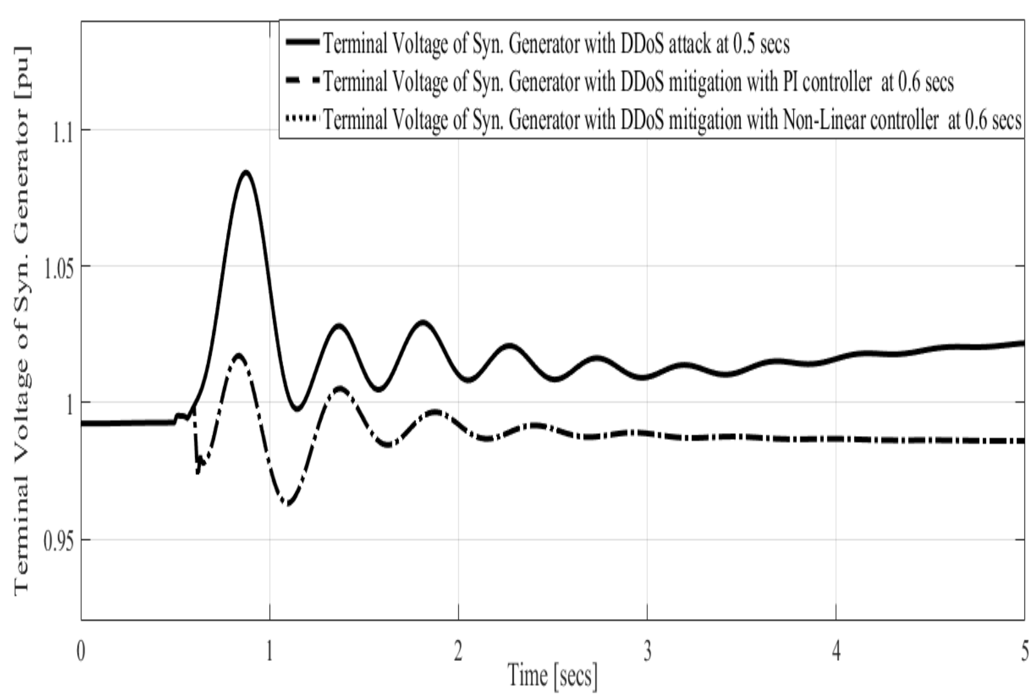

Figure 83. Terminal Voltage of Synchronous Generator.

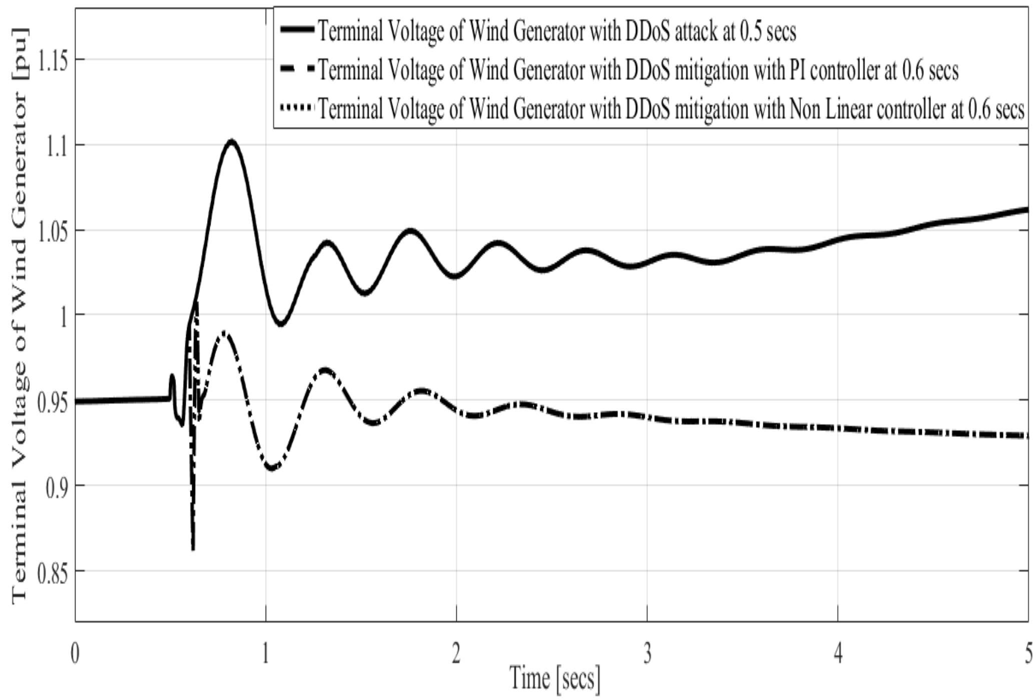

Figure 84. Terminal Voltage of Wind Generator.

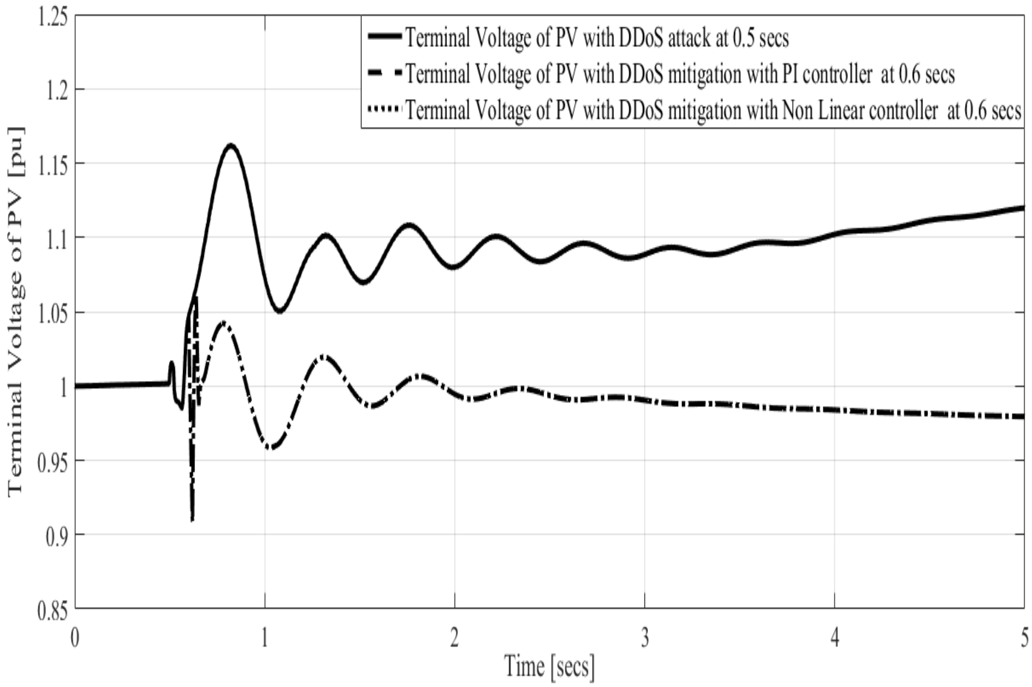

Figure 85. Terminal Voltage of PV.

2. FDI Attack Case

Figures 86-91 show the voltage responses at the PCC, current at PCC, power at PCC, terminal voltage of synchronous generator, terminal voltage of wind generator and terminal voltage of PV. From the responses, it is observed that the FDI cyber-attack affects the performance of the hybrid grid, but the proposed controllers mitigate the adverse effects of the cyber-attack. However, the Non-Linear controller performs better than the PI controller.

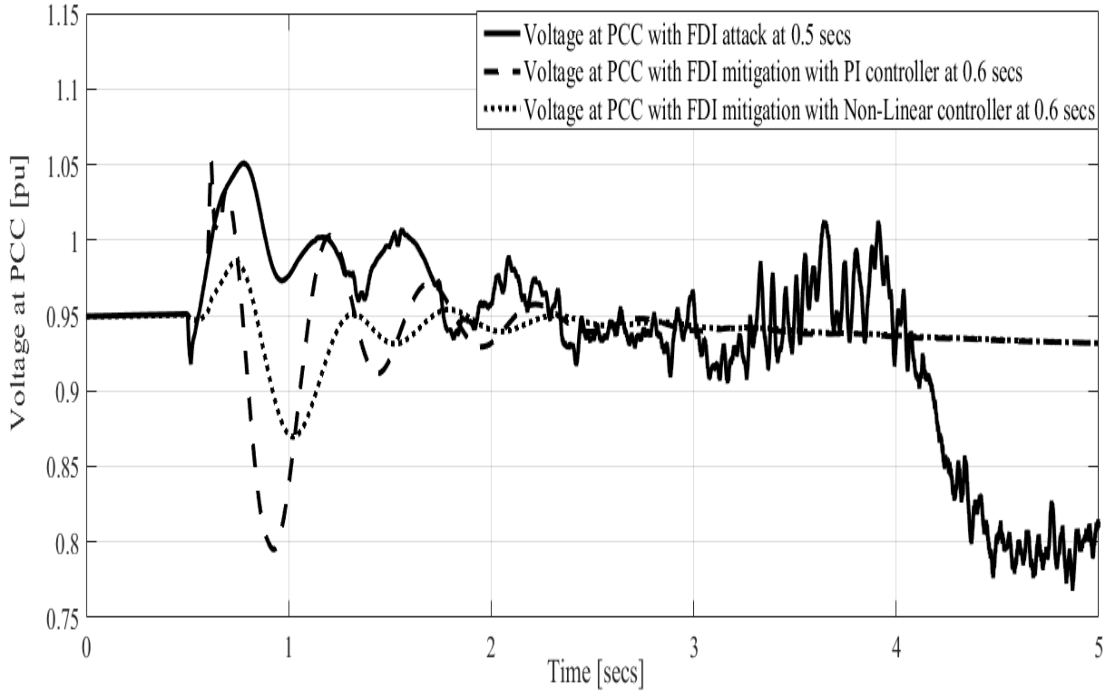

Figure 86. Voltage at PCC

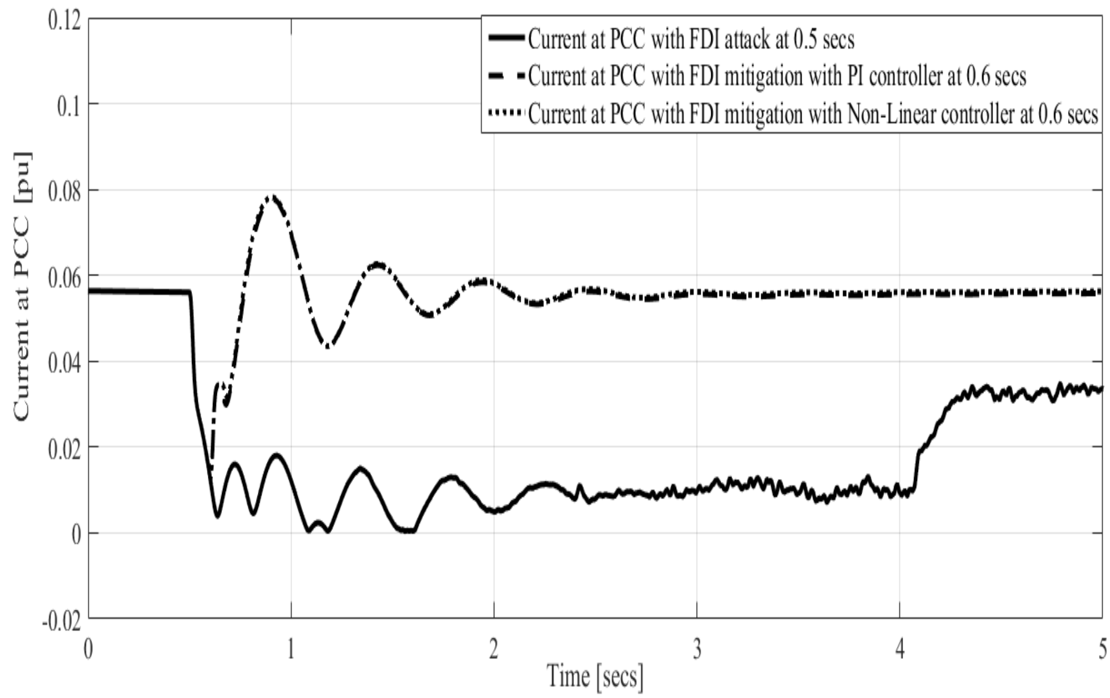

Figure 87. Current at PCC

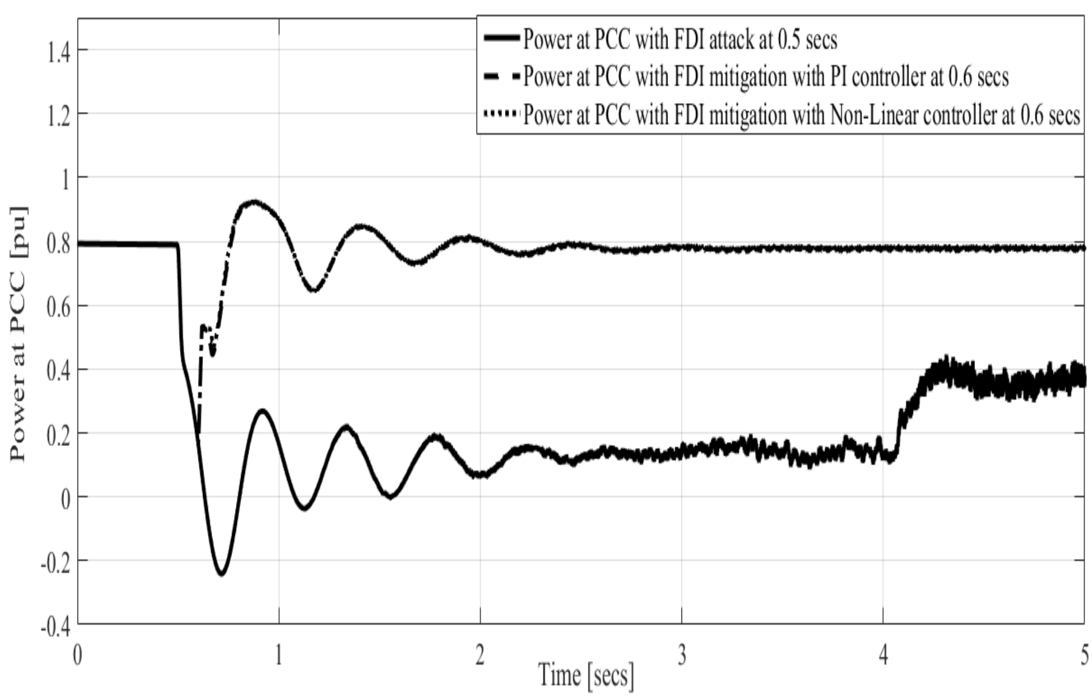

Figure 88. Power at PCC

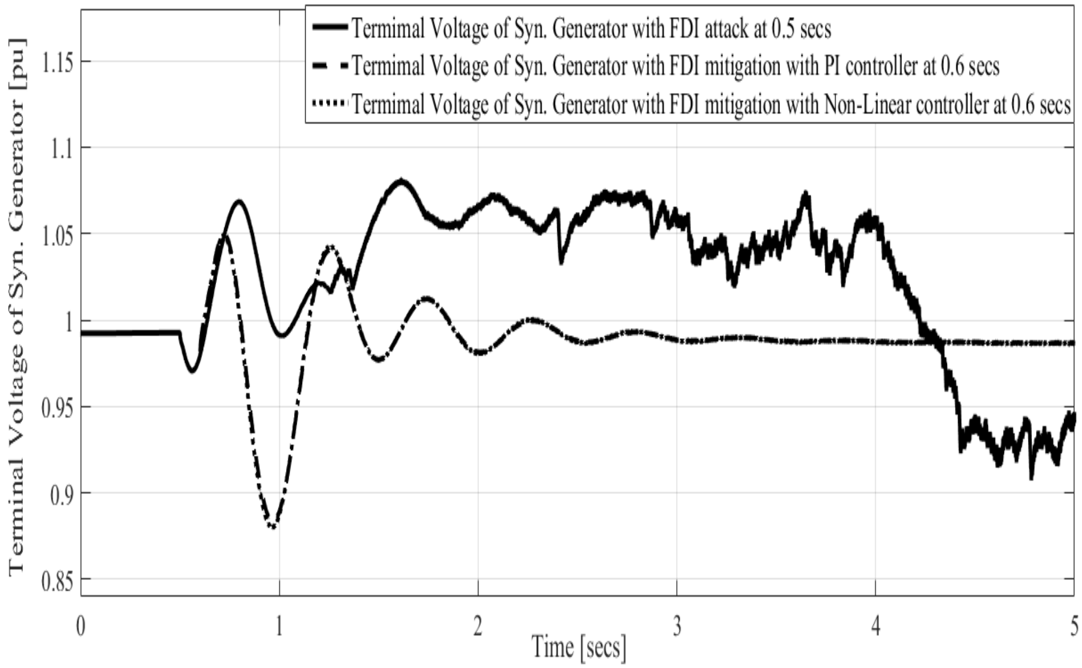

Figure 89. Terminal Voltage of Syn. Generator

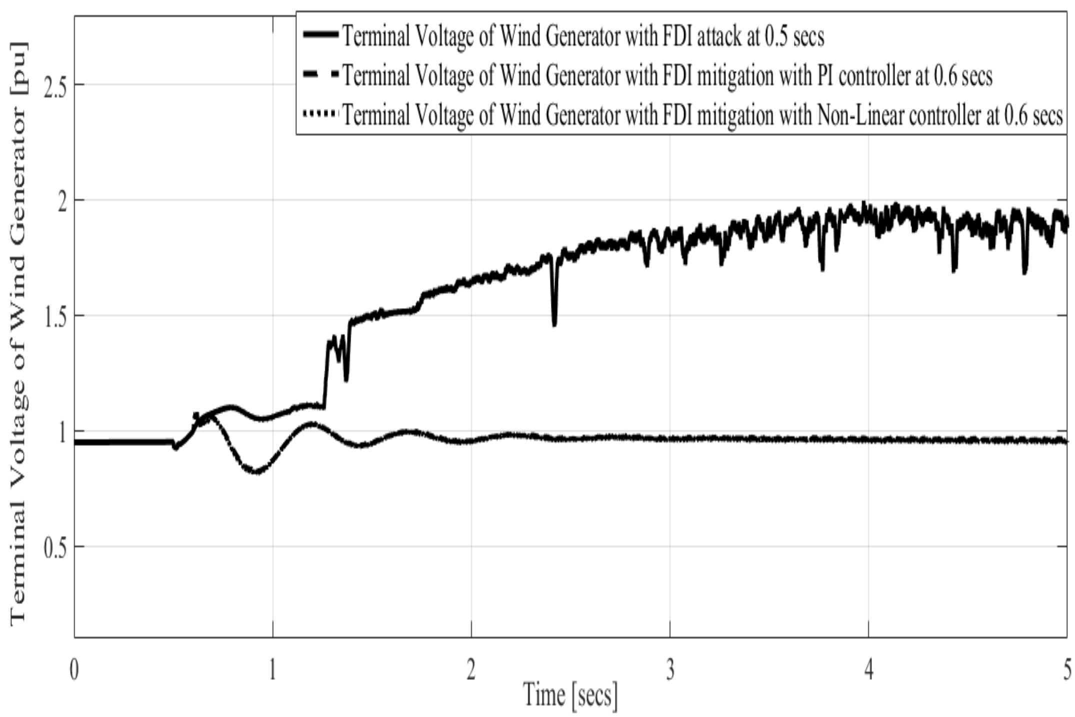

Figure 90. Terminal Voltage of Wind Generator

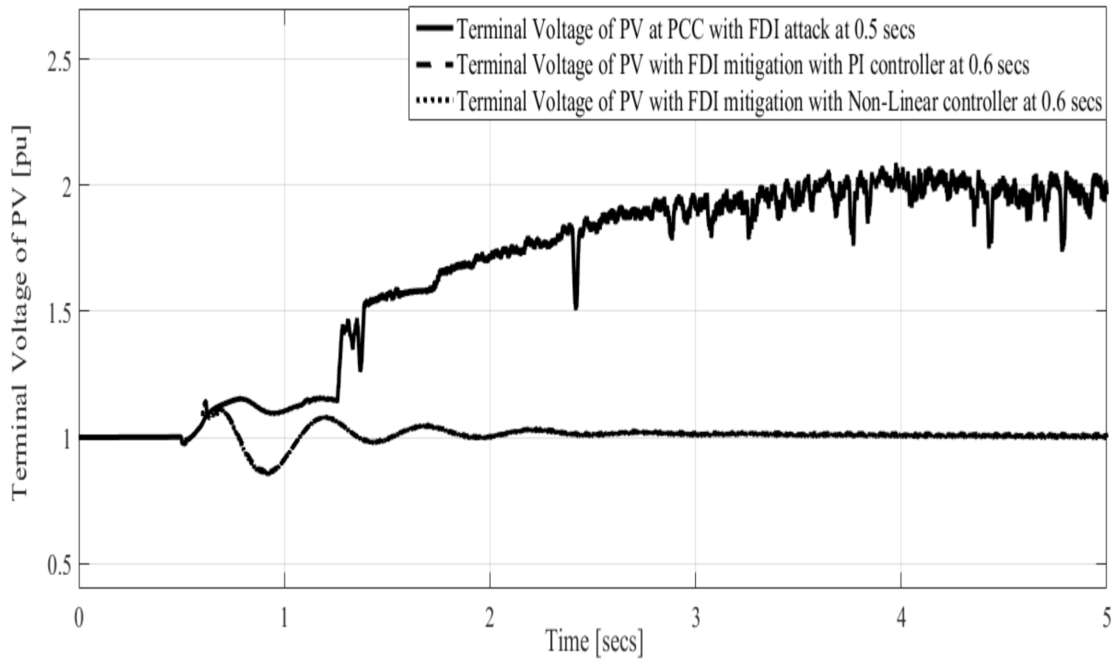

Figure 91. Terminal Voltage of PV

iii. Effects and Mitigation of DDoS and FDI Cyber-Attacks on AVR Controller of SG

For this scenario, it is assumed that the DDoS and FDI attacks disrupt the AVR controller of the SG at 0.5 secs and continue until 5 sec. To mitigate the cyber-attack, the proposed controllers start operating at 0.6 secs and improve the performance of the system. Figures 92-93 show the E_{dfo} reference voltage (E_{fdo}) of the AVR of the SG system with and without the DDoS and FDI cyber-attacks and with the proposed controllers. From the response, it is evident that the DDoS and the FDI cyber-attacks change the dc reference voltage and deteriorate the performance of the system. Also, the proposed controllers can detect the cyber-attack and mitigate the adverse effects. For the DDoS attack on the AVR of the synchronous generator, the Non-Linear controller works better than the PI controller, and in case of the FDI attack, the PI controllers performs better.

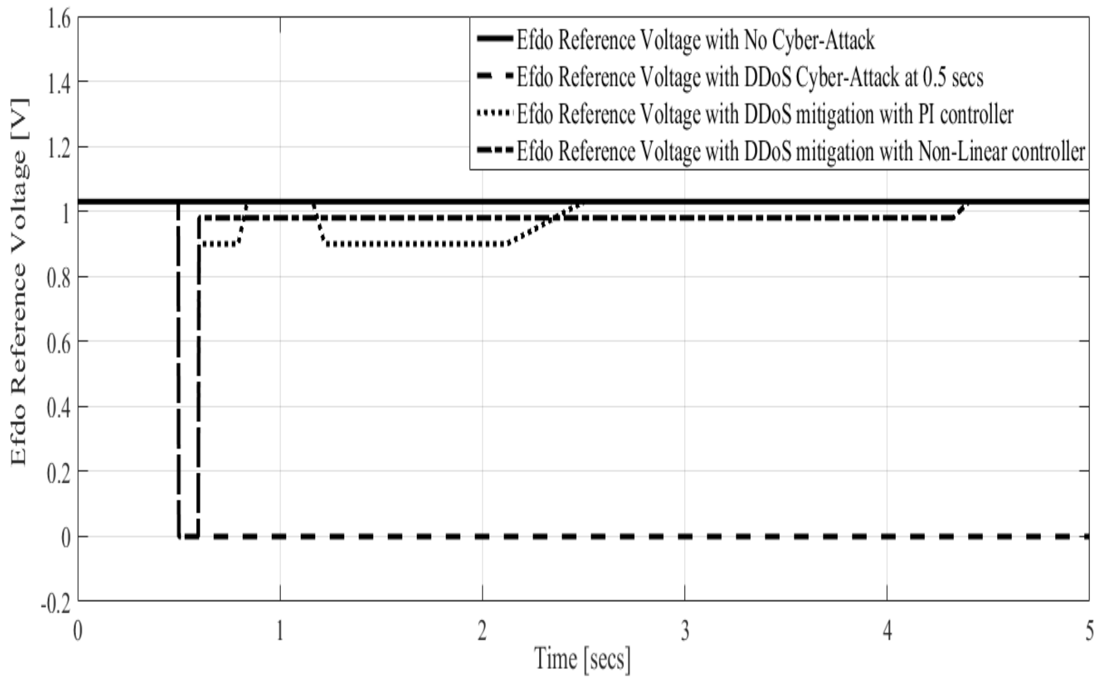

Figure 92. E_{fdo} Reference Voltage of AVR for DDoS

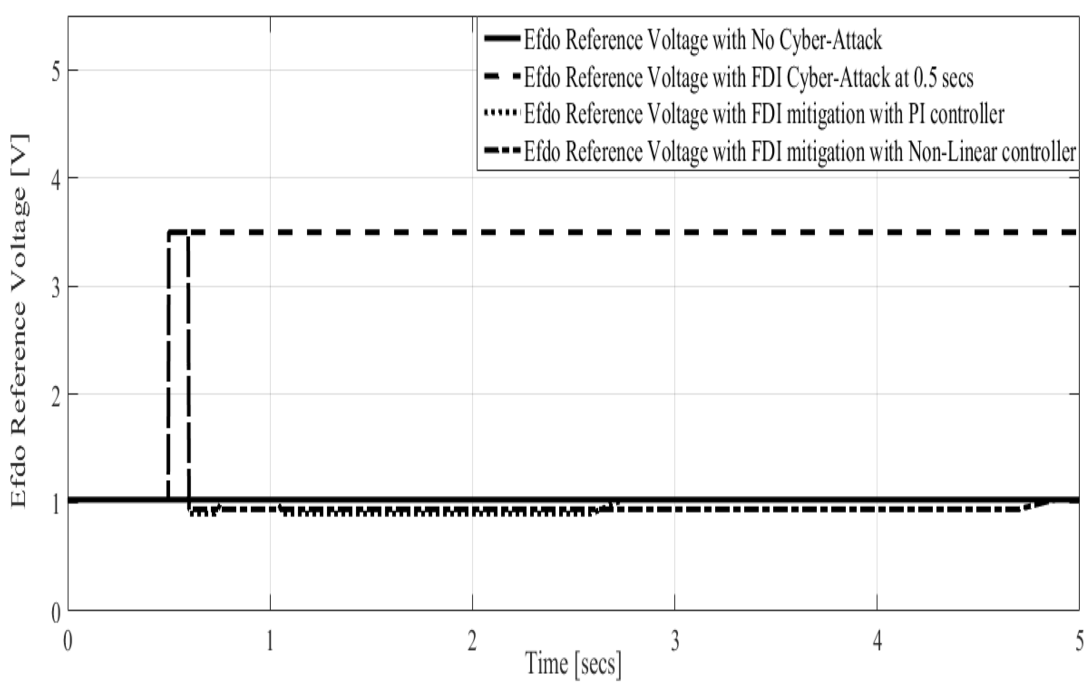

Figure 93. E_{fdo} Reference Voltage of AVR for FDI

1. DDoS Attack Case

Figures 95-99 show the voltage responses at the PCC, current at PCC, power at PCC, terminal voltage of synchronous generator, terminal voltage of wind generator and terminal voltage of PV. From the responses, it is observed that the DDoS cyber-attack affects the performance of the hybrid grid, but the proposed controllers mitigate the adverse effects of the cyber-attack. However, the Non-Linear controller performs better than the PI controller.

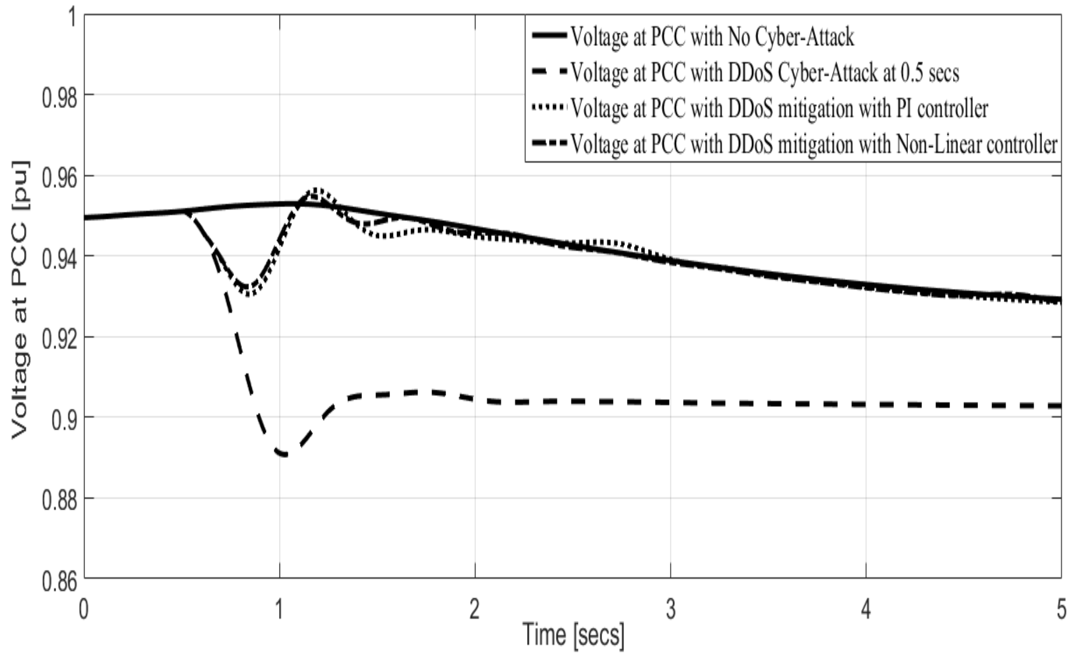

Figure 94. Voltage at PCC

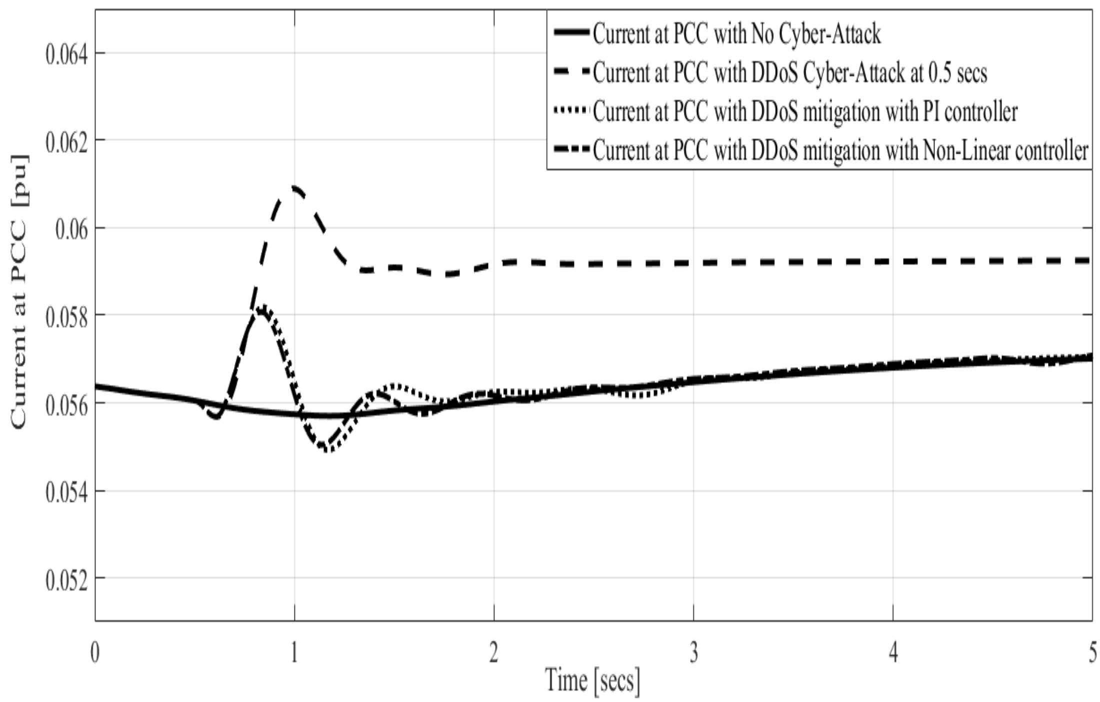

Figure 95. Current at PCC

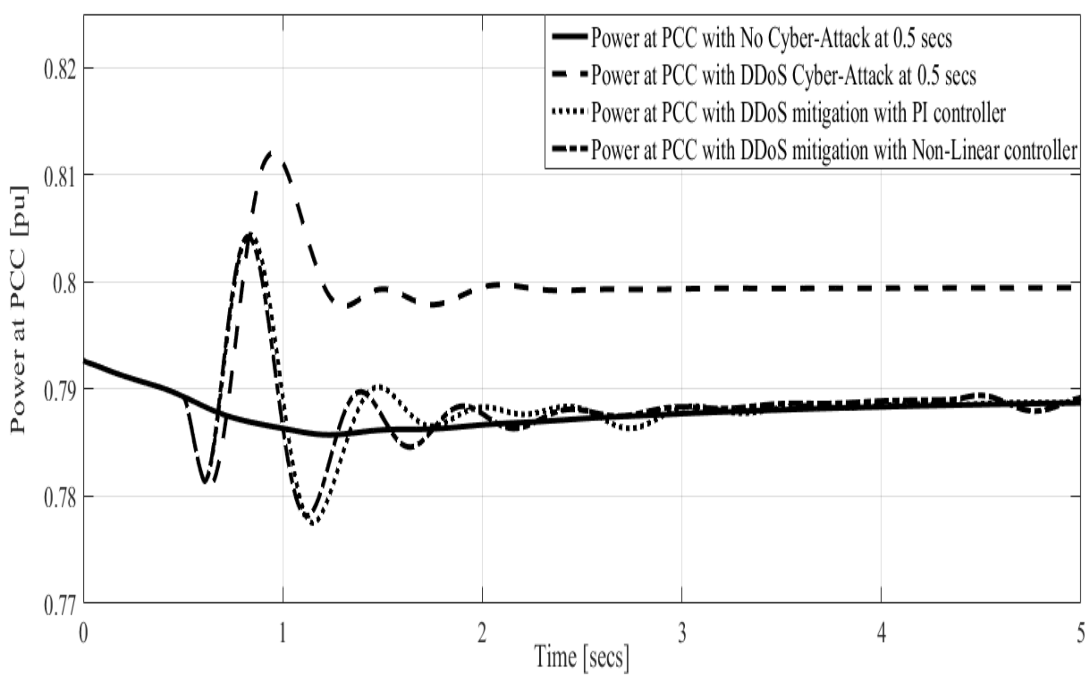

Figure 96. Power at PCC

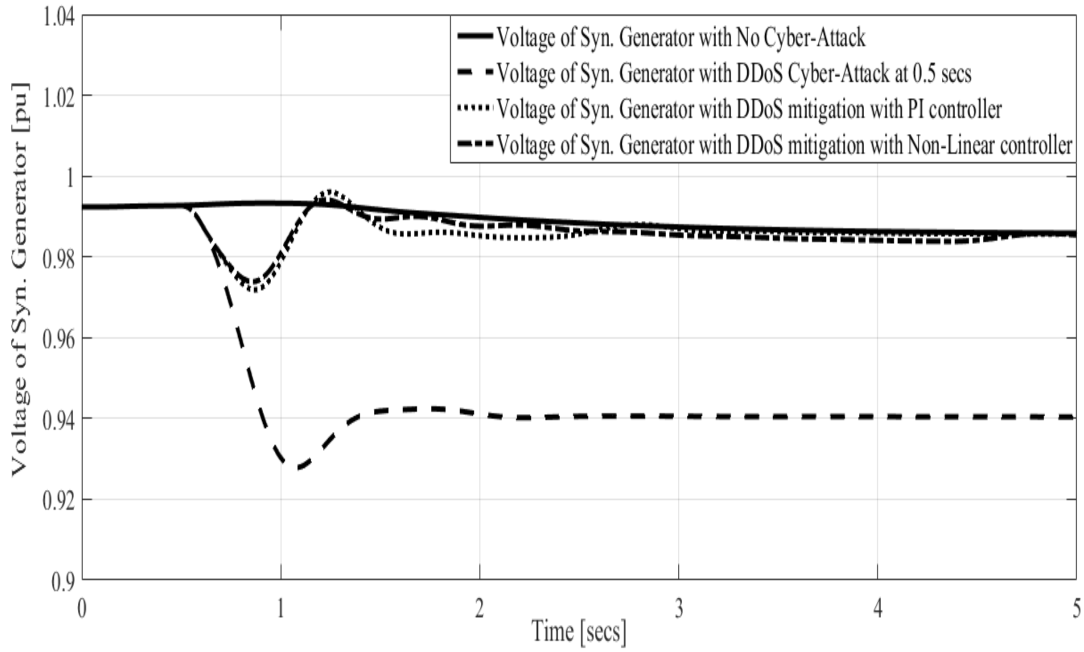

Figure 97. Terminal Voltage of Synchronous Generator

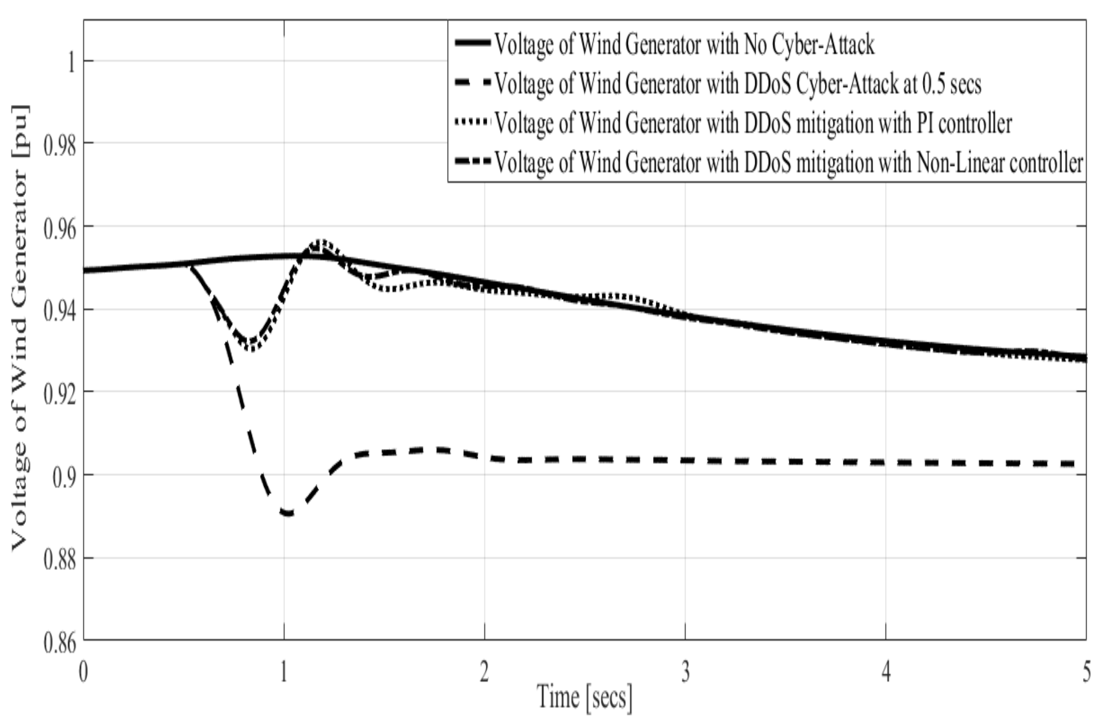

Figure 98. Terminal Voltage of Wind Generator

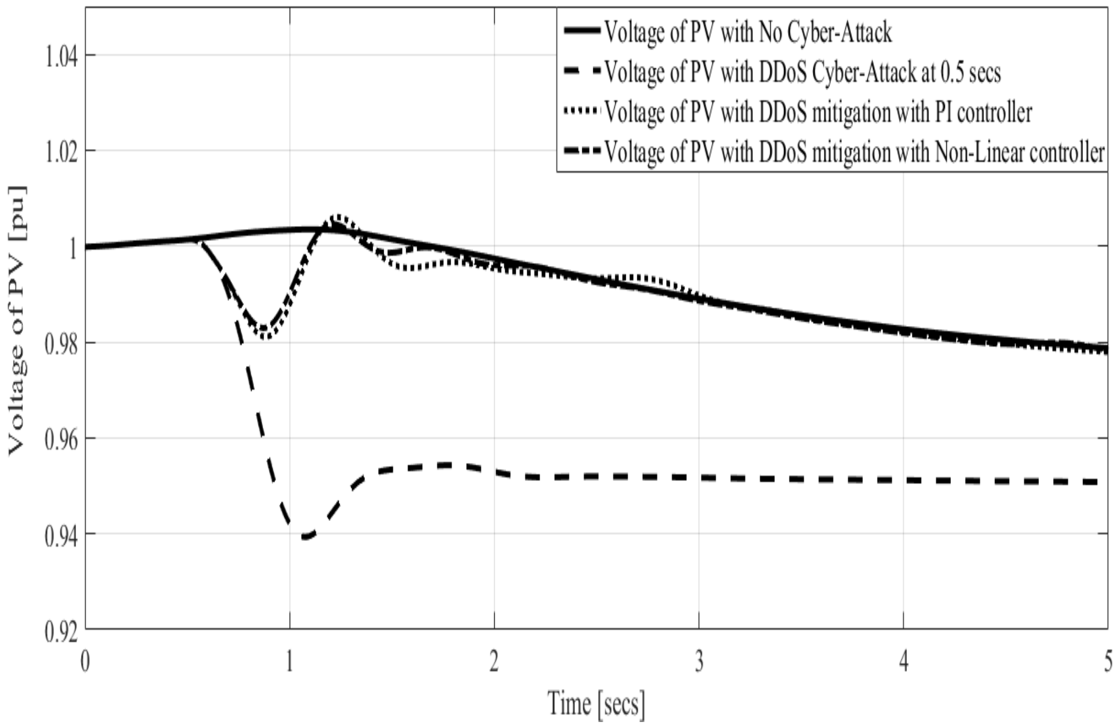

Figure 99. Terminal Voltage of PV

2. FDI Attacks Case

Figures 100-105 show the voltage responses at the PCC, current at PCC, power at PCC, terminal voltage of synchronous generator, terminal voltage of wind generator and terminal voltage of PV. From the responses, it is observed that the FDI cyber-attack affects the performance of the hybrid grid, but the proposed controllers mitigate the adverse effects of the cyber-attack. However, the PI controller performs better than the Non-Linear controller.

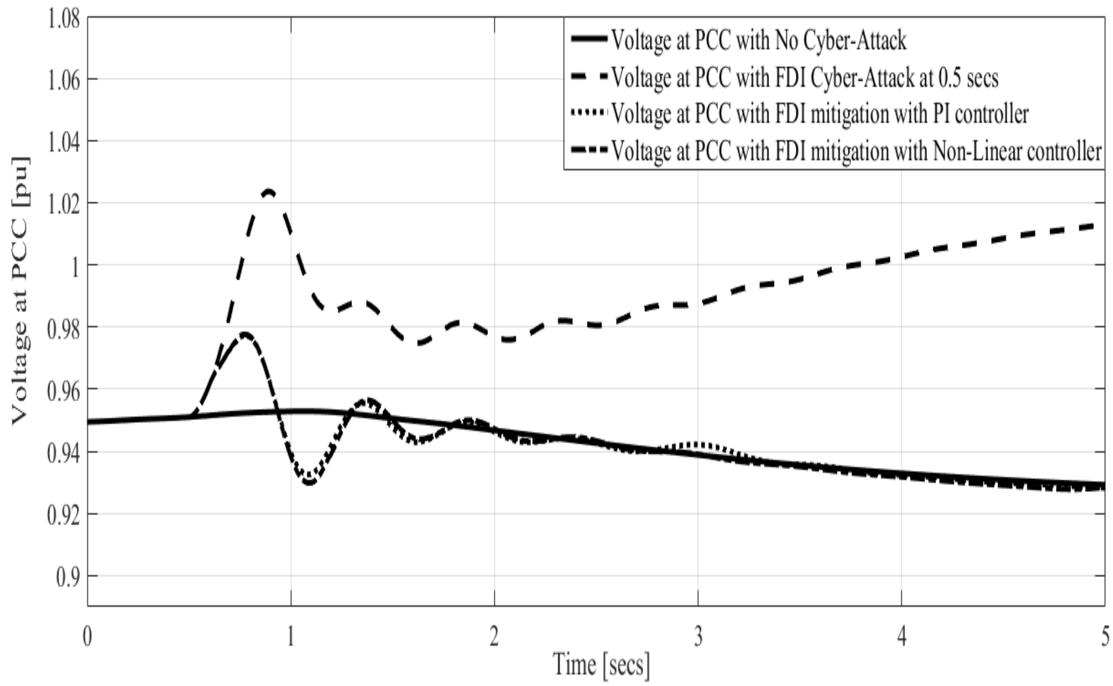

Figure 100. Voltage at PCC

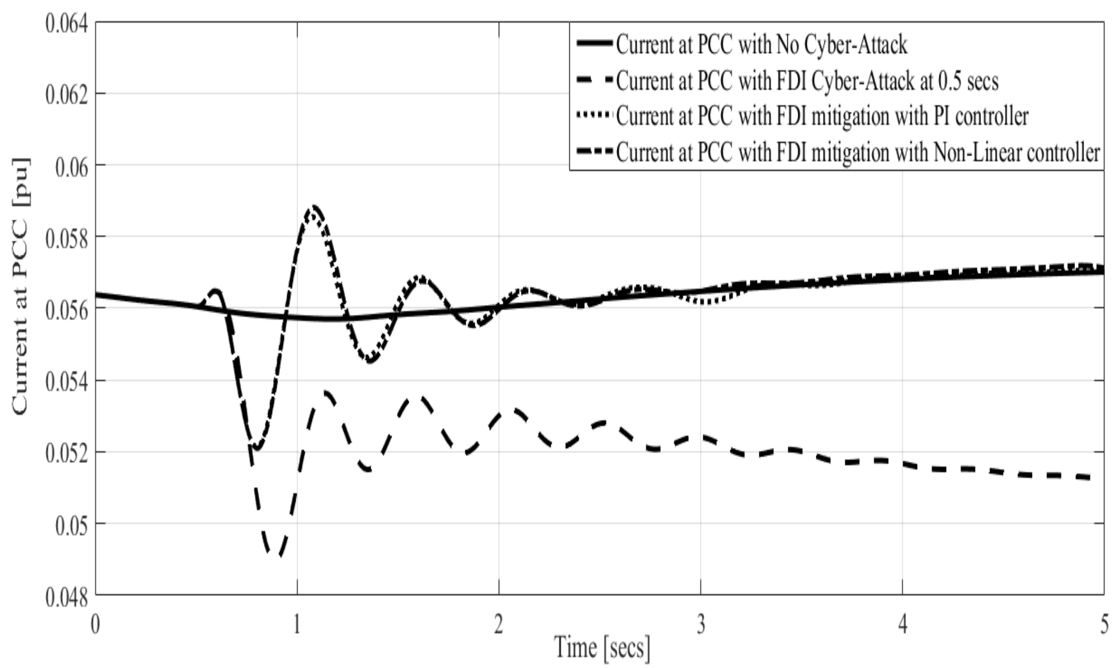

Figure 101. Current at PCC

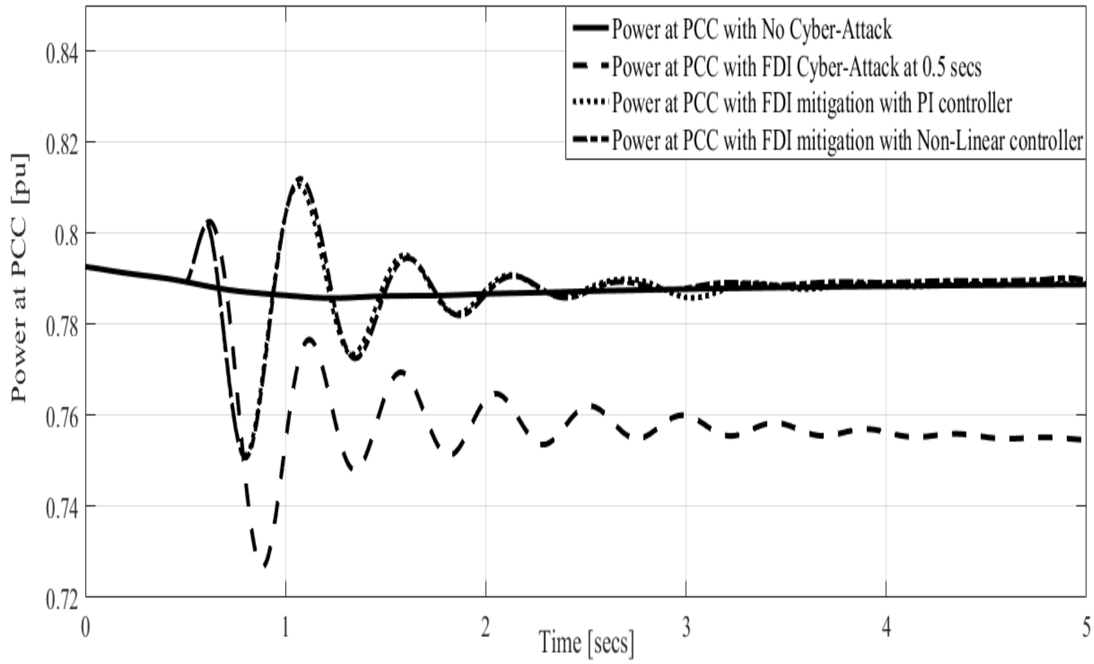

Figure 102. Power at PCC

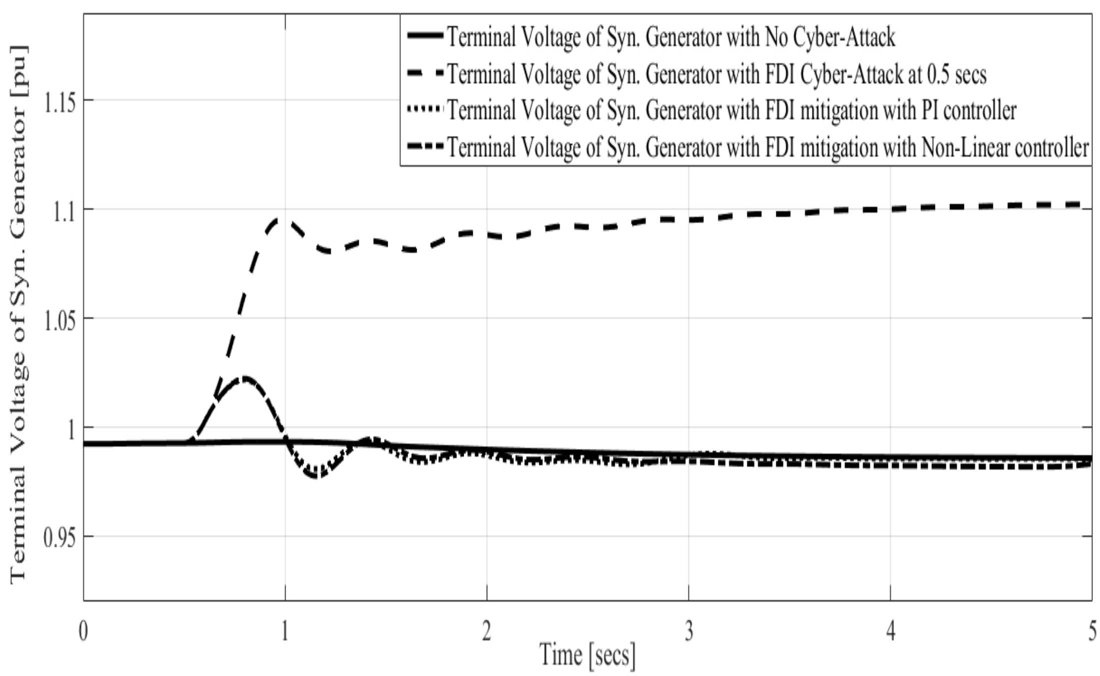

Figure 103. Terminal Voltage of Synchronous Generator

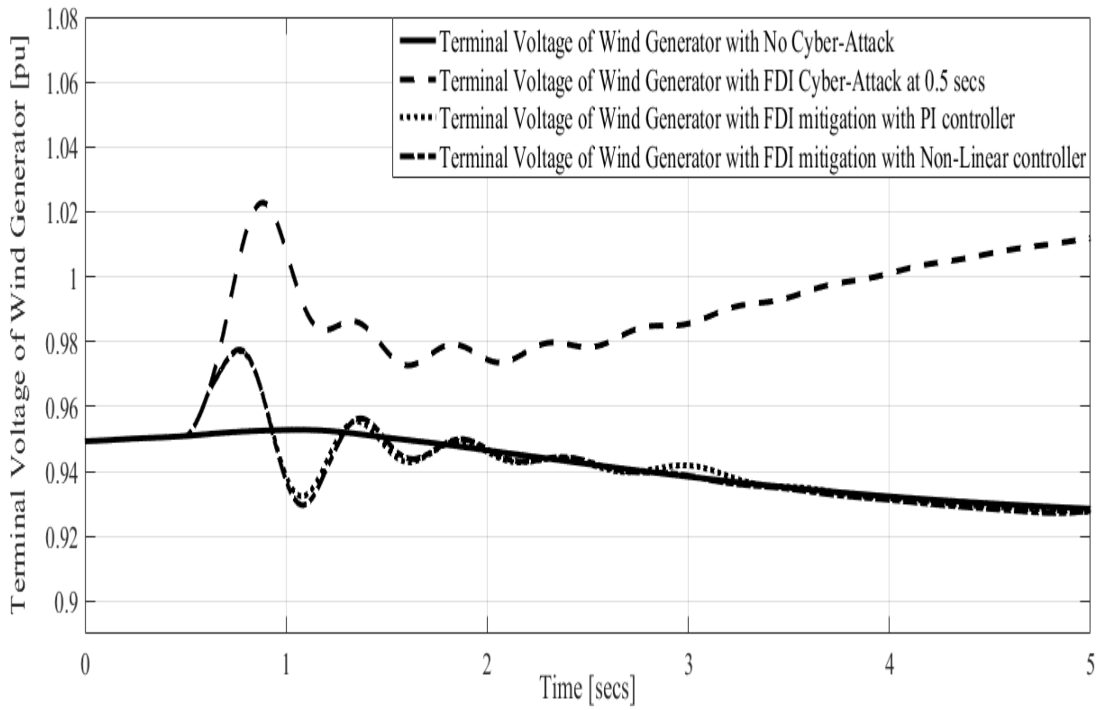

Figure 104. Terminal Voltage of Wind Generator

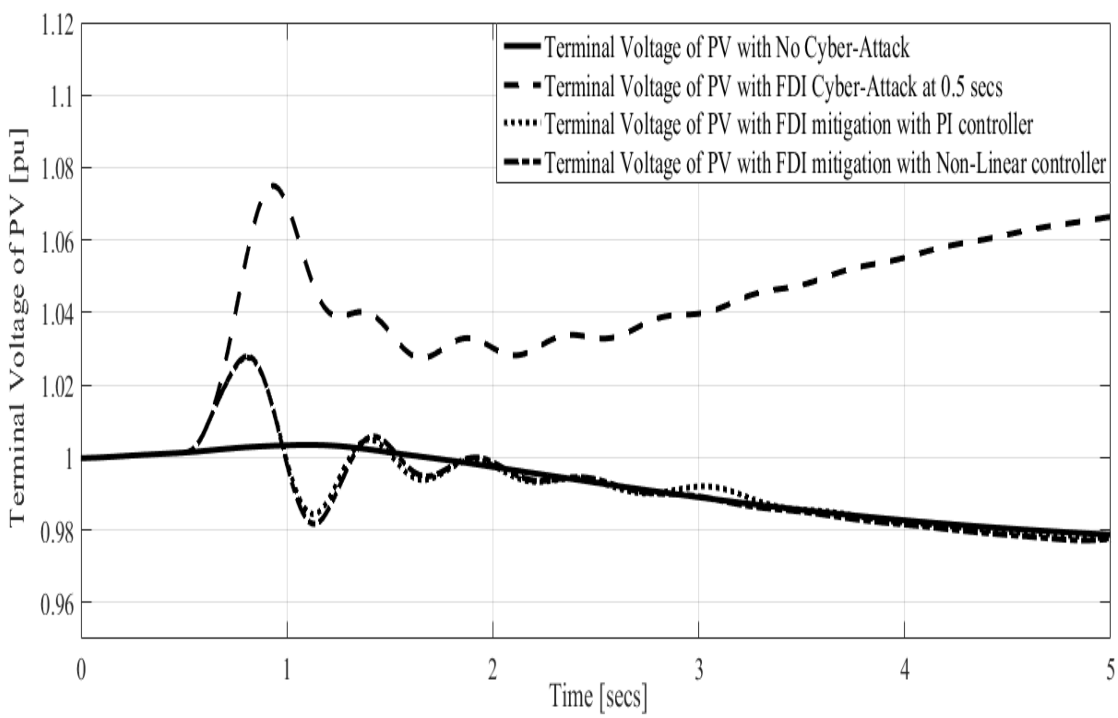

Figure 105. Terminal Voltage of PV

iv. Effects and Mitigation of DDoS and FDI Cyber-Attacks on SES

For this scenario, it is assumed that the PV system is turned off at 0.5 sec and the SES is turned on at 0.5 sec. The DDoS and FDI attacks occur on the SES (i.e., $P_{SES} \neq$ 2MW due to change in one gate pulse signal of the VSC) at 2.5 sec and continue until 5 sec. Figures 106 shows the response of the IGBT gate signal for the VSC of the SES with no cyber-attack, with FDI attack and with the proposed mitigation technique. The zoomed in portion of the figure shows the response from 2.5 secs (when the attack occurs) to 2.6 secs (when the mitigation strategy works). It has been shown that the cyber-attack affected the gate signal to change to 5 in case of FDI attack. However, the proposed mitigation technique changes the signal back to its original value.

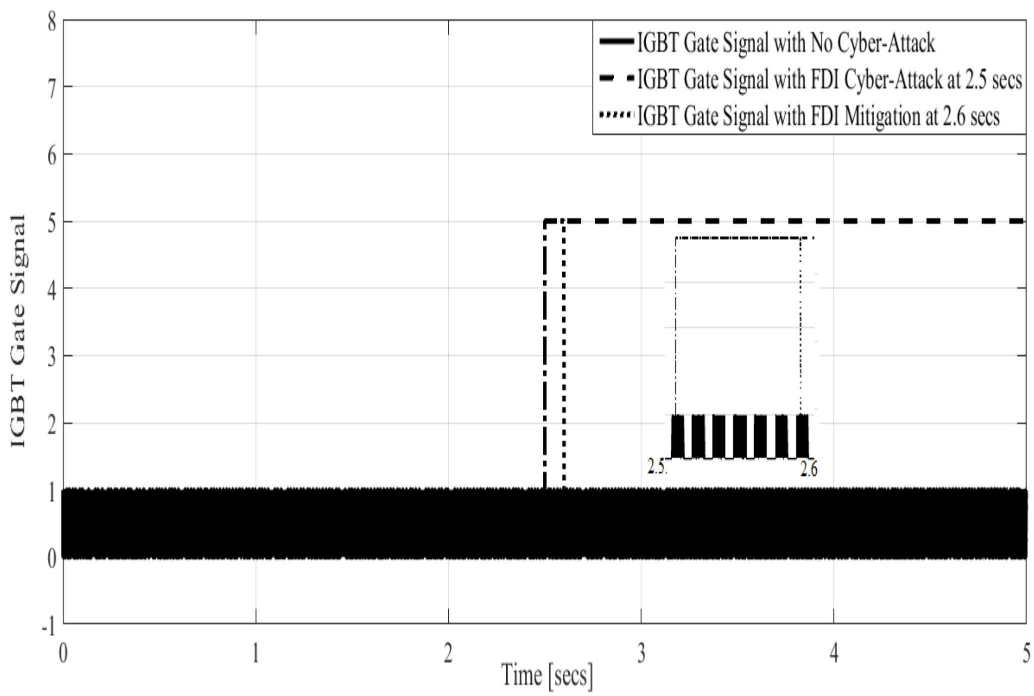

Figure 106. IGBT gate pulse signal for VSC of SES for FDI attack

1. DDoS Attack Case

Figures 107-113 show the voltage responses at the PCC, current at PCC, power at PCC, power of energy storage system, terminal voltage of synchronous generator, terminal voltage of wind generator and terminal voltage of PV. From the responses, it is shown that the DDoS attack affects the power quality of the hybrid grid. It is also evident from the responses that the proposed technique detects the cyber-attack and properly mitigates it.

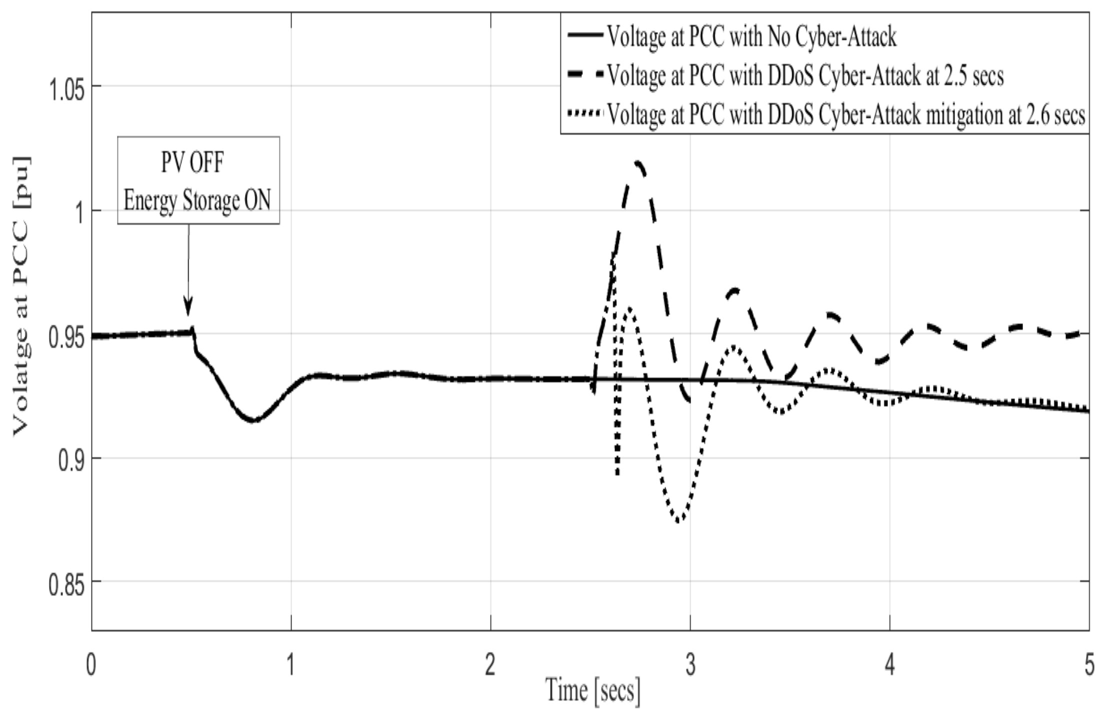

Figure 107. Voltage at PCC

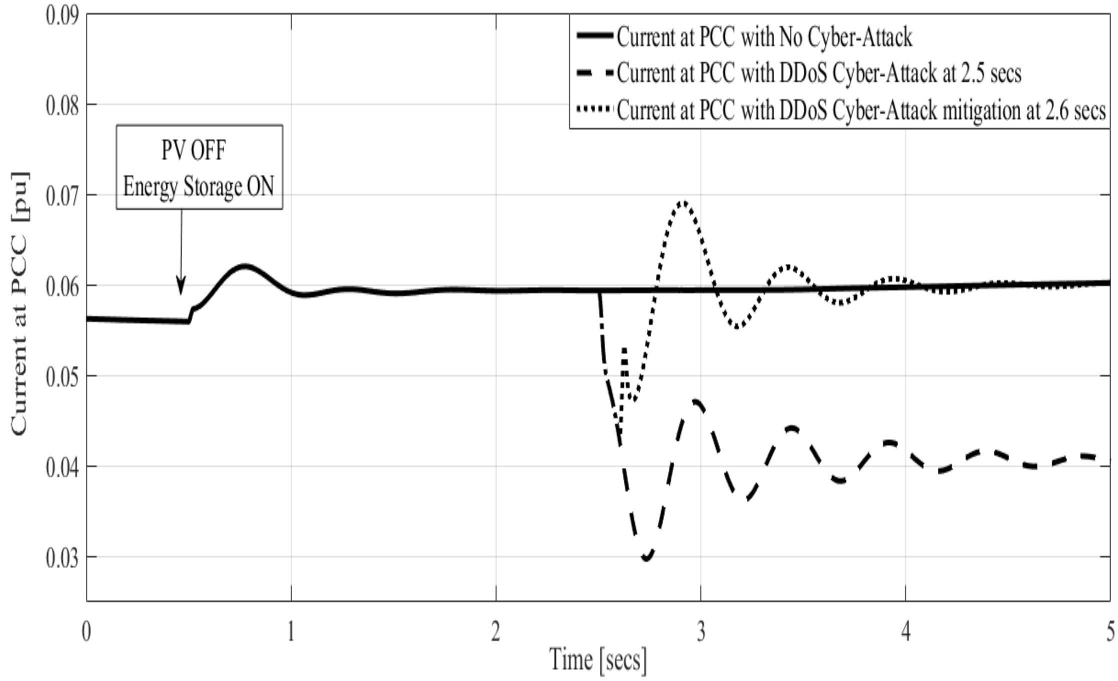

Figure 108. Current at PCC

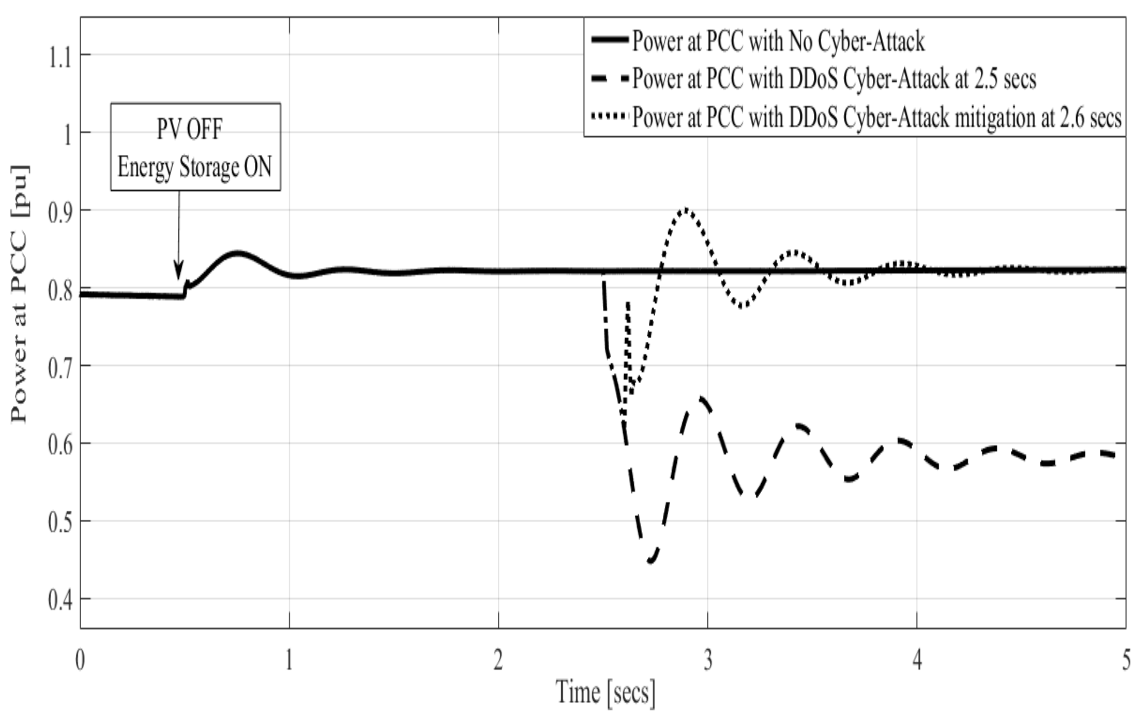

Figure 109. Power at PCC

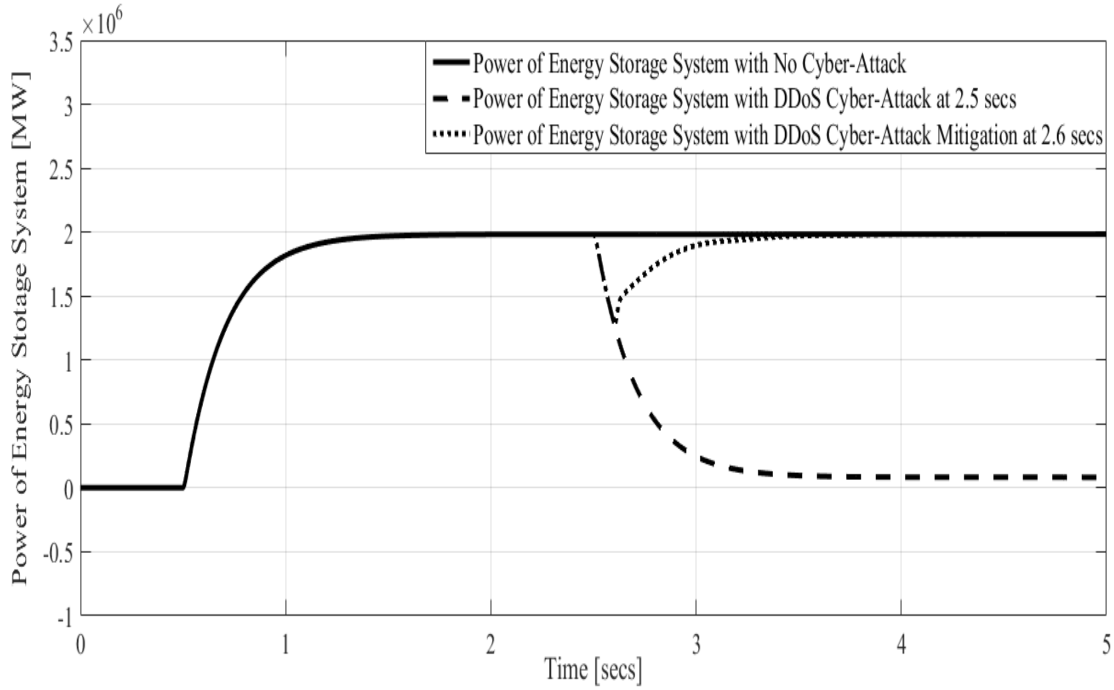

Figure 110. Power of ESS

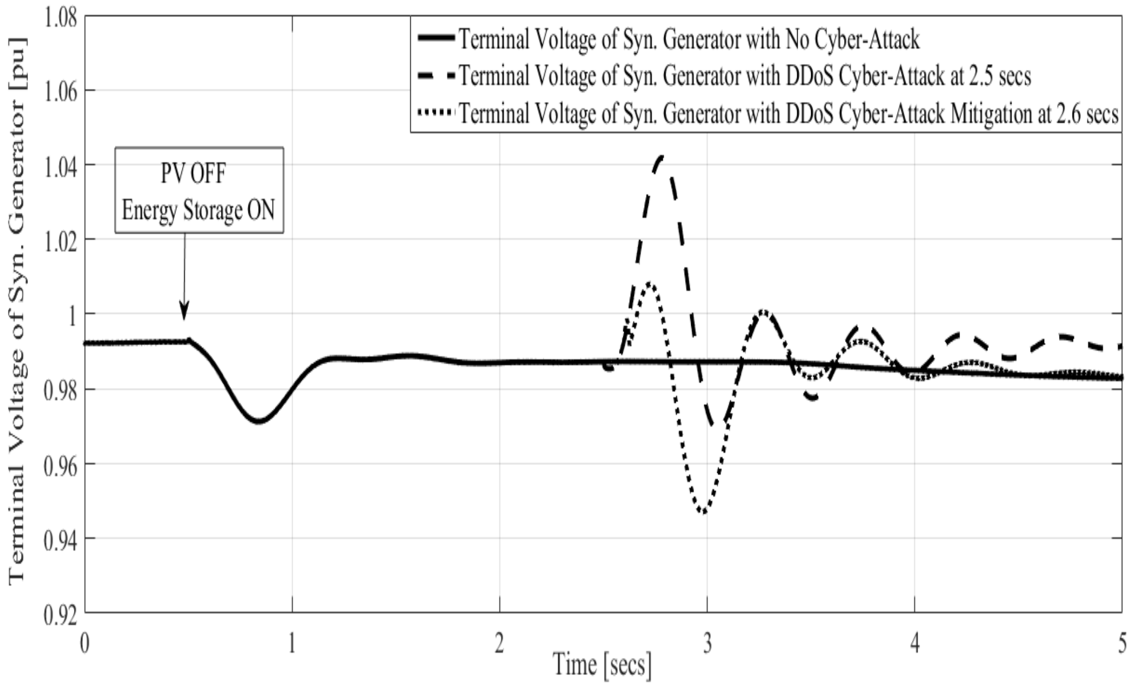

Figure 111. Terminal Voltage of Synchronous Generator

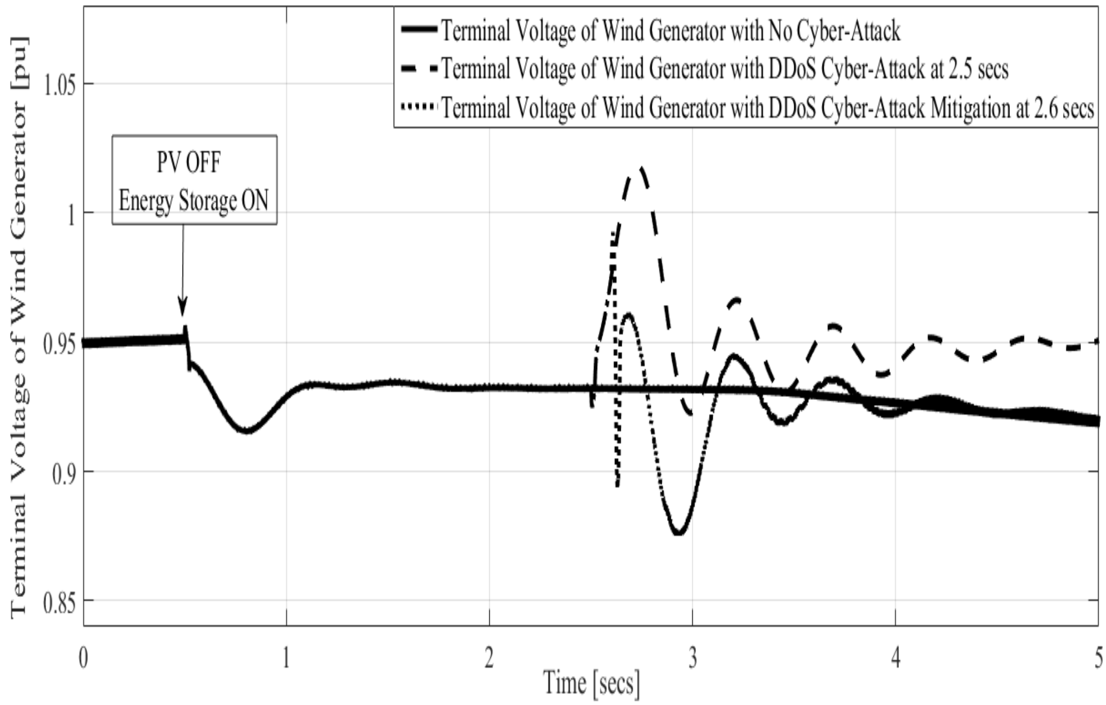

Figure 112. Terminal Voltage of Wind Generator

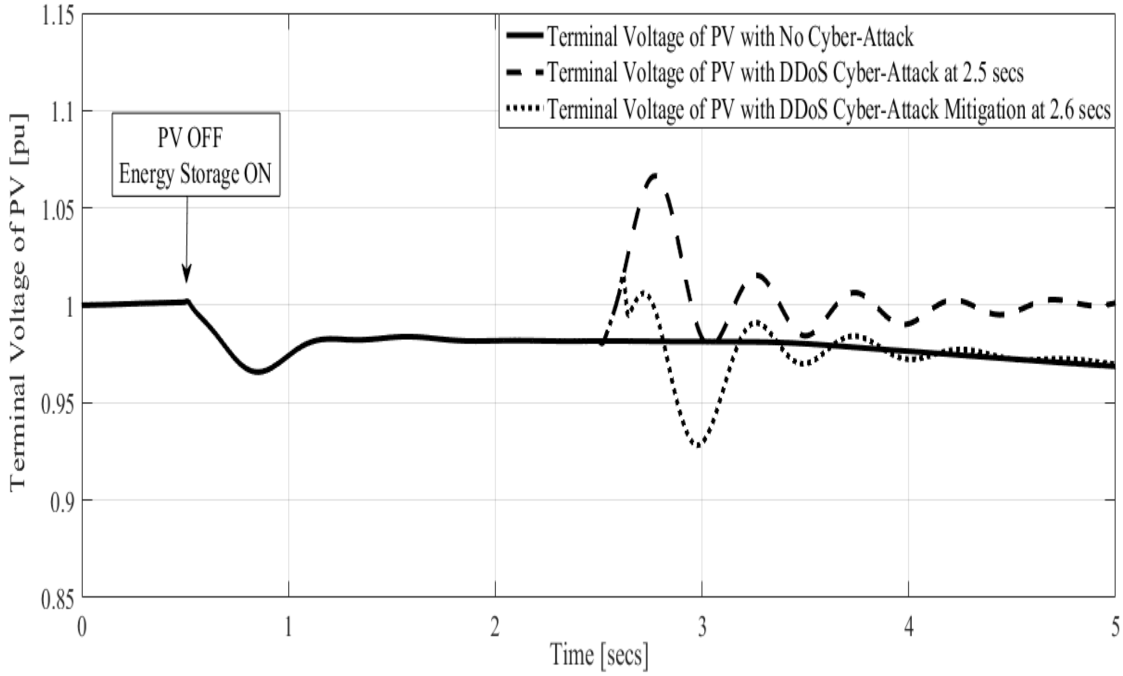

Figure 113. Terminal Voltage of PV

2. FDI Attack Case

Figures 114-120 show the voltage responses at the PCC, current at PCC, power at PCC, power of energy storage system, terminal voltage of synchronous generator, terminal voltage of wind generator and terminal voltage of PV. From the responses, it is shown that the FDI attack affects the power quality of the hybrid grid. It is also evident from the responses that the proposed technique detects the cyber-attack and properly mitigates it.

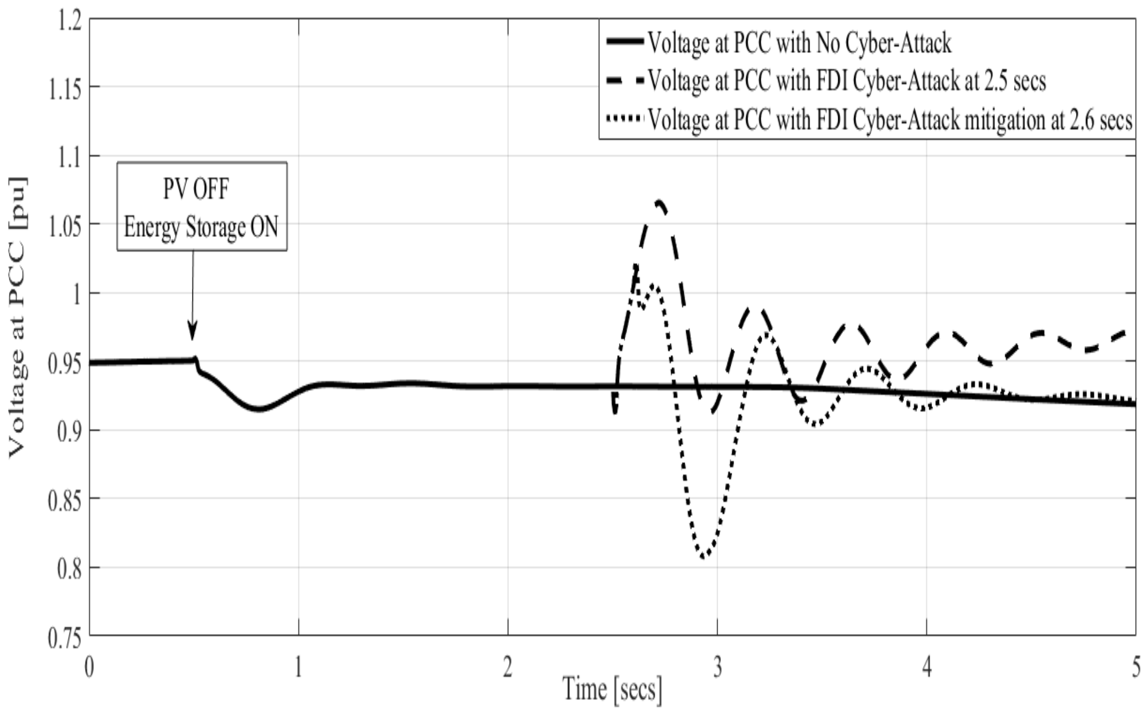

Figure 114. Voltage at PCC

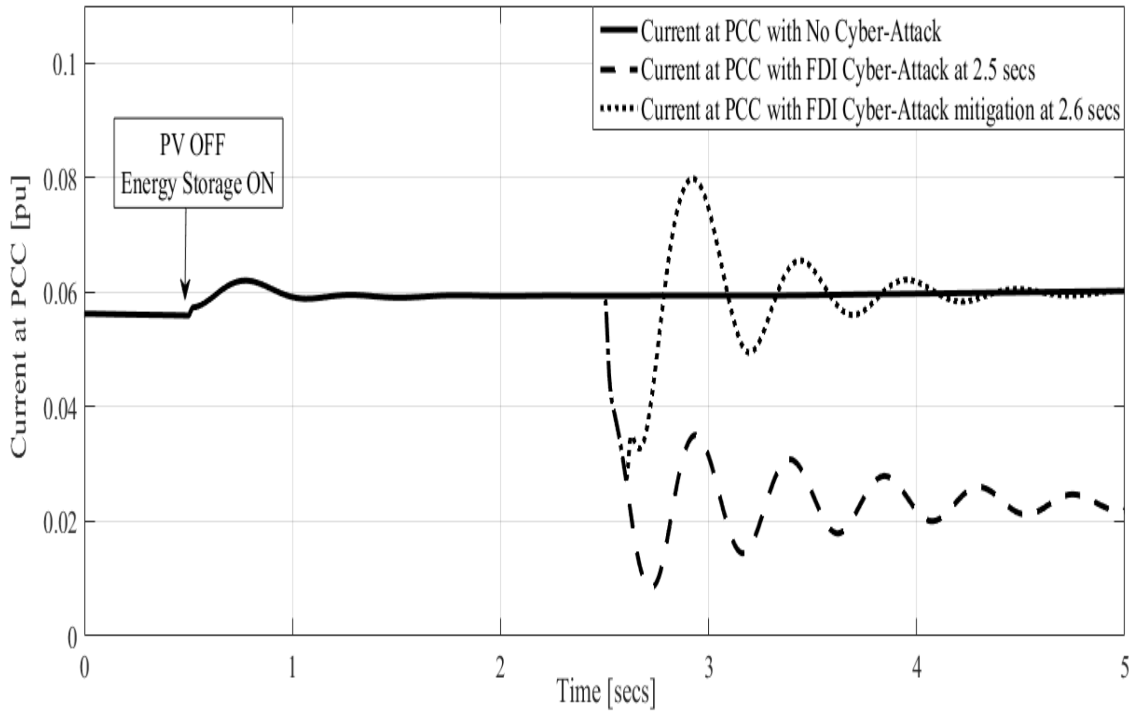

Figure 115. Current at PCC

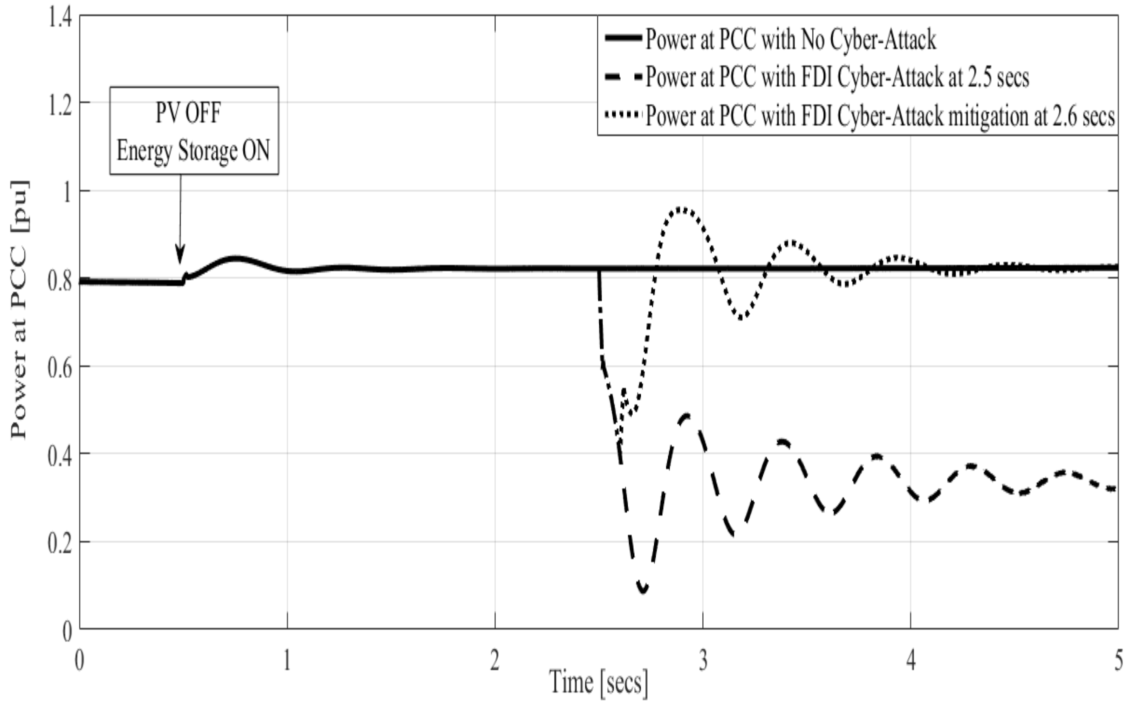

Figure 116. Power at PCC

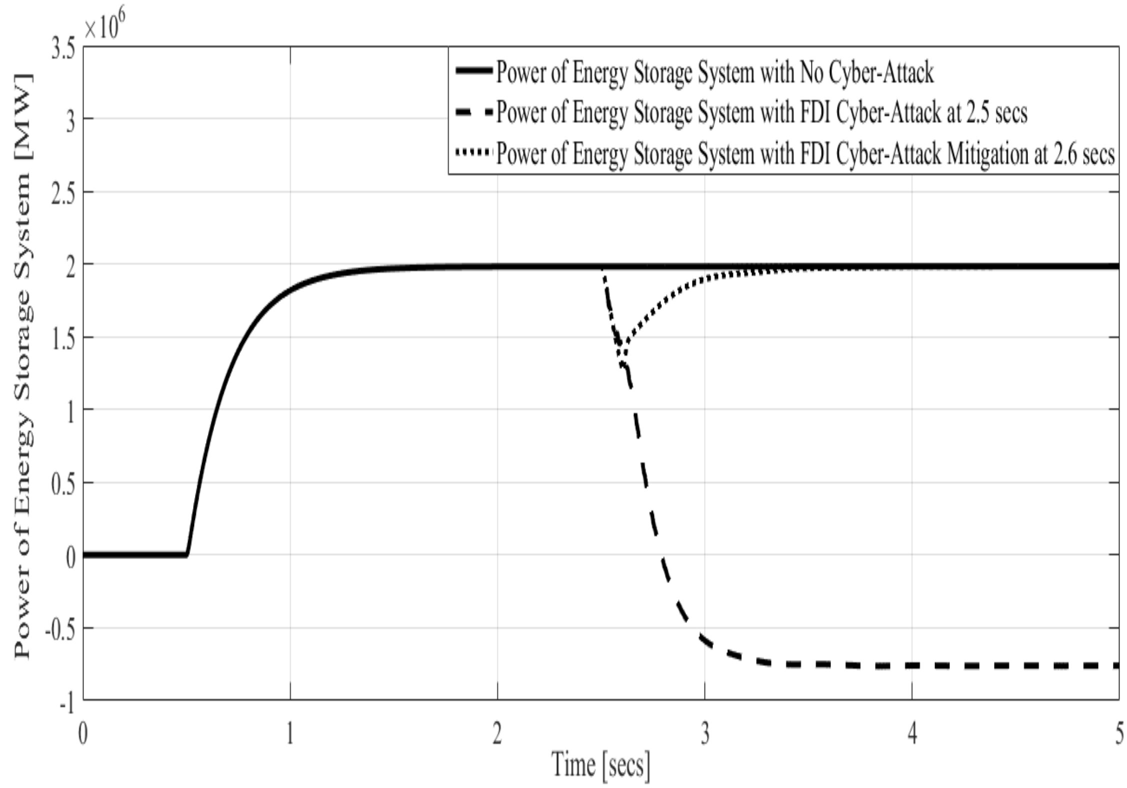

Figure 117. Power of ESS

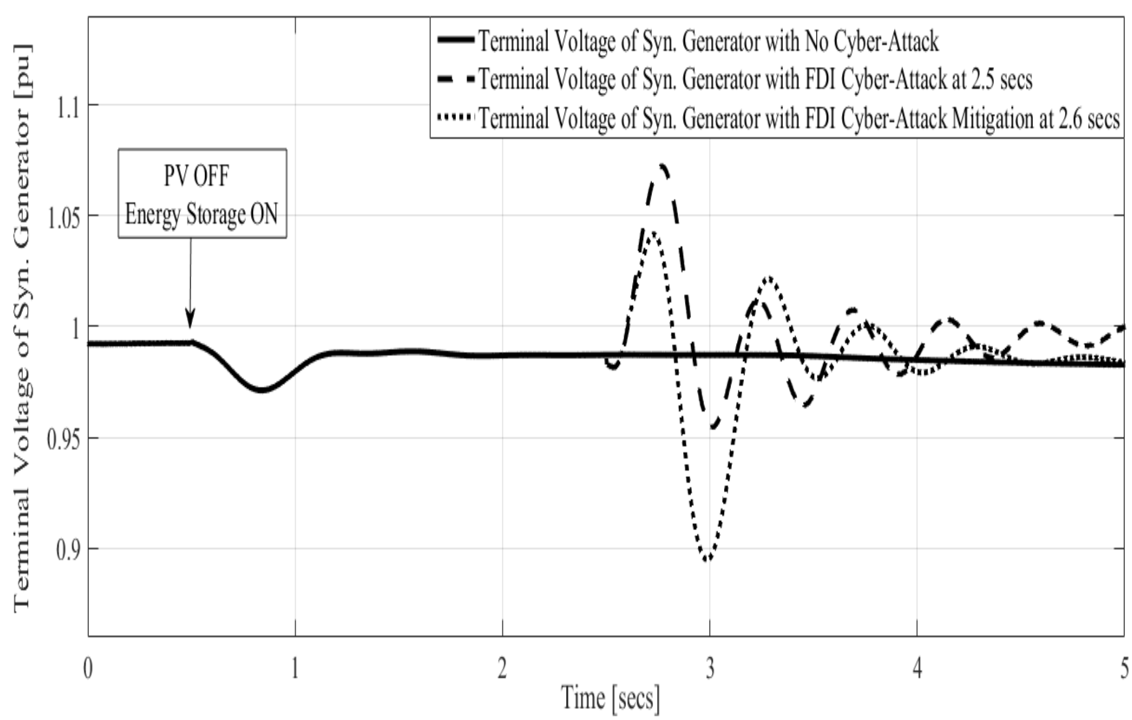

Figure 118. Terminal Voltage of Synchronous Generator

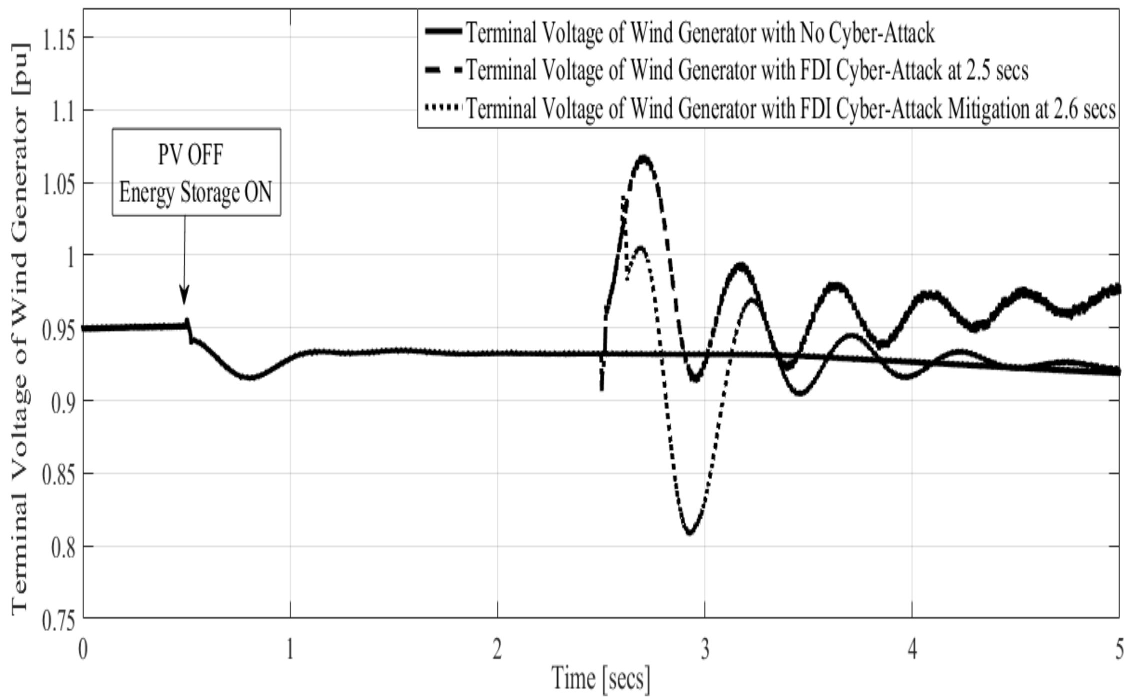

Figure 119. Terminal Voltage of Wind Generator

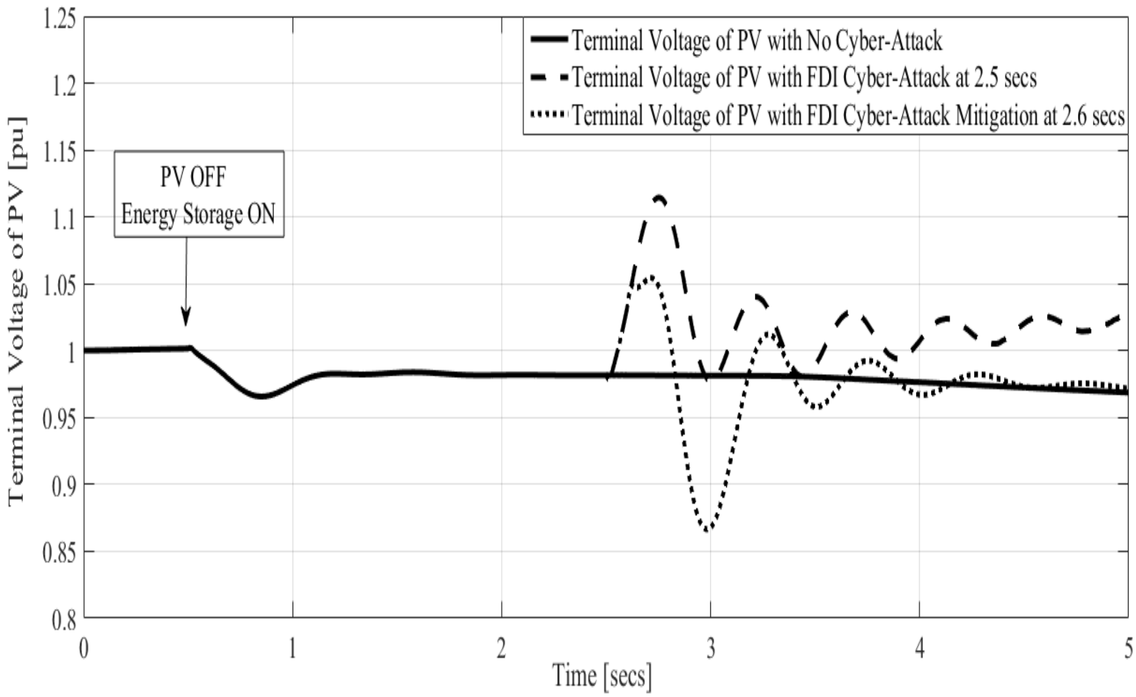

Figure 120. Terminal Voltage of PV

v. Index Based Performance Evaluation of the Proposed Mitigation Techniques

The performance of the proposed cyber security mitigation techniques has been evaluated through the voltage index calculation using equation (17). The lower the value of voltage index, the better the system performance. In other words, the less deviation of the PCC voltage with respect to time ensures the system stability.

Tables XXVII-XXX show the voltage index values for the two cyber-attack scenarios with and without the proposed controllers for GSC, VSC, AVR and SES. From these index values, it is evident that the cyber-attack deteriorates the performance of the hybrid grid. Also, the proposed detection and mitigation techniques for the GSC, VSC, AVR and SES perform well and improve the power quality of the hybrid grid. Moreover, for the DDoS and FDI attack on the GSC, the PI controller performs better than the Non-Linear controller. In case of VSC, the PI controller works better for the DDoS attack and the Non-Linear controller works better for the FDI attack. For the AVR, the Non-Linear controller performs better than PI in case of DDoS attack and the PI controller works better for the FDI attack.

Table XXVII: Voltage Index Values for GSC

Attack Point	Type of Attack	Voltage Index			
		No Attack	With attack but no controller	PI controller	Non-linear Controller
GSC	**FDI**	0.0435	0.3291	0.06541	0.06981
	DDoS		0.8460	0.0896	0.1063

Table XXVIII: Voltage Index Values for VSC

Attack Point	Type of Attack	Voltage Index			
		No Attack	With attack but no controller	PI controller	Non-linear Controller
VSC	**FDI**	0.0435	0.2159	0.09748	0.06077
	DDoS		0.4029	0.06023	0.06029

Table XXIX: Voltage Index Values for AVR

Attack Point	Type of Attack	Voltage Index			
		No Attack	With attack but no controller	PI controller	Non-linear Controller
AVR	**FDI**	0.0435	0.1911	0.05429	0.05688
	DDoS		0.2002	0.05097	0.04935

Table XXX: Voltage Index for SES

Type of Attack	Voltage Index		
	No Attack	With attack but no mitigation	Mitigation
FDI	0.0799	0.1259	0.0981
DDoS		0.1054	0.0679

vi. Analysis of Effects of Different Types Cyber-Attacks on SES

This section deals only with the effects of different cyber-attacks that were applied at the breaker of the SES. This section doesn't include mitigation techniques. Only the effect of cyber-attacks on the power quality of the system are demonstrated.

1. Impact of DDoS Cyber-Attack

For this case, it is assumed that the PV system is turned off at 0.5 sec and the SES is turned on at 0.5 sec. The DDoS attack on the energy storage (i.e., energy storage disabled) occurs at 3.5 sec and persists till 5 sec. Figs. 121- 123 show the voltage responses at PCC, current response at PCC, and power response at PCC during the DDoS cyber-attack. From the responses, it is shown that the DDoS attack on the energy storage deteriorates the power quality of the hybrid power system.

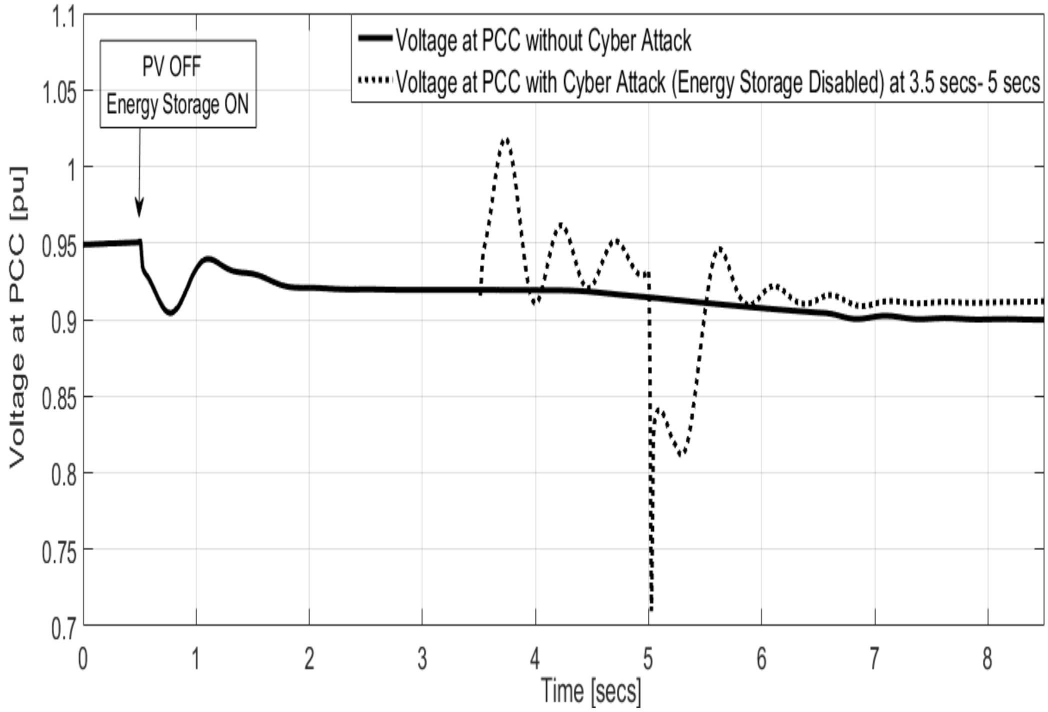

Figure 121. Voltage at PCC

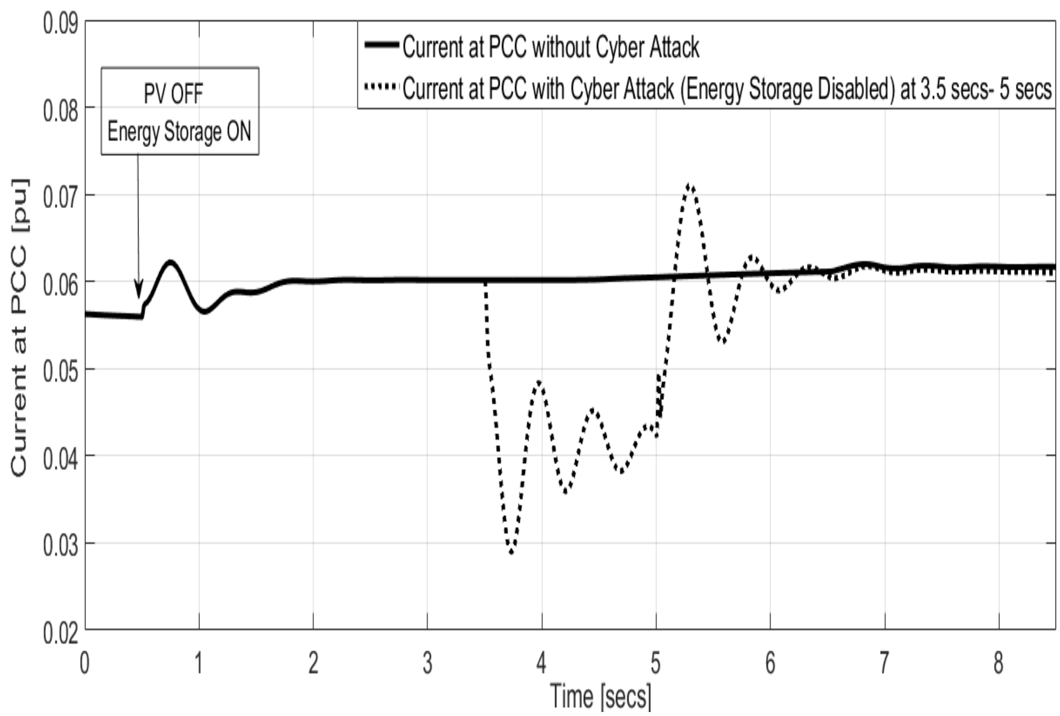

Figure 122. Current at PCC

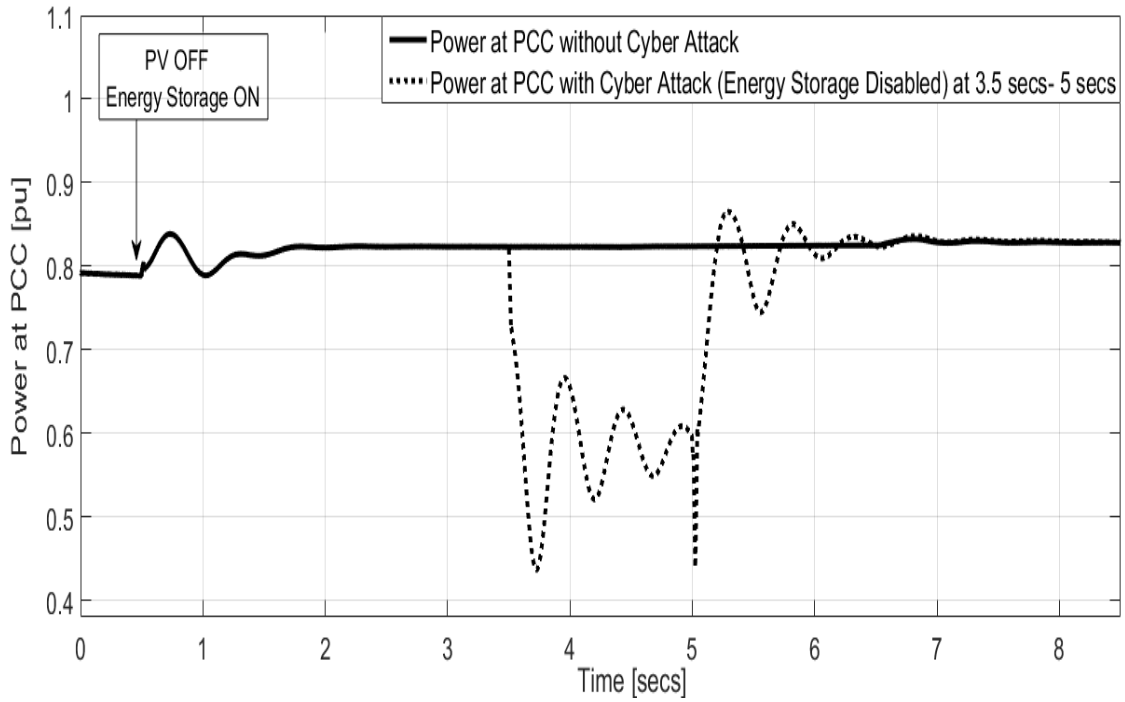

Figure 123. Power at PCC

2. Impact of Bad Data Injection Attack

For this case, the PV is assumed to be on always. This means the SES system was off at 0.5 sec, unlike the previous scenario. It is considered that the bad data injection cyber-attack enables the energy storage system from 3.5 sec to 5 sec. Figs. 124-126 show the voltage responses at PCC, current at PCC, and power responses at PCC during the bad-data injection cyber-attack. From the responses, it is shown that the bad data injection cyber-attack on the energy storage deteriorates the power quality of the hybrid power system.

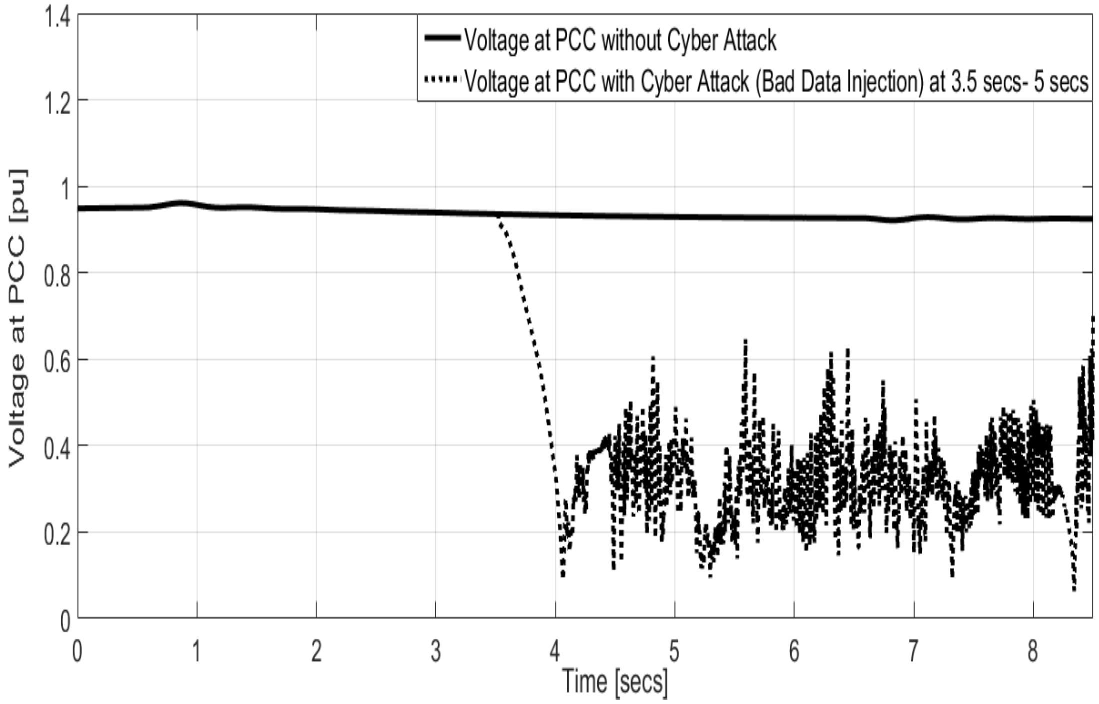

Figure 124. Voltage at PCC

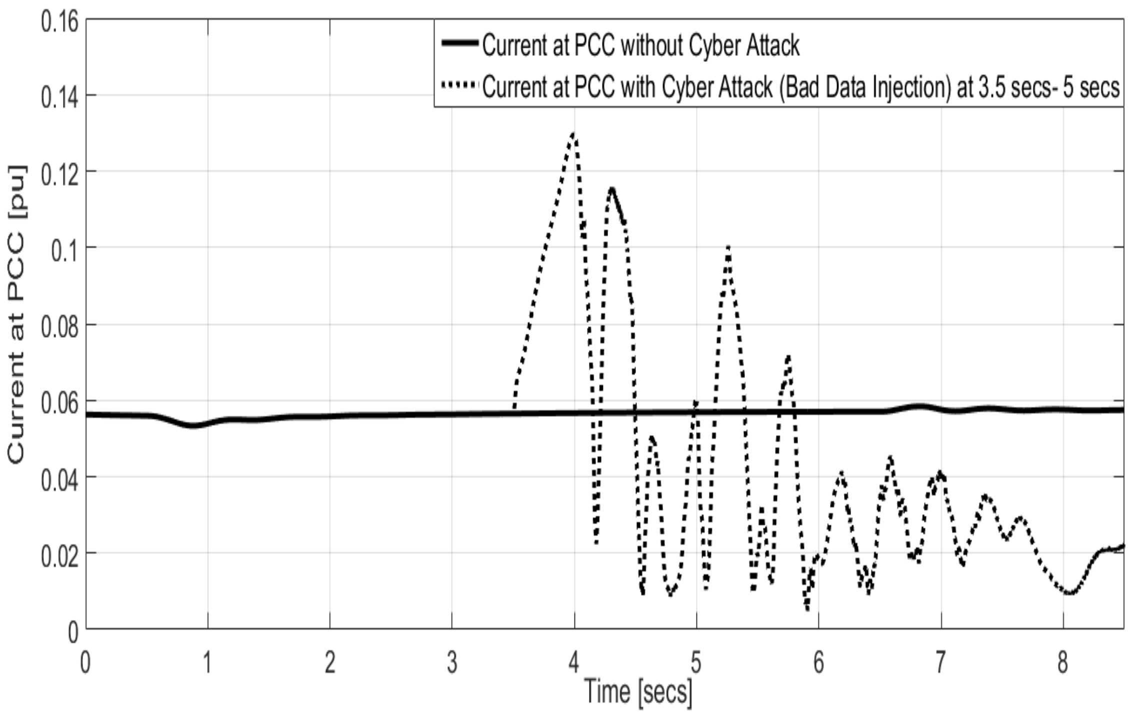

Figure 125. Current at PCC

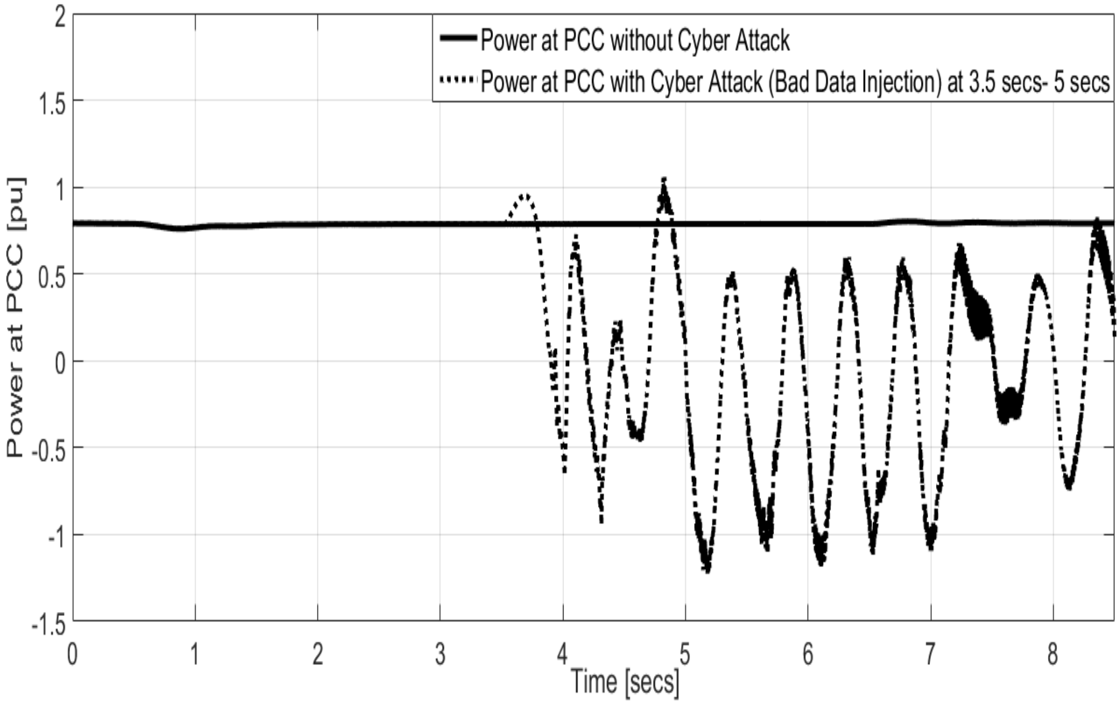

Figure 126. Power at PCC

3. Effects of Crash Override Cyber-Attack

For this case, it is assumed that the PV system is turned off at 0.5 sec and the SES is turned on at 0.5 sec. The Crash Override attack on the circuit breaker of the energy storage (i.e., energy storage disabled) occurs at 2.5 sec- 3 secs, 4.5-5 secs, and 6.5 secs-8.5 secs. Figs. 127-131 show the voltage responses at PCC, current at PCC, power at PCC, terminal voltage of synchronous generator and terminal voltage of wind generator during the Crash Override attack. From the responses, it is shown that the Crash Override attack on the energy storage deteriorates the performance of the hybrid grid system.

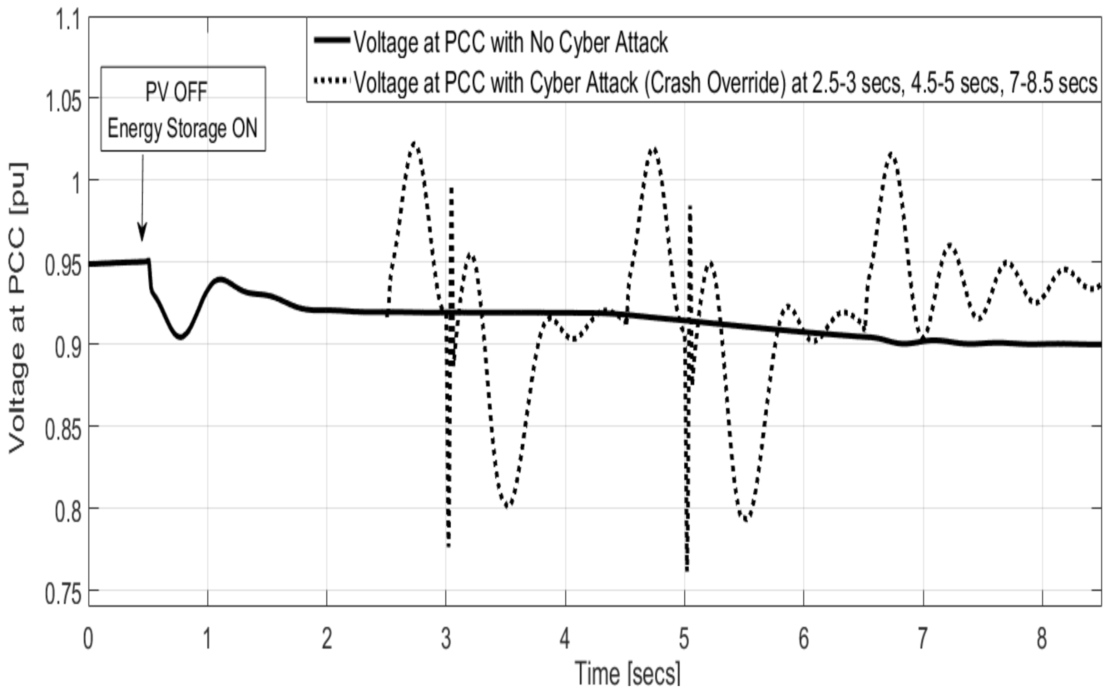

Figure 127. Voltage at PCC

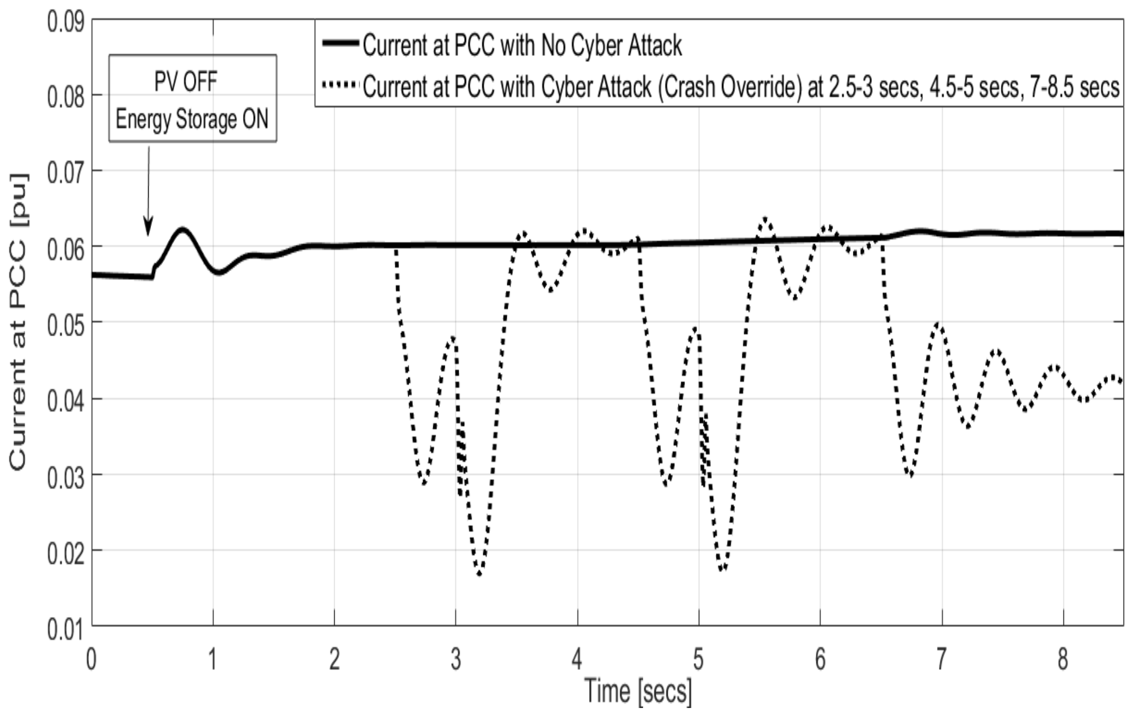

Figure 128. Current at PCC

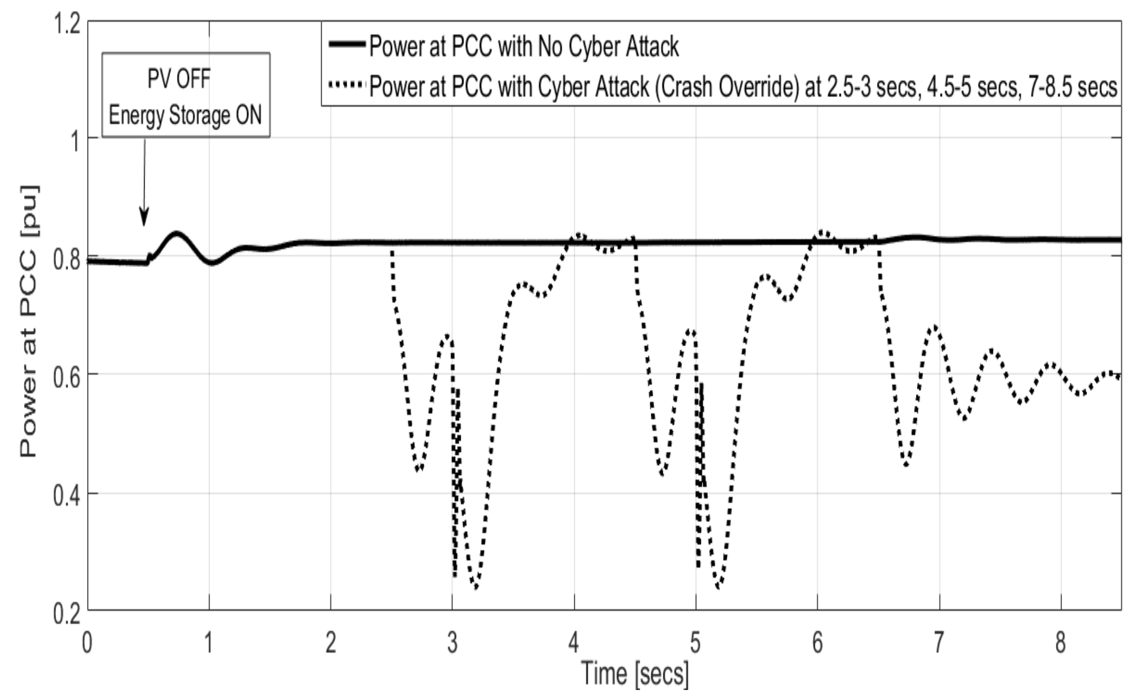

Figure 129. Power at PCC

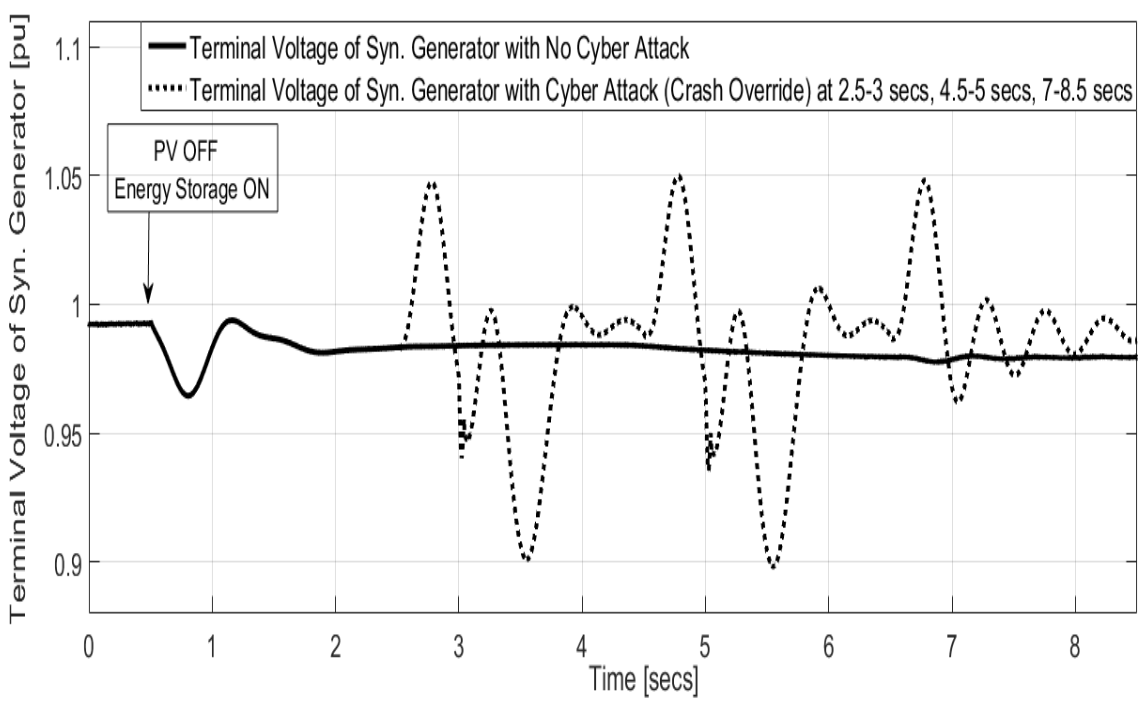

Figure 130. Terminal Voltage of Synchronous Generator

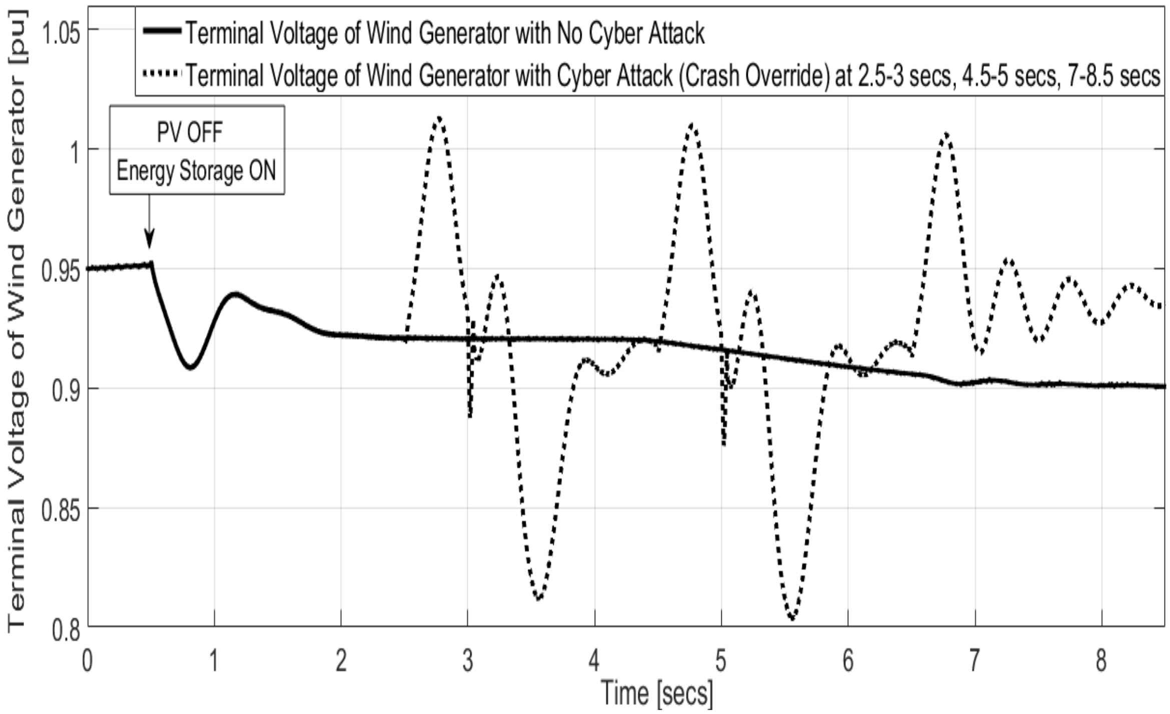

Figure 131. Terminal Voltage of Wind Generator

4. Effects of Tampering Communication Data/Signal Cyber Attack

For this case, it is assumed that the PV system is turned off at 0.5 sec and the SES is turned on at 0.5 sec. For the tampering communication data attack, the energy storage controller is attacked and the signal to start the energy storage is delayed from 0.5 secs to 2.5 secs. Figs. 132-136 show the voltage responses at PCC, current at PCC, power at PCC, terminal voltage response of synchronous generator, and terminal voltage of wind generator. From the responses, it is shown that the tampering communication data/signal cyber-attack on the energy storage deteriorates the performance of the hybrid grid system.

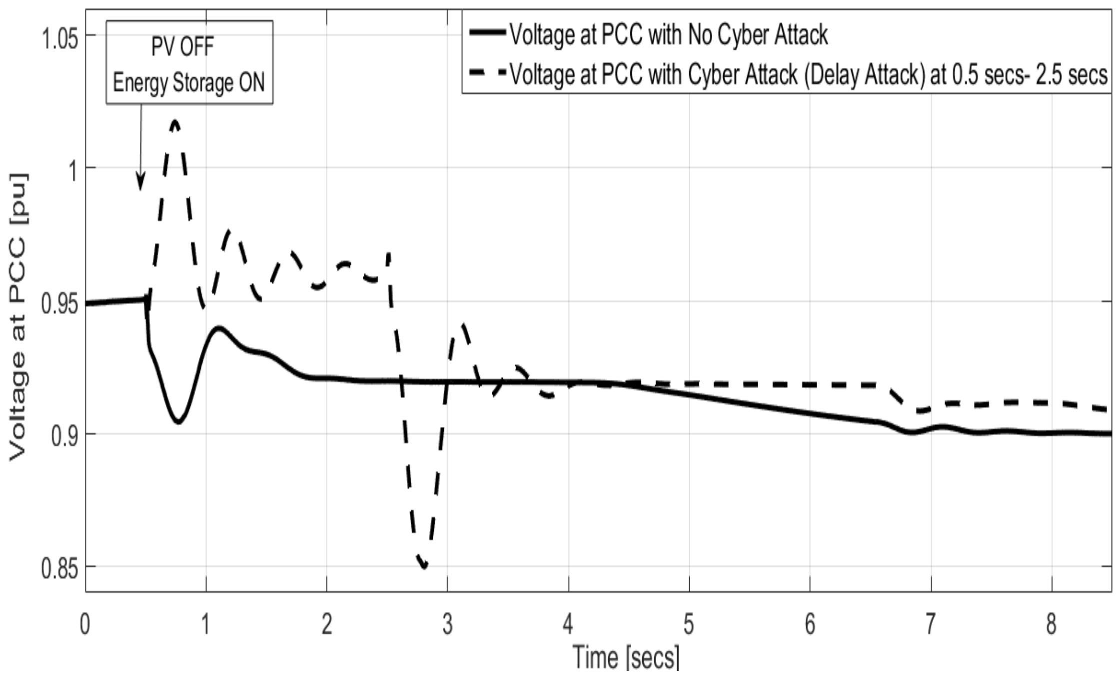

Figure 132. Voltage at PCC

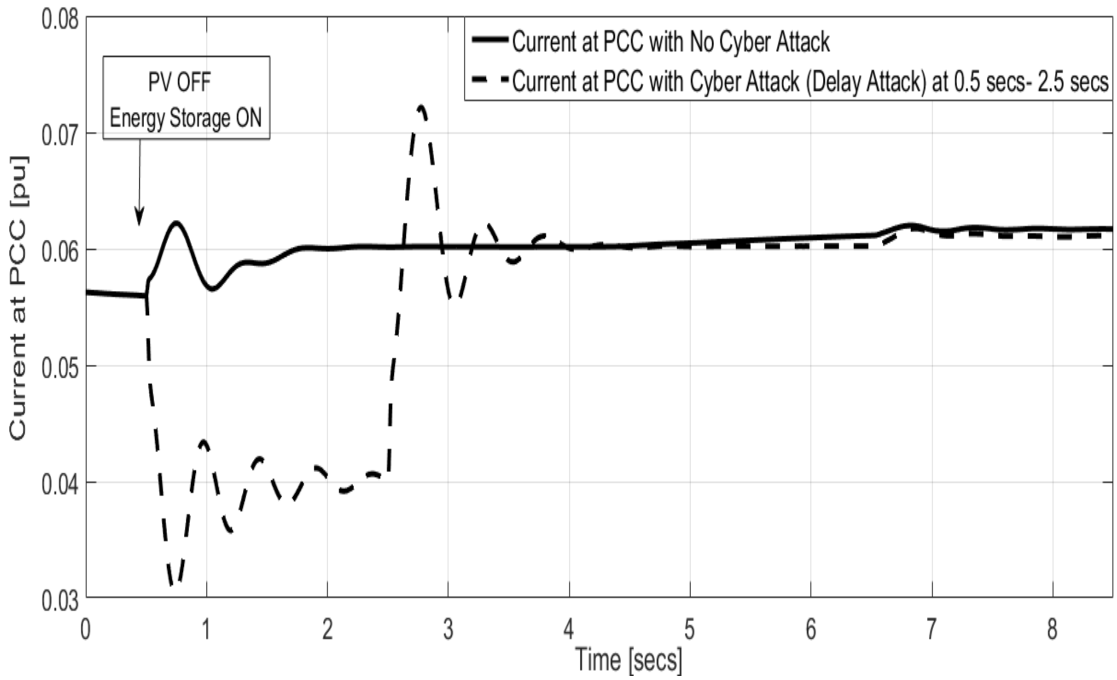

Figure 133. Current at PCC

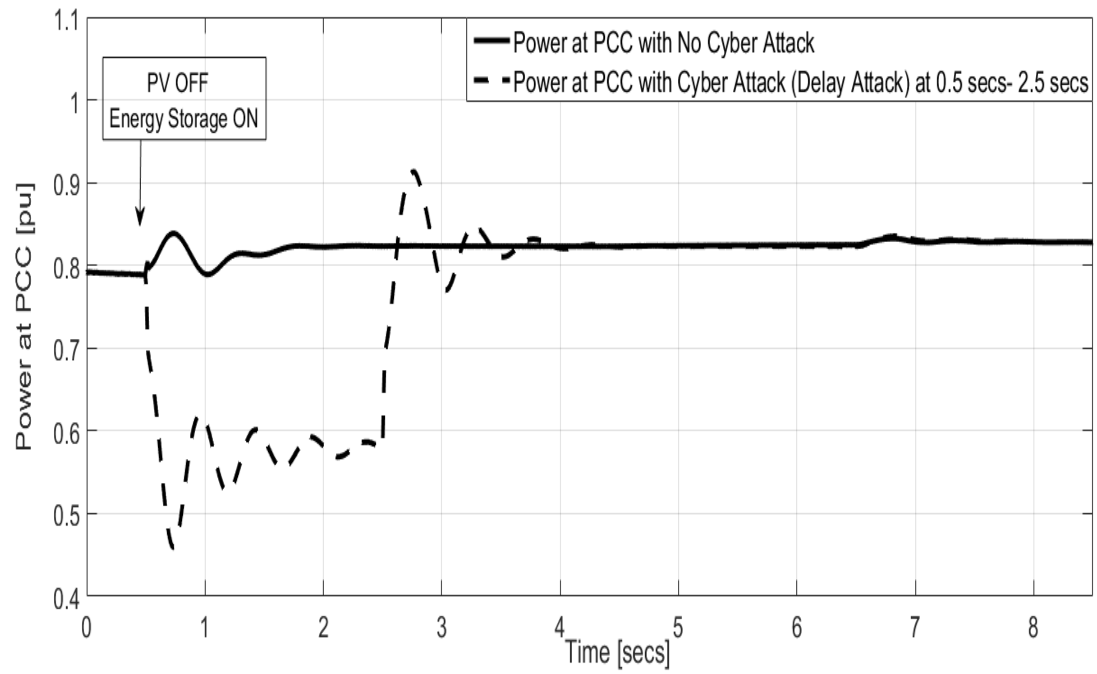

Figure 134. Power at PCC

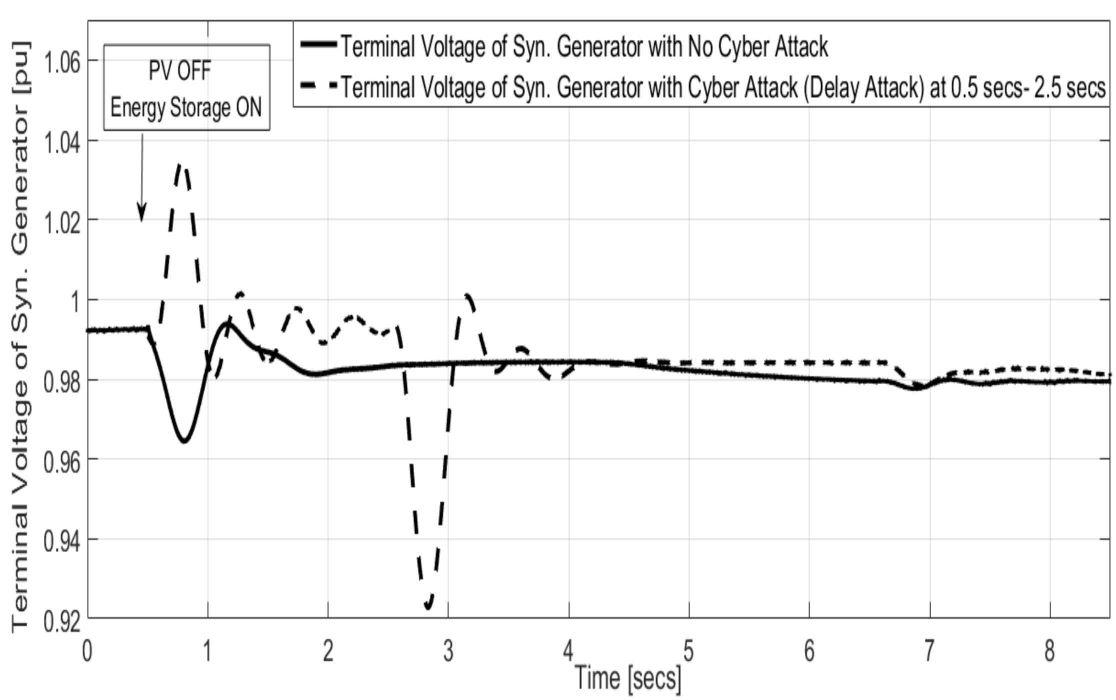

Figure 135. Terminal Voltage of Synchronous Generator

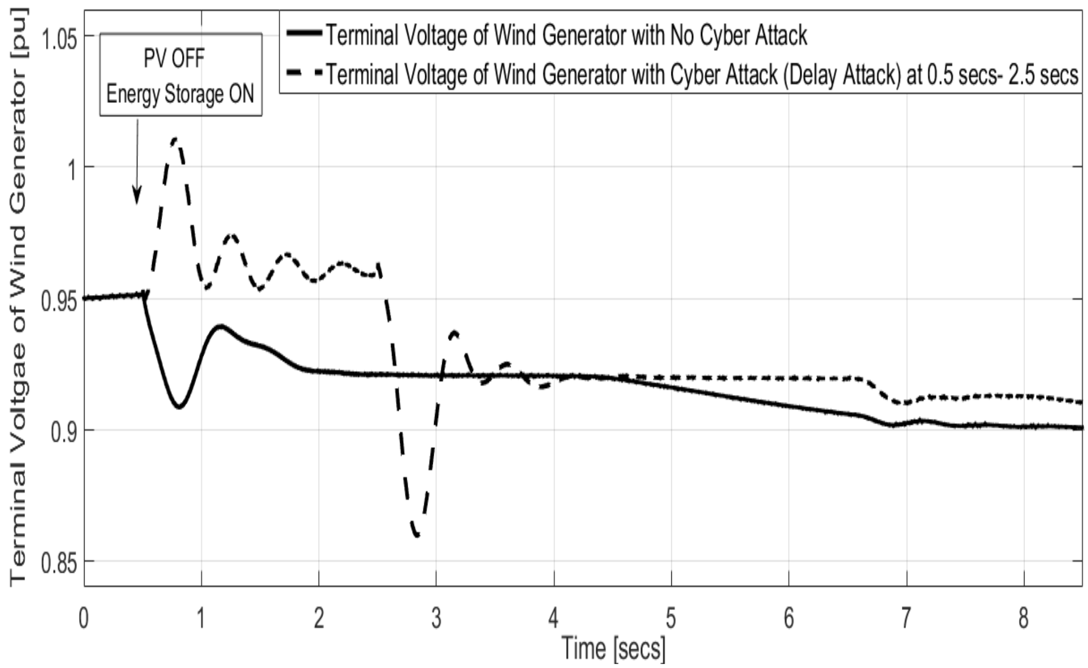

Figure 136. Terminal Voltage of Wind Generator

G. Conclusion

This chapter analyzes the effects of cyber-attacks on various components such as the SES system, GSC of wind generator, VSC of the PV system, and AVR of the synchronous system in a hybrid power grid. The DDoS attack, FDI attack, crash override attack, and tampering communication data/signal attacks are considered on the mentioned devices. Two new mitigation methods based on Non-Linear controller and PI controller for the GSC and VSC, and one new detection and mitigation method for the SES, have been proposed. The effects of cyber-attacks through circuit breakers analysis is carried out only for the SES. Based on the simulation results, the following conclusions can be drawn.

i) The DDoS and FDI cyber-attacks on the GSC of the wind generator affects the power quality of the hybrid grid. The responses also show that the two proposed controllers, NL controller and PI controller mitigate the adverse effects of cyber-attack well and improve the power quality of the system.

ii) The DDoS and FDI cyber-attacks affects the VSC of PV system and the performance of the hybrid grid, but the proposed controllers, i.e., the NL controller and the PI controller mitigate the adverse effects of the cyber-attack. The controllers also improve the power quality of the system.

iii) The DDoS and FDI cyber-attacks affects the AVR of SG system and the performance of the hybrid grid, but the proposed controllers, i.e., the NL controller and the PI controller mitigate the adverse affects of the cyber-attack. The controllers also improve the power quality of the system.

iv) The DDoS and FDI attacks affect the SES. The gate signal of the IGBT of the VSC is tampered with, and the mitigation method is successful in returning the signal back to original thus mitigating the attack and hence improving the power quality of the system.

v) The effects of different types cyber-attacks on circuit breaker of SES shows that the cyber-attacks impact the operation of SES and deteriorate the performance of the entire system.

VI. CONCLUSION AND FUTURE WORK

A. Conclusion

The main objective of this dissertation is to make significant contribution in the field of power quality improvement in case of various issues like faults, communication delays and cyber-attacks. The conclusions can be summarized as follows.

1. Different non-linear controllers like the ANFIS controlled TSC, Static Non-Linear control based TSC, and Fuzzy Logic controlled TSC are proposed to overcome the nonlinearity issue of the system and improve the performance of the network. At first the performance of the FLC based TSC was compared with that of the conventional PID controlled TSC. Later, the effectiveness of the ANFIS controlled TSC and static Non-Linear controlled TSC was compared with that of the Fuzzy controlled TSC. Quantitative analysis is done in terms of voltage index and THD to evaluate the performance of the system and to observe the effectiveness of the proposed controllers. From the results it is shown that the fuzzy logic controlled TSC is effective to enhance the power quality of the hybrid system. Also, the performance of the proposed fuzzy logic controlled TSC is better than that of the PID controlled TSC. Moreover, the proposed ANFIS and static nonlinear control based TSC methods are effective to enhance the power quality of the hybrid grid system. Also, the proposed non-linear controlled TSC perform better than the fuzzy controlled TSC.
2. This dissertation also deals with the communication delays. Two controllers, namely the FLC based method and the Modified Predictor method, are proposed to minimize the adverse affects of time delay on the power quality enhancement of a hybrid power grid. Effect of time delays ranging from 0-700 ms have been considered for the analysis. The performance of the FLC based method has been compared with that of

the Modified Predictor method in terms of voltage index at PCC. The Fuzzy controller and Modified Predictor Methods are effective in reducing the negative effects of time delay on the power quality improvement of the hybrid power system. The fuzzy controlled method performs better than the modified predictor method in most of the cases. In some cases, like the 2LG temporary fault at points F2 and F1, the performance of the Modified Predictor method is better than that of the 2-Input Fuzzy controller method.

3. Furthermore, this dissertation analyzes the affects of cyber-attacks on the controllers of hybrid power grid like the GSC of wind generator, the VSC of the PV system, the AVR of the synchronous generator, and the SES system. To analyze the affects, two types of cyber-attacks, DDoS and FDI attacks have been considered. This dissertation also proposed two controllers, such as the Non-Linear controller and PI controller to detect and mitigate the cyber-attacks. The simulation results show that cyber-attacks deteriorate the performance of the system. The DDoS and FDI cyber-attacks on the GSC of the wind generator, VSC of the PV system, AVR of the SG system affect the power quality of the hybrid grid. The responses also show that the two proposed controllers, i.e., the NL controller and PI controller mitigate the adverse affects of cyber-attack well and improve the power quality of the system. It is evident that the DDoS and FDI attacks affect the SES. The gate signal of the IGBT of the VSC is tampered with and the mitigation method is successful in returning the signal back to original thus mitigating the attack and hence improving the power quality of the system. Furthermore, different types of cyber-attacks on the circuit breaker of SES impact the operation of SES and deteriorate the performance of the entire system.

It is to note here that the validity of the results has been tested analytically. The results obtained from the simulations have been manually calculated using the required equations. The manually calculated results were found to be almost close to the ones obtained from the Matlab/Simulink simulations.

B. Contribution of this Thesis

There are several works which have applications of the nonlinear controllers, such as the FLC, ANFIS, and static nonlinear controller in the power system stability analysis. But none of the work dealt with the application of these controllers for power quality improvement of hybrid power grid. The originality of this work also lies with proposing two new controllers such as the 2-input based fuzzy logic controller and modified predictor method to minimize the adverse effects of time delay introduced in the network of a hybrid power grid consisting of IEEE 9 bus system and a DFIG-based wind generator system. This work also analyzes the effects of cyber-attacks on different controllers of the hybrid power system like the GSC, VSC, AVR, and SES. Two different controllers, such as the Non-Linear controller and PI controller have also been proposed to detect and mitigate the cyber-attacks.

C. Future Work

1. In future, a comparative stability analysis will be performed for the proposed non-linear controllers. For the stability analysis of the controllers, the Lyapunov method will be used. This method provides the system with robustness to (bounded) uncertainty in the system dynamics and adds certain (non-smooth) terms to the control that ensures stability for most of the uncertainties. For tuning the PI/PID controllers, one of the well-known optimization methods, such as the Particle Swarm Optimization [250], Bat Algorithm [251], Bacterial Foraging Optimization [252], Genetic Algorithm [253], Bee

Swarm [254], Ant Colony Optimization [255], Shuffled Frog-Leaping [256], etc., will be used.

2. Other new methods to minimize the negative impact of random delays will be explored. Moreover, delays due to cyber-attacks will be considered, and appropriate minimization methods will be investigated.
3. New methods for cyber-attacks detection and mitigation in smart hybrid grids will be explored. Appropriate control algorithm will be investigated and developed for microgrid operation. Data Driven algorithms will be developed to ensure secure power delivery to the consumers.
4. Centralized controller implementation will be explored for different types of power quality issues in hybrid power grid.
5. Repeated applications of cyber-attacks scenario will be considered. Moreover, the robustness of the proposed attack mitigation controller parameters will be studied for different set point changes by the attackers.

VII. BIBLIOGRAPHY

[1] R. C. Dugan, M. F. McGranaghan, S. Santoso and H. W. Beaty, Electrical Power Systems Quality, McGraw-Hill, 2003.

[2] A. Dolara and S. Leva, "Power quality and harmonic analysis of end user devices," *Energies,* vol. 15, no. 5, pp. 5453-5466, 1996.

[3] M. H. J. Bollen, "Understanding Power Quality Problems: Voltage Sags and Interruptions," *IEEE Press*, 2000.

[4] T. C. Shute, H. T. V. Jr. and J. L. Kirkpatrick, "Survey of harmonic levels on the American electric power distribution system," *IEEE Trans. Power Delivery,* vol. 4, pp. 2204-2213, 1989.

[5] A. E. Emanuel, J. A. Orr, D. Cyganski and E. M. Gulchenski, "A survey of harmonics voltages currents at the customer's bus," *IEEE Trans. Power Delivery,* vol. 8, pp. 411-421, 1993.

[6] J. A. Martinez and J. M. Arnedo, "Voltage sag studies in distribution networks-part T: System modeling," *IEEE Trans. Power Deliv.*, vol. 21, no. 3, pp. 338-345, 2012.

[7] C. K. Subasri, R. S. Charles and P. Venkatesh, "Power quality improvement in a wind farm connected to grid using FACTS device," *Power Electron Renew. Energy Syst.,* vol. 326, no. 4, pp. 1203-1212, 2012.

[8] M. Liao H, "On capability of different FACTS devices to mitigate a range of power quality phenomena," *IET Gener. Trans. Distribution,* vol. 11, no. 5, pp. 2002-2012, 2017.

[9] X. Wang, F. Blaabjerg and W. Wu, "Modeling and analysis of harmonic stability in an ac power-electronics-based power system," *IEEE Trans. Power Electronics,* vol. 29, no. 12, pp. 6421-6432, 2014.

[10] Z. Chen and E. Spooner, "Grid power quality with variable speed wind turbines," *IEEE Trans. Energy Conversion,* vol. 16, no. 5, pp. 148-158, 2001.

[11] F. H. Gandoman, A. Ahmadi, A. M. Sharaf, P. Siano, B. H. J. Pou and V. G. Agelidis, "Review of FACTS technologies and applications for power quality in smart grids with renewable energy systems," *Renewable and Sustain. Energy reviews,* vol. 82, pp. 502-514, 2018.

[12] Primen, "The cost of power disturbances to industrial & digital economy companies," EPRI CEIDS, 2001.

[13] Targosz, Roman and J. Manson, "European Power Quality Survey," LPQI, 2008.

[14] Y. Shih-An, S. Chun-Lien and C. Rung-Fang, "Assessment of PQ cost for high-tech industry," IEEE Power India Conference, 2006.

[15] S. B. Choi, K. Y. Nam, D. K. Kim, S. H. Jeong, H. S. Ryoo and a. J. D. Lee, "Evaluation of interruption costs for industrial customers in Korea," in *Power System Conference and Exposition (PSCE)*, 2006.

[16] Q. Zhong, W. Huang, S. Tao and a. X. Xiao, "Survey on Assessment of Power Quality Cost in Shanghai China," in *IEEE Proceedings*, 2014.

[17] G. Ramanal and B. V. S. Ram, "Power System Stability Improvement Using FACTS and Expert Systems," *International Journal of Advances in Engineering & Technology,* 2011.

[18] A. K. Mohanty and a. A. K. Barik, "Power System Stability Improvement Using FACTS Devices," *INternational Journal of Modern Engineering Research (IJMER),* vol. 1, no. 2, pp. 666-672.

[19] A. Ledwich and a. G. Ghosh, Power quality enhancement using custom power devices, Kluwer's Power Electronics and Power system series,, 2002.

[20] S. D. Swain, P. K. Ray and a. K. B. Mohanty, "Improvement of Power Quality usimg a Robust Hybrid Series Active Power Filter," *IEEE Transactions on Power Electronics,* vol. 32, no. 5, pp. 3490-3498, 2017.

[21] V. Yarlagadda, B. V. S. Ram and a. K. R. M. Rao, "Testing and Control of TSC-TCR Type Static Var Compensator (SVC)Using Microcontroller," *International JOurnal of Control and Automation,* vol. 5, no. 3, 2012.

[22] J. Subrahmanyam, S. R. Reddy, P. K. Sahoo, C. Sashidhar and a. N. M. Reddy, "A Novel Method for Improvement of Power Factor Using Thyristor Switched Capacitor in Wind Mill Power," *International Journal of Emerging Technology and Advanced Engineering,* vol. 2, no. 2, 2012.

[23] A. Ohtake, F. Zhang, T. Fujimoto and a. N. Nakayama, "Development of 200-Mvar class thyristor switched capaciotr supporting fault ride-through," in *International Power Electronics Conference (IPEC-Hiroshima)*, 2014.

[24] L. Zhang, S.-C. Qi, H.-G. Zhao and a. J. Yao, "Study of TSC Plus SVG Basd on the Mixture of Hot Rolling Mill Control of Reactive Power Compensation," in *International Conference on Control, Automation and Systems Engineering (CASE)*, 2011.

[25] S. Ebrahimi, V. Najmi and a. H. Mokhtari, "Reactive compensation investigation of TSC systems based on different power factor definiations," in *IECON 2012-38th Annual Conference on IEEE Industrial Electronics Society*, 2012.

[26] A. D. Baing and a. J. G. Jamnani, "Closed loop control of Thyristor Switched Capaciotr (TSC) for instantaneous Reactive Power Compensation," *International Journal of Engineering Development and Research (IJEDR)*, pp. 84-87, 2014.

[27] P. B. and a. B. V. Sumangala, "Implementation of Thyristor Switched Capacitor for Reactive Power Compensation at Secondary of Distribution Level Feeders for Voltage Stability," *International Journal of Engineering Reaserch & technology (IJERT)*, vol. 2, no. 5, 2013.

[28] A. Goyal, N. Kapil and a. S. Mahapatra, "Implementation of Thyristor Switched Capacitors for pOwer Factor Improvement," *Advance in Elcetronic and Electric engineerin*, vol. 4, no. 3, pp. 225-230, 2014.

[29] P. B. and a. B. V. Sumangala, "Implementation of Thyristor Switched Capacitor for Reactive Power Compensation at Secondary of Distribution Level Feeders for Voltage Stability," *International JOurnal of Engineering Research & Technology (IJERT)*, vol. 2, no. 5, 2013.

[30] H. Su and a. Q. Li, "Rough Controlling TSC for Reactive Current Compensation in traction Substations," in *5th International Power Electronics and Motion Control Conference (IPEMC),CES/IEEE*, 2006.

[31] S. Omar, F. M. Fotuhi-Firuzabad and a. R. Billinton, "Subtransmission System Reliability Enhancement Using a Thyristor Controlled Series Capacitor," *IEEE Transactuons on Power Delivery*, vol. 15, no. 1, pp. 443-449, 2000.

[32] R. Sharma, A. Singh and a. A. N. Jha, "Performance evaluation of tuned PI controller for power quality enhancement for linear and non linear loads," in *Recent Advances and Innovations in Engineering (ICRAIE)*, 2014.

[33] K. Sharma and S. S. a. Sudhir, "EFFECTS ON MAJOR POWER QUALITY ISSUES DUE TO INCOMING INDUCTION GENERATORS IN POWER SYSTEM," *ARPN Journal of Engineering and Applied Sciences,* vol. 5, no. 2, p. 9, 2010.

[34] C. T. Leondes, Fuzzy Theory Systems: techniques and Applications, London: U. K. : Academics, 1999.

[35] M. E. El-Hawary, Electric Power Applications of Fuzzy Systems, New York: IEEE Press, 1998.

[36] A. T. Johns, Y. H. Song, R. W. Dunn, D. S. Fitton and a. R. K. Aggarwal, "Neural-network basd adaptive single-pole autoreclosure techniques for EHV transmissions systems," *IEE Proceedings of Generation, Transmission and Distribution,* vol. 141, no. 2, pp. 155-160, 1994.

[37] M. Zarghami, M. L. Crow and a. S. Jagannathan, "Nonlinear control of FACTS controllers for damping inter-area oscillations in power systems," *IEEE Transactions on Power Delivery,* vol. 25, no. 4, pp. 3113-3121, 2010.

[38] L. W. a. K. H. Wang, "Dynamic stability analysis of a DFIG-based offshore wind farm connected to a power grid through an HVDC link," *IEEE Tran. Power Syst.,* vol. 26, no. 3, pp. 1501-1510, 2011.

[39] L. Wang and a. L.-Y. Chen, "Reduction of Power Fluctuations of a Large-Scale Grid-Connected Offshore Wind Farm Using a Variable Frequency Transformer," *IEEE Transaction on Sustainable Energy,* vol. 2, no. 3, pp. 226-234, 2011.

[40] R. G. Agarwal and a. V. Wandhare, "Novel Stability Enhancing Control Strategy for Centralized PV-Grid Systems for Smart Grid Applications," *IEEE Trans. on Smart Grid,* 2014.

[41] A. S. Leger, J. James and D. Frederick, "Smart Grid Modeling Approach for Wide Area Control Applications," 2012.

[42] T. Lin, A. Domijan and a. F. C. Jr., "A Survey of Techniques for Power Quality Monitoring," *International Journal of Power Energy Syst.,* vol. 25, no. 3, pp. 167-172, 2012.

[43] B. Naduvathuparambil, M. C. Valenti and a. A. Feliachi, "Communication delays in wide area measurement systems," in *Proceedings of the Thirty-Fourth Southeastern Symposium on System Theory*, 2002.

[44] H. X. Wu, K. S. Tsakalis and a. G. T. Heydt, "Evaluation of time delay effects to wide-area power system stabilizer design," *IEEE Trans. Power Syst.*, vol. 19, no. 4, pp. 1935-1941, 2004.

[45] S. Ayasun and a. A. Gelen, Stability analysis of a generator excitation control system with time delays, 2010.

[46] S. Ayasun, "Computation of time delay margin for power system small-signal stability," *International Journal on Electrical Energy Systems,* vol. 19, pp. 949-968, 2008.

[47] S. Sonmez and a. S. Ayasun, "Effect of load increase and power system stabilizer on stability delay margin of a," *Turkish Journal of Electrical Engineering & Computer Sciences,* vol. 24, pp. 5183-5194, 2016.

[48] G. Cai, D. Yang and C. Liu, "Adaptive Wide-Area Damping Control Scheme for Smart Grids with Consideration of Signal Time Delay," *Energies,* vol. 6, pp. 4841-4858, September 2013.

[49] S. S. Mamidala, "A Review of Cybersecurity for the Power Grid".

[50] K. G. J. L. K. a. M. A.-R. M. S. El. Moursi, "Application of series voltage boosting schemes for enganced fault ride-through performance of fixed speed wind turbines," *IEEE Trans. Power Deliv.* , vol. 29, no. 1, pp. 61-71, 2014.

[51] S. Alarai, S. Member, A. Moawwad, S. Member, M. Shawky, E. Moursi and a. V. Khadkikar, "Voltage Booster Schemes for Fault Ride-Through enhancement of variable Speed Wind Turbines," vol. 4, no. 4, pp. 1071-1081, 2013.

[52] M. Daoud and X. Fernando, "On the Communication Requirements for the Smart Grid," *Energy and Power Engineering,* vol. 3, pp. 53-60, February 2011.

[53] K. Alagar and a. V. Wan, "Context-Aware Security Solutions for Cyber-Physical Systems," *Institute for Computer Sciences, Social Informatics and Telecommunications Engineering,* vol. 109, pp. 18-29, 2013.

[54] J. B. Zhang, C. Y. Han and a. Y. D. Chung, "A novel modal decomposition control and its application to PSS design for damping inter-area oscillations in power system," *IEEE Trans. Power Syst.,* vol. 27, no. 4, pp. 2015-2025, 2012.

[55] S. Kaur and a. G. Bharti, "Two Input Two Output Fuzzy Controller System Design using MATLAB," *International Journal of Advances in Engineering, Science and Technology (IJAEST),* vol. 2, no. 3, pp. 209-218, 2012.

[56] H. Kala, D. Deepakraj, P. Gopalakrishnan, P. Vengadesan and a. M. K. Iyyar, "Performance Evaluation of Fuzzy logic and PID Controller or Liquid Level Process," *International Journal of Innovative Research in Electrical, Electronics, Instrumentation and Control Engineering,* vol. 2, no. 3, 2014.

[57] Y. Mo, T. H.-J. Kim, K. Brancik, D. Dickinson, H. Lee, A. Perrig and a. B. Sinopoli, "Cyber Physical security of a smart grid infrastructure," *Proceedings of IEEE,* vol. 100, no. 1, pp. 195-209, 2012.

[58] J. Yan, C. C. Liu and a. M. Govindarasu, "Cyber Intrusion of Wind Farm SCADA system and Its Impact Analysis," in *IEEE PSCE*, 2011.

[59] X. Liu, M. Shahidehpour, Y. Cao, L. Wu, W. Wei and a. X. Liu, "Microgrid Risk Analysis Considering the Impact of Cyber-Attacks on Solar PV and ESS Control Systems," *IEEE Trans. Smart Grid,* vol. 8, no. 3, pp. 1330-1339, 2017.

[60] M. e. al, "Electric power quality and artificial intelligence: Overview and applicability," *IEEE Power engineering review,* vol. 19, no. 6, pp. 5-10, June'99.

[61] R. Wael, "A power quality perspective to system operational diagnosis using fuzzy logic and adaptive technique," *IEEE trans.on Power Delivery,* vol. 19, no. 3, pp. 903-909, July'2003.

[62] R. A. Flores, "State of the Art in the Classification of Power Quality Events, An Overview".

[63] S. Bhattacharyya and a. S. Cobben, "Consequences of Poor Power Quality- An Overview," 2011.

[64] S. Gupta, "POWER QUALITY: PROBLEMS, EFFECTS AND ECONOMIC IMPACTS," *International Journal of Electrical and Electronics Engineering (IJEEE),* vol. 1, no. 1, pp. 83-91, 2012.

[65] M.H.J.Bollen, "Fast assessment method for voltage sag in distribution system," *IEEE Trans. on Industry Application,* vol. 32, no. 6, pp. 1414-1423, Nov/Dec 96.

[66] P. o. IWANN, "Detection and classification of PQ problems," 8th international workconference on artifical neural network.

[67] M. Hemmingsson and a. D. Karlsson, "Power Quality and system stability," Elforsk report 12:39.

[68] N. P. &. A. Guide, "Power Quality," pp. 410-421.

[69] S. A. Mohammed, A. G. Cerrada, A.-M. M. A. and B. Hasanin, "Dynamic Voltage Restorer (DVR) System for Compensation of Voltage Sags, State-of-the-Art Review," *International Journal of Computational Engineering Reseach,* vol. 3, no. 1, pp. 177-183, 2013.

[70] D. Chapman, "Harmonics Causes and Effects," in *Power Quality Application Guide*, Copper Development Association, 2001, p. 15.

[71] N. Rich, "Mitigating harmonics in electrical systems," 2014.

[72] UST, "Power Quality Glossary".

[73] I. Littelfuse, "Protect your LED designs from over-voltage transient surges," 2015.

[74] Zenatix, "Current And Voltage Unbalance- Causes And Counter Measures," 2015.

[75] S. Debdas and a. M. F. Qureshi, "Application of Wavelet Transform for Power Quality Studies of Signal Notches in Weak AC System," *International Journal of Scientific & Engineering Research,* vol. 2, no. 11, 2011.

[76] "Electrical Power Systems Qulaity," [Online]. Available: http://halimnurrokhman.blogspot.com/2011/09/power-quality-evaluation-procedure.html.

[77] I. S. 446-1987, "IEEE Recommended Practice for Emergency and Standby Power Systems for Industrial and Commercial Applications," IEEE Orange Book.

[78] P. M. Balasubramaniam and a. S. U. Prabha, "Power Quality Issues, Solutions and Standards: A Technology Review," *Journal of Applied Science and Engineering*, vol. 18, no. 4, pp. 371-380, 2015.

[79] R. N. Rao, "Harmonic Analysis of Small Scale Industrial Loads and Harmonic Mitigation Techniques in Industrial Distribution System," *IJERA*, vol. 3, no. 4, pp. 1511-1540, 2013.

[80] S. Saha and a. C. Nandi, "Modelling and Harmonic Analysis of Domestic/Industrial Loads," in *National Seminar on Energy Science and Enngineering (NSESE)*, 2013.

[81] S. Selvakumaran and a. S. M. Kalidasan, "Power quality improvement in transmission systems using facts devices," in *2016 Online International Conference on Green Engineering and Technologies (IC-GET)*, Coimbatore, 2017.

[82] A. Singh and a. B. S. Surjan, "Power Quality Improvemnet Using FACTS Devices: A Review," *International Jpiurnal of Engineering and Advanced Technology (IJEAT),* vol. 3, no. 2, pp. 383-390, 2013.

[83] M. P. Donsion, J. A. Guemes and a. J. M. Rodriguez, "Power Quality Benefits of Utilizing FACTS Devices in Electrical Power Systems".

[84] A. R. Krishna and a. C. H. K. R. K. Reddy, "Power Quality Problems and it's improvement using FACTS devices," *International Journal of Engineering Trends and Technology (IJETT),* vol. 4, no. 5, pp. 1462-1466, 2013.

[85] L. Wang, S. Member and a. D. Troung, "Stability Enhancement of a Power System with a PMSG-based and a DFIG-based offshore Wind Farms Using a SVC with an Adaptive-Network-based Fuzzy Inference System," vol. 60, no. c, pp. 2799-2807, 2011.

[86] L. Wang and a. D. N. Troung, "Stability enhancement of DFIG-based offshore wind farm led to a multimachine system using a STACOM," *IEEE Trans. Power Syst.,* vol. 28, no. 3, pp. 2882-2889, 2013.

[87] S. Ghosh and a. M. H. Ali, "Power Quality Enhancement by Coordinated Operation of Thyristor Switched Capacitor and Optimal Reclosing of Circuit Breakers," *Journal of the Institute of Engineering and Technology, Generation, Transmission, and Distribution*, vol. 9, no. 12, pp. 1301-1307, 2015.

[88] D.-N. Truong, "Designed damping controller for SSSC to improve stability of a hybrid offshore wind farms considering time delays," *Electr. Power Energy Syst.*, vol. 65, pp. 425-431, 2015.

[89] S. W. D. d. Haan, H. Polinder, W. L. Kling and a. J. G. Slootweg, "General model for representing variable speed wind turbines in power system dynamics simulations," *IEEE Trans. Power Syst.*, vol. 18, no. 1, pp. 144-151, 2003.

[90] A. Ramasamy, R. Vibin and a. S. K. Gowdham, "A New approach for controlling the power flow in a transmission system using Unified Power Flow Controller," *International Journal of Modern Engineering Research (IJMER)*, vol. 4, no. 2, pp. 8-14, 2014.

[91] Z. Wang, K. T. Chau, B. Yuwen, Z. Zhang and a. F. Li, "Power Compensation and Power Quality Improvement Based on Multiple-Channel Current Source Converter Fed HT SMES," *IEEE Trans. Applied Superconductivity*, vol. 22, no. 3, 2012.

[92] R. T. Hock, Y. R. d. Novaes and a. A. L. Batschauer, "A Voltage Regulator for Power Quality Improvement in Low-Voltage Distribution Grids," *IEEE Trans. Power Electronics*, vol. 33, no. 3, pp. 2050-2060, 2017.

[93] Y. Prakash and a. S. Sankar, "Power quality improvement using DVR in power system," in *Power and Energy Systems Conference: Towards Sustainable Energy*, 2014.

[94] T. C. Archana and a. P. Reji, "Power quality improvement using self-supported Dynamic Voltage Restorer (DVR) in distribution system," in *2015 International Conference on Power, Instrumentation, Control and Computing (PICC)*, 2015.

[95] J. Gutierrez, J. C. Montano, M. Castilla and a. A. Lopez, "Power-quality improvement in reactive power control using FC-TCR circuits," in *IECON*, 2002.

[96] E. Sofras, J. Prousalidis and a. A. Sourlangas, "Improving electric power quality in ships via surge protection devices (SPDs)," *Journal of MArine Engineering & Technology*, vol. 14, no. 2, pp. 103-110, 2015.

[97] M. Weinhold, R. Zurowski, T. Mangold and a. L. Voss, "Power Conditioning Equipment for Improvement of Power Quality in Distribution Systems".

[98] V. Salehi, S. Kahrobaee and a. S. Afsharnia, "Power Flow Control and Power Quality Improvement of Wind Turbine Using Universal Custom Power Conditioner," in *2006 IEEE International Symposium on Industrial Electronics*, 2007.

[99] M. Costea and a. T. Leonida, "The effect of using isolation transformer to supply small nonlinear loads," in *2014 16th International Conference on Harmonics and Quality of Power (ICHQP)*, 2014.

[100] P. K. Dhal and a. C. C. A. Ranjan, "Power quality improvement based on uninterruptible power supply (UPS) in distribution system," in *International Conference on Electronics and Communication Systems (ICECS)*, 2015.

[101] B. Singh, K. Al-Haddad and a. A. Chandra, "A Review of Active Filters for Power Quality Improvement," *IEEE Trans. Industrial Electronics*, vol. 46, no. 5, pp. 960-971, 1999.

[102] S. S. Patil and a. R. A. Metri, "Power quality improvement using shunt active power filter," in *International Conference on Data Management, Analytics and Innovation (ICDMAI)*, 2017.

[103] A. Chauhan and a. R. Thakur, "Power Quality Improvement using Passive & Active Filter," *International Journal of Engineering & Technology (IJETT)*, vol. 36, no. 3, pp. 130-136, 2016.

[104] S. Khalid and a. B. Dwivedi, "Power Quality Issues, Problems, Standards," *International Journal of Advances in Engineering & Technology*, 2011.

[105] G. S. Stavrakakis and a. G. N. Kariniotakis, "A general simulation algorithm for the accurate assessment of isolated diesel-wind turbines systems interaction. Part I: A general multimachine power system model," *IEEE Transactions on Energy Conversion*, vol. 10, no. 9, pp. 577-583, 1995.

[106] L. Wang and a. K. H. Wang, "Dynamic stability analysis of a DFIG-based offshore wind farm connected to a power grid through an HVDC link," *IEEE Transaction on Power Systems*, vol. 26, no. 3, pp. 1501-1510, 2011.

[107] O. A.-L. N. J. a. G. S. F. M. Hughes, "A power system stabilizer for DFIG-based wind generation," *IEEE Trans. Power Syst.*, vol. 21, no. 2, pp. 763-772, 2006.

[108] I. Erlich, J. Kretschmann, J. Fortmann, S. Mueller-Engelhardt and a. H. Wrede, "Modelling of wind turbines based on doubly-fed induction generators for power system stability studies," *IEEE Trans. Power Sys.,* vol. 22, no. 3, pp. 909-919, 2007.

[109] A. D. Hansen and a. G. Michalke, "Fault ride-through capability of DFIG wind turbines," *Renewable Energy,* vol. 32, no. 9, pp. 1594-1610, 2007.

[110] M. Rahimi and a. M. Parniani, "Transient performance improvement of wind turbines with doubly fed induction generators usig nonlinear control strategy," *IEEE Trans. Energy Conversion,* vol. 25, no. 2, pp. 514-525, 2010.

[111] B. Pokharel and a. W. Gao, "Mitigation of disturbances in DFIG-based wind farm connected to weak distribution system using STATCOM," in *North American Power Symposium 2010, NAPS 2010,* 2010.

[112] H. Mohammadpour, M. Islam, E. Santi and a. Y.-J. Shin, "SSR Damping in Fixed-Speed Wind Farms Using Series FACTS Controllers," *IEEE Trans. Power Deliv.,* vol. PP, no. 99, pp. 1-1, 2015.

[113] H. Liao, S. Abdelrahman and a. J. V. Z. Milanović, "Mitigation of power quality using FACTS devices for provision of differentiated quality of electricity supply in networks with renewable generation," *IEEE Trans. Power Deliv.,* vol. 32, no. 4, pp. 1975-1985, 2017.

[114] S. K. Khadem, M. Basu and a. M. F. Conlon, "A comparative analysis of placement and control of UPQC in DG integrated grid connected network," *Sustain Energy Grids Network,* vol. 6, no. 2, pp. 46-57, 2016.

[115] A. K. Goswami, C. P. Gupta and a. G. K. Singh, "Minimization of voltage sag induced financial losses in distribution systems using FACTS devices," *Electric Power Syst. Reearch,* vol. 81, no. 3, pp. 767-774, 2011.

[116] J. Khazaie, M. Mokhtari, M. Khalilyan and a. D. Nazarpour, "Sub-synchronous resonance damping using distributed static series compensator (DSSC) enhanced with fuzzy logic controller," *Electric Power Energy Syst.,* vol. 43, no. 1, pp. 80-89, 2012.

[117] W. U. Tareen, S. Mekhilef, M. Seyedmahmoudian and a. B. Horan, "Active power filter (APF) for mitigation of power quality issues in grid integration of wind and photovoltaic energy conversion system," *Renew. Sustain. Energy Rev.,* vol. 70, no. 4, pp. 635-655, 2017.

[118] A. Mohanty, M. Viswavandya, D. Mishra, P. K. Ray and a. S. Pragyan, "Modelling&simulation of a PV based micro grid for enhanced stability," *Energy proceeding,* vol. 109, pp. 94-101, 2017.

[119] N. D. G. MPI for Dynamics and Self-Organization Göttingen, "Dynamics of Modern Power Grids," 2018.

[120] W. E. Ferro and a. W. B. Gish, "Overvoltages Caused by DSG Operation: Synchronous and Induction Generators," *IEEE Trans. Power Deliv.,* pp. 258-264, 1986.

[121] L. Wang and a. M. S. N. Thi, "Stability enhancement of large-scale integration of wind, solar, and marine-current power generation fed to an SG-based power system through an LCC-HVDC link," *IEEE Trans. Sustain. Energy,* vol. 5, no. 1, pp. 160-170, 2014.

[122] N. Walia, H. Singh and a. A. Sharma, "ANFIS: Adaptive Neuro-Fuzzy Inference System- A Survey," *International Journal of Computer Applications,* vol. 123, no. 13, pp. 32-38, 2015.

[123] M. Zarghami, M. L. Crow and a. S. Jagannathan, "Nonlinear control of FACTS controllers for damping inter-area oscillations in power systems," *IEEE Trans. Power Deliv.,* vol. 25, no. 4, pp. 3113-3121, 2010.

[124] L. Gao, L. Chen, Y. Fan and a. H. Ma, "A nonlinear control design for power systems," *Automatica,* vol. 28, no. 5, pp. 975-979, 1992.

[125] M. E. El-Hawary, Electric Power Applications of Fuzzy Systems: New York, IEEE Press, 1998.

[126] V. Rajkumar and a. R. Mohler, "Nonlinear Control Methods for Power Systems: A Comparison," *IEEE Trans. on Control Systems Technology,* vol. 3, no. 2, pp. 231-237, 1995.

[127] J. S. R. Jang, "ANFIS: adaptive-network-based fuzzy inference system," *IEEE Trans. Syst. Man Cybern.,* vol. 23, no. 3, pp. 665-685, 1993.

[128] S. R. Khuntia and a. S. Panda, "ANFIS approach for TCSC-based controller design for power system stability improvement," in *Commun. Control Compu. Technol. (ICCCCT)*, 2010.

[129] S. R., Panda and a. S. Khuntia, "ANFIS approach for SSSC controller design for the improvement of transient stability performance," *Math. Comput. Model*, vol. 57, no. 1-2, pp. 289-300, 2013.

[130] A. R. Roosta, D. Georges and a. N. Hadj-Said, "Decentralized Nonlinear Controller Design for Multimachine Power Systems Via Backstepping".

[131] H. E. Psillakis and a. A. T. Alexandridis, "A New Excitation Control for Multimachine Power Systems I: Decentralized Nonlinear Adaptive Control Design and Stability Analysis," *International Journal of Control, Automation, and Systems,* vol. 3, no. 2, pp. 278-287, 2005.

[132] T. Hiyama, "Rule-based stabilizers for multi-machine power system," *IEEE Trans. Power Syst.*, vol. 5, no. 2, pp. 403-411, 1990.

[133] N. Mathur, I. Glesk and a. A. Buis, "Comparison of adaptive neuro-fuzzy inference system (ANFIS) and Gaussian processes for machine learning (GPML) algorithms for the prediction of skin temperature in lower limbprotheses," *Medical Engineering and Physics Journal*, vol. 38, pp. 1083-1089, 2016.

[134] H. Sahraie, A. Ghaffari and a. M. Amidpour, "Adaptive Neuro-Fuzzy Inference system (ANFIS) Approach to Evaluate the Debutanizer Top Product," *International Journal of Engineering and Applied Sciences,* vol. 6, no. 2, 2014.

[135] A. Kusagur, S. F. Kodad and a. S. Ram, "Modelling & Simulation of an ANFIS controller for an AC drive," *World Journal of Modelling and Simulation*, vol. 8, no. 1, pp. 36-49, 2012.

[136] A. Albakkar and a. O. P. Malik, "Adaptive Neuro-Fuzzy Controlled Based on Simplified ANFIS Network," in *IEEE Power and Energy Society General Meeting*, 2013.

[137] M. Mahdavi, L. Li1, J. Zhu1 and a. S. Mekhilef, "An Adaptive Neuro-Fuzzy Controller for Maximum Power Point Tracking of Photovoltaic Systems," in *TENCON 2015-2015 IEEE Region 10 Conference*, 2015.

[138] M. Sahin and a. R. Erol, "A Comparative Study of Neural Networks and ANFIS for Forecasting Attendance Rate of Soccer Games," *Mathematical and Computational Applications,* vol. 22, no. 4, 2017.

[139] B. Bhargave, "Synchronize phasor measurement system project at Southern California Edison Co," in *IEEE Power Engineering Society Summer Meeting*, 1999.

[140] G. Chen, Y. Sun, V. Venkatasubramanium, L. Cheng, J. Lin, A. Bose, W. Zhao and a. C. Lin, "Wide Area Control Framework Design Considering Different Feedback Time Delays," in *IEEE Power and Energy Society General Meeting*, San Diego, 2012.

[141] M. Chenine, K. Zun and a. L. Nordstrom, "Survey on priorities and communication requirements for PMU-based applications in the nordic region," in *IEEE Power Tech*, 2009.

[142] P. Kamsal and a. A. Bose, "Smart grid communication requirements for the high voltage power system," in *IEEE Power and Energy Society*, 2011.

[143] M. H. Ali, M. Tamura and a. T. J, "Influence of Communication Delay on the Performance of Fuzzy Logic-Controller Braking Resistor Against Transient Stability," *IEEE trans. on Control Systems Technology,* vol. 16, no. 6, pp. 1232-1241, November 2008.

[144] J. Qi, Q. Jiang, G. Wang and a. Y. Cao, "Wide-area time-delay robust control for power system," *European Trans. of Electrical Power*, vol. 10, pp. 899-910, 2009.

[145] S. Sönmez, S. Ayasun and a. C. O. Nwankpa, "An Exact Method for Computing Delay Margin for Stability of Load Frequency Control Systems with Constant Communication Delays," *IEEE Trans. Power Syst.,* vol. 31, no. 1, 2016.

[146] S. Sonmez, S. Ayasun and a. U. Eminoglu, "Computation of time delay margin for stability of a single-area load frequency control system with communication delays," *WSEAS Trans. Power Syst.,* vol. 9, pp. 67-76, 2014.

[147] W. Yao, L. Jiang, Q. H. Wu, J. Y. Wen and a. S. J. Cheng, "Delay-dependent stability analysis of the power system with a wide-area damping controller embedded," *IEEE Trans. Power Syst.,* vol. 26, no. 1, pp. 233-240, 2011.

[148] W. Yao, L. Jiang, Q. H. Wu, J. Y. Wen, Q. H. Wu and a. S. J. Cheng, "Wide-area damping controller of FACTS devices for inter-area oscillations considering communication time delays," *IEEE Trans. Power Syst.*, vol. 29, no. 1, pp. 318-329, 2014.

[149] Y. Zhou, S. Ghosh, M. H. Ali and a. T. E. Wyatt, "Minimization of negative Effects of Time Delay in Smart Grid System," in *IEEE SoutheastCon*, Florida, 2013.

[150] M. H. ALi and a. D. Dasgupta, "Effects of communication delays in electric grid," in *Future of Instrumentation International Workshop*, 2011.

[151] M. Gamal, N. Sadek, M. R. M. Rizk and a. A. K. Abou-elSaoud, "Delay Compensation using Smith predictor for wireless network control system," *Alexandria Engineering Journal*, vol. 55, pp. 1421-1428, 2016.

[152] M. Mokhtari, F. Aminifar, D. Nazarpour and a. S. Golshannavaz, "Wide-Area Power Oscillation Damping with a Fuzzy Controller Compensating the Continous Communication Delays," *IEEE TRans. Power Systems*, vol. 28, no. 2, pp. 1997-2005, 2013.

[153] J. W. Stahlhut, T. J. Browne, G. T. Heydt and a. V. Viittal, "Latency viewed as a stochastic process and its impact on widearea power system control signals," *IEEE Trans. Power Syst.*, vol. 23, no. 1, 2008.

[154] R. E. Wilson, "An investigation of time transfer accuracies over a utility microwave communications channel," *IEEE Trans. Power Deliv.*, vol. 8, no. 3, pp. 993-999, 1993.

[155] B. Chaudhuri, R. Majumder and a. B. C. Pal, "Wide-area Measurement-Based Stabilizing Control of power System Considering Signal Transmission Delay," *IEEE Trans. Power Syst.*, vol. 19, no. 4, pp. 1971-1979, 2004.

[156] C. W. Taylor, D. C. Erickson, K. E. Martin, R. E. Wilson and a. V. Venkatasubramanian, "WACS-wide-area stability and voltage control system: R&D and online demonstration," *IEEE Proceedings*, vol. 93, no. 5, pp. 892-906, 2005.

[157] H. Ota, Y. Kitayama, H. Ito, N. Fukushima, K. Omata, K. Morita and a. Y. Kokai, "Development of transient stability control system (TSC system) based on online stability calculation," *IEEE Trans. Power Syst.*, vol. 1, pp. 84-89, 1996.

[158] M. Koaizawa, M. Nakane, K. Omata and a. Y. Kokai, "Actual operating experiencve of online transient stability control system (TSC systems)," in *IEEE PES Winter Meeting*, 2000.

[159] K. S. Ko and a. D. K. Sung, "The Effect of EV Aggregators with Time-Varying Delays on the Stability of a Load Frequency Control System," *IEEE Trans. Power Syst.*, 2017.

[160] Q. Jiang, Z. Zou and a. Y. Cao, "Wide-area TCSC controller design in consideration of feedback signals' time delays," in *IEEE Power Energy Society General Meeting*, San Francisco, 2005.

[161] M. S. Saad, M. A. Hassoumeh, E. H. Abed and a. A. A. Edris, "Delaying instability and voltage collapse in power systems using SVXs with washout filter-aided feedback," in *American Control Conference*, Portland, 2005.

[162] B. Chaudhuri, R. Majumder and a. B. Pal, "Wide area measurement based stabilizing control of power system considering signal transmission delay," in *IEEE Power Energy Society General Meeting*, San Francisco, 2005.

[163] E. C. Martins and a. F. G. Jota, "Design of networked control systems with explicit compensation for time-delay variations," *IEEE Trans. Syst. Man Cybern.*, vol. 40, no. 3, 2010.

[164] J. Yool, Y. Zhoul, S.-M. Leel, M. G. Joo2 and a. J. H. Park, "An adaptive delay compensation technique for wireless sensor and actuator network," *International Journal of Smart Home*, vol. 6, no. 4, 2012.

[165] G. Kishore, N. S. Beniwal and a. S. Mishra, "Study of compensation of variable delay in communication link using communication disturbance observer (CDOB) and network disturbance (ND)," *International Journal of Science and Research Development*, vol. 2, no. 9, 2014.

[166] F. Zhang, L. Cheng and a. W. Gao, "Prediction Based Hierarchical Compensation for Delays in WIde-area Control Systems," *IEEE Trans. Smart Grid.*

[167] F. Zhang, Y. Sun, L. Cheng, X. Li, J. H. Chow and a. W. Zhao, "Measurement and modelling of delays in wide-area closed loop control systems," *IEEE TRans. Power Syst.*, vol. 30, no. 5, pp. 2426-2433, 2015.

[168] S. B. Wang, X. Y. Meng and a. T. W. Chen, "Wide-area control of power systems through delayed network communication," *IEEE Trans. Control Syst. Technology*, vol. 20, no. 2, pp. 495-503, 2012.

[169] N. R. Chaudhuri, S. Ray, R. Majumder and a. B. Chaudhuri, "A new approach to continous lentency compensation with adaptive phasor power oscillation damping controller (POD)," *IEEE Trans. Power Syst.*, vol. 25, no. 2, pp. 939-946, 2010.

[170] P. Zhang, D. Y. Yang, K. W. Chan and a. G. W. Chai, "Adaptive wide-area damping control scheme with stochastic subspace identification and signal time delay compensation," *IET Transm. Distrib.*, vol. 6, no. 9, pp. 844-852, 2012.

[171] J. H. Chow and a. S. G. Ghiocel, "An adaptive wide-area power system damping controller using synchro phasor data," *Control Optim. Methods Elect. Smart Grids Power Electron Power Syst.*, vol. 3, no. 3, pp. 327-342, 2012.

[172] C. L. Lai and a. P. L. Hsu, "Design the Remote-Control System with the Time Delay Estimator and the Adaptive Smith Predictor," *IEEE Trans. Indus. Informatics*, vol. 6, no. 1, 2010.

[173] S. Ghosh and a. M. H. Ali, "Minimization of Adverse Effects of Time Delay in Smart Power Grid," in *IEEE ISGT*, Washington D. C., 2014.

[174] A. Ashok, S. Krishnaswamy and M. Govindarasu, "PowerCyber: A Remotely Accessible Testbed for Cyber Physical Security of the Smart Grid," 2016.

[175] L. Langer, P. Smith, M. Hutle and A. Schaeffer-Filho, "Analysing Cyber-physical Attacks to a Smart Grid: A Voltage Control Use Case".

[176] A. Hahn, A. Ashok, S. Sridhar and M. Govindarasu, "Cyber-Physical Security Testbeds: Architecture, Application, and Evaluation for Smart Grid," *IEEE Transactions on Smart Grid*, vol. 4, no. 2, pp. 847-855, 2013.

[177] H. T. Zhang and a. L. L. Lai, "Monitoring system for smart grid," in *IEEE ICMLC*, 2012.

[178] M. Jin, J. Lavaei and K. H. Johansson, "Power Grid AS-based State Estimation: Vulnerability Analysis Against Cyber Attacks," in *IEEE Allerton Conference on Communication, Control, and Computing*, 2017.

[179] M. Mallouhi, Y. Al-Nashif, D. Cox, T. Chadaga and a. S. Hariri, "A testbed for analyzing security of SCADA control systems(TASSCS)," in *IEEE ISGT*, 2011.

[180] G. N. Ericsson, "Cyber security and power syste communications-Essential parts of a smart grid infrastructure," *IEEE Transactions on Power Delivery*, vol. 25, no. 3, 2010.

[181] T. Lu, J. Zhao, L. Zhao, Y. Li and a. X. Zhang, "Towards a Framework for Assuring Cyber Physical System Security," *International Journal of Security and Its Applications*, vol. 9, no. 3, pp. 25-40, 2015.

[182] P. Li, Y. Liu, H. Xin and a. X. Jiang, "A Robust Distributed Economics Dispatch Strategy of Virtual Power Plant Under Cyber-Attacks," *IEEE Trans. Ind. Informatics*, vol. 2303, no. c, 2017.

[183] S. Kakran and a. S. Chanana, "Smart operations of smart grids integrated with distributed generation: A review," *Renew. Sustain. Energy Rev.*, vol. 81, pp. 524-535, 2018.

[184] H. He and a. J. Yan, "Cyber-physical attacks and defenses in the smart grid: a survey," *IET Cyber-Physical Systems: Theory & Applications*, vol. 1, no. 1, pp. 13-27, 2016.

[185] K. Edemacul, M. Euku and a. R. Ssekibuule, "Packet Drop Attack Detection Techniques in Wireless Ad Hoc Networks: A Review," *International Journal of Network Security & Its Applications (IJNSA)*, vol. 6, no. 5, 2014.

[186] Y. Yuan, Z. Quanyan, S. Fuchun, W. Qinyi and a. T. Basar, "Resilent control of cyber-physical system against Denial-of-Service attacks," in *6th International Synposium on Resilient Control Systems (ISRCS)*, 2013.

[187] Z. Heng, C. Peng, S. Ling and a. C. Jiming, "Optimal DoS attack policy against remote state estimation," in *IEEE 52nd Annual Conference on Decision and Control (CDC)*, 2013.

[188] A. Rai and a. R. K. Challa, "Survey on Recent DDoS Mitigation Techniques and Comparative Analysis," in *IEEE CICT*, 2016.

[189] P. Shengyi, "Cybersecurity testing and intrusion detection for cyber-physical power systems," Mississippi State University, 2014.

[190] Y. Huang, M. Smalifalak, H. Nguyen, R. Zheng, Z. Han, H. Li and a. L. Song, "Bad Data Injection in Smart Grid: Attack and Defense Mechanisms," IEEE Communications Magazine, 2013.

[191] J.-C. Kao and a. R. Marculescu, "Eavesdropping Minimization via Transmission Power Control in Ad-Hoc Wireless Networks," in *3rd Annual IEEE Communications Society on Sensor and Ad Hoc Communications and Networks*, 2006.

[192] K. Cheolhyeon, L. Weiyi and a. H. Inseok, "Security analysis for cyber-Physical Systems agianst stealthy deception attacks," in *American Control Conference (ACC)*, 2013.

[193] K. Chalkias, F. Baldimtsi, D. Hristu-Varsakelis and a. G. Stephanides, "Two Types of Key-Compromise Impersonation Attacks against One-Pass Key Establishment Protocols," *Communications in Computer and Information Science*, vol. 23, pp. 227-238, 2009.

[194] M. Conti, N. Dragoni and a. V. Lesyk, "A Survey of Man in the Middle Attacks," in *IEEE Communications Surveys & Tutorials*, 2016.

[195] L. Yuzhe, S. Ling, C. Peng, C. Jiming and a. D. E. Quevedo, "Jamming attack on Cyber-Physical Systems: A game-theoretic approach," in *IEEE 3rd Annual International Conference on Cyber Technology in Automation, Control and Intelligent Systems (CYBER)*, 2013.

[196] T.-T. Tran, O.-S. Shin and a. J.-H. Lee, "Detection of replay attacks in smart grid systems," in *Computing, Management and Telecommunications (ComManTel)*, 2013.

[197] S. Bakjer, N. Filipiak and a. K. Timlin, "In the dark: Crucial industries confront cyberattacks," McAfee 2nd annual critical infrastructure protection report, 2011.

[198] S. Asri and a. B. Pranggono, "Impact of Distributed Denial-of-Service Attack on Advanced Metering Infrastructure," *Wireless Pers. Communication,* vol. 83, pp. 2211-2223, 2015.

[199] D. Wang, X. Guan, T. Liu, Y. Gu, Y. Sun and a. Y. Liu, "A survey on bad data injection in smart grid," in *IEEE PES Asia-Pacific*, 2013.

[200] K. Wan and a. V. Alagar, "Context-Aware Security Solutions for Cyber-Physical Systems," 18-29, 2013.

[201] A. R. Metke and a. R. L. Ekl, "Security technology for smart grid networks," *IEEE Transactions on Smart Grid,* vol. 1, no. 1, pp. 99-107, 2010.

[202] T. H. Morris, A. K. Srivastava, B. Reaves, K. Pavurapu, S. Abdelwahed, R. Vaughn, W. McGrew and a. Y. Dandass, "Engineering future cyber-physical energy systems: challenges, research needs, and roadmap," in *North American Power Symposium (NAPS),* Starkville, 2009.

[203] S. Sridhar, A. Hahn and a. M. Govindarasu, "Cyber Physical system security for the electric power grid," *IEEE Proceedings,* vol. 100, no. 1, pp. 210-224, 2012.

[204] J. M. Weiss, "Control systems cyber security - the need for appropriate regulations to assure cyber security of the electric grid," 2007.

[205] A. Hahn, "Cyber security of the smart grid: Attack exposure analysis, detection algorithms, and testbed evaluation," 2013.

[206] P. J. Hawrylak, M. Haney and a. M. H. Papa, "Using hybrid attack graphs to model cyber-physical attacks in the Smart Grid," in *5th International Symposium on Resilient Control System (ISRCS)*, 2012.

[207] F. Pasqualetti, F. Dorfler and a. F. Bullo, "Cyber-physical attacks in power networks: Models, fundamental limitations and monitor design," in *IEEE Conference on Decision and Control and European Control Conference (CDC-ECC)*, 2011.

[208] S. Liu, D. Kundur, T. Zourntos and a. K. Butler-Purry, "Coordinated Variable Structure Switching in Smart Power Systems: Attacks and Mitigation," in *1st International conference on High Confidence Networked Systems*, 2012.

[209] S. Liu, X. Feng, D. Kundur, T. Zourntos and a. K. L. Butler-Purry, "A class of cyber-physical switching attacks for power system disruption," in *Seventh Annual Workshop on Cyber Security and Information Intelligence Research*, 2011.

[210] T. Li, F. Tan, Q. Wang, L. Bu, J.-N. Cao and a. X. Liu, "From offline toward real-time: A Hybrid Systems Model Checking and CPS Co-Design Approach for Medical Device Plug-and Play (MSPnP)," in *IEEE/ACM Third Conference on Cyber-Physical Systems (ICCPS)* , 2012.

[211] F. Dorfler, F. Pasqualetti and a. F. Bullo, "Distributed detection of cyber-physical attacks in power networks: A waveform relaxation approach," in *49th Annual Allerton Conference on Communication, Control, and Computing* , 2011.

[212] E. M. Ferragu, J. L. B. Czejdo and a. A. Melin, "Addressing the Challenges of Anomaly Detection for Cyber-Physical Energy Grid Systems," in *Eighth Annual Cyber Security and Information Intelligence Research Workshop*, 2013.

[213] P. M. Esfahani, M. Vrakopoulou, G. Andersson and a. J. Lygeros, "A Tractable Nonlinear Fault Detection and Isolation Technique with Application to the CYber-Physical Security of Power Systems," in *51st IEEE Conference on Decision and Control*, 2012.

[214] D. Callaway and a. I. Hiskens, "Detecting false data injection attacks on DC state estimation," in *1st Workshop Secure Control Syst.*, 2010.

[215] S. Ghosh and a. M. H. Ali, "Augmentation of Power Quality of Grid Connected Wind Generator by Fuzzy Logic Controlled TSC," in *IEEE PES Transm. and Distri.(T&D) Conference & Exposition*, Denver, 2018.

[216] R. Angu and R. K. Mehta, "A single machine infinite bus power system damping control design with extended state observer," *Journal of Cogent Engineering,* vol. 4, no. 1, 2017.

[217] A. R. V. V. Bergen, Power Systems Analysis, T. Robbins, Ed., Prentice-Hall Series, 2000.

[218] M. H. Ali, T. Murata and a. J. Tamura, "Effect of Coordination of Optimal Reclosing and Fuzzy Controlled Braking Resistor on Transient Stability During Unsuccessful Reclosing," *IEEE Trans. on Power Systems, vol. 21, no. 3,* pp. 1321- 1330, August 2006.

[219] "http://www.edaboard.com/thread130090.html," [Online].

[220] "http://www.cdeep.iitb.ac.in/nptel/Electrical%20Engineering/Power%20System%20Operation%20and%20Control/module%203/html/l6_s1.html," [Online].

[221] J. Mohammadi, S. Vaez-Zadeh, S. Afsharnia and a. E. Daryabeigi, "A Combined Vector and Direct Power Control for DFIG_Based Wind Turbines," *IEEE Trans. Sustain. Energy,* vol. 5, no. 3, pp. 767-775, 2014.

[222] "hindawi," [Online]. Available: https://www.hindawi.com/journals/cpis/2013/125801/fig1/.

[223] J. Tamura, T. Yamazaki, M. Ueno, Y. Matsumura and a. S. Kimoto, "Transient stability simulation pf power system including wind generatorby PSCAD/EMTDC," in *IEEE Porto Power Tech*, 2001.

[224] M. Rahimi, "Mathematical modeling, dynamic response analysis and control of PMSG-based wind turbines operating with an alternative control structure in power control mode," *International Trans. Electrical Energy Systems,* 2017.

[225] A. A. AbdElhafez, S. H. Alruways, Y. A. Alsaif, M. F. Althobaiti, A. B. Alotaibi and a. N. A. Alotaibi, "Reactive Power Problem and Solutions: An Overview," *Journal of Power and Energy Engineering,* vol. 5, pp. 40-54, 2017.

[226] M. Mokhtari, F. Aminifar, D. Nazarpour and a. S. Golshannavaz, "Wide-Area Power Oscillation Damping with a Fuzzy Controller Compensating the Continous Communication Delays," *2013,* vol. 28, no. 2, IEEE Trans. Power Syst..

[227] M. H. Ali, Y. Soma, T. Murata and a. J. Tamura, "A Fuzzy logic controlled braking resistor scheme for stabilization of synchronous generator," in *IEEE Int. Electric Machines Drives Conf.*, 2001.

[228] M. K. H and a. M. H. Ali, "Transient Stability Augmentation of PV/DFIG/SG-Based Hybrid Power System by Nonlinear Control-Based Variable Resistive FCL," *IEEE Trans. Sustain. Energy,* vol. 6, no. 4, 2015.

[229] S. R. Khuntia and a. S. Panda, "ANFIS approach for TCSC-based controller design for power system stability improvement," in *Communication and Control in Computer Technology (ICCCCT),* 2010.

[230] M. A. Hosen, A. Khosravi, S. Nahavandi and a. L.Sinnott, "Prediction Interval-Based ANFIS Controller for Nonlinear Processes," in *International Joint Conference on Neural Networks (IJCNN*, 2016.

[231] T. Salomao and a. J. A. Marin, "Adaptive Neuro-Fuzzy Inference System Control for a Two Tanks Hydraulic System Model," in *IEEE International Autumn Meeting on Power Electronics and Computing (ROPEC)*, 2013.

[232] M. K. Hossain and M. H. Ali, "Transient Stability Augmentation of PV/DFIG/SG-Based Hybrid Power System by Nonlinear Control-Based Variable Resistive FCL," *IEEE Transactions on Sustainable Energy,* vol. 6, no. 4, pp. 1638-1648, October 2015.

[233] M. A. G. D. Brito, L. P. Sampaio, G. Luigi, G. A. E. Melo and a. C. A. Canesin, "Comparative analysis of MPPT techniques for PV applications," in *3rd Int. Conf. Clean Electr. Power Renew. Energy Resour. Impact, ICCEP 2011*, 2011.

[234] T. P. Sahu and a. T. V. Dixit, "Modelling and analysis of perturb and observe and incremental conductance MPPT algorithm for PV array using Cuk converter," in *IEEE Students' Conf. Electr. Electron. Comput. Sci. (SCEECS)*, 2014.

[235] M. G. Villalva, J. R. Gazoli and a. E. R. Filho, "Comprehensive approach to modelling and simulation of photovoltaic arrays," *IEEE Trans. Power Electronics*, vol. 24, no. 5, pp. 1198-1208, 2009.

[236] M. K. Hossain and a. M. H. Ali, "Overview on maximum power point tracking (MPPT) techniques for photovoltaic power systems," *International Review of Electronics Engineering,* vol. 8, no. 4, pp. 1363-1378, 2013.

[237] M. G. Villalva, J. r. Gazoli and a. E. R. Filho, "Comprehensive Approach to Modelling and Simulation of Photovoltaic Arrays," *IEEE Trans. Power Electron.,* vol. 57, no. 1-2, pp. 1198-1208, 2009.

[238] U. Yilmaz, A. Kircay and a. S. Borekci, "PV system fuzzy logic MPPT method and PI control as a charge controller," *Renew. Sustain. Energy Rev.*, vol. 81, pp. 994-1001, 2018.

[239] B. S. Kumar and a. K. Sudhakar, "Performance Evaluation of 10 MW grid connected solar photovoltaic power plant in India," Energy Reports, 2015.

[240] C. Solar, "Why is Energy Storage Such an Important Part of the Renewables Mix".

[241] CAP-X, "The Supercapacitor Advantage," 2018.

[242] A. Burke, "Ultracapacitors: Why, how, and where is the technology", J. Power Sources," *Journal of Power Sources*, vol. 91, pp. 37-50, 2000.

[243] Y. Y. Yao, D. L. Zhang and a. D. G. Xu, "A Study of Supercapacitor Parameters and Characteristics," in *IEEE Conf. Power Syst. Technology*, 2006.

[244] T. Wei, S. Wang and a. Z. Qi, "A Supercapacitor Based Ride-Through System for Industrial Drive Applications," in *IEEE Conf. Mech. and Autom.*, 2007.

[245] J. M. Miller, "Electrical and Thermal Performance of the Carbon-carlbon Ultracapacitor under Constant Power Conditions," in *IEEE Conference on Vehicle Power and Propulsion*, 2007.

[246] G. Alcicek, H. Gualous, P. Venet, R. Gallay and a. A. MIraoui, "Experimental Study of temperature effect on Ultracapacitor ageing," in *IEEE Conference on Power Electronics and Applications*, 2007.

[247] S. Basu, "voltage and Current Ripple Considerations for Improving Lifetime of Ultra-Capacitors used for Energy Buffer Applications at Converter Inputs," in *IEEE Conference on Power Electronics Specialists*, 2007.

[248] P. Agarwal and a. R. Gupta, "Grid Integration of Solar PV power using shunt connected VSC," in *IEEE SCES*, 2013.

[249] P. Srithorn, M. Sumner, L. Yao and a. R. Prashar, "A STATCOM with supercapacitors for enhanced power stability," in *IET Conference on Power Electronics*, 2008.

[250] F. Marini and a. B. Walczak, "Particle swarm optimization (PSO). A tutorial," *Chemometrics and Intelligent Laboratory Systems*, vol. 149, no. b, pp. 153-165, 2015.

[251] X.-S. Yang, "A New Metaheuristic Bat-Inspired Algorithm," 2010.

[252] N. K. Jhankal and a. D. Adhyaru, "Bacterial foraging optimization algorithm: A derivative free technique," in *2011 Nirma University International Conference on Engineering*, Ahmedabad, India, 2012.

[253] J. McCAll, "Genetic algorithms for modelling and optimisation," *Journal of Computational and Applied Mathematics,* Vols. 205-222, no. 184, 2005.

[254] R. Akbari, A. Mohammadi and a. K. Ziarati, "A powerful bee swarm optimization algorithm," in *IEEE 13th International Multitopic Conference,* Islamabad, Pakistan, 2010.

[255] M. Dorigo, M. Birattari and a. T. Stutzle, "Ant colony optimization," *IEEE Computational Intelligence Magazine,* vol. 1, no. 4, pp. 28-39, 2006.

[256] L. Wang and a. Y. Gong, "A fast shuffled frog leaping algorithm," in *Ninth International Conference on Natural Computation (ICNC)*, Shenyang, China, 2014.